arXiv:1608.03011v2 [math.SG] 28 Oct 2016

CELLULAR LEGENDRIAN CONTACT HOMOLOGY FOR SURFACES, PART II

DAN RUTHERFORD AND MICHAEL SULLIVAN

Abstract. This article is a continuation of [15]. For Legendrian surfaces in 1-jet spaces, we prove that the Cellular DGA defined in [15] is stable tame isomorphic to the Legendrian contact homology DGA.

Contents

1. Introduction 1
2. Background 3
3. Transverse Square Decompositions 10
4. Blueprint for enumeration of GFTs 17
5. Computation of LCH, Part 1: 0-cells and 1-cells 21
6. Computation of LCH, Part 2: 2-cells without swallowtail singularities 29
7. Computation of LCH, Part 3: 2-cells with swallowtail singularities 51
8. Isomorphism between the cellular DGA and LCH 80
9. Proof of Theorem 5.1 Part 1: Construction of squares without swallowtails 92
10. Proof of Theorem 5.1 Part 2: Construction of squares with swallowtails 106
11. Proof of Theorem 5.1 Part 3: Verification of Properties 121
12. Proof of Theorem 5.1 Part 4: Transversality 148
References 154

1. Introduction

This article is a continuation of [15]. Together the two articles provide a formulaic computation of the Legendrian contact homology (LCH) differential graded algebra (DGA) for any Legendrian surface in a 1-jet space. In [15] we compute the LCH DGA for several families of examples, and in [16] we apply our results to study augmentations and generating families.

Let S be a surface, and let $L \subset J^1(S)$ be a closed Legendrian surface in the 1-jet space of S. In [15], we defined the cellular DGA of L, denoted here as $(\mathcal{A}_{cell}, \partial)$. The definition of $(\mathcal{A}_{cell}, \partial)$ requires as input a cellular decomposition of the base projection of L that contains in its 1-skeleton the projection of all crossings arcs, cusp edges, and swallowtail points from the front projection. For each cell, we have one generator of $\mathcal{A}_{cell}$ for each pair of sheets above the cell that and do not cross one another. After collecting generators into upper triangular matrices, the differential ∂ is characterized by simple matrix formulas as summarized in Figure 1. (Additional terms appear when swallowtail points are present.)

We have established in Theorem 4.1 of [15] that $(\mathcal{A}_{cell}, \partial)$ is determined, up to stable tame isomorphism, by the Legendrian L, i.e., it does not depend on the cellular decomposition or other choices involved in the definition. In the present article, we prove the following:

Theorem 1.1. *Let $L \subset J^1(S)$ be a closed Legendrian surface. The cellular DGA of L is stable tame isomorphic to the Legendrian contact homology DGA of L with coefficients in $\mathbb{Z}/2$.*

In particular, the cellular DGA is an invariant of the Legendrian isotopy class of L. We remark that it would be interesting to have an independent, low-tech proof of invariance that skirts the theory of holomorphic curves.

We thank Tobias Ekholm for explaining his transversality argument. The second author is supported by grant 317469 from the Simons Foundation. He thanks the Centre de Recherches Mathematiques for hosting him while some of this work was done.

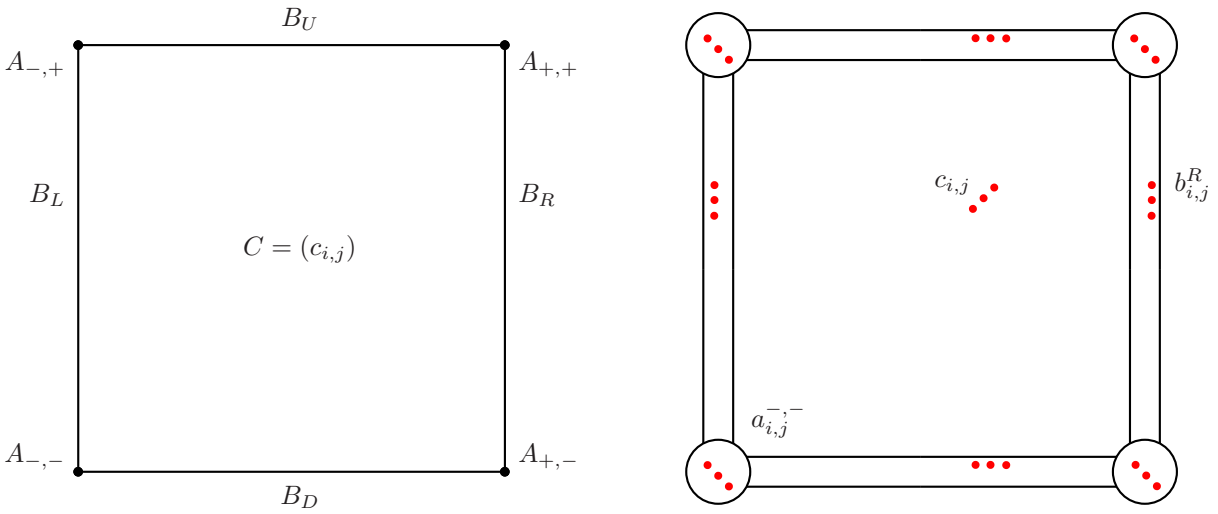

$$\partial A = A^2; \qquad \partial B = A_+(I+B) + (I+B)A_-;$$
$$\partial C = A_{-,-}C + CA_{+,+} + (I+B_U)(I+B_L) + (I+B_R)(I+B_D).$$

FIGURE 1. (left) Matrix formulas for the differential in the Cellular DGA. (right) Geometrically, the generators of the Cellular DGA correspond to Reeb chords $a_{i,j}$, $b_{i,j}$, and $c_{i,j}$ that are local minima, saddle points, and local maxima located in neighborhoods of the 0-, 1-, and 2-cells of a decomposition of S into squares.

1.0.1. *Outline of proof.* The proof of Theorem 1.1 occupies this entire article, and we now provide an outline of the argument. In this introduction, we denote the LCH DGA as $(\mathcal{A}_{LCH}, \partial)$.

Our starting point is the work of Ekholm [4] that allows the differential in $(\mathcal{A}_{LCH}, \partial)$, that was originally defined in [6] and [8] by a count of holomorphic disks, to be computed via a count of rigid *gradient flow trees* (abbrv. GFTs). In Section 2, we recall relevant background about the LCH DGA and GFTs. In Section 3, we construct a cellular decomposition of S into squares, $\mathcal{E}_{\pitchfork}$, so that, in the front projection of L, the form of the singular set above each square matches one of 14 standard types. (See Figure 4, below.) In addition, we construct a related cellular decomposition, $\mathcal{E}_{\|}$, that is suitable from the point of view of the cellular DGA.

For computing LCH, we modify L by a Legendrian isotopy to a Legendrian $\tilde{L}$ that has several properties that aid in the explicit enumeration of rigid GFTs. Most importantly, the sheets of $\tilde{L}$ are pinched together above the 1-skeleton of $\mathcal{E}_{\pitchfork}$ with the pinching most exaggerated above the 0-skeleton. As a result, above each cell of dimension $0 \leq d \leq 2$, each pair of sheets are connected by a Reeb chord that when viewed as a critical point of the difference of z-coordinates of sheets has index d. (Some additional Reeb chords that we call exceptional generators appear as well and are discussed below.) Labeling Reeb chords between the i-th and j-th sheet above 0-cells, 1-cells, and 2-cells in the form $a_{i,j}$, $b_{i,j}$, and $c_{i,j}$, gives a rough indication of the correspondence between generators of $\mathcal{A}_{cell}$ and $\mathcal{A}_{LCH}$ underlying the isomorphism of Theorem 1.1. See Figure 1. As an additional consequence of the pinching near the 1-skeleton, the GFTs used in computing the differential of $(\mathcal{A}_{LCH}, \partial)$ become localized and must remain entirely within a neighborhood of the square that they begin in. The Reeb chords that appear above suitable neighborhoods of any closed cell from $\mathcal{E}_{\pitchfork}$ then generate a sub-DGA, so that computation of $(\mathcal{A}_{LCH}, \partial)$ may be carried out on a square-by-square basis.

The enumerations of GFTs required for computation of the sub-DGAs corresponding to individual cells of $\mathcal{E}_{\pitchfork}$ are carried out in Sections 5-7. A common argument applies for all squares that do not contain swallowtail points. To orient the reader for this general computation, the logically independent Section 4 outlines in detail the computation for two of the most basic square types with technical details simplified or ignored. In Section 5, we compute the sub-DGAs associated to 0-cells and 1-cells. In Section 6, we compute in a uniform manner the sub-DGAs of all 2-cells that do not contain swallowtail points. In Section 7, we address squares with swallowtail points.

To be more precise, in Sections 5-7 we only give a partial calculation of the differential in $(\mathcal{A}_{LCH}, \partial)$. The reason for this is that the presence of crossing arcs above a square forces additional Reeb chords

that we call *exceptional generators* to appear. In turn, these exceptional generators lead to GFTs that can be quite complicated, so that a complete calculation would require special arguments for many of the different square types. To keep the computation as uniform as possible, in Sections 5-7 we only compute ∂ up to terms belonging to an ideal I involving these exceptional generators. Aside from these terms, for each of the first 12 square types the differential is given by a common matrix formula where certain matrix entries are replaced with 0's and 1's in a way that is determined by the location of crossing arcs and cusp edges. The final two square types contain swallow tail points, and as a result differentials in these square types have a form that is genuinely distinct from the other twelve square types.

To avoid having to explicitly identify the remaining terms involving exceptional generators, we show in the first half of Section 8, that the quotient of $(\mathcal{A}_{LCH}, \partial)$ by the differential ideal I is stable tame isomorphic to $(\mathcal{A}_{LCH}, \partial)$. Moreover, our partial calculations from Sections 5-7 give a complete calculation of the differential in $\mathcal{A}_{LCH}/I$. Section 8 is then concluded by establishing Theorem 1.1 via a stable tame isomorphism between $(\mathcal{A}_{LCH}/I)$ and the cellular DGA.

The final Sections 9-12 give a rather explicit coordinate model for $\tilde{L}$ that is used for the calculation of $(\mathcal{A}_{LCH}, \partial)$ in the earlier sections of the paper. This construction is technical (although elementary). To allow the reader to understand the computation of LCH without worrying about the details of this coordinate construction, we have listed those properties of $\tilde{L}$ that are required for the arguments as Properties 1-19 appearing in Sections 5-7. We expect that most readers will not find it surprising that a Legendrian satisfying Properties 1-19 exists. However, as many properties involving the critical points and gradient vector fields of local defining functions for $\tilde{L}$ and their difference functions are demanded simultaneously, we did not feel that the existence of $\tilde{L}$ was entirely obvious. An outline of the construction appears at the start of Section 9.

1.0.2. *Strategies for reading.* For a first reading, the details of the construction from Section 9-12 may be omitted. The reader may also reduce the length of the proof by considering only the case of Legendrians without swallowtail points. This eliminates Sections 7 and 10, and simplifies the isomorphism in Section 8 as well as parts of Section 11. In fact, for some purposes considering only Legendrian surfaces without swallowtail points may suffice. By work of Entov [11, Corollary 1.8 and Section 1.8], assuming the base surface S and Legendrian L are orientable, it is always possible to remove all swallowtail points from L via a Legendrian isotopy. However, in practice, it can be difficult to explicitly find such an isotopy for a given Legendrian, and the number of generators of the cellular DGA may be greatly increased by removing swallowtail points. Thus, aside from removing any assumptions on the orientability of L and S, the extra work involved to include swallow tail points is justified in order to make the cellular DGA a flexible tool for computations. For example, a configuration of four swallowtail points can collapse to a cone point, whose DGA we compute in Section 5.3 of [15], and the cone points appear in the work-in-progress by Casals and Murphy on Lefschetz fibrations.

2. Background

We assume familiarity with [15, Sections 2 and 3]. In particular, the reader should be familiar with the generic appearance of the base and front projection of a Legendrian surface in a 1-jet space; the latter may include **cusp edges**, **crossing arcs**, and (upward and downward) **swallowtail points**. We refer to this subset of the front projection (cusp edges, crossing arcs and swallowtail points) and sometimes its base projection as the **singular set**. The definition of the **cellular DGA** from [15, Section 3] as well as algebraic results on **DGAs** (differential graded algebras) and **stable tame isomorphism** as found in [15, Section 2] are required for the proof of Theorem 1.1. In this section, we recall background on Legendrian contact homology, focusing on Ekholm's work on gradient flow trees which is fundamental for this article.

Let S be a surface. Denote the 1-jet space of S as $J^1S = T^*S \times \mathbb{R}$. Define the **front projection** $\pi_{xz} : J^1S \to J^0S = S \times \mathbb{R}$, the **base projection** $\pi_x : J^1S \to S$ and the **Lagrangian projection** $\pi_{xy} : J^1S \to T^*S$. In coordinates $(x_1, x_2, y_1, y_2, z) \in J^1S$ arising from a choice of local coordinates (x_1, x_2) on S, the standard contact structure on J^1S is the kernel of the contact form $dz - y\,dx := dz - y_1\,dx_1 - y_2\,dx_2$. Let ω be the standard symplectic structure on T^*S, where locally $\omega = dx \wedge dy$.

2.1. **LCH.** Let $L \subset J^1S$ be a Legendrian surface. The Legendrian contact homology (LCH) of L is the homology of a differential graded algebra (DGA) denoted $(\mathcal{A}_{LCH}, \partial)$ whose definition is based on the theory of J-holomorphic curves. The LCH DGA was first introduced in [10] and was then rigorously defined in [6, 8]. In reviewing the definition, it is natural to use $\mathbb{Z}/2[H_1(L)]$-coefficients and introduce a $\mathbb{Z}$-grading on $\mathcal{A}_{LCH}$, but in the remainder of the article we will specialize to coefficients in $\mathbb{Z}/2$ (all group ring generators are replaced with 1) and collapse the grading modulo the Maslov number of L.

2.1.1. *Reeb chords and the algebra $\mathcal{A}_{LCH}$.* The Reeb vector field X_α associated to a contact form α is defined as the unique vector field which satisfies $\alpha(X_\alpha) = 1$ and $d\alpha(X_\alpha, \cdot) = 0$. For our contact form on J^1S, the Reeb vector field is ∂_z. The **Reeb chords** $R(L)$ for our Legendrian L are the (non-constant) flows lines of the Reeb vector field that begin and end on the Legendrian.

Assuming that L has a generic front projection, we can write $L = L_0 \sqcup L_1 \sqcup L_2$ where $L_i \subset L$ has codimension i and the front projection $\pi_{xz}|_L$ satisfies:

- $\pi_{xz}|_L$ is an immersion when restricted to L_0;
- $\pi_{xz}|_L$ has a cusp edge singularity along L_1;
- $\pi_{xz}|_L$ has (upward or downward) swallowtail singularities at points in L_2.

Any $p \in L_0$ has a neighborhood $U \subset L$ that is the 1-jet of a function $F : \pi_x(U) \to \mathbb{R}$. We say that F is a **local defining function** for L at p. The Reeb chords $R(L)$ are in one-to-one correspondence with the critical points $F_i - F_j$ of positive critical value, where F_i and F_j are two such local defining functions for L. [The critical points are in the intersection of the domains of F_i and F_j.] As an additional generic assumption on L the front projection of L, we assume that the critical points of the $F_i - F_j$ are Morse.

The restriction of π_{xy} to L is an exact Lagrangian immersion. Reeb chords are also in one-to-one correspondence with the double points of $\pi_{xy}(L)$, which are transverse due to the previous assumption on the $F_i - F_j$.

The underlying algebra $\mathcal{A}_{LCH} = \mathcal{A}_{LCH}(L)$ of the LCH DGA is defined to be the free unital associative (non-commutative) over the group ring $\mathbb{Z}/2[H_1(L)]$ with generating set $R(L)$. This is the tensor algebra of the $\mathbb{Z}/2[H_1(L)]$-module generated by $R(L)$.

2.1.2. *The grading on $\mathcal{A}_{LCH}$.* We review the (Maslov) grading of a Reeb chord and the (minimal) Maslov number of the Legendrian, as formulated in [7, Section 3]. Let $\gamma \in C^\infty([0,1], L)$ be such that $\gamma([0,1]) \subset L_0$ except for at isolated points where γ intersects L_1 transversely. Define $D(\gamma)$ (resp. $U(\gamma)$) to be the number of intersections of γ with L_1 where $\pi_{xz}(\gamma)$ (oriented by $[0,1]$) goes from the upper (resp. lower) sheet to the the lower (resp. upper) sheet of the pair of cusping sheets. Let $\mu(\gamma) := D(\gamma) - U(\gamma)$. Define the **Maslov number** of L, $\mu(L)$, to be the minimum non-negative integer value achieved by $\mu(\gamma)$ over all loops $\gamma \in C^\infty(S^1, L)$.

Denote the connected components of L as $L = \bigsqcup_{i=1}^{\ell} L^i$, and choose base points $p_i \in L^i$. Given a Reeb chord $c \in R(L)$, let $c \cap L = \{c^+, c^-\}$ where c^+ has the greater z-coordinate of the two. Supposing that $c^+ \in L^i$ and $c^- \in L^j$, we choose generic **base point paths** $\gamma_c^\pm \in C^\infty([0,1], L)$, such that $\gamma_c^\pm(0) = c^\pm$, $\gamma_c^+(1) = p_i$, and $\gamma_c^-(1) = p_j$, and let $\gamma_c = \gamma_c^+ \cup -\gamma_c^-$ which is a single oriented path from c^+ to c^- when $i = j$ and a disjoint union of oriented paths when $i \neq j$. Define the **grading** of c, $|c| \in \mathbb{Z}$ by

$$|c| = \mu(\gamma_c) + \mathrm{Ind}(c, F_i - F_j) - 1 \tag{1}$$

where F_i and F_j are local defining functions for the sheets containing c^+ and c^- respectively, and $\mathrm{Ind}(c, F_i - F_j)$ denotes the Morse index of c as a critical point of $F_i - F_j$.

We extend the grading of Reeb chords to a grading of $\mathcal{A}_{LCH}$ as a direct sum of $\mathbb{Z}/2$-modules, $\mathcal{A}_{LCH} = \oplus_{k \in \mathbb{Z}} \mathcal{A}_k$, by requiring that for a homology class $A \in H_1(L)$, $e^A \in \mathbb{Z}/2[H_1(L)]$ has $|e^A| = -\mu(A)$, and that $|x \cdot y| = |x| + |y|$ holds when x and y are homogeneous elements.

Remark 2.1. For Legendrian isotopy invariance of $(\mathcal{A}_{LCH}, \partial)$ in the multiple component case where $\ell \geq 2$, we need to allow for an overall grading change determined by a choice of integers $m = (m_1, \ldots, m_\ell) \in \mathbb{Z}^\ell$. Given m, we obtain an alternate grading of Reeb chords by replacing each $|q|$ with $|q| + m_j - m_i$ when q has lower endpoint on L^j and upper endpoint on L^i.

Alternatively, a grading of Reeb chords by $\mathbb{Z}/m(L)$ may be defined without reference to base point paths as follows. Fix a choice of **Maslov potential**, i.e. a locally constant function $\mu : L_0 \to \mathbb{Z}/m(L)$

whose value increases by 1 when passing from the lower sheet to the upper sheet at cusp edges. Then,

$$|c| = \mu(c^+) - \mu(c^-) + \mathrm{Ind}(c, F_i - F_j) - 1 \qquad (\mathrm{mod}\ m(L)). \tag{2}$$

Note that when Λ is connected, the grading is independent of the choice of Maslov potential and is the reduction of the grading from (1) mod $m(L)$. In the multi-component case, gradings resulting from different Maslov potentials are related to one another and to the grading from (1) as in Remark 2.1.

2.1.3. *The LCH differential.* For any non-negative integer n, let D_{n+1} be the space of closed unit disks in $\mathbb{C}$ centered on the origin, with punctures $p_0, \dots, p_n$ removed from the boundary in counter-clockwise order such that $p_0 = 1$, $p_1 = i$, $p_2 = -1$ (if p_1, p_2 exist). Let $\mathcal{J}$ be the set of ω-tame almost complex structures $\mathcal{J} := \{J \in \mathrm{End}(TT^*M) \mid J^2 = -Id, \omega(Jv, v) \geq 0\}$, with equality holding if and only if $v = 0$. As a technical condition, we also need to assume for $J \in \mathcal{J}$ there exists some neighborhood of the double points in $\pi_{xy}(L)$ where J looks like the standard complex structure of $\mathbb{C}^2$ [8, page 3305]. Let $J \in \mathcal{J}$ and let i denote the complex structure on any $\Delta \in D_{n+1}$ inherited from $\mathbb{C}$. Fix $a, b_1, \dots, b_n \in R(L)$ with base point paths $\gamma_a^{\pm}, \gamma_{b_1}^{\pm}, \dots, \gamma_{b_n}^{\pm}$. Fix an element $A \in H_1(L)$. For $n \geq 0$, let $\mathcal{M}(a; b_1, \dots b_n; A)$ be the moduli space of equivalence class of pairs (u, Δ) such that the following hold.

- The pair is comprised of $\Delta \in D_{n+1}$ and $u : (\Delta, \partial\Delta) \to (T^*M, \pi_{xy}(L))$.
- The image under u of a sequence of points $\{z_n\} \subset \Delta$ converging to the puncture p_0 (resp. p_j) converges to the double point $\pi_{xy}(a)$ (resp. $\pi_{xy}(b_j)$). Moreover, the image of $u(\partial\Delta)$ near p_0 (resp. p_j) in the positive (resp. negative) oriented boundary direction runs from the branch (of the two branches that intersect at the double point $\pi_{xy}(a)$ (resp. $\pi_{xy}(b_j)$)) of $\pi_{xy}(L)$ with the lower z-coordinate lift in L to the branch with the higher z-coordinate lift.
- Combining the continuous lift of $u(\partial\Delta \backslash \{p_0, p_1, \dots, p_n\})$ in L with the base point paths $-\gamma_a^+ \cup \gamma_a^-$ and $\gamma_{b_i}^+ \cup -\gamma_{b_i}^-$ produces a representative for $A \in H_1(L)$.
- The map u restricted to the interior of Δ is J-holomorphic, $J \circ du = du \circ i$.
- Two pairs (u, Δ) and (u', Δ') are equivalent if there exists a biholomorphic map ψ of the unit disk taking the punctures of Δ to those of Δ' such that $u = u' \circ \phi$.

Define the **formal dimension** of the moduli space $\mathcal{M}(a; b_1, \dots b_n; A)$ to be

$$\mathrm{fdim}\mathcal{M}(a; b_1, \dots b_n; A) = |a| - \sum_{j=1}^{n} |b_j| + \mu(A) - 1.$$

For any $a, b_1, \dots b_n, A$ such that $\mathrm{fdim}\mathcal{M}(a; b_1, \dots b_n; A) \leq 1$, there exists an open dense subset $\mathcal{J}_{reg} \subset \mathcal{J}$ such that $\mathcal{M}(a; b_1, \dots b_n; A)$ is a manifold, compact in the sense of Gromov (see [6], for example) whose dimension equals its formal dimension [8]. So for $J \in \mathcal{J}_{reg}$, $\mathcal{M}(a; b_1, \dots b_n; A)$ is a finite set of points when $\mathrm{fdim}\mathcal{M}(a; b_1, \dots b_n; A) = 0$, cf. [6, 8].

We can now define the differential $\partial : \mathcal{A}_{LCH} \to \mathcal{A}_{LCH}$. For Reeb chords $a \in R(L)$, set

$$\partial a = \sum_{|e^A b_1 \cdots b_n| = |a| - 1} \sharp\mathcal{M}(a; b_1, \dots, b_n; A) e^A b_1 \cdots b_n,$$

and then extend ∂ to all of $\mathcal{A}_{LCH}$ with the ($\mathbb{Z}/2[H_1(L)]$-linear) Leibniz rule. Here $\sharp\mathcal{M}(a; b_1, \dots, b_n; A)$ is a $\mathbb{Z}/2$-count. If $n = 0$, then the empty word is $b_1 \cdots b_n = 1$.

Theorem 2.2 ([6, 8])**.** *The differential has degree -1 and satisfies $\partial^2 = 0$. Moreover, if L and L' are Legendrian isotopic, then for any $J \in \mathcal{J}_{reg}(L)$, $J' \in \mathcal{J}_{reg}(L')$ and any choice of base point paths, the DGAs $(\mathcal{A}_{LCH}, \partial) = (\mathcal{A}_{LCH}(L), \partial(L, J))$ and $(\mathcal{A}'_{LCH}, \partial') = (\mathcal{A}_{LCH}(L'), \partial(L', J'))$ are stable tame isomorphic (after possibly applying a grading change as in Remark 2.1).*

In particular, the homology $H_*(\mathcal{A}_{LCH}, \partial)$, called the **Legendrian contact homology**, is a well-defined Legendrian isotopy invariant.

2.2. **Gradient flow trees.** In [4], Ekholm showed that the count of homolorphic disks appearing in the definition of LCH may be replaced with a count of suitable gradient flow trees (abbrv. GFTs). This is a significant extension of earlier results of Floer [12] and Fukaya-Oh [13] that relate holomorphic strips and disks to gradient trajectories and flow trees in the case of graphical Legendrians. In this article, we only consider GFTs with a single positive puncture. This allows a definition of GFT that

appears somewhat different from the general definition given in [4], but more closely parallels the presentation of flow trees from [13]. See Remark 2.5.

We consider **rooted trees**, i.e. trees with a finite number of edges and with a chosen 1-valent **initial vertex**, v_0. (For those familiar with [4], we recast 2-valent initial vertices as discussed later in Remark 2.8.) We orient the edges of a rooted tree so that all edges are oriented away from v_0. Note that any other vertex $v \neq v_0$ has precisely one incoming edge that is oriented towards v while any other adjacent edges are oriented away from v. Vertices with valence 1 (resp. valence greater than 1) are called **external** (resp. **internal**). Sometimes, we refer to v_0 as the **input** vertex, and to the remaining external vertices as **output** vertices. Edges with both endpoints at internal vertices are **internal**, while edges with at least one endpoint at an external vertex are **external**.

A **metric tree** with 1 input is a rooted tree Γ equipped with the following additional structure:

(1) Each edge e is assigned a length $l(e) \in (0, +\infty]$ such that (i) all internal edges have finite length, and (ii) the initial edge that starts at v_0 has length $+\infty$.
(2) At each internal vertex an ordering of the outgoing edges is chosen.

To each edge, e, of a metric tree, we assign an interval $[c, d] \subset [-\infty, +\infty]$ according to:

- The initial edge beginning at v_0 has $[c, d] = [-\infty, 0]$ unless it is the only edge of Γ in which case $[c, d] = [-\infty, +\infty]$.
- All other edges, e, have $[c, d] = [0, l(e)]$.

Fix a Riemannian metric g on S.

Definition 2.3. A **gradient flow tree** (abbrv. **GFT**) of L (with respect to the metric g) is a metric tree Γ together with for each edge e a continuous map

$$\gamma : [c, d] \to S$$

together with a pair of 1-jet lifts

$$\gamma^+ : [c, d] \to L \quad \text{and} \quad \gamma^- : [c, d] \to L, \quad \pi_x \circ \gamma^{\pm} = \gamma$$

satisfying:

(1) For all, $t \in (c, d)$, $z(\gamma^+(t)) > z(\gamma^-(t))$.
(2) For all $t \in (c, d)$, $\gamma'(t) = -\nabla(f^+ - f^-)(\gamma(t))$ where f^+ and f^- are local defining functions for L at $\gamma^+(t)$ and $\gamma^-(t)$, respectively.
(3) If e is an internal edge, then γ is non-constant.
(4) At each internal vertex, v, write the edges adjacent to v as $e_0, e_1, \ldots, e_r$, $r \geq 1$, where e_0 is the unique edge oriented into v and $e_1, \ldots, e_r$ are the outgoing edges at v appearing according to their order. Notate corresponding edge maps as $\gamma_i : [c_i, d_i] \to S$, $0 \leq i \leq r$. We require that the 1-jet lifts $\gamma_i^{\pm}$ fit together continuously at v as follows
$$\gamma_0^+(d_0) = \gamma_1^+(c_1); \quad \gamma_i^-(c_i) = \gamma_{i+1}^+(c_{i+1}) \text{ for } 1 \leq i \leq r-1; \quad \gamma_r^-(c_r) = \gamma_0^-(d_0).$$
(See Figure 2.)
(5) The initial edge, e, that begins at v_0, satisfies $\lim_{t \to -\infty} \gamma(t) = a$ where the Reeb chord a is a critical point of $f_+ - f_-$.
(6) An external vertex at the end of an edge e, we either have
   (a) $l(e) = +\infty$ and $\lim_{t \to +\infty} \gamma(t) = b$ where the Reeb chord b is a critical point of $f_+ - f_-$, or
   (b) the images $\gamma^+(b) = \gamma^-(b)$ agree and belong to a cusp edge of L.

A **partial flow tree** (abbrv. **PFT**) is a rooted tree Γ satisfying all of the properties of a GFT except that the initial edge starting at v_0 is parametrized with $[c, d]$ where $-\infty < c < 0$, and no requirement is placed on the image at c other than $z(\gamma^+(c)) > z(\gamma^-(c))$. In particular, this input edge is no longer required to begin at a Reeb chord.

We introduce some additional terminology associated with a GFT or PFT Γ. When the input vertex v_0 begins at the Reeb chord a we say that the vertex v_0 is a **positive puncture** at a. When an output vertex v limits to a Reeb chord b as $t \to +\infty$, we say that v is a **negative puncture** at b. We refer to output vertices that end at a point on the cusp edge of L as **e-vertices**.

Often, we will provide a labeling of the sheets of L above some subset $U \subset S$ as $S_1, \ldots, S_n$, and denote the corresponding local defining functions by $F_1, \ldots, F_n$. (We emphasize that such an enumerations

of sheets of L only makes sense locally.) Typically, we shorten notation for the local **difference functions** to

$$F_{i,j} := F_i - F_j.$$

When the 1-jet lifts, γ^+ and γ^-, of an edge e of a GFT or PFT have their images in S_i and S_j respectively, we say that S_i (resp. S_j) is the **upper sheet** (resp. **lower sheet**) of e. Note that in this case γ is a trajectory for $-\nabla F_{i,j}$, and we say that γ is an (i,j)**-flow line**.

Observation 2.4. (i) For any point x belonging to the interior of one of the edges of a GFT or PFT Γ, there is a unique PFT whose initial vertex is x that consists of the portion of Γ that lies below x (with respect to the orientation of edges of the domain tree of Γ). Usually, we refer to this PFT as simply **the PFT starting with** x.

(ii) External edges may be mapped to Reeb chords as constant maps. In fact this must be the case for GFTs that have a positive (resp. negative) puncture at a Reeb chord that is a local minimum (resp. maximum) of $f^+ - f^-$.

(iii) The sheet difference $z(\gamma^+(t)) - z(\gamma^-(t))$ decreases not only along every non-constant edge (as a standard consequence of the negative gradient flow equation), but also when passing internal vertices (from the incoming edge to an outgoing edge). Thus, if x and y are any points in the domain of a PFT Γ with x above y (with respect to the orientation of edges of Γ), then the sheet difference at x is larger than at y.

Remark 2.5. (i.) Our definition of PFT is much more restrictive than in [4], where more than one exceptional vertex is allowed.

(ii.) In [4], the definition of GFT does not allow constant external edges (mapped to Reeb chords). However, [4] does allow punctures to occur at internal vertices, as we explicitly do not. The equivalence of these conventions is easily seen: A constant edge may be replaced with a puncture at an internal vertex in a unique way and the converse statement holds also.

(iii.) The condition $z(\gamma^+) > z(\gamma^-)$ is not included in the definition of GFT from Ekholm. Indeed, this condition may fail for GFTs with more than one positive puncture. However, Lemma 2.8 from [3], establishes this condition for GFTs with 1 positive puncture.

2.2.1. *Words of GFTs and PFTs.* We define the **word**, $w(\Gamma)$, of a PFT or GFT, Γ, using induction on the number of internal vertices. If Γ has no internal vertices then, its domain is a single edge with one output vertex, v. In this case, declare

$$w(\Gamma) = \begin{cases} b, & \text{if } v \text{ has a negative puncture at } b \\ 1, & \text{if } v \text{ is an } e\text{-vertex.} \end{cases}$$

Now, supposing $w(\Gamma)$ has been defined for PFTs with fewer internal vertices, we consider the first internal vertex, v, of Γ. Let the outgoing edges at v be ordered as $e_1, \dots, e_r$, for some $r \geq 1$. Let $\Gamma_1, \dots, \Gamma_r$ denote the PFTs of Γ that begin at interior points of the edges $e_1, \dots, e_r$ respectively, and define

$$w(\Gamma) = w(\Gamma_1) \cdots w(\Gamma_r).$$

An alternate formulation of $w(\Gamma)$ is as follows: The ordering of outgoing edges at internal vertices, allows us to embed the domain tree of Γ into D^2 by requiring that the outgoing edges $e_1, \dots, e_r$ at an internal vertex v appear in counterclockwise order when we travel around v starting at the incoming edge. Moreover, we can arrange the external vertices to sit on ∂D^2, and their cyclic ordering is well defined. We then take the product of all negative punctures, $b_1, \dots, b_n$, as they appear in counterclockwise order around ∂D^2, starting at v_0. That is,

$$w(\Gamma) = b_1 \cdots b_n.$$

Yet another perspective on $w(\gamma)$ is the following: The union of the Lagrangian projections of the one jet lifts γ^+ and $-\gamma^-$ (the negative indicates orientation reverse) of all edges of Γ fit together to give a continuous closed curve, C, with image in $\pi_{xy}(L)$. We call C the **boundary curve** of Γ. See Figure 2. When instead considered as a curve on L, C has discontinuities that are in bijection with the positive and negative punctures of Γ. (The z-coordinate increases (resp. decreases) when passing a positive (resp. negative) puncture.) From this perspective, $w(\Gamma)$ is the product of negative punctures as they appear along the curve C, when starting with the upper lift γ^+ of the initial edge of Γ.

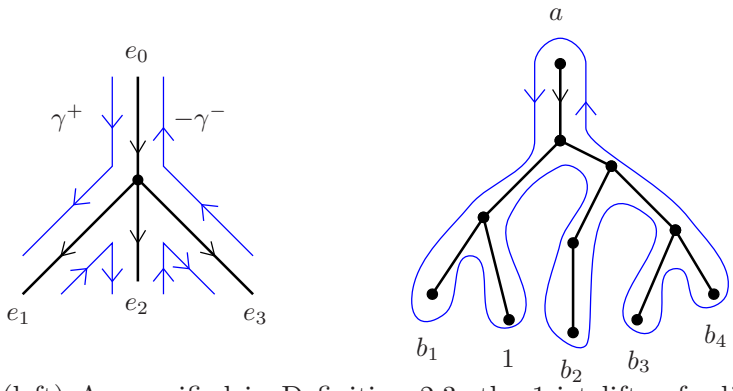

FIGURE 2. (left) As specified in Definition 2.3, the 1-jet lifts of adjacent edges fit together continuously at internal vertices. (right) A GFT with $w(\Gamma) = b_1b_2b_3b_4$. All edges of Γ are oriented downward, and the output vertex labelled with a 1 is an e-vertex. The 1-jet lifts fit together as indicated to form a continuous closed curve, C, on $\pi_{xy}(L)$.

When Γ is a GFT with positive puncture at a and $w(\Gamma) = b_1 \cdots b_n$, we say that Γ is a GFT **from** a **to** $b_1, \dots, b_n$.

2.3. **GFTs and Holomorphic Disks.** The connection between GFTs and Legendrian contact homology is the following.

In Section 3 of [4], Ekholm associates a **formal dimension** to a GFT, Γ, from a to $b_1, \dots, b_n$ written, $fdim(\Gamma)$. It is equal to the formal dimension of the moduli space of holomorphic disks $\mathcal{M}(a; b_1, \dots, b_n; [\widehat{C}])$, where $\widehat{C}$ is the lift of the boundary curve of Γ to L (this is discontinuous at punctures) together with the base point paths $-\gamma_a^+ \cup \gamma_a^-$ and $\gamma_{b_i}^+ \cup -\gamma_{b_i}^-$. The pair consisting of the Legendrian and metric (L, g) is **1-regular** when (i) there are no GFTs with $fdim(\Gamma) < 0$, (ii) all trees with $fdim(\Gamma) = 0$ are transversally cut out (i.e. they are obtained via iterated transverse intersection of certain suitably defined ascending and descending manifolds), and (iii) the set of trees with $fdim(\Gamma) = 0$ is finite. (The "1" in 1-regular refers to the number of positive punctures.) When (L, g) is 1-regular, GFTs with formal dimension 0 are called **rigid**.

It is shown in [4, Theorem 1.1 (a)] that any (L, g) can be made 1-regular after a C^∞-small perturbation. For the Legendrians that we consider we will use a mild strengthening of this statement; see Proposition 12.2.

Theorem 2.6 ([4], Theorem 1.1)**.** *Suppose that (L, g) is 1-regular. There exists a Legendrian $\widehat{L} \subset J^1S$ such that*

1. *$\widehat{L}$ is Legendrian isotopic to L, and has its Reeb chords canonically identified with those of L, and*
2. *there exists $J \in \mathcal{J}_{reg}$ for $\widehat{L}$ such that when $fdim(\mathcal{M}(a; b_1, \dots, b_n; A)) = 0$, disks in $\mathcal{M}(a; b_1, \dots, b_n; A)$ for $\widehat{L}$ are in bijection with the set of (equivalence classes of) rigid GFTs for L from a to $b_1, \dots, b_n$ whose boundary curves satisfy $[\widehat{C}] = A$.*

In particular, the differential in the LCH DGA of L may be computed by

$$\partial a = \sum_{\Gamma} [\widehat{C}] \cdot w(\Gamma)$$

where the sum is over all rigid GFTs for L that begin at a.

2.4. **Generic behavior at vertices.** In Section 3 of [4], it is shown that when (L, g) is 1-regular the internal vertices that appear in rigid GFTs are limited to the following types:

- A Y_0**-vertex**, v, is a 3-valent vertex with image in S disjoint from the cusp locus of L. At v, there exist sheets S_i, S_m, S_j with defining functions satisfying $F_i(v) > F_m(v) > F_j(v)$, such that the incoming edge e_0 at v is an (i, j)-flow line while the outgoing edges e_1 and e_2 are respectively (i, m)- and (m, j)-flow lines.
- A Y_1**-vertex**, v, is a 3-valent vertex with image at a point of S belonging to the cusp locus of L such that the sheets corresponding to edges adjacent to v are as follows. Near v there are sheets S_i, S_k, S_{k+1}, S_j of L such that sheets S_k and S_{k+1} meet at a cusp edge so that S_k has

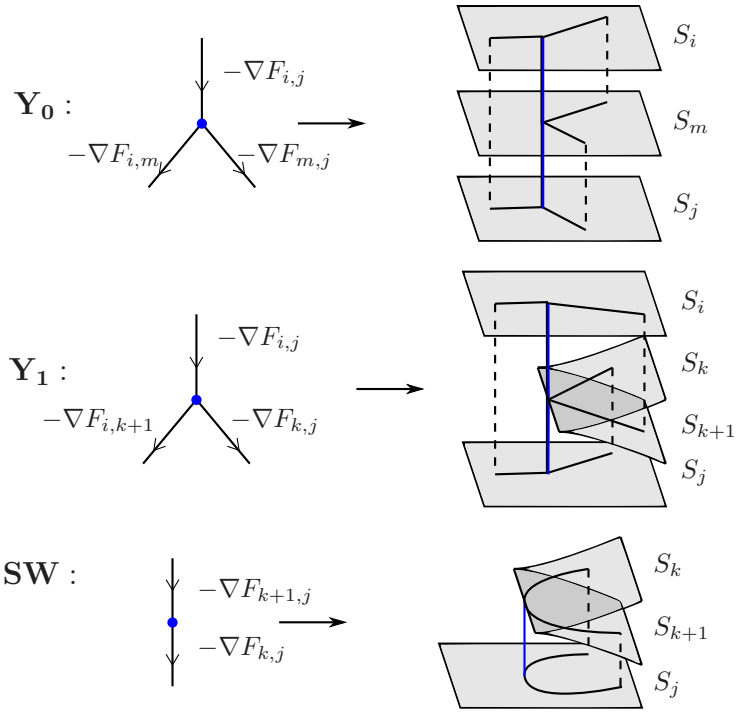

FIGURE 3. The generic internal vertices pictured via their domain trees and 1-jet lifts.

larger z-coordinate than S_{k+1}; S_i sits above the cusp edge; and S_j sits below the cusp edge. The incoming edge e_0 is an (i,j)-flow line while the out going edges e_1 and e_2 are respectively $(i,k+1)$- and (k,j)-flow lines. In addition, $-\nabla F_{i,j}, -\nabla F_{i,k+1}$ and $-\nabla F_{k,j}$ are all transverse to the cusp locus of L at v, and necessarilly point to the side of the cusp locus where S_k and S_{k+1} exist.

- A *sw*-**vertex** (also called a **switch vertex**), v, is a 2-valent vertex with image at the base projection of a cusp edge where sheets S_k and S_{k+1} meet with S_k the upper sheet of the cusp edge. In addition, one of the following holds:
  - (i) The incoming (resp. outgoing) edge at v is an (i,k)-flow line (resp. an $(i,k+1)$-flow line) for some sheet S_i that sits above the cusp edge at v. Note that $-\nabla F_{i,k} = -\nabla F_{i,k+1}$ must be tangent to the cusp locus at v.
  - (ii) The incoming (resp. outgoing) edge at v is a $(k+1,j)$-flow line (resp. a (k,j)-flow line) for some sheet S_j that sits below the cusp edge. Note that $-\nabla F_{k,j} = -\nabla F_{k+1,j}$ is tangent to the cusp locus at v.

See Figure 3.

We use the terminology **switch point** for a point along the projection of a cusp edge between sheets S_k and S_{k+1} where a third sheet S_i or S_j as in (i) or (ii) has $-\nabla F_{i,k}$ or $-\nabla F_{k,j}$ tangent to the projection of the cusp edge. A switch point is **non-degenerate** when the tangency of the restriction of the corresponding $-\nabla F_{i,k}$ or $-\nabla F_{k,j}$ to the cusp locus has order 1. Of course, switch vertices can only have their images at switch points.

Theorem 2.7 ([4])**.** *Assume (L,g) is 1-regular. Then, all internal vertices of rigid GFTs must be either Y_0-, Y_1-, or sw-vertices. (External vertices may be punctures or e-vertices.)*

Proof. In Section 3 of [4], GFTs are assigned a geometric dimension, $gdim(\Gamma)$. [4, Proposition 3.14] shows that when Γ is transversally cut out, a space of nearby GFTs with similar geometric properties, eg. homeomorphic domain trees with corresponding branches having the same upper and lower sheet in L, is a manifold of dimension $gdim(\Gamma)$. In particular, a transversally cut out tree has $gdim(\Gamma) \geq 0$. Moreover, [4, Lemma 3.7] shows that in general $gdim(\Gamma) \leq fdim(\Gamma)$, so that a rigid tree must have $gdim(\Gamma) = fdim(\Gamma) = 0$. Possible vertices of trees with $gdim(\Gamma) = fdim(\Gamma)$ are listed in [4, Lemma 3.7]. □

Remark 2.8. In [4, Lemma 3.7], 2-valent vertices with a positive (resp. negative) puncture at a local minimum (resp. local maximum) are also listed as possible internal vertices. However, with our conventions for GFTs, such punctures become Y_0's with an adjacent external edge mapped to a constant trajectory at the corresponding critical point. See Remark 2.5 (ii).

Moreover, for GFTs with these generic vertices, formal dimension may be computed from the count of vertices of various types and the Morse index of punctures.

Proposition 2.9. *Suppose that (L, g) is 1-regular. Let Γ is a rigid GFT with a postive puncture at a and negative punctures at $b_1, \dots, b_m$. Let E, Y_1, and SW denote the number of $e-$, Y_1-, and sw-vertices of Γ respectively, and $Ind(a)$ and $Ind(b_i)$ denote the Morse indices of a and b_i as critical points of local difference functions $F_i - F_j$ with $F_i > F_j$. Then, we have*

$$2 - Ind(a) = \sum_{i=1}^{m} (1 - Ind(b_i)) + E - Y_1 - SW. \tag{3}$$

Proof. The first formula for the formal dimension, $fdim(\Gamma)$, from [4, Definition 3.4] reads

$$\dim(\Gamma) = (n-3) + \sum_{p \in P(\Gamma)} (I(p) - (n-1)) - \sum_{q \in Q(\Gamma)} (I(q) - 1) + \sum_{r \in R(\Gamma)} \mu(r).$$

Comparing the notation there with ours, $\dim(\Gamma) = fdim(\Gamma) = 0$, $n = 2$, $\sum_{p \in P(\Gamma)}(I(p) - (n-1)) = \mathrm{Ind}(a) - 1$, $\sum_{q \in Q(\Gamma)}(I(q) - 1) = \sum_{i=1}^{m}(\mathrm{Ind}(b_i) - 1)$ and $\sum_{r \in R(\Gamma)} \mu(r) = E - Y_1 - SW$. The equation (3) follows. □

3. Transverse Square Decompositions

Let $L \subset J^1 S$ be a Legendrian with generic front projection and base projection, and let Σ denote the singular set (cusps, crossings and swallowtails) of the front projection of L. In this section, we construct a cell decomposition of S into squares. The 1-skeleton will be transverse to $\pi_x(\Sigma)$, so we will denote the decomposition as $\mathcal{E}_{\pitchfork}$. Above each square of $\mathcal{E}_{\pitchfork}$, Σ is required to match one of a finite collection of standard forms that are introduced in Section 3.2 below, and a few additional technical requirements are imposed on $\mathcal{E}_{\pitchfork}$ for later use. In addition, we construct a related cellular decomposition $\mathcal{E}_{||}$ that will be used in Section 8 when working with the Cellular DGA.

3.1. Regularity requirements.

We impose some regularity requirements on our square decomposition. In this section we use the notation $I = [-1, 1]$.

For the transverse cell decomposition $\mathcal{E}_{\pitchfork} = \{e^i_\alpha\}$ constructed below, we always require the following conditions. Note that these requirements may be obtained from an arbitrary polygonal decomposition (as in Section 3.1 of [15]) into squares by altering the original characteristic maps first near 0-cells and then in a neighborhood of 1-cells.

(1) We have characteristic maps
$$c^i_\alpha : I^i \xrightarrow{\cong} \overline{e^i_\alpha} \subset S$$
which are homeomorphisms and are smooth with smooth inverse except possibly at the corners of 2-cells. (Compare with requirement (2) below).

(2) Each 0-cell e^0_α has a disk coordinate neighborhood $U \subset S \to D^2$ so that if N distinct 2-cells meet at e^0_α then near the corner each of their characteristic maps rescales the angle. More precisely, for a given 2-cell e^2_β containing e^0_α as a corner, we use polar coordinates on I^2 centered at the corner of I^2 corresponding to e^0_α with the angle coordinate rotated so that $0 \le \theta \le \pi/2$ parametrizes a neighborhood of this corner. We require that the characteristic map for e^2_β takes $\{0 \le r \le 1/8\}$ into $U \cong D^2$ and has the form
$$c(r, \theta) = \left(r, \pm\frac{4}{N}\theta + (m2\pi)/N\right)$$
for $0 \le r \le 1/8$, for some $0 \le m < N$.

(3) Along each 1-cell, the characteristic maps of the 2-adjacent faces may be glued together to give smooth maps $(-\epsilon, \epsilon) \times (-1, 1) \to S$.

3.1.1. *Where do the technical requirements come into play?* In Sections 9-12, we will define a front projection for a Legendrian $\tilde{L}$ that is isotopic (but not literally equal to) the original front projection of L. This is done by providing local defining functions $F_i : I^2 \to \mathbb{R}$ for the sheets of $\tilde{L}$ above each square using coordinates given by the characteristic maps. This explains (1). Near corners each local defining function will have the form $ar^2 + b$ in the polar coordinate system centered at the corner of I^2 as described in (2) with the coefficients a and b agreeing for sheets in distinct squares that meet at the 0-cell. Therefore, the requirements from (2) show that the front will be smooth in a neighborhood of a 0-cell. Moreover, the construction of sheets will be standard near edges as well, so that (3) will guarantee the smoothness of the pieced together front above 1-cells.

In addition, the conditions allow the following:

Construction 3.1. Let $L \subset J^1S$ be a Legendrian with local defining functions given by $ar^2 + b$ in the coordinate neighborhoods of 0-cells prescribed in (2). There exists a metric on S with respect to which the gradients of local defining functions (and hence also local difference functions) agree with the gradients taken in each square with respect to the standard Euclidean metric on I^2.

Proof. The Euclidean metrics on squares piece together to give a metric on the complement of the 0-cells of S. In a D^2 coordinate neighborhood (as in (2)) of a 0-cell adjacent to N faces, the metric appears in polar coordinates as $dr^2 + (\frac{4}{Nr})^2 d\theta^2$. In order to extend smoothly to $r = 0$, we alter the metric inside D^2 to $dr^2 + [(1 - \alpha(r))(\frac{4}{Nr})^2 + \alpha(r)(\frac{1}{r})^2]d\theta^2$ where $\alpha(r)$ is a bump function that is 0 outside values of r where all local defining functions have the form $ar^2 + b$ and is 1 in a neighborhood of 0.

This change to the metric does not alter gradients of functions of the form $f(r, \theta) = g(r)$. □

3.2. **Elementary squares.** In Figure 4, some standard forms for the base projection of the crossing and cusp loci of a Legendrian L to a square $[-1, 1] \times [-1, 1]$ are presented and divided into Types (1)-(14). Note that parametrizations of squares may be orientation reversing (supposing S is oriented, which we do not require in general) so that the images of the cusp and crossing locus in S may appear reflected across $x_1 = x_2$ in some squares.

For some edges of the squares of type (5), (6), (8) or (12), a pair of arcs of the crossing locus intersect a single edge. Along such an edge either the x_1 or x_2-coordinate goes from -1 to 1 while the other coordinate remains fixed. Denote the coordinate that varies by x_i. We require that the two crossings that appear along the restriction of L to that edge arise from a strand with larger z-coordinate at $x_i = -1$ passing through two consecutive strands with lesser z-coordinate at $x_i = -1$ as x_i increases. See the image labelled (2Cr) in Figure 5. Thus, when viewed with this prescribed orientation, above each edge of a square of Type (1)-(14) the singular set L matches 1 of the 4 forms pictured in Figure 5.

We refer to a square in S above which L has one of the types (1)-(14) as an **elementary square** for L.

3.3. **Requirements for the transverse square decomposition $\mathcal{E}_{\pitchfork}$.** We will want to construct a transverse square decomposition $\mathcal{E}_{\pitchfork}$ for L together with a choice of orientation for each of the 1-cells of $\mathcal{E}_{\pitchfork}$ so that a list of conditions (A1)-(A4) is satisfied. We state (A1)-(A3) now, and postpone (A4) until 3.4.

(A1) All 2-cells are elementary squares for L parametrized so that all orientations of 1-cells are from the lower left corner to upper right corner.

(A2) For any 0-cell, e^0_α, and pair of sheets S_i, S_j above e^0_α consider the set of 1-cells,

$$T(e^0_\alpha, S_i, S_j) = \{e^1_\beta \,|\, e^0_\alpha \text{ is the initial vertex of } e^1_\beta; \text{ and } S_i \text{ and } S_j \text{ intersect above } e^1_\beta\}.$$

The cardinality of $T(e^0_\alpha, S_i, S_j)$ satisfies

$$|T(e^0_\alpha, S_i, S_j)| \leq 2,$$

and if $|T(e^0_\alpha, S_i, S_j)| = 2$ then the two 1-cells in $T(e^0_\alpha, S_i, S_j)$ form the bottom and left edge of a single Type (3) square that has e^0_α as its lower left vertex.

(A3) No two Type (3) squares share a common boundary edge or vertex.

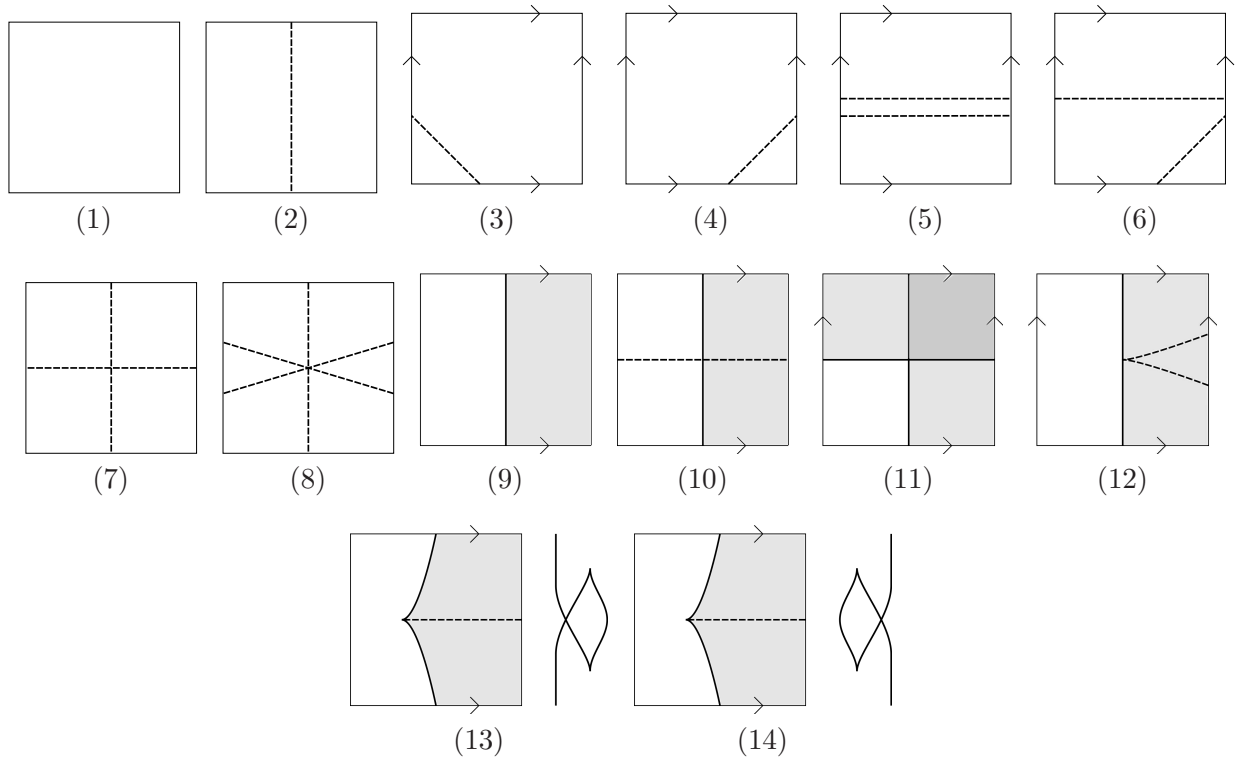

FIGURE 4. Allowed base projections of the cusp and crossing locus for elementary squares. Solid lines denote cusp edges and dotted lines denote intersection of sheets. The side of the cusp locus where the cusp sheets lie is shaded. Codimension 2 phenomena appear in (7), (8) and (10)-(14). In (7), (10), and (11) the two crossing and/or cusp lines involve 4 distinct sheets. The squares (9), (12), and (13)-(14) are base projections of a triple point, a sheet crossing a cusp edge, and the upward and downward swallow tails respectively.

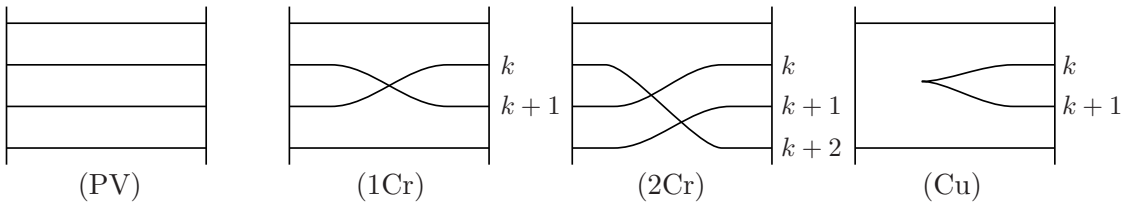

FIGURE 5. The four possibilities for the singular set of L above edges of elementary squares, pictured in the front projection: (PV) Plain vanilla, i.e. no crossings or cusps; (1Cr) 1 Crossing; (2Cr) 2 Crossings; and (Cu) a single left cusp. The left and right vertical lines denote the endpoints of the edge where $x_i = -1$ and $x_i = +1$ respectively for either $i = 1$ or 2. There may be many additional strands that are disjoint from those pictured and do not have any crossings or cusps. Note that in the (2Cr) square if strands are numbered from top to bottom as they appear at $x_i = +1$, crossings occur first between the $k + 2$ and k strands and then between the $k + 2$ and $k + 1$ strands.

3.4. **Shifting $\pi_x(\Sigma)$ into the 1-skeleton.** In order to later make contact with the cellular DGA, we will want to be able to associate an L-compatible cell decomposition to $\mathcal{E}_{\pitchfork}$ which we will denote $\mathcal{E}_{\parallel}$. (Recall from [15] that a polygonal decomposition is L-compatible if its 1-skeleton contains the projection of the singular set of L.) The remaining condition (A4) is designed to ensure that such a procedure is successful.

To begin, we shift the base projection of the singular set, denoted $\pi_x(\Sigma)$, into the 1-skeleton of $\mathcal{E}_{\pitchfork}$. This is done one square at a time. Except in the case of squares of type (12)-(14), the intersection of an arc of the cusp or crossing locus with a given elementary square has its endpoints in the interiors

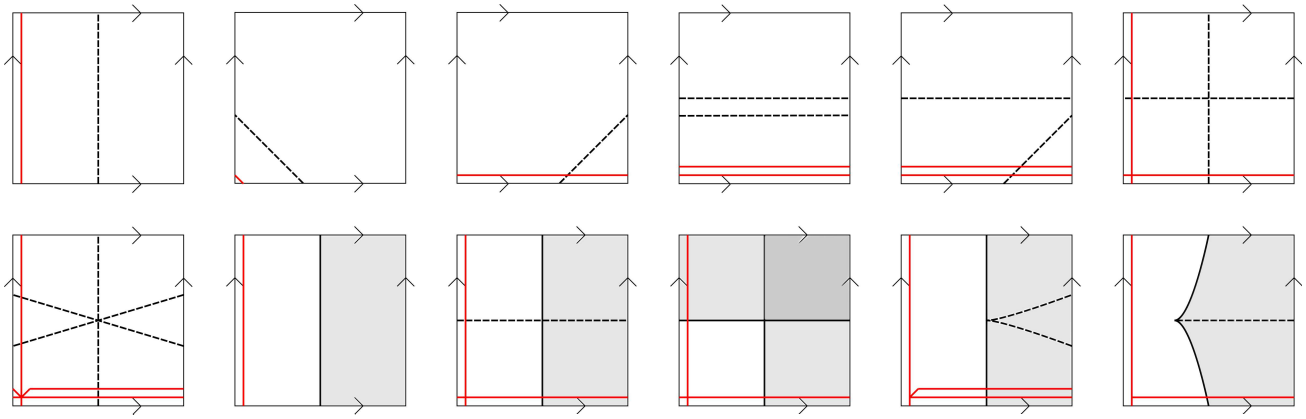

FIGURE 6. Homotoping the singular set into the 1-skeleton. Red lines are drawn next to the edge or vertex that an arc of $\pi_x(\Sigma)$ is moved to.

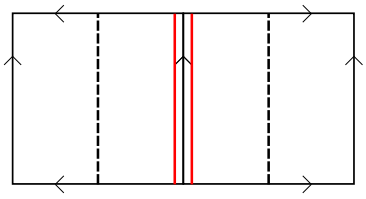

FIGURE 7. An example where crossing arcs from distinct squares are shifted to the same 1-cell so that (A4) fails.

of some 1-cells at the boundary of the square. We move these endpoints so that they sit at the initial vertex (with respect to the orientation) of the given 1-cell. This specifies a unique edge of the square that we shift the arc into, or in the case of a square of type (3) the arc is shifted into a single vertex. For Type (12)-(14) cells, we place the codimension 2 point in the lower left corner of the square and then proceed as above. See Figure 6.

As the relocation of endpoints is determined by the orientation of the 1-cells, this shifting of segments pieces together to give a global homotopy of $\pi_x(\Sigma)$ into the 1-skeleton of $\mathcal{E}_{\pitchfork}$. In general, this homotopy cannot be realized by an isotopy of S since for elementary squares of type (5), (6), (8), and (12) two distinct arcs are homotoped to the same edge of a square. Also, it is possible that a closed component of the crossing locus only intersects squares of type (3) and hence is collapsed to a point. We can now state the remaining requirement (A4).

(A4) In the above homotopy, no closed component of $\pi_x(\Sigma)$ is shrunk to a point, and the only distinct arcs that are placed on the same edge are those arising from squares of type (5), (6), (8), and (12) as described above.

For instance, we do not allow two squares of type (2) to be located next to one another with the orientation of horizontal borders pointing away from a shared vertical edge. See Figure 7.

3.5. **Construction of $\mathcal{E}_{\pitchfork}$.** After constructing $\mathcal{E}_{\pitchfork}$ we construct the associated L-compatible decomposition $\mathcal{E}_{\|}$ in 3.6 below.

Proposition 3.2. *For any $L \subset J^1S$ with generic front and base projection, we can find a transverse square decomposition $\mathcal{E}_{\pitchfork}$ of a neighborhood of S satisfying (A1)-(A4).*

Proof. Let $A, B \subset S$ denote the (base projection of the) cusp and crossing locus respectively. Generically, they have the following form.

The cusp locus, A, is a union of transversely intersecting and self-intersecting closed curves which are immersed except for cusp points at the projections of swallow tail points. The crossing locus, B, is a union of closed curves and arcs with endpoints at swallow tails. The crossing locus has cusp points at some points of $A \cap B$ where a sheet crosses a cusp edge as in Figure 4 (12). In addition, there are a finite number of transverse double points between parts of the crossing locus and itself as well as

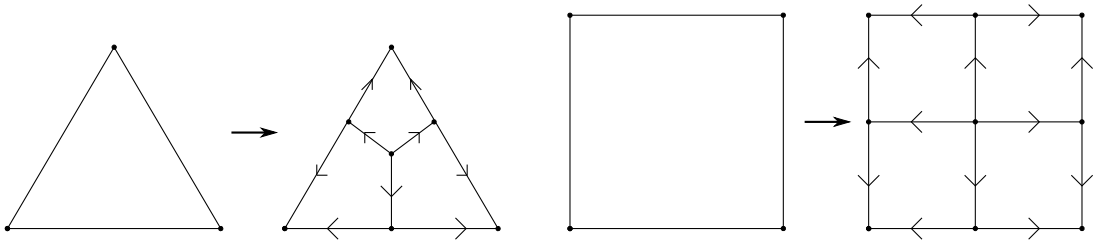

FIGURE 8. Subdividing triangles and squares. Orientations for edges are pictured after the subdivision.

transverse double points between crossing and cusp curves. Finally, there are a finite number of triple points of B, as in Figure 4 (8), that correspond to an intersection of 3 sheets of L.

We will construct the required decomposition of S into squares in the following steps:

1. At the codimension 2 parts of $A \cup B$.
2. In a neighborhood of A.
3. In a neighborhood of $A \cup B$.
4. The rest of S.
5. Subdivide the result, and assign orientations to edges.

Step 1. Begin with squares around all codimension 2 singularities, with various edges intersecting arcs of A and B as perscribed in Figure 4 (7)-(8) and (10)-(14).

Step 2. Next, square the remaining portion of a regular neighborhood $N(A)$ of the cusp locus so that boundaries of individual squares have two opposite boundary edges perpendicular to A and the other two opposite edges on $\partial N(A)$. (We choose the neighborhood $N(A)$ so that this is also the case for the squares surrounding codimension 2 points except for the case of a transverse intersection of two cusp edges for which only the vertices of the square lie on the boundary of $N(A)$.) If necessary, add extra edges perpendicular to A to ensure that no two codim 2 squares share a common edge.

Step 3. Now we extend the squaring to a neighborhood of $A \cup B$. Of the squares containing codimension 2 front singularities there are two types with edges having two intersections with the crossing locus; see Figure 4 (8) and (12). Begin by placing an adjacent square next to each of these edges with the boundary edges chosen so that the crossing locus appears as in the first half of Figures 9 and 10 below. (These new squares are as in Figure 1 (6).) Now, the remainder of B should be a union of arcs with boundaries on edges that contain just one intersection with B. Use a single Type (2) square for the neighborhoods of each of these arcs. (Note that we do require that between any two codimension 2 points of the crossing locus there is one square of type (2).)

Step 4. We now have squares in a neighborhood of $A \cup B$, $N(A \cup B)$. The complement of the interior of this neighborhood, $T = S \setminus Int(N(A \cup B))$, is a surface with boundary with a triangulation of the boundary already constructed. We can extend this triangulation of ∂T to a triangulation of all of T (into triangles not squares). To see that this is possible, first, triangulate T up to a collar neighborhood of the boundary. Then, observe that a triangulation of the boundary of an annulus (which we now have along the boundary of each component of this collar) can always be extended to a triangulation of the annulus.

Step 5. Now, we subdivide our current polygonal decomposition into squares and orient the corresponding edges. Subdivide the triangles in T into 3 squares by dividing each edge in half and adding edges from the midpoints of edges to a new vertex in the center of the triangle. Orient the edges of these squares so that they point away from the center of the triangle. This is indicated in Figure 8. Subdivide each of the squares in $N(A \cup B) - N(A)$ into 4 smaller squares by cutting the square into quarters. Again, orient all edges to point away from the center of the original square; see Figure 8. Finally, cut squares in $N(A)$ in half along the direction that is perpendicular to the cusp edge with the exception of those squares that contain double points of A which we do not subdivide at all. Orient the edges that are perpendicular to the cusp edge so that they point from the side of the cusp locus with fewer sheets to the side with more sheets. Orient the remaining edges away from the newly added edge in the middle of the original squares.

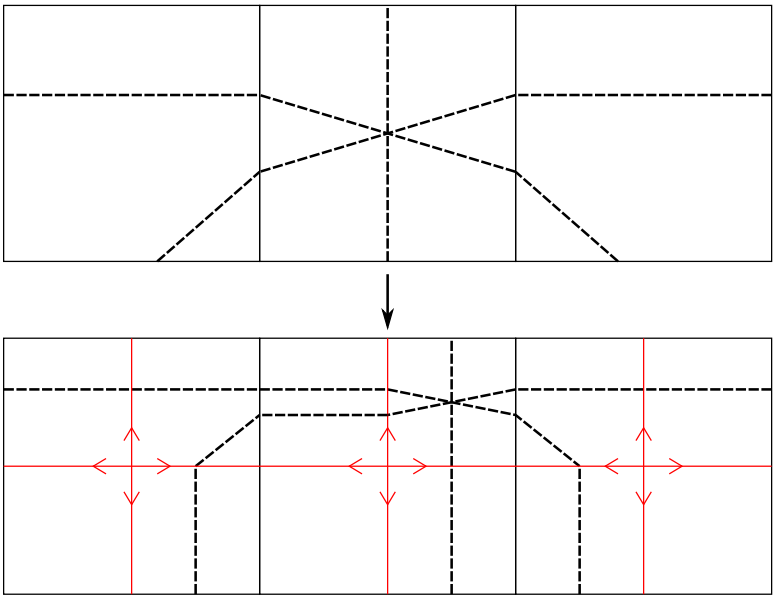

FIGURE 9. Subdivision near a triple point.

Each edge of the original decomposition is shared by two squares, so it is important to note that the subdivision and orientation prescribed for these edges is the same with respect to either face. This is the case since all edges are subdivided in half except for edges that intersect the cusp locus; the orientation of the two subdivided pieces is always away from the new vertex. Also, note that all squares have opposite edges oriented in the same direction.

Finally, one should take some care in subdividing squares that intersect the crossing locus, B, so that the subdivided pieces all fit one of the forms specified in Figure 4. This is particularly important at squares of the form (8) and (12) which contain triple points and sheets intersecting the cusp edge. We subdivide these squares and their adjacent squares as pictured in Figure 9 and 10 respectively. The edges that intersect the crossing locus twice can be made to have the form indicated in Figure 5 (2Cr) by the following considerations. For squares of type (8), choose the identification of the given square (before subdivision) with the pictured one so that the vertical sides have this property when oriented from lower to upper corners. For squares of type (12), exactly one of the subdivisions pictured in Figure 10 has the desired property, and this is the subdivision that we use.

Note that our subdivisions prescribe particular halves of the original edges that the crossing arc should leave these squares along. This extra restriction can be met, since in our original decomposition we required one square containing a single arc of type (2) between any two codimension 2 portions of B. The subdivision of such a square can be chosen so that the crossing arc will leave along any perscribed halves of the bottom and top edges, and so that the subdivision uses only squares of type (2), (3), and (4). See Figure 11.

With the construction complete, we verify that (A1)-(A4) holds. Property (A1) is clear from the construction, keeping in mind that in our figures the singular set in the image of an elementary square may appear in a manner that differs from the depiction in Figure 4 by reflected across $x_1 = x_2$. Property (A2) is seen to hold by considering the appearance of the crossing locus in relation to the orientations of squares after Step 5. is completed. (In particular, examine Figures 9, 10, and 11.)

For (A3), note that Type (3) squares only appear when some of the Type (12) and Type (2) squares are subdivided during Step 5. (See the Figures 10 and 11.) Examining the placement of squares after the subdivision shows that no two Type (3) squares share an edge or vertex.

To verify (A4), first check that the condition holds near codimension 2 points (examine Figures 9 and 10). Before the subdivision, all remaining squares that intersect $A \cup B$ have type (2) or (9) and are bordered on the right and left by squares of type (1). After the subdivision and resulting orientation of 1-cells, the crossing arc for a subdivided Type (2) square will be homotoped to the center two 1-cells of the four squares arising from the subdivision. The cusp arcs for subdivided Type (9) squares are homotoped to the left sides of these squares (which are bordered by squares of type (1)).

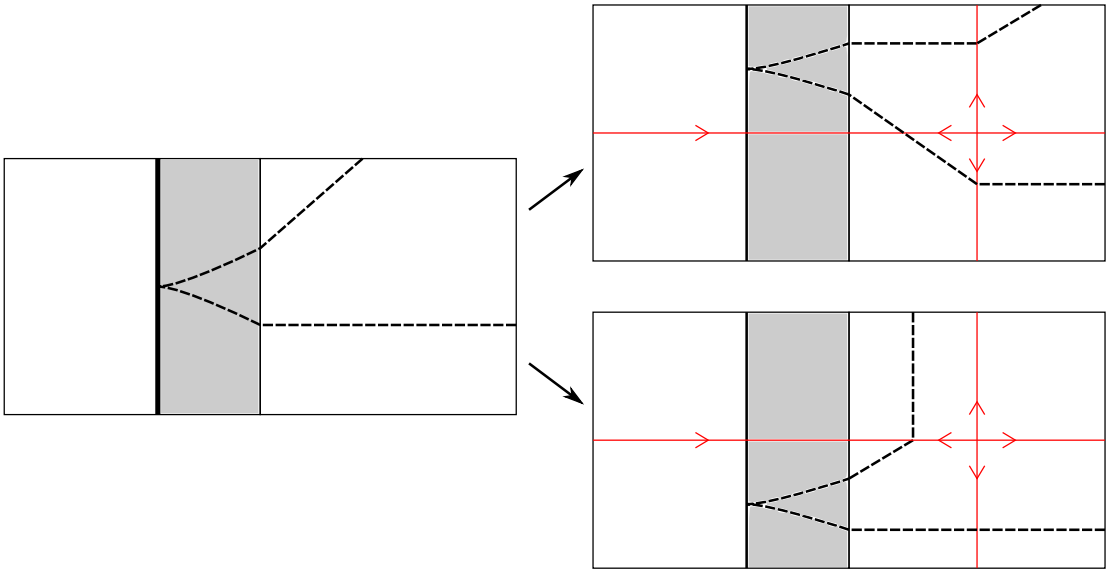

FIGURE 10. Subdivision near a sheet intersecting a cusp edge. Note that the left square contains a cusp edge, so it is only subdivided into two smaller squares. Of the two subdivisions pictured, we use the one that results in the edge with two crossings matching the form given in Figure 5 (2Cr). (This way, only one version of (12) is necessary.)

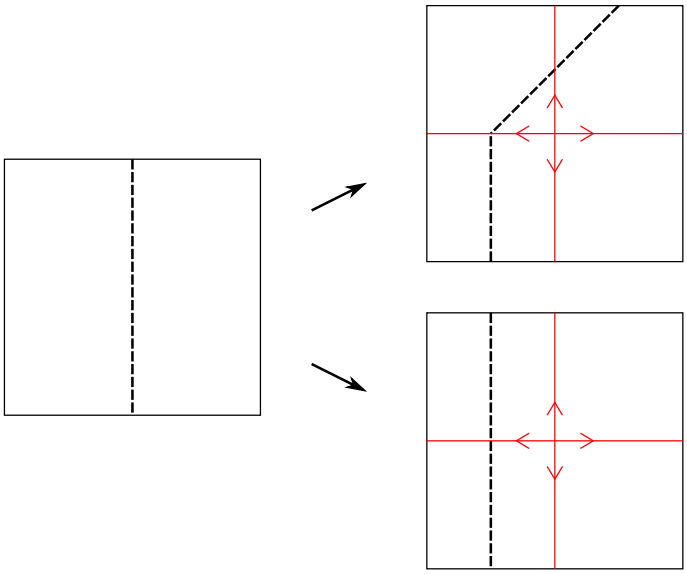

FIGURE 11. Subdividing a Type (2) square. Using one of the pictured subdivisions or their reflections across a vertical axis, we arrange for the crossing arc to intersect any perscribed halves of the boundary.

□

Remark 3.3. As constructed, some squares of $\mathcal{E}_{\pitchfork}$ may be disjoint from $\pi_x(L)$. These squares can be safely ignored so that we view $\mathcal{E}_{\pitchfork}$ as a square decomposition of a neighborhood of $\pi_x(L)$.

3.6. **Construction of $\mathcal{E}_{\|}$.** From this construction of $\mathcal{E}_{\pitchfork}$ we can now produce a related L-compatible polygonal decomposition of $\pi_x(L) \subset S$ denoted $\mathcal{E}_{\|}$. As in 3.4, we have a map of $\pi_x(\Sigma)$ into the 1-skeleton of $\mathcal{E}_{\pitchfork}$ that is not realized by an isotopy of S only because in squares of type (5), (6), (8) and (12) two crossing arcs are mapped to the same edge. Note that all apperances of these squares in $\mathcal{E}_{\|}$ are as specified in Figures 9 and 10). To arrive at the decomposition $\mathcal{E}_{\|}$ we simply seperate these edges by placing new 2-cells and 1-cells between them in an appropriate manner. See Figures 12 and 13.

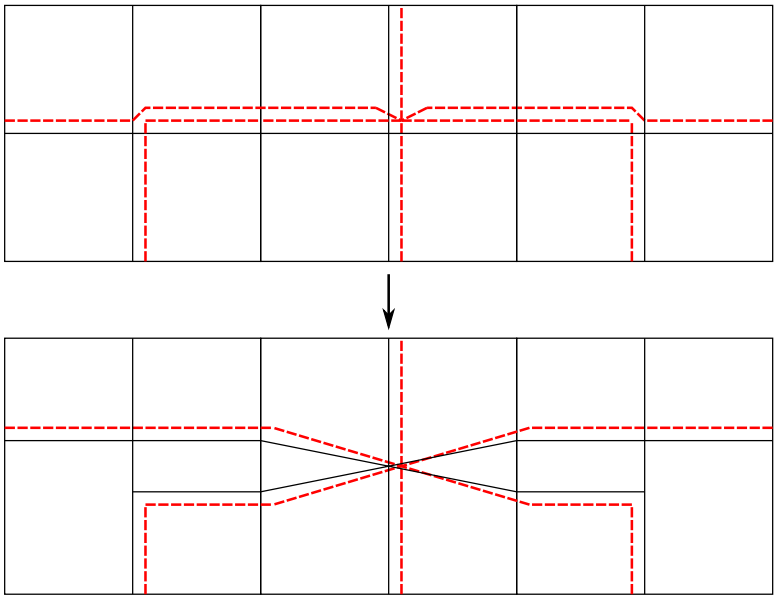

FIGURE 12. (Top) The result of shifting $\pi_x(\Sigma)$ into the 1-skeleton of $\mathcal{E}_{\pitchfork}$ is pictured near a Type (8) square. (Bottom) We obtain $\mathcal{E}_{\|}$ by subdividing squares of type (5),(6),(8) and (12) and seperating the crossing arcs that previously belonged to the same 1-cells. The dotted red lines represent the crossing locus, and are intended to coincide with parts of the 1-skeleton (black).

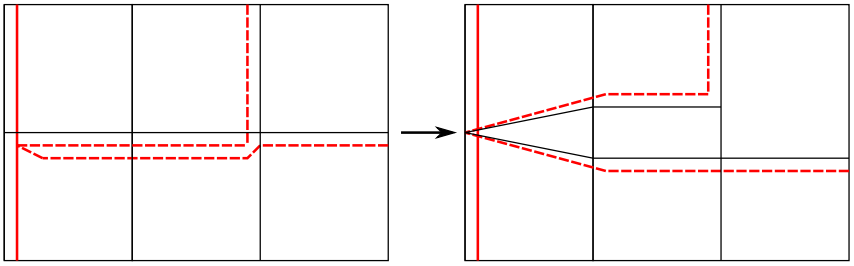

FIGURE 13. Shifting $\pi_x(\Sigma)$ into the 1-skeleton and forming $\mathcal{E}_{\|}$ near a Type (12) square. The solid red line is the cusp locus while the dotted red lines represent the crossing locus. Both are intended to coincide with parts of the 1-skeleton (black).

More precisely, the relationship between the cells of $\mathcal{E}_{\pitchfork}$ and $\mathcal{E}_{\|}$ is the following:

Proposition 3.4. *The L-compatible polygonal decomposition $\mathcal{E}_{\|}$ is obtained by applying a homeomorphism to the cell decomposition $\mathcal{E}_{\pitchfork}$ and then making the following subdivisions:*

- *The cell decompositions of closed squares of type (5), (8), and (12) from $\mathcal{E}_{\pitchfork}$ are subdivided by placing an extra 0-cell in the interior of the edge of the square that corresponds to the right edge in Figure 4 and then connecting this new 0-cell to the lower left corner of the square with a new 1-cell.*
- *The cell decompositions of closed squares of type (6) are subdivided by placing an extra 0-cell on both the left and right edges and then connecting these new 0-cells with a new 1-cell.*

4. Blueprint for enumeration of GFTs

The next step of the proof is to perform a (partial) computation of the LCH DGA above each square of the decomposition $\mathcal{E}_{\pitchfork}$ using a Legendrian isotopic surface, $\tilde{L}$, for which the Reeb chords near any particular square form sub-DGAs. This is carried out in Sections 5-7. To compute the LCH differential using Theorem 2.6, we will need to enumerate relevant rigid GFTs for each of the 14 square types. To help prepare the reader for the general enumeration procedure, in this section we outline a computation for the Type (1) square using a simplified model for $\tilde{L}$. This should serve as a blue print for the unified

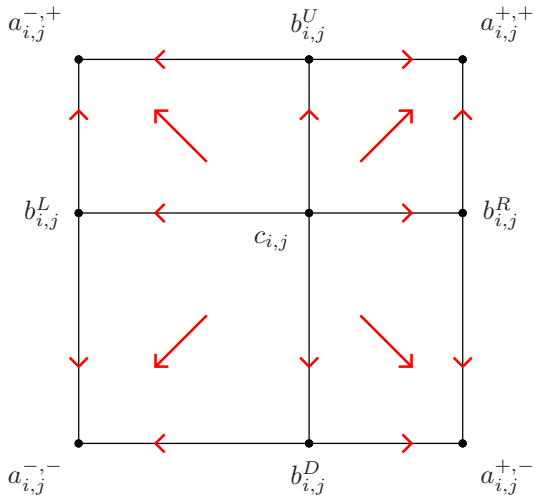

FIGURE 14. Location of the critical points of $F_{i,j}$. Red arrows indicate the sign of the components of $-\nabla F_{i,j}$.

approach used for square types (1)-(12). (The (13) and (14) squares which have swallowtail points require an additional argument.) We then explain some of the challenges that are later addressed in extending this approach to other square types.

Section 4 is intended as a guide for the proof of Theorem 1.1. The remainder of the article is independent of Section 4, both logically and in exposition.

4.1. **Type (1) square as an example.** We consider a square, in coordinates $[-1,1]\times[-1,1]$, above which L consists of n non-intersecting sheets without cusp edges. (This is a Type (1) square in Figure 4.) Above the square, the front projection of L appears as a subset of $[-1,1]\times[-1,1]\times\mathbb{R}$ that consists of the union of the graphs of n functions $F_1,\dots,F_n : [-1,1]\times[-1,1]\to\mathbb{R}$, which we label to satisfy $F_1 > \dots > F_n$. We take F_i of the form

$$F_i(x_1,x_2) = f_i(x_1) + f_i(x_2)$$

where $f_i : [-1,1]\to\mathbb{R}$ are 1-dimensional functions designed so that for any $1\le i<j\le n$, the difference function $f_i - f_j$ has local minima at -1 and 1 and a single local maximum $\beta_{i,j}\in(-1,1)$. Moreover, we can arrange that the locations of the local maxima are lexicographically ordered in i and j,

$$\beta_{1,2} < \beta_{1,3} < \dots < \beta_{2,3} < \beta_{2,4} < \dots < \beta_{n-1,n}.$$

(Figure 67, below illustrates how this ordering of critical points may be arranged.) The Reeb chords in $[-1,1]\times[-1,1]$, are critical points of difference functions $F_{i,j} := F_i - F_j$ with $i<j$, and for each $F_{i,j}$ we have 9 critical points

$$a^{\pm,\pm}_{i,j}, b^{U}_{i,j}, b^{R}_{i,j}, b^{D}_{i,j}, b^{L}_{i,j}, c_{i,j}, \qquad 1\le i<j\le n$$

located as pictured in Figure 14. Critical points labeled with a's, b's, and c's are respectively local minima, saddle points, and local maxima. The horizontal and vertical segments connecting the $b^X_{i,j}$ to $c_{i,j}$ are flow lines for $-\nabla F_{i,j}$ that divide the square into four closed (i,j)**-quadrants**. We call the upper right and the lower left of these quadrants the 1-st and 3-rd (i,j)-quadrant.

We now compute the differential $\partial c_{i,j}$ (with $\mathbb{Z}/2$ coefficients) which counts rigid GFTs begining at $c_{i,j}$. Due to the absence of cusp edges, internal vertices can only be Y_0-vertices. (We assume the 1-regular condition is satisfied with respect to the Euclidean metric on $[-1,1]\times[-1,1]$.) Thus, by Proposition 2.9, a GFT beginning at $c_{i,j}$ is rigid if and only if the number of outputs at local minima, $a^{\pm,\pm}_{k,l}$, is the same as the number of outputs at local maxima, $c_{k,l}$. For each, $X\in\{U,L,R,D\}$, the single edge tree that is the $-\nabla F_{i,j}$ flow line from $c_{i,j}$ to $b^X_{i,j}$ is rigid, and 4 other families of rigid GFTs are pictured in Figure 15. We will show that these are the only rigid GFTs, so that

$$\partial c_{i,j} = b^U_{i,j} + b^L_{i,j} + b^R_{i,j} + b^D_{i,j} + \sum_{i<m<j}\left(a^{+,+}_{i,m}c_{m,j} + c_{i,m}a^{-,-}_{m,j} + b^U_{i,m}b^L_{m,j} + b^R_{i,m}b^D_{m,j}\right)$$

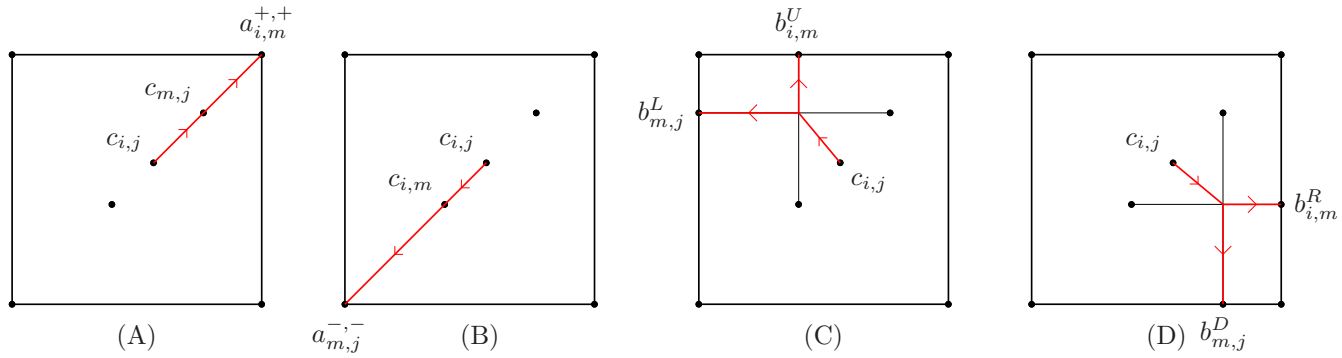

FIGURE 15. For each $i < m < j$ there are 4 rigid GFTs with a single Y_0-vertex, and two outputs. Note that edges that precede outputs at c's are constant.

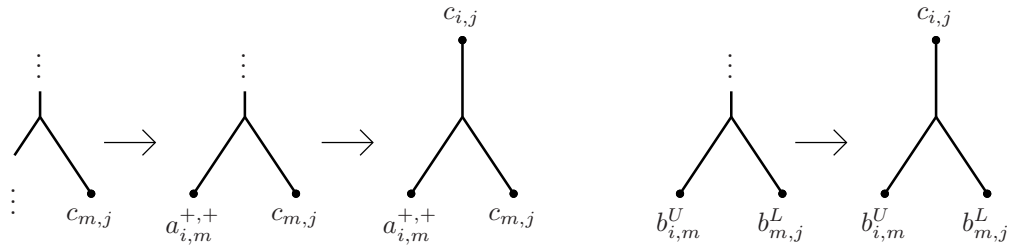

FIGURE 16. Pictorial summary of the arguments in Case 1 and Case 2.

Putting $C = (c_{i,j})$, $B_U = (b^U_{i,j})$, etc., (with 0's for entries when the corresponding Reeb chord does not exist), we get the matrix equation

$$\partial C = A_{+,+}C + CA_{-,-} + (I + B_U)(I + B_L) + (I + B_R)(I + B_D) \tag{4}$$

which is identical to the differential of the cellular DGA for a square without crossings or cusps above its boundary.

Proof that there are no other rigid GFTs beginning at c's. The steps of the proof are summarized in Figure 16. We will use the following:

Lemma 4.1 (1st and 3rd Quadrant Lemma)**.** *Suppose that an edge $\gamma \subset \Gamma$ on a GFT is a $-\nabla F_{i,j}$ flow line.*

1. *If γ has a point that is mapped to the 1-st (j,l)-quadrant for some $i < j < l$. Then, all outputs on the part of Γ below γ are at $a^{+,+}$ critical points.*
2. *If γ has a point that is mapped to the 3-rd (h,i)-quadrant for some $h < i < j$. Then, all outputs on the part of Γ below γ are at $a^{-,-}$ critical points.*

Proof. We prove (1) as (2) is similar. Any edge of Γ below γ (with respect to the orientation of the domain tree of Γ) must be an (i',j')-flow line (i.e. a trajectory for $-\nabla F_{i',j'}$) for some $i \leq i' < j' \leq j$. For all such (i',j'), the 1-st (j,l)-quadrant is contained in the 1-st (i',j')-quadrant where $-\nabla F_{i',j'}$ has both components positive. Thus, all edges below γ must remain entirely within the 1-st (j,l)-quadrant. Moreover, since the only critical points of the $F_{i',j'}$ in the 1-st (j,l)-quadrant are the $a^{+,+}_{i',j'}$, (1) follows. □

With Lemma 4.1 in hand, let Γ be a rigid GFT beginning at some c Reeb chord.

Case 1: Γ has at least one output at a c.

The only way that a $c_{m,l}$ can occur as an output of a GFT is when a Y_0-vertex has its image at $c_{m,l}$ with one of the outgoing edges the constant (m,l)-flow line. Supposing the other outgoing edge is an (i,m)-flow line (resp. an (l,j)-flow line), (using the lexicographical ordering of the $c_{i,j}$ along the diagonal) the 1-st and 3-rd quadrant lemma shows that all outputs that occur below this edge can only be at $a^{+,+}$'s (resp. $a^{-,-}$'s). Since the number of outputs at c's and a's must agree, we see that:

(i) At a Y_0 with one outgoing edge having an output at a c, the other outgoing edge must proceed directly to an a without branching.
(ii) Moreover, any edge with an output at an a must begin with such a Y_0-vertex at a c-vertex.

So far, we know Γ has a Y_0-vertex x where one of the outgoing edges is a constant map limiting to a c. Suppose that the incoming edge at x is an (i,j)-flow line. We consider the case where for some $i<m<j$ the constant outgoing edge of x is at $c_{m,j}$, so that (i) implies the other outgoing edge limits to a puncture at some $a_{i,m}^{+,+}$. We show that the incoming edge α at x must begin at a positive puncture at $c_{i,j}$, so that Γ is as in (A) of Figure 15. (In the case where the outgoing edges have punctures at $c_{i,m}$ and $a_{m,j}^{-,-}$ a similar argument will show that Γ is as in (B) of Figure 15.)

Suppose that this is not the case, so that α begins at another Y_0 vertex, y. As t increases, α traces out some part of the $-\nabla F_{i,j}$ trajectory from $c_{i,j}$ to $c_{m,j}$, so the image of α is entirely contained in the intersection of the 1-st (i,j)-quadrant and the 3-rd (m,j)-quadrant.

- Subcase: The other outgoing edge at y is a (j,l)-flow line for some $j<l$. Then, since y is in the 3-rd (m,j)-quadrant, Lemma 4.1 (2) applies to contradict (ii).
- Subcase: The other outgoing edge at y is a (h,i)-flow line for some $h<i$. Then, since y is in the 1-st (i,j)-quadrant, Lemma 4.1 (1) applies to contradict (ii).

Case 2: Γ does not have any outputs at c's.

Since the number of outputs at a's and c's is equal, Γ has all outputs at b's. The rigid GFTs with only one edge (these are simply gradient trajectories of $-\nabla F_{i,j}$) are as specified. Assuming more than one edge, we can find a "lower most" Y_0 vertex, x, where for some $i<j$, an (i,j)-flow line branches into two edges that limit to critical points of the form $b_{i,m}^X$ and $b_{m,j}^Y$. For this to occur, x must have its image at the intersection of flow lines from $c_{i,m}$ and $c_{m,j}$ to $b_{i,m}^X$ and $b_{m,j}^Y$, and since these flow lines are horizontal or vertical line segments, we see that either $(X,Y)=(U,L)$ or $(X,Y)=(R,D)$. We show that the incoming edge α at x must begin at a positive puncture at $c_{i,j}$, so that Γ is as in (C) or (D) of Figure 15.

Suppose that instead α begins at a Y_0 vertex, y. Since α is a portion of the (i,j)-flow line from $c_{i,j}$ to the image of x, the image of α is entirely contained in the intersection of the 1-st (i,m)-quadrant and the 3-rd (m,j)-quadrant. Then, arguing as in the sub-cases above, considering the other outgoing edge at y and applying Lemma 4.1 contradicts (ii).

□

4.2. **Issues with extending the argument to other square types.** The biggest difficulty with extending the argument to remaining squares of type (1)-(12) is that for squares with crossing arcs additional Reeb chords are present. As an example, consider the Type (2) square where a crossing between sheets k and $k+1$ runs vertically through the center of the square. To the left of the crossing locus, an additional local maximum $\tilde{c}_{k+1,k}$ appears and two new saddle points $\tilde{b}_{k+1,k}^U$ and $\tilde{b}_{k+1,k}^D$ appear along the edges U and D. (We order the subscripts, so that the first subscript indicates the upper endpoint of the Reeb chord.) The new Reeb chords can appear as outputs in GFTs beginning at some $c_{i,j}$ that do not have the form identified in Figure 15. For instance, $\partial c_{i,j}$ may have terms of the form $c_{i,k+1}\tilde{b}_{k+1,k}^U a_{k,j}^{-,-}$; see Figure 17.

To avoid having to identify these additional trees, we instead observe the (more easily derived) formulas

$$\partial\tilde{c}_{k+1,k}=\tilde{b}_{k+1,k}^U+\tilde{b}_{k+1,k}^D+b_{k+1,k}^L;\quad \partial\tilde{b}_{k+1,k}^U=a_{k+1,k}^{-,+};\quad \partial\tilde{b}_{k+1,k}^D=a_{k+1,k}^{-,-}.$$

Then, (using [15, Theorem 2.1]) the quotient of the DGA by the ideal generated by the *exceptional generators* $\tilde{c}_{k+1,k},\tilde{b}_{k+1,k}^U,\tilde{b}_{k+1,k}^D,b_{k+1,k}^L,a_{k+1,k}^{-,+},a_{k+1,k}^{-,-}$ is stable tame isomorphic to the original DGA. In this quotient, terms in the differential arising from the new GFTs with endpoints at exceptional generators all become 0, so that the formula (4) remains valid with the caveat that the matrices $A_{-,+},B_L$ and $A_{-,-}$ have the $(k,k+1)$-entry equal to 0. This is precisely the form of the part of the cellular DGA associated to the corresponding square of $\mathcal{E}_{||}$ (where the crossing arc now sits directly above the left edge of the square). In Section 8, we carry out a similar quotient procedure for all squares, with care taken when canceling a or b Reeb chords that appear in the boundary of more than one 2-cell. (This is the reason that the technical requirements (A2)-(A4) were imposed on the square decomposition $\mathcal{E}_{\Cap}$.)

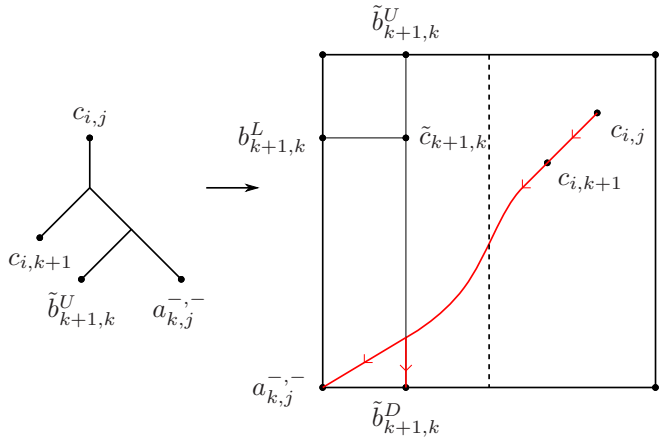

FIGURE 17. A rigid GFT in a Type (2) square giving $\partial c_{i,j} = c_{i,k+1}\tilde{b}^U_{k+1,k}a^{-,-}_{k,j} + \cdots$.

We mention briefly some of the other adjustments to the above argument that appear in Sections 5-7.

(1) The construction of $\tilde{L}$ needs to allow for a perturbation to obtain the 1-regular condition; see Section 12 for details. As a result, in Sections 9-12 the location of Reeb chords is only specified up to ϵ, and the behavior of individual flow lines is not as precisely known. Typically, to restrict the locations of flow lines we require that $-\nabla F_{i,j}$ points transversally to particular curves in $[-1,1]\times[-1,1]$, as such conditions are preserved by perturbation.
(2) No major changes are required for the 1-st Quadrant Lemma. However, extra care is required in the 3-rd Quadrant Lemma, for instance to allow the possibility that GFTs terminate at an e-vertex along a cusp edge.
(3) The location of the gradient trajectories connecting the $c_{i,j}$ to surrounding saddle points $b^X_{i,j}$ is no longer precisely known. (The relative location of saddle points $b^X_{i,j}$ and $b^Y_{i,j}$ along edges seperated by a crossing or cusp arc are different, so that, even ignoring the perturbation, we should no longer expect these trajectories to be straight lines.) In identifying rigid GFTs without endpoints at c's we make a more radical departure, and give a topological argument to show that the $\mathbb{Z}/2$-count of such GFTs is independent of the precise location of these flow lines. See Section 6.5. (This added flexibility is also important in the case of (13)-(14) squares.)

5. Computation of LCH, Part 1: 0-cells and 1-cells

In this section, we replace L with the Legendrian isotopic surface $\tilde{L}$. We then establish in Corollary 5.6 that the Reeb chords of $\tilde{L}$ located in a suitable neighborhood of any given cell of $\mathcal{E}_{\pitchfork}$ generate a sub-algebra that is preserved by the LCH differential. In Propositions 5.9 and 5.10, we compute the sub-DGAs associated to 0-cells and 1-cells.

5.1. **The Legendrian $\tilde{L}$.** Recall from Section 3 that we have found a cell decomposition, $\mathcal{E}_{\pitchfork}$, of a neighborhood of $\pi_x(L)\subset S$ into squares so that the projection of the crossing and cusp locus of L to each square matches (up to isotopy) one of 14 model squares. Moreover, the closed squares are parametrized by $[-1,1]^2$, and (except possibly at the corners) the parametrizations provide smooth local coordinates on S that we notate as (x_1,x_2). Coordinates of neighboring squares fit together at 1-cells and 0-cells as specified in Section 3.

Theorem 5.1. *Let $\mathcal{E}_{\pitchfork}$ be a transverse square decomposition for the front generic Legendrian $L\subset J^1(S)$. Then, there exists a Legendrian $\tilde{L}\subset J^1(S)$ and a Riemannian metric g on S such that:*

- *Above each of the squares of $\mathcal{E}_{\pitchfork}$, the singular sets of L and $\tilde{L}$ have the same topological form, i.e. they match the same square type with the same sheets meeting at crossing and cusp arcs and swallowtail points. In particular, $\tilde{L}$ and L are Legendrian isotopic.*
- *The Legendrian and metric pair $(\tilde{L},g)$ is 1-regular.*
- *In the local coordinates given by $\mathcal{E}_{\pitchfork}$, the local defining functions of $\tilde{L}$ and their gradients with respect to g satisfy Properties 1-19 as stated below.*

The proof of Theorem 5.1 will be given in Sections 9-12. The Properties 1-7 of Theorem 5.1 are stated in the current section; Properties 8-13 appear in Section 6; and Properties 14-19 which concern the form of $\tilde{L}$ above the swallow tail squares (13) and (14) are stated in Section 7.

Notation 5.2. We denote the LCH DGA of $\tilde{L}$ with coefficients in $\mathbb{Z}/2$ (specialize all homology classes in $\mathbb{Z}/2[H_1(\tilde{L})]$ to 1) and grading reduced modulo $m(L)$ by $(\mathcal{A}_{LCH}, \partial)$.

From Theorem 2.6, the differential of $(\mathcal{A}_{LCH}, \partial)$ can be computed by summing over rigid GFTs of $\tilde{L}$. This DGA is computed up to stable tame isomorphism over the course of Sections 6-8 with the end result stated in Proposition 8.6 below.

Notation 5.3. We use the notation $\nabla F = (\delta_{x_1} F, \delta_{x_2} F)$ for the components of the gradient of a function F with respect to the metric g from Theorem 5.1.

5.1.1. *Cusp locus, crossing locus.* As stated in Theorem 5.1, the projection of the singular set of $\tilde{L}$ to each square of $\mathcal{E}_{\pitchfork}$ matches one of the square types (1)-(14) up to an ambient isotopy of $[-1,1]\times[-1,1]$. The following property provides a stronger restriction on the location of the cusp and crossing locus.

Property 1 (The square models)**.** All crossing loci are contained in the region $\{-1/4 < x_1 < 1/4\} \cup \{-1/4 < x_2 < 1/4\}$. All cusp loci are straight lines in $\{x_1 = -3/8\}$ or $\{x_2 = -3/8\}$, except possibly in disks of radii 3/32 containing the swallowtail points.

5.2. **Invariant neighborhoods of 0-cells and 1-cells and the sub-DGAs $\mathcal{A}_{LCH}(e^d_\alpha)$.** Recall from Section 3.1 that each 0-cell, e^0_α, has a disk neighborhood consisting of the union of balls of radius 1/16 (with respect to the euclidean metric used in the domain of parametrization $[-1,1]^2$) centered at all corners of 2-cells where e^α_0 appears. Denote this neighborhood as $N(e^0_\alpha)$, and note that requirement (2) of Section 3.1 shows that $\partial N(e^0_\alpha)$ is a smooth circle in S.

Property 2 (0-cells)**.** Let e^0_α be a 0-cell. For all local defining functions F_i and F_j with $F_i > F_j$ in $N(e^0_\alpha)$, the gradient $-\nabla F_{i,j}$ points inward along the boundary $\partial N(e^0_\alpha)$.

Property 3 (1-cells)**.** Let e^1_α be a 1-cell with endpoints at the 0-cells e^0_- and e^0_+. Then, e^1_α has a neighborhood $N(e^1_\alpha) \subset S$ with the following features.

(1) We have $N(e^0_-), N(e^0_+) \subset N(e^1_\alpha)$ and the boundary of $N(e^1_\alpha)$ is a piecewise smooth curve consisting of the union of an arc from the boundary of $N(e^0_-)$, an arc from the boundary of $N(e^0_+)$, and two paths P_1 and P_2.
(2) Each of P_l is contained in the interior of a single 2-cell that contains e^1_α as an edge. In $[-1,1]\times[-1,1]$ coordinates, P_l is piecewise linear, contained within a distance of 1/32 from e^1_α, and monotonically increasing in the coordinate, x_i, that is parametrizes e^1_α, and is parallel to e^1_α for $1/2 \leq x_i \leq 3/4$.
(3) For any $(x_1,x_2) \in P_l$ and i,j such that $F_{i,j}(x_1,x_2) > 0$, we have that $-\nabla F_{i,j}(x_1,x_2)$ is transverse to P_l at (x_1,x_2) and points into $N(e^1_\alpha)$. (If (x_1,x_2) is a non-smooth point of P_l, then $-\nabla F_{i,j}(x_1,x_2)$ should be transverse to both segments of P_l that meet at (x_1,x_2).)
(4) Suppose the sheets defined by F_i and F_j cross at $(x_1,x_2) \in P_l$. Then (x_1,x_2) is a non-smooth point of P_l where two line segments of P_l meet. Label these segments Q_1 and Q_2 so that $F_i \geq F_j$ along Q_1 and $F_j \geq F_i$ along Q_2. Then, at (x_1,x_2), $-\nabla F_{i,j}$ (resp. $-\nabla F_{j,i}$) is transverse to Q_1 (resp. Q_2) and points to the side of Q_1 (resp. Q_2) that borders $N(e^1_\alpha)$.

Remark 5.4. The item (4) in Property 3 is included to simplify the proof of Theorem 5.1 and is not needed for computing $(\mathcal{A}_{LCH}, \partial)$.

For any 2-cell, e^2_α, we define a neighborhood $N(e^2_\alpha)$ that is the union of e^2_α and the neighborhoods of its boundary 0- and 1-cells given by Properties 2 and 3. See Figure 18.

The following allows us to localize the computation of LCH to a square-by-square calculation.

Lemma 5.5. *Let N denote any of the neighborhoods $N(e^0_\alpha)$, $N(e^1_\alpha)$ or $N(e^2_\alpha)$. Any (partial or complete) gradient flow tree for $\tilde{L}$ that starts at a point in N must have its entire image contained in N.*

Proof. From Properties 2 and 3, we have that at any point on the boundary of N all negative gradients of positive local difference functions point into N. Therefore, no branch of the tree can ever cross out of N as t increases. □

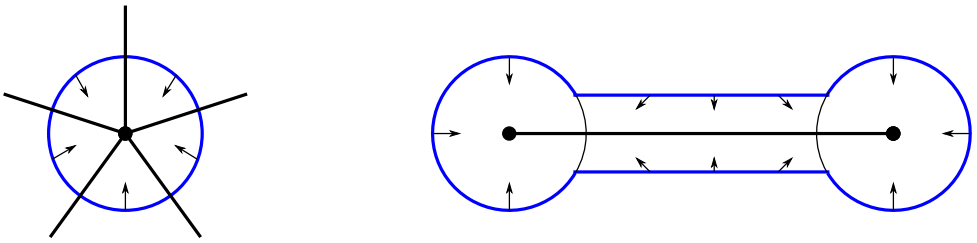

FIGURE 18. Neighborhoods of 0-cells and 1-cells. (left) The neighborhood $N(e^0_\alpha)$ is pictured (boundary in blue) along with the 1-skeleton near e^0_α. (right) The boundary of $N(e^1_\alpha)$ appears in blue with the polygonal paths P_1 and P_2 pictured as horizontal segments. The division of $N(e^1_\alpha)$ into $N(e^0_-)$, $\widehat{N}(e^1_\alpha)$, and $N(e^0_+)$ is indicated by the thin black lines. The arrows indicate the direction of negative gradients $-\nabla F_{i,j}$ with $F_i > F_j$ as specified by Properties 2 and 3.

For any cell e^d_α, $d = 0, 1$, or 2, of $\mathcal{E}_{\Gamma}$, let $\mathcal{A}_{LCH}(e^d_\alpha)$ denote the sub-algebra of $\mathcal{A}_{LCH}$ generated by Reeb chords belonging to $N(e^d_\alpha)$.

Corollary 5.6. *For any cell e^d_α, of $\mathcal{E}_{\Gamma}$, the sub-algebra $\mathcal{A}_{LCH}(e^d_\alpha)$ is a sub-DGA of $(\mathcal{A}_{LCH}, \partial)$.*

Proof. Since the differential of $(\mathcal{A}_{LCH}, \partial)$ may be computed via a count of rigid GFTs of $\tilde{L}$, the corollary follows from Lemma 5.5. □

5.2.1. *Notations for sheets and Reeb chords.* In computing the sub-DGAs $\mathcal{A}_{LCH}(e^d_\alpha)$, we will use a notation for Reeb chords arising from a numbering of the sheets restricted to e^d_α as $S_1, \dots, S_n$. The notation for a Reeb chord uses two subscripts to indicate the endpoints of the Reeb chord by the following:

Convention 5.7. The order of sub-scripts for a Reeb chord $x_{i,j}$ is always chosen so that the first (resp. second) subscript indicates the upper (resp. lower) sheet of the Reeb chord

In general, the enumeration of sheets cannot be carried out in a consistent manner globally, and, as a result, the same Reeb chord may be denoted with different notations in the context of different $\mathcal{A}_{LCH}(e^d_\alpha)$. We pay special attention to this point in Section 8 where we combine our local calculations of the $\mathcal{A}_{LCH}(e^d_\alpha)$ to compute the full DGA $(\mathcal{A}_{LCH}, \partial)$.

Remark 5.8. This issue is parallel to the choice of total orderings of sheets required in defining the differential in the cellular DGA.

5.3. **Computation of $(\mathcal{A}_{LCH}, \partial)$ near the 0-skeleton.** Recall from Section 2.2 that we denote local defining functions for sheets of $\tilde{L}$ labeled $S_1, \dots, S_n$ as $F_1, \dots, F_n$, and that a Reeb chord starting on sheet S_j and ending on sheet S_i (with respect to the Reeb vector field ∂_z) corresponds to a critical point of $F_{i,j} := F_i - F_j$ with positive critical value. Trajectories of $-\nabla F_{i,j}$ are referred to as (i,j)-flow line. The abbreviations GFT and PFT respectively refer to gradient flow trees and partial flow trees of $\tilde{L}$.

Consider a 0-cell, e^0_α. By Property 1, above $N(e^0_\alpha)$, $\tilde{L}$ is a union of non-intersecting sheets that we label $S_1, \dots, S_n$ with (pointwise) decreasing z-coordinate, i.e. $F_1 > F_2 > \dots > F_n$ above $N(e^0_\alpha)$.

Property 4 (Reeb chords above 0-cells)**.** For any pair of sheets, S_i, S_j, above e^0_α with $F_i > F_j$, there is a unique Reeb chord $a_{i,j}$ in $N(e^0_\alpha)$. Each $a_{i,j}$ is a non-degenerate local minimum of $F_{i,j}$, and there are no other Reeb chords in $N(e^0_\alpha)$.

Proposition 5.9. *For some 0-cell, e^0_α, let $a_{i,j}$, $1 \le i < j \le n$, be the Reeb chords $N(e^0_\alpha)$. In $(\mathcal{A}_{LCH}(e^0_\alpha), \partial)$ we have*

$$\partial a_{i,j} = \sum_{i<k<j} a_{i,k} a_{k,j}.$$

Proof. By Theorem 2.6 and Theorem 5.1, $\partial a_{i,j}$ is computed as a sum over rigid GFTs with a postive puncture at $a_{i,j}$. Any such flow tree, Γ, is contained entirely in $N(e^0_\alpha)$ (by Lemma 5.5. Since the

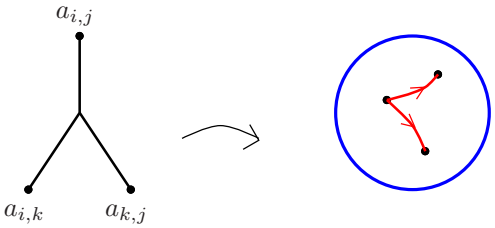

FIGURE 19. A rigid GFT Γ beginning at $a_{i,j}$ with domain and image pictured. The top branch of the tree maps to the constant $-\nabla F_{i,j}$ at $a_{i,j}$.

cusp locus of $\tilde{L}$ is disjoint from $N(e^0_\alpha)$, internal vertices of Γ can only be Y_0-vertices, and all outputs of Γ must be at Reeb chords in $N(e^0_\alpha)$. Thus, Proposition 2.9 shows that Γ must have two negative punctures and, therefore, a single Y_0. As the initial branch of Γ must be constant (since $a_{i,j}$ is a local minimum), we have exactly one such tree for each intermediate sheet S_k with $F_i > F_k > F_j$ as follows: After the Y_0 the outgoing edges of Γ are flow lines for $-\nabla F_{i,k}$ and $-\nabla F_{k,j}$ that must limit to $a_{i,k}$ and $a_{k,j}$ respectively. See Figure 19. □

5.4. **Computation of $(\mathcal{A}_{LCH}, \partial)$ near the 1-skeleton.** Consider now a 1-cell e^1_α parametrized by $[-1,1]$, and label the sheets above $N(e^1_\alpha)$ as $S_1, \dots, S_n$ with descending z-coordinate in the order they appear above $+1$. As in Section 3.2, above e^1_α the front projection of $\tilde{L}$ has one of four forms that we refer to with the abbreviations

(PV) Plain Vanilla: The sheets do not intersect.
(1Cr) 1-crossing: Sheets k and $k+1$ cross one another somewhere in $[-1/4, 1/4]$.
(2Cr) 2-crossing: Sheet $k+2$ crosses sheets $k+1$ and k somewhere in $[-1/4, 1/4]$ as $x \in [-1,1]$ decreases from $x = +1$ to $x = -1$.
(Cu) Left cusp: Sheets k and $k+1$ meet at a cusp at $x = -3/8$.

See Figure 5. As specified by Property 1, the location of the cusp point in (Cu) is at $x = -3/8$, and the location of crossings in (1Cr) and (2Cr) are between $x = -1/4$ and $x = 1/4$.

Let $\widehat{N}(e^1_\alpha)$ denote $N(e^1_\alpha)$ with the the interior of each $N(e^0_\pm)$ removed where e^0_+ and e^0_- are the endpoints of e^1_α. Then, $N(e^1_\alpha) = N(e^0_+) \cup N(e^0_-) \cup \widehat{N}(e^1_\alpha)$ with all subsets compact, see Figure 18. Moreover, $\widehat{N}(e^1_\alpha)$ consists of a portion of e^1_α together with subsets of two squares that contain e^1_α in their boundary. In each of these squares, the intersection of $\widehat{N}(e^1_\alpha)$ lies, with respect to the parametrization by $[-1,1]^2$, within a strip of distance $1/32$ from e^1_α. According to the third regularity requirement stated in Section 3.1, the parametrizations of these bordering squares can be combined in a suitable manner to realize $\widehat{N}(e^1_\alpha)$ as a subset of $(-1,1) \times [-1/32, 1/32]$. The boundary of $\widehat{N}(e^1_\alpha)$ consist of some subsets of $\partial N(e^0_\pm)$ which are circular arcs centered at $(\pm 1, 0)$ together with polygonal paths P_1 and P_2 which respectively belong to $[-1,1] \times (0, 1/32]$ and $[-1,1] \times [-1/32, 0)$ and project to the first component in a one-to-one manner.

Label sheets above $N(e^1_\alpha)$ as $S_1, \dots, S_n$ with decreasing z-coordinate as they appear above e^+_0. For $p \in \widehat{N}(e^1_\alpha) \subset [-1,1] \times [-1/32, 1/32]$ we let $x_1(p) \subset [-1,1]$ denote the first coordinate of p.

Property 5 (Reeb chords above 1-cells)**.** The only Reeb chords in $\widehat{N}(e^1_\alpha)$ are as follows.

- For every $i < j$, there is a Reeb chord $b_{i,j}$ with $x_1(b_{i,j}) \in [1/2, 3/4]$.
- If sheets i and j with $i < j$ cross above e^1_α, then there is a Reeb chord $\tilde{b}_{j,i}$ with $x_1(\tilde{b}_{ji}) \in [-3/4, -1/2]$.

Moreover, all of the $b_{i,j}$ and $\tilde{b}_{j,i}$ are non-degenerate saddle points.

(We follow Convention 5.7; in all cases the first and second subscripts refer respectively to the upper and lower sheets of the Reeb chord.)

Note that the only Reeb chords of the second type are $\tilde{b}_{k+1,k}$ for a (1Cr) edge and $\tilde{b}_{k+2,k+1}, \tilde{b}_{k+2,k}$ for a (2Cr) edge.

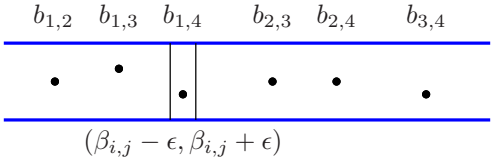

FIGURE 20. The $b_{i,j}$ are lexicographically ordered by their x_1-coordinates.

5.4.1. *Statement of the differential.* Let $a^-_{i,j}, a^+_{i,j}, b_{i,j}, \tilde{b}_{i,j}$ denote Reeb chords in $N(e^0_-)$, $N(e^0_+)$, and $N(e^1_\alpha)$ respectively, where subscripts of all Reeb chords now correspond to the ordering of sheets as $S_1, \dots, S_n$ above e^+_0.

We place these generators into strictly upper triangular matrices A_-, A_+, and B whose respective (i,j)-entries with $i<j$ are given by $a^-_{i,j}, a^+_{i,j}$, and $b_{i,j}$, when they exist. (The $\tilde{b}_{i,j}$ do not appear in any of these matrices.) All other entries are 0 with the exception that if S_k and S_{k+1} meet at a cusp edge above e^1_α, then the $(k,k+1)$-entry of A_- is 1. (Note that for $i<j$, if S_i and S_j cross above e^1_α or exactly one of these sheets ends at a cusp edge, then the (i,j)-entry of A_- is 0.)

Proposition 5.10. *Let e^1_α be a 1-cell with Reeb chords $a^-_{i,j}, a^+_{i,j}, b_{i,j}, \tilde{b}_{i,j}$ as above. In $(\mathcal{A}_{LCH}(e^1_\alpha), \partial)$ we have*

$$\partial B = A_+(I+B) + (I+B)A_- + X$$

where all entries of X belongs to the ideal generated by the $\tilde{b}_{i,j}$.

After discussing relevant properties of $\tilde{L}$ above 1-cells, the proof of Proposition 5.10 is given at the conclusion of this section.

5.4.2. *Properties of Reeb chords and gradients above 1-cells.* Locations of Reeb chords are specified more precisely in the following.

Property 6 (Location of 1-cell Reeb chords)**.** For a 1-cell e^1_α with n sheets above $x=+1$, there exists a collection of numbers $\beta_{i,j} \in [1/2, 3/4]$, for any $i<j$ and $\epsilon>0$, depending only on n, such that

- the intervals $[\beta_{i,j}-\epsilon, \beta_{i,j}+\epsilon]$ are all disjoint;
- the $\beta_{i,j}$ appear in lexicographic order, i.e.

$$\beta_{i,j} < \beta_{i',j'} \quad \text{whenever } i<i', \text{ or } i=i' \text{ and } j<j'; \text{ and} \tag{5}$$

- $x_1(b_{i,j}) \in (\beta_{i,j}-\epsilon, \beta_{i,j}+\epsilon)$

Moreover, in the case of a (1Cr) or (2Cr) edge respectively, there are in addition $\tilde{\beta}_{k+1,k} \in [-3/4, -1/2]$ or $\tilde{\beta}_{k+2,k+1}, \tilde{\beta}_{k+2,k} \in [-3/4,-1/2]$ such that $x_1(\tilde{b}_{j,i}) \in (\tilde{\beta}_{j,i}-\epsilon, \tilde{\beta}_{j,i}+\epsilon)$ and, in the (2Cr) case, the $[\tilde{\beta}_{i,j}-\epsilon, \tilde{\beta_{i,j}}+\epsilon]$ are disjoint with $\tilde{\beta}_{k+2,k} < \tilde{\beta}_{k+2,k+1}$.

Property 6 is illustrated in Figure 20.

Property 7 (Monotonicity above 1-cells)**.** Let $(x_1,x_2) \in \widehat{N}(e^1_\alpha)$, and $\nabla F_{i,j} = (\delta_{x_1}F_{i,j}, \delta_{x_2}F_{i,j})$.
Suppose $F_i > F_j$ when $x_1 \in [1/4, 1]$.

- If $\beta_{i,j}+\epsilon \le x_1$, then $-\delta_{x_1}F_{i,j}(x_1,x_2) > 0$.
- If $x_1 \in [1/4, \beta_{i,j}-\epsilon]$, then $-\delta_{x_1}F_{i,j}(x_1,x_2) < 0$.

Suppose $F_i > F_j$ when $x_1 \in [-1,-1/4]$ and that sheets S_i and S_j do not cross in $\widehat{N}(e^1_\alpha)$.

- If $x_1 \le -1/4$, then $-\delta_{x_1}F_{i,j}(x_1,x_2) < 0$

Suppose $F_i > F_j$ when $x_1 \in [-1,-1/4]$ and that sheets S_i and S_j cross in $\widehat{N}(e^1_\alpha)$.

- If $x_1 \in [\tilde{\beta}_{i,j}+\epsilon, -1/4]$, then $-\delta_{x_1}F_{i,j}(x_1,x_2) > 0$.
- If $x_1 \le \tilde{\beta}_{i,j}-\epsilon$, then $-\delta_{x_1}F_{i,j}(x_1,x_2) < 0$.

See Figure 21.

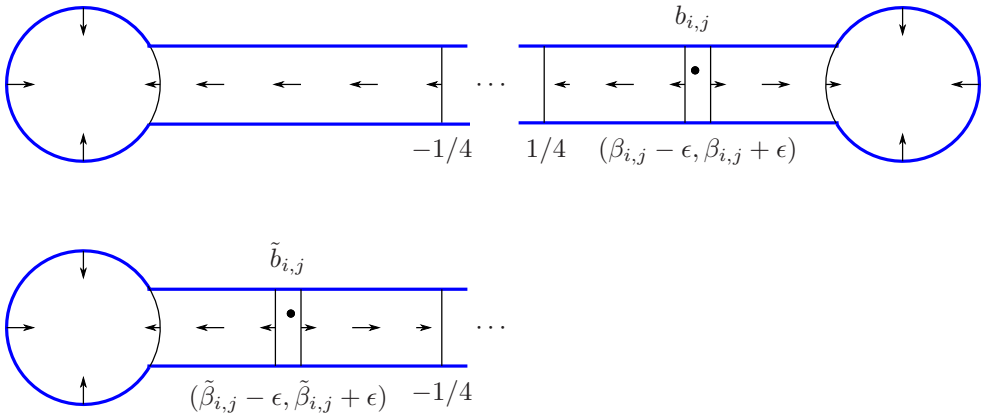

FIGURE 21. The horizontal component of $-\nabla F_{i,j}$ with $F_i > F_j$ in the neighborhood of a 1-cell when (top) the S_i and S_j do not cross or when (bottom) sheets S_i and S_j cross in the 1-cell with S_i above S_j when $x_1 \leq -1/4$.

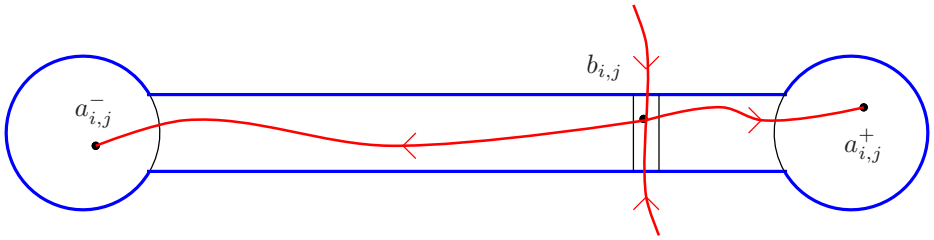

FIGURE 22. The stable and unstable manifold of $b_{i,j}$. If sheet S_i is no longer above S_j when $x_1 \leq -1/4$ due to a crossing or cusp, then the left flowline of the unstable manifold ends at the crossing or cusp locus.

5.4.3. *Stable and unstable manifolds of the $b_{i,j}$.* The $b_{i,j}$ are saddle points of $F_i - F_j$, and thus their *stable* and *unstable* manifolds with respect to $-\nabla F_{i,j}$ are 1-dimensional open disks. The stable (resp. unstable) manifold of $b_{i,j}$ consists of $b_{i,j}$ together with two non-constant (i,j)-flow lines ending (resp. beginning) at $b_{i,j}$, i.e. limiting to $b_{i,j}$ as $t \to +\infty$ (resp. $t \to -\infty$). By Properties 2 and 3, a flow line belonging to the unstable manifold of $b_{i,j}$ is entirely contained in $N(e^1_\alpha)$ as long as it remains in a region where $F_i - F_j$ is positive. Thus, as t increases towards $+\infty$, such a flow line may either limit to a Reeb chord above $N(e^0_\pm)$, reach the cusp edge at an e-vertex, or *terminate at the cusp or crossing locus*. In more detail, for 1-cells of Type (1Cr) or (2Cr), the flowline may pass the crossing locus and enter a region where $F_i - F_j < 0$; for 1-cells of Type (Cu) the flowline may reach the cusp locus where, if the graphs of F_i and F_j meet at the cusp edge, it ends as a e-vertex, or, when exactly one of the sheets S_i and S_j is a cusp sheet, the difference function $F_i - F_j$ ceases to be defined.

Proposition 5.11. *Consider a Reeb chord $b_{i,j}$ in $N(e^1_\alpha)$ where e^1_α is a 1-cell with endpoints $e^0_\pm$.*

1. *One of the non-constant flow lines of the unstable manifold of $b_{i,j}$ limits to a Reeb chord in $N(e^0_+)$, while the other either limits to a Reeb chord in $N(e^0_-)$; reaches an e-vertex; or terminates at the cusp or crossing locus.*
2. *Any point p in the intersection of the stable manifold of $b_{i,j}$ with $N(e^1_\alpha)$ satisfies $x_1(p) \in [\beta_{i,j}-\epsilon, \beta_{i,j}+\epsilon]$ with respect to the coordinates $\widehat{N}(e^1_\alpha) \subset [-1,1]\times[-1/32,1/32]$.*
3. *The two flowlines of the stable manifold of $b_{i,j}$ exit $N(e^1_\alpha)$ along opposite sides of the boundary.*

See Figure 22.

Proof. To verify (1), suppose that instead both flow lines of the unstable manifold limit to the same point or that they both end at the cusp/crossing locus. Then, the unstable manifold of $b_{i,j}$ together with the limiting critical point, or some appropriate portion of the crossing or cusp locus, bounds a region $R \subset N(e^1_\alpha)$ that does not contain any critical points of $F_{i,j}$ in its interior. As the unstable manifold of $b_{i,j}$ seperates the two non-constant flow lines of the stable manifold of $b_{i,j}$, one of the two (i,j)-flow lines from the stable manifold of $b_{i,j}$ would have to be entirely contained in R. This is impossible since

as t decreases toward $-\infty$ this flow line cannot limit to critical points above $N(e^0_\pm)$, since they are local minimums, and cannot run into the crossing locus (since $F_{i,j}$ increases as t decreases) or the cusp locus (by Property 7).

For (2), Property 7 shows that as t decreases from $+\infty$ a flowline of the stable manifold cannot cross the vertical lines $x_1 = \beta_{i,j} \pm \epsilon$. Finally, (3) follows from (1) and (2), since the unstable manifold of $b_{i,j}$ seperates $\widehat{N}(e^1_\alpha)$ into two halves. □

Lemma 5.12. *For any $i < j$ and $i' < j'$ with $(i,j) \neq (i',j')$, the unstable manifold of $b_{i,j}$ intersects the stable manifold of $b_{i',j'}$ transversally in an odd number of points. Any such intersection point $(x_1, x_2) \in \widehat{N}(e^1_\alpha) \subset [-1,1] \times [-1/32, 1/32]$ satisfies $x_1 \in (\beta_{i',j'} - \epsilon, \beta_{i',j'} + \epsilon)$.*

Proof. The unstable manifold of $b_{i,j}$ is entirely contained in $N(e^1_\alpha)$ (by Lemma 5.5) while the intersection of the stable manifold of $b_{i',j'}$ with $N(e^1_\alpha)$ belongs to the subset where $x_1 \in (\beta_{i',j'} - \epsilon, \beta_{i',j'} + \epsilon)$ (by Proposition 5.11). Thus, the location of any intersection points must be as claimed.

That the unstable and stable manifolds intersect transversally follows from the 1-regularity of $\tilde{L}$ stated in Theorem 5.1. Finally, the intersections points are odd in number since the unstable manifold of $b_{i,j}$ (resp. the stable manifold of $b_{i',j'}$) intersects $T = N(e^1_\alpha) \cap \big([\beta_{i',j'} - \epsilon, \beta_{i',j'} + \epsilon] \times [-1/32, 1/32]\big)$ in a single line segment with endpoints on the left and right boundary of T (resp. on the upper and lower boundary of T) by Property 7 (resp. by Proposition 5.11 and Property 3).

□

5.4.4. *Computation of $\partial b_{i,j}$.*

Proof of Proposition 5.10. In this proof, we make the convention that if $F_i < F_j$ at e^0_- or either F_i or F_j is not defined at e^0_-, then $a^-_{i,j} = 0$ with the exception that if S_k and S_{k+1} meet at a cusp edge above e^1_α, then $a^-_{k,k+1} = 1$. Then, the stated formula for ∂B is equivalent to the term-by-term formula,

$$\partial b_{i,j} = a^+_{i,j} + a^-_{i,j} + \sum_{i<m<j} (a^+_{i,m} b_{m,j} + b_{i,m} a^-_{m,j}) + x$$

where x belongs to the ideal generated by the $\tilde{b}_{l,l'}$.

We first identify an odd number of rigid GFTs contributing each of the terms, other than x, that appear in the formula for $\partial b_{i,j}$. Then, to complete the proof we show that any other rigid GFT would have to have an endpoint at one of the $\tilde{b}_{i,j}$.

First, consider rigid flow trees beginning at $b_{i,j}$ that do not have any internal vertices, i.e. flow lines of $-\nabla F_{i,j}$ that start at $b_{i,j}$ and limit to a Reeb chord as $t \to +\infty$ or terminate at an e-vertex. There are two non-constant (i,j)-flow lines beginning at $b_{i,j}$, and, from Proposition 5.11, one of these two flow lines must limit to $a^+_{i,j}$, while the other either limits to $a^-_{i,j}$; ends at an e-vertex; or terminates at the cusp or crossing locus. Notice that with our conventions for the meaning of $a^-_{i,j}$ these rigid flow trees contribute exactly the term $a^+_{i,j} + a^-_{i,j}$ to $\partial b_{i,j}$, and there are no other rigid flow trees without internal vertices.

We now specify some rigid flow trees with exactly 1 internal vertex. For any $i < m < j$, consider a flow tree Γ whose initial branch is a portion of the $-\nabla F_{i,j}$ flowline beginning at $b_{i,j}$ that intersects the stable manifold of $b_{i,m}$ (resp. $b_{m,j}$), as specified by Lemma 5.12. Next, a Y_0 occurs in Γ at one of the odd number of intersection points; the outgoing edges are (i,m)-flows and (m,j)-flows. If the Y_0 point is on the stable manifold of $b_{i,m}$, then the outgoing branch that is an (i,m)-flow line limits to $b_{i,m}$, while other outgoing branch is an (m,j)-flow line that has initial point (x_1, x_2) with

$$x_1 \leq \beta_{i,m} + \epsilon < \beta_{m,j} - \epsilon \qquad \text{by (2) of Proposition 5.11 and equation (5).}$$

Property 7 applies to show that this (m,j)-flow must remain to the left of $x_1 = \beta_{m,j} - \epsilon$ in $N(e^1_\alpha)$, and will therefore either limit to $a^-_{m,j}$; reach an e-vertex at the cusp locus; or terminate at a crossing arc or cusp edge. (In the final case, Γ is not actually a flow tree.) As we use $\mathbb{Z}/2$ coefficients, trees of this type contribute precisely the term $b_{i,m} a^-_{m,j}$ to $\partial b_{i,j}$, since we have set $a^-_{m,j} = 0$ (resp. 1) exactly when the (m,j)-flow terminates at the cusp or crossing edge (resp. ends at an e-vertex). In a similar manner, when the Y_0 point belongs to the stable manifold of $b_{m,j}$, the outgoing edges limit to $a^+_{i,m}$ and $b_{m,j}$ respectively, and these trees give the $a^+_{i,m} b_{m,j}$ terms. See Figure 23.

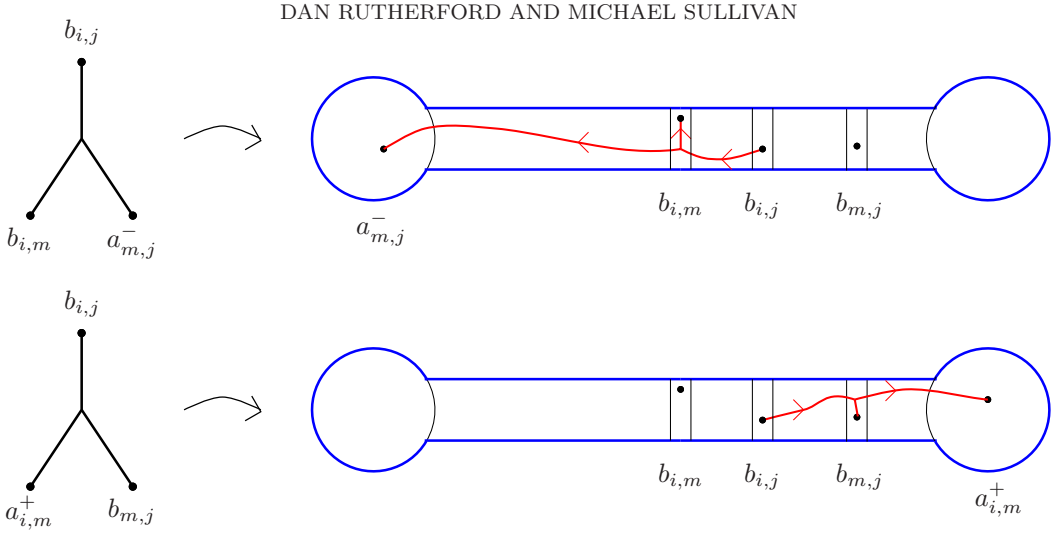

FIGURE 23. The domain and image of rigid flow trees beginning at $b_{i,j}$ and having 1 Y_0-vertex.

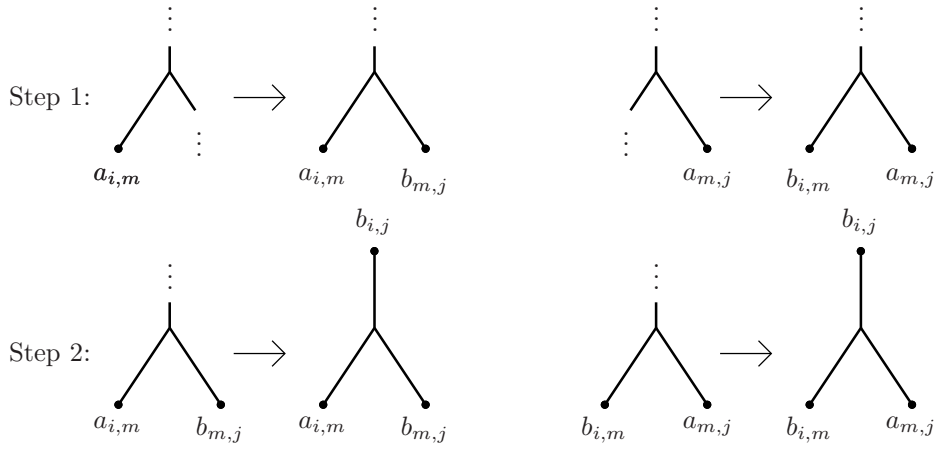

FIGURE 24. Steps 1 and 2 from the proof of Proposition 5.10.

To complete the proof, we need to show that any rigid GFT Γ begining at some $b_{i,j}$ with at least 1 internal vertex, and without endpoints at any $\tilde{b}_{i,j}$ must be one of the trees from the previous paragraph. Such a flow tree can only have endpoints at Reeb chords of the form $a^{\pm}_{l,l'}$, $b_{l,l'}$ or e-vertices, and cannot have any Y_1 or sw-vertices because Properties 1 and 7 show that all $-\nabla F_{i,j}$ with $F_i > F_j$ point transversally to the cusp edge in the direction where the cusp sheets are not defined. Therefore, Proposition 2.9 gives

$$1 = A + E$$

where A and E are respectively the number of endpoints of Γ at a Reeb chords and at e-vertices. Therefore, Γ has all but one endpoint at b Reeb chords, with the remaining endpoint at an a Reeb chord or an e-vertex.

Consider the edge that has its endpoint at an a Reeb chord or an e-vertex. The initial vertex of this edge, x, must be a Y_0.

Step 1. Suppose that the incoming edge at x is an (i,j)-flow with the outgoing edges (i,m) and (m,j)-flows. If the (i,m) edge (resp. the (m,j) edge) ends at an a Reeb chord or e-vertex, then the (m,j) edge (resp. the (i,m) edge) ends at $b_{m,j}$ (resp. at $b_{i,m}$). See Figure 24.

The partial flow tree that starts with the edge in question has all of its endpoints at b Reeb chords. Therefore, Step 1. follows from

Lemma 5.13. *Any PFT that begins in $N(e^1_\alpha)$ and has all endpoints at Reeb chords of the form $b_{i',j'}$ has no internal vertices.*

Proof of Lemma 5.13. Suppose that such a PFT has some internal vertex. Then, by the combinatorics of rooted trees, we can find a pair of edges that end at Reeb chords b_{i_1,j_1} and b_{i_2,j_2} respectively and

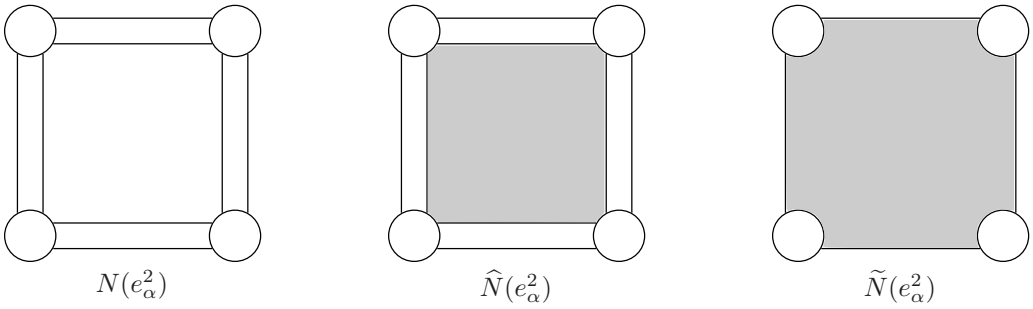

FIGURE 25. The neighborhood $N(e^2_\alpha)$ (left) with the subsets $\widehat{N}(e^2_\alpha)$ (center) and $\widetilde{N}(e^2_\alpha)$ (right) shaded.

start at a common Y_0-vertex. The image of this Y_0-vertex would be an intersection in $N(e^1_\alpha)$ of the stable manifolds of b_{i_1,j_1} and b_{i_2,j_2}. However, no such intersection point can exist by (2) of Proposition 5.11 since the intervals $[\beta_{i_1,j_1}-\epsilon, \beta_{i_1,j_1}+\epsilon]$ and $[\beta_{i_2,j_2}-\epsilon, \beta_{i_2,j_2}+\epsilon]$ are disjoint. □

As a consequence of Step 1., note that since x belongs to the stable manifold of $b_{i,m}$ or $b_{m,j}$ it is to the right of any crossings in the case e^1_α is a (1Cr) or (2Cr) edge. Thus, the sheets $S_1, \dots, S_n$ appear with z-coordinates strictly descending at x, so it follows that $i < m < j$.

Step 2. The incoming edge at x must begin at $b_{i,j}$. See Figure 24.

To establish Step 2., we need to show that the (i,j) edge, E, that ends at x cannot begin at a Y_0 vertex. From Step 1., we know that x is located on either the stable manifold of $b_{i,m}$ or $b_{m,j}$. Therefore by Properties 6 and 7 and Proposition 5.11, any point in the image of E must have x_1-coordinates in $[b_{i,m}-\epsilon, b_{m,j}+\epsilon]$. If the initial endpoint of E were at a Y_0, y, then the other outgoing edge of y, F, would either be a (j,l)-flow or an (h,i)-flow for some $h < i < j < l$. By Lemma 5.13, F would have to belong to the stable manifold of either $b_{j,l}$ or $b_{h,i}$, but, by Proposition 5.11 and Property 6, this is impossible since $\beta_{h,i}+\epsilon < \beta_{i,m}-\epsilon$ and $\beta_{m,j}+\epsilon < \beta_{j,l}-\epsilon$.

With Step 1. and Step 2. established, we see that the Y_0 vertex x is at one of the odd number of intersection of the unstable manifold of $b_{i,j}$ with either the stable manifold of $b_{i,m}$ or $b_{m,j}$. There are no other internal vertices in the tree, so Γ is indeed one of the previously identified GFTs. □

6. Computation of LCH, Part 2: 2-cells without swallowtail singularities

In this section, we compute in Theorem 6.5 the sub-DGAs associated to 2-cells of type (1)-(12).

6.1. **Reeb chords above a 2-cell: Types (1)-(12).** Let e^2_α be a 2-cell of type (1)-(12). The closure of e^2_α is parametrized by $[-1,1]^2$, and we use $e^0_{+,+}, e^0_{-,+}, e^0_{-,-}, e^0_{+,-}$ to denote the 0-cells that appear above the corners of e^2_α at $(x_1,x_2) = (1,1),(-1,1),(-1,-1),(1,-1)$ respectively. We denote the 1-cells that form the edges $\{-1\}\times[-1,1]$, $[-1,1]\times\{-1\}$, $\{+1\}\times[-1,1]$, $[-1,1]\times\{+1\}$ by e^1_L, e^1_D, e^1_R, e^1_U respectively. (Here and elsewhere, the subscripts L, D, R, U are intended to convey "Left", "Down", "Right", and "Up".) We recall that, since the transverse square decomposition $\mathcal{E}_{\pitchfork}$ satisfies the requirement (A1) from Section 3.3, the orientation of both e^1_L and e^1_R (resp. e^1_D and e^1_U) is from the bottom edge to the top edge (resp. the left edge to the right edge) of $[-1,1]^2$.

We define a subset $\widehat{N}(e^2_\alpha) \subset N(e^2_\alpha)$ to satisfy

$$N(e^2_\alpha) = N(e^1_L) \cup N(e^1_D) \cup N(e^1_R) \cup N(e^1_U) \cup \widehat{N}(e^2_\alpha)$$

so that $\widehat{N}(e^2_\alpha)$ is compact and only intersects neighborhoods of 1-cells along subsets of their boundaries. In coordinates, $\widehat{N}(e^2_\alpha)$ is a subset of the interior of $[-1,1]^2$. Note in addition that the earlier parametrizations of the subsets $\widehat{N}(e^1_X)$ for $X \in \{L,D,R,U\}$ by subsets of $[-1,1]\times[-1/32,1/32]$ can be suitably modified and pieced together with the parametrization of e^2_α to realize $N(e^2_\alpha)$ with the interiors of the $N(e^0_{\pm,\pm})$ removed as a subset of $[-1-1/32,1+1/32]\times[-1-1/32,1+1/32]$. Denote this subset of $N(e^2_\alpha)$ by $\widetilde{N}(e^2_\alpha)$. See Figure 25.

6.1.1. *Reeb chords above $N(e^2_\alpha)$.* Above e^2_α, the components of the complement of the cusp edge of $\tilde{L}$ each project in a one-to-one manner to $[-1,1]$. Thus, within e^2_α we can label the sheets of $\tilde{L}$ as $S_1,\dots,S_n$ so that above $(x_1,x_2)=(+1,+1)$ their z-coordinates appear in decreasing order. For $X\in\{L,D,R,U\}$, we have Reeb chords in neighborhoods of $N(e^0_{\pm,\pm})$ and $N(e^1_X)$ as specified by Properties 4 and 5, which we denote by $a^{\pm,\pm}_{i,j}$, $b^X_{i,j}$, and $\tilde{b}^X_{i,j}$. We follow Convention 5.7 so that the subscript i,j indicates a Reeb chord whose upper (resp. lower) endpoint is on S_i (resp. S_j). The location of $b^X_{i,j}$ is determined by Property 6 to lie within the subset of $N(e^1_X)$ that is specified in our current coordinate system by a requirement of the form

$$x_1(b^X_{i,j})\in(\beta^X_{i,j}-\epsilon,\beta^X_{i,j}+\epsilon) \text{ when } X\in\{D,U\}, \text{ or } \quad x_2(b^X_{i,j})\in(\beta^X_{i,j}-\epsilon,\beta^X_{i,j}+\epsilon) \text{ when } X\in\{L,R\},$$

for appropriate $\beta^X_{i,j}\in[1/2,3/4]$. Similarly, we have $\tilde{\beta}^X_{i,j}\in[-3/4,-1/2]$ that specify the location of the $\tilde{b}^X_{i,j}$ should they exist.

Remark 6.1. (i) In general, $\beta^U_{i,j}=\beta^R_{i,j}=\beta_{i,j}$. (Recall, that the $\beta_{i,j}$ specify the position of Reeb chords in neighborhoods of 1-cells and depend only on n and not the type of the 1-cell.) However, we caution that,

$$\beta^L_{i,j}=\beta_{\sigma_L(i),\sigma_L(j)} \text{ and } \beta^D_{i,j}=\beta_{\sigma_D(i),\sigma_D(j)}$$

where $\sigma_L(i)$ and $\sigma_D(i)$ indicate the position (with respect to descending z-coordinate) that sheet S_i appears above $(x_1,x_2)=(-1,+1)$ and $(x_1,x_2)=(+1,-1)$ respectively. Thus, if a crossing or cusp appears above U or R, then for some values of i,j we may have $\beta^L_{i,j}\neq\beta_{i,j}$, or $\beta^D_{i,j}\neq\beta_{i,j}$.

(ii) In parallel to (i), note that the indices provided on Reeb chords of the form $b^L_{i,j}$ or $b^D_{i,j}$ may be distinct from the indices that would be used to specify the same Reeb chord when considering e^1_L or e^1_D in the setting of Section 5.4. This is because if a crossing or cusp appears along edges U or R, then the sheets $S_1,\dots,S_n$ are labeled in a different manner above e^1_L and e^1_D than in Section 5.4. For instance, if sheets k and $k+1$ cross above e^1_U, then there is a Reeb chord $b^L_{k+1,k}$ with $x_2(b^L_{k+1,k})\in[1/2,3/4]$, while in Section 5.4 all Reeb chords above the upper half of $N(e^1_L)$ would be labeled with subscripts i,j with $i<j$. The use of different labellings of Reeb chords in the context of the sub-DGAs $\mathcal{A}(e^d_\alpha)$ for different e^d_α is addressed in Section 8.

Property 8. The only Reeb chords in $\widehat{N}(e^2_\alpha)$ are as follows.

- For any $i<j$, there is a unique Reeb chord $c_{i,j}$ within $[1/2,3/4]^2$. The location of $c_{i,j}$ is more precisely specified by
$$c_{i,j}\in(\beta^U_{i,j}-\epsilon,\beta^U_{i,j}+\epsilon)\times(\beta^R_{i,j}-\epsilon,\beta^R_{i,j}+\epsilon).$$
- For each pair of sheets S_i and S_j with $i<j$ that cross one another somewhere in $[-1,1]^2$, there is a unique Reeb chord with upper sheet S_j and lower sheet S_i that we denote $\tilde{c}_{j,i}$.

Moreover, all of the $c_{i,j}$ and $\tilde{c}_{j,i}$ are non-degenerate local maxima.

See Figure 26.

To specify the location of $\tilde{c}_{j,i}$ we make the following observation. By considering the squares of type (1)-(12) in a case-by-case manner, we see that if sheets S_i and S_j cross somewhere in $[-1,1]^2$, then they either cross above exactly one of e^1_U or e^1_L, or, as happens only in the case of the Type (3) square, they cross above both e^1_D and e^1_R.

Property 9. Let $i<j$.

- If sheets S_i and S_j cross above e^1_R, then
$$\tilde{c}_{j,i}\in(\beta^D_{j,i}-\epsilon,\beta^D_{j,i}+\epsilon)\times(\tilde{\beta}^R_{j,i}-\epsilon,\tilde{\beta}^R_{j,i}+\epsilon).$$
- If sheets S_i and S_j cross above e^1_U, then
$$\tilde{c}_{j,i}\in(\tilde{\beta}^U_{j,i}-\epsilon,\tilde{\beta}^U_{j,i}+\epsilon)\times(\beta^L_{j,i}-\epsilon,\beta^L_{j,i}+\epsilon).$$
- If sheets S_i and S_j cross above both e^1_L and e^1_D, then
$$\tilde{c}_{j,i}\in(\tilde{\beta}^D_{j,i}-\epsilon,\tilde{\beta}^D_{j,i}+\epsilon)\times(\tilde{\beta}^L_{j,i}-\epsilon,\tilde{\beta}^L_{j,i}+\epsilon).$$

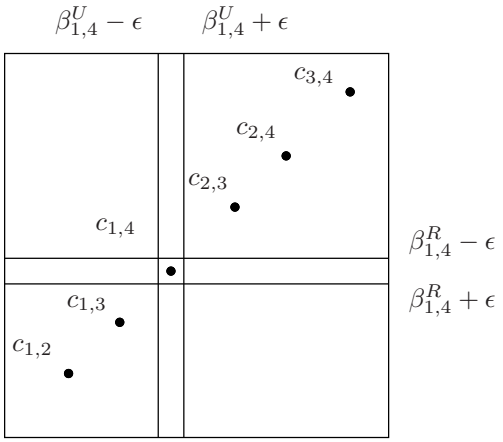

FIGURE 26. The critical points, $c_{i,j}$, that occur in $[1/2, 3/4] \times [1/2, 3/4]$ have both coordinates increasing with i and, for a fixed i, increasing with j.

6.1.2. *Exceptional generators.* The equivalence between the cellular DGA and $(\mathcal{A}_{LCH}, \partial)$ of Theorem 1.1 will actually be realized by comparing the cellular DGA with a certain stable tame isomorphic quotient of $(\mathcal{A}_{LCH}, \partial)$. In this quotient, we will remove the following generators from the generating set.

Definition 6.2. We say that a Reeb chord is an **exceptional generator** in $N(e^2_\alpha)$ if either of the following conditions applies:

(1) The generator has the form $\tilde{b}_{i,j}$ or $\tilde{c}_{i,j}$, i.e. the Reeb chord sits in the half of an edge where $-3/4 < x_i < -1/2$ or in the interior of the square but outside of the region $[1/2, 3/4] \times [1/2, 3/4]$. OR
(2) When the singular set is pushed into the boundary of e^2_α as in Section 3.4, a crossing arc between the sheets that form the end points of the Reeb chord sits above the 0-cell or 1-cell that the chord corresponds to.

Remark 6.3. In particular, according to (2) of Definition 6.2, any generator of the form $b^X_{i,j}$ or $a^{\pm,\pm}_{i,j}$ such that $i > j$ will be an exceptional generator. However, in some cases there are also exceptional generators of the form $b^X_{i,j}$ or $a^{\pm}_{i,j}$ with $i < j$, eg. above a Type (4) square $a^{-,-}_{k,k+1}$ is an exceptional generator. A complete square-by-square list of exceptional generators appears in Section 8.1.

6.2. **Computation of $(\mathcal{A}_{LCH}(e^2_\alpha), \partial)$: the statement.** For a given 2-cell, e^2_α, of type (1)-(12) we define strictly upper triangular matrices $A_{+,+}$, $A_{-,-}$, B_X for $X \in \{L, D, R, U\}$, and C. All (i, j)-entries with $i \geq j$ are 0. For $i < j$, the (i, j)-entries are respectively the Reeb chords of the form $a^{+,+}_{i,j}$, $a^{-,-}_{i,j}$, $b^X_{i,j}$, and $c_{i,j}$. If no such Reeb chord exists, the (i, j)-entry is 0 with the following exceptions: For squares of type (9)-(12), a pair of sheets S_k and S_{k+1} meet at a cusp before reaching the lower left side of the square. In these cases, the matrices B_L and $A_{-,-}$ have all entries in the k and $k + 1$ rows and columns equal to 0 except for the $(k, k + 1)$-entry of $A_{-,-}$ which is taken to be 1. For a Type (11) square an additional, similar adjustment is made to the two columns of B_D and $A_{-,-}$ that correspond to the sheets that meet at a cusp before reaching the bottom edge of the square.

Remark 6.4. Reeb chords of the form $\tilde{b}^X_{i,j}$ or $\tilde{c}_{i,j}$ do not appear as entries of these matrices, nor do Reeb chords of the form $a^{\pm,\pm}_{i,j}$ or $b^X_{i,j}$ with $i > j$. For instance, if e^2_α has type (2), then both the $(k, k+1)$- and $(k + 1, k)$-entries are 0 in the matrices $A^{-,-}$ and B_L.

Theorem 6.5. *For a 2-cell e^2_α of type (1)-(12), in $(\mathcal{A}_{LCH}(e^2_\alpha), \partial)$ we have*

$$\partial C = A_{+,+}C + CA_{-,-} + (I + B_R)(I + B_D) + (I + B_U)(I + B_L) + X. \tag{6}$$

where all of the entries of the matrix X belong to the ideal generated by the exceptional generators in $N(e^2_\alpha)$.

The proof of Theorem 6.5 appears at the conclusion of this section after relevant properties of gradients have been stated and several preliminary results about GFTs in $N(e^2_\alpha)$ have been established.

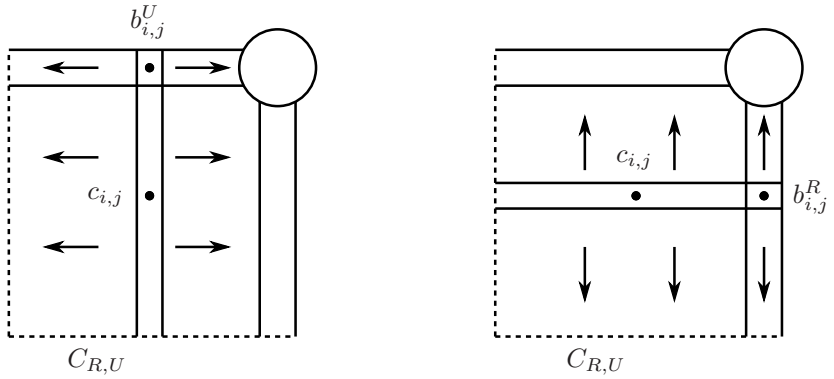

FIGURE 27. The direction of the x_1- and x_2-components of $-\nabla F_{i,j}$ in $C_{R,U}$ as determined by Property 10.

6.3. **Properties of gradients above 2-cells.** The following Properties 10 and 11 may be viewed as extensions of the monotonicity property of the $-\nabla F_{i,j}$ above 1-cells, i.e. Property 7, to the interiors of 2-cells.

For a given 2-cell e^2_α with boundary edges $e^1_L, e^1_D, e^1_R, e^1_U$, we label the four components of

$$\left\{(x_1,x_2)\in[-1,1]^2 \;\middle|\; |x_1|\geq\frac{1}{4}\text{ and }|x_2|\geq\frac{1}{4}\right\}\setminus\left(N(e^1_L)\cup N(e^1_D)\cup N(e^1_R)\cup N(e^1_U)\right)$$

as $C_{R,U}$, $C_{L,U}$, $C_{L,D}$, $C_{R,D}$ so that for $X\in\{L,R\}$ and $Y\in\{D,U\}$ the subset $C_{X,Y}$ shares some portion of its boundary with $N(e^1_X)$ and $N(e^1_Y)$.

Property 10 (Monotonicity in corners)**.** For $X\in\{L,R\}$ and $Y\in\{D,U\}$, suppose that $F_i>F_j$ in $C_{X,Y}$ and that S_i and S_j are both defined in all of $C_{X,Y}$ (i.e., neither sheet meets a cusp edge in $C_{X,Y}$). Write $\nabla F_{i,j}=(\delta_{x_1}F_{i,j},\delta_{x_2}F_{i,j})$.

- Suppose there is a Reeb chord in $\widehat{N}(e^1_X)$ with upper sheet S_i and lower sheet S_j. If the Reeb chord has the form $b^X_{i,j}$ (resp. $\tilde{b}^X_{i,j}$), set $\alpha^X_{i,j}=\beta^X_{i,j}$ (resp. $\alpha^X_{i,j}=\tilde{\beta}^X_{i,j}$). Then,
$$-\delta_{x_2}F_{i,j}(x_1,x_2)>0 \quad \text{if } x_2\geq\alpha^X_{i,j}+\epsilon, \text{ and}$$
$$-\delta_{x_2}F_{i,j}(x_1,x_2)<0 \quad \text{if } x_2\leq\alpha^X_{i,j}-\epsilon.$$
- Suppose there is no Reeb chord in $\widehat{N}(e^1_X)$ with upper sheet S_i and lower sheet S_j. Then,
$$-\delta_{x_2}F_{i,j}(x_1,x_2)<0.$$

In a similar manner, the sign of $-\delta_{x_1}F_{i,j}(x_1,x_2)$ is specified in regions of $C_{X,Y}$ that are determined by the location of Reeb chords with upper sheet S_i and lower sheet S_j in $\widehat{N}(e^1_Y)$.

See Figure 27 for an illustration of Property 10 in $C_{R,U}$, and see Figure 28 for an example.

Remark 6.6. The location of Reeb chords and signs of partial derivatives specified in Properties 8-10 are explained by the following considerations. Up to a C^∞-small perturbation, the defining functions F_i (and also the difference functions $F_{i,j}$) for sheets of $\tilde{L}$ above any of the corners $C_{X,Y}$ are sums

$$F_i(x_1,x_2)=F_i^Y(x_1)+F_i^X(x_2) \tag{7}$$

where, up to additive constants, F_i^Y and F_i^X are the restriction of F_i to the 1-cells e^1_Y and e^1_X. Thus, we have the following: The Reeb chords in $C_{X,Y}$ are precisely at points $(x_1,x_2)\in C_{X,Y}$ such that $d_xF^Y_{i,j}(x_1)=0$ and $d_xF^X_{i,j}(x_2)=0$ where Reeb chords $b^Y_{i,j}$ and $b^X_{i,j}$ sit along the 1-skeleton. In $C_{X,Y}$, the horizontal line through $b^X_{i,j}$ and vertical line through $b^Y_{i,j}$ are flow lines of $-\nabla F_{i,j}$, and they divide $C_{X,Y}$ into regions where the signs of the components of $-\nabla F_{i,j}$ are uniform.

The set up from Properties 8-10 is just the portion of this picture that remains after an arbitrary suitably small perturbation. See Section 9 for details.

Property 11 (Monotonicity in half spaces)**.** Let $1\leq i<j\leq n$, and write $\nabla F_{i,j}=(\delta_{x_1}F_{i,j},\delta_{x_2}F_{i,j})$.

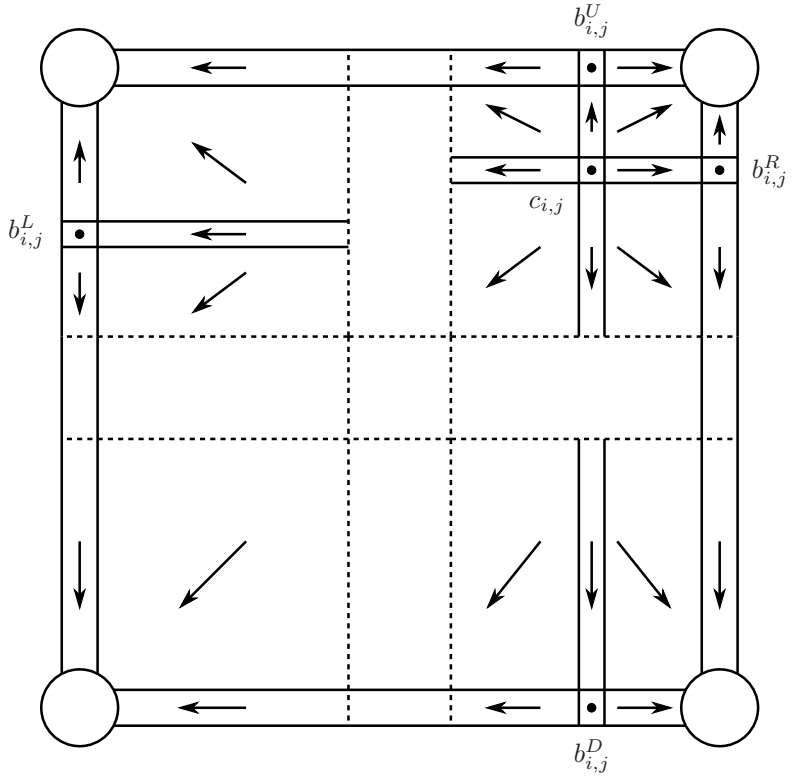

FIGURE 28. Signs of the components of $-\nabla F_{i,j}$ specified by Properties 7 and 10. A diagonal arrow indicates the sign of both components while a horizontal or vertical arrow indicates only one component. No sign has been specified in regions without an arrow. The dotted lines are $x_1 = \pm 1/4$ and $x_2 = \pm 1/4$. In this example, $\beta^R_{i,j} < \beta^L_{i,j}$ as may happen, for instance, if the square has Type (2) with $i < k$ and $j = k+1$.

- Suppose S_i and S_j do not cross above e^1_U and at most one of them ends at a cusp edge above e^1_U. Then, for $(x_1, x_2) \in \widehat{N}(e^2_\alpha)$ we have

$$-\delta_{x_2} F_{i,j}(x_1, x_2) < 0, \quad \text{whenever } x_2 = 1/2. \tag{8}$$

- Similarly, if S_i and S_j do not cross above e^1_R and at most one of them ends at a cusp edge above e^1_R. Then, for $(x_1, x_2) \in \widehat{N}(e^2_\alpha)$ we have

$$-\delta_{x_1} F_{i,j}(x_1, x_2) < 0, \quad \text{whenever } x_1 = 1/2. \tag{9}$$

See Figure 29.

Property 12. There are line segments B_1 and B_2, such that the following hold.

- The segment B_1 begins on $x_1 = 1/2$, ends on $x_1 = 3/4$ and is contained in the rectangle $[1/2, 3/4] \times (1/4, 1/2)$.
- For all $i < j$, and $(x_1, x_2) \in B_1$ with $1/2 \le x_1 \le \beta^U_{i,j} - \epsilon$, $-\nabla F_{i,j}(x_1, x_2)$ is transverse to B_1 and points in to the region above B_1.
- The segment B_2 satisfies analogous conditions with all locations reflected across $x_1 = x_2$.

See Figure 33, below, where portions of the segments B_1 and B_2 are pictured.

6.3.1. *Transversality at cusps.* Recall from Section 2.2 that if sheets S_k and S_{k+1} meet at a cusp, then a point along the $(k, k+1)$-cusp edge where $\nabla F_{i,k}$ or $\nabla F_{k+1,j}$ is tangent to the (base projection) of the cusp locus for some S_i above S_k or S_j below S_{k+1} is called an (i,k)- or $(k+1, j)$-switch point. Note also that along the cusp locus $\nabla F_{i,k} = \nabla F_{i,k+1}$ and $\nabla F_{k,j} = \nabla F_{k+1,j}$.

Property 13 (Cusp transversality)**.** For a square of type (1)-(11), suppose sheets S_k, S_{k+1} form a cusp edge. Then, at any point, (x_1, x_2) where S_i (resp. S_j) is above (resp. below) the cusp edge the vector fields $-\nabla F_{i,k+1}$, $-\nabla F_{k,j}$, and $-\nabla F_{i,j}$ are transverse to the cusp locus and point towards the region with fewer sheets.

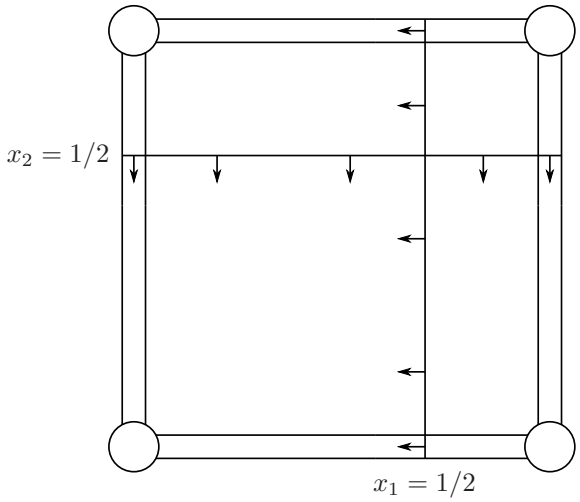

FIGURE 29. Components of $-\nabla F_{i,j}$ point down along $x_1 = 1/2$ and left along $x_2 = 1/2$ (in most cases) as specified by Properties 11 and 7.

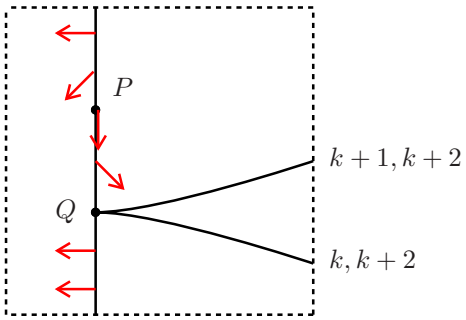

FIGURE 30. The unique $(k+1, k+2)$-switch point at P. The vertical line denotes the $(k, k+1)$-cusp locus. The upper (resp. lower) branch of the horizontal curve is the $(k+1, k+2)$-crossing locus (resp. the $(k, k+2)$-crossing locus). Above Q the arrows denote $-\nabla F_{k+1,k+2}$, while below Q the arrows denote $-\nabla F_{k+2,k+1}$.

In each Type (12) square, the above condition holds with the following exception: With sheets labeled $S_1, \ldots, S_n$ as they appear above $(+1, +1)$ such that S_k and S_{k+1} meet at the cusp edge, there is a unique non-degenerate $(k+1, k+2)$-switch point, P, located with x_2-coordinate above the point Q where the crossing locus and the cusp locus intersect and below $x_2 = 1/2$. Between P and Q, $-\nabla F_{k+1,k+2}$ is transverse to the cusp locus and points towards the region with more sheets.

See Figure 30.

6.3.2. *Stable manifolds of the $b^X_{i,j}$.* For $X \in \{L, D, R, U\}$, any Reeb chord $b^X_{i,j}$ or $\tilde{b}^X_{i,j}$ is a saddle point of $F_{i,j}$, and has stable manifold, with respect to $-\nabla F_{i,j}$, consisting of the point itself and two non-constant flow lines that limit to the point as $t \to +\infty$. Moreover, Proposition 5.11 shows that precisely one of these flow lines is contained entirely in $N(e^2_\alpha)$. (The other flow line is contained in the other 2-cell that borders e^1_X.) We refer to this non-constant flow line as the **$b^X_{i,j}$-line** or the **$\tilde{b}^X_{i,j}$-line** in $N(e^2_\alpha)$.

Lemma 6.7 (Limits of b-lines)**.** *For squares of type (1)-(12), as $t \to -\infty$, the $b^X_{i,j}$-line limits to $c_{i,j}$ (resp. $\tilde{c}_{i,j}$) if $i < j$ (resp. if $i > j$), while (if it exists) the $\tilde{b}^X_{i,j}$-line limits to $c_{i,j}$ (resp. $\tilde{c}_{i,j}$) if $i < j$ (resp. if $i > j$).*

See Figure 31.

Proof. Follow the flow line, γ, as t decreases towards $-\infty$. Once γ enters $\widehat{N}(e^2_\alpha)$ it cannot leave (by Property 3). Moreover, as $t \to -\infty$, γ must either limit to a critical point of $F_{i,j}$, or terminate at a cusp edge. (Since $F_{i,j}$ increases as t decreases, the flow line cannot terminate at a crossing.) The only

FIGURE 31. The $b^L_{i,j}$-line.

critical point of $F_{i,j}$ in $\widehat{N}(e^2_\alpha)$ with $F_{i,j} > 0$ is $c_{i,j}$ (resp. $\tilde{c}_{i,j}$), so the result follows once we show that γ cannot terminate at a cusp edge.

Suppose γ does terminate at a point x of the cusp edge. Then $-\nabla F_{i,j}(x)$ must point to the side of the cusp locus where more sheets exist, and one of i or j must be a cusp sheet. [Near a cusp locus, $-\nabla F_{i,j}$ is only defined on the side where S_i and S_j both exist. Therefore if γ runs into a cusp locus involving S_i or S_j it must approach this cusp locus from the side where S_i and S_j both exist, and since we follow γ in the direction where t decreases it follows that $-\nabla F_{i,j}(x)$ points to the side of the cusp locus where S_i and S_j both exist.] By Property 13, the square is then of type (12) with $i = k+1$ and $j = k+2$, so γ belongs to either the stable manifold of $b^U_{k+1,k+2}$ or $b^R_{k+1,k+2}$. [These are the only Reeb chords with upper and lower sheets S_{k+1} and S_{k+2} respectively.] However, by Proposition 5.11, these stable manifolds enter $\widehat{H}(e^2_\alpha)$ in the upper right corner where $x_1 \geq 1/4$ and $x_2 \geq 1/4$. Then, Property 10 shows that the stable manifolds of $b^U_{k+1,k+2}$ or $b^R_{k+1,k+2}$ must remain in the region where $x_1 \geq 1/4$ and $x_2 \geq 1/4$, so they cannot reach the cusp locus. □

6.3.3. *Non-existence of switches and Y_1 vertices.*

Proposition 6.8. *Consider any 2-cell of e^2_α of type (1)-(12). No GFT in $N(e^2_\alpha)$ has a Y_1- or sw-vertex.*

Proof. The image of a Y_1-vertex must be at a point on the cusp locus. Moreover, at this image there there must be sheets S_i and S_j that respectively lie above and below the cusp edge and have the property that $-\nabla F_{i,j}$ points into the side of the cusp locus where the number of sheets increases by 2. Such a point cannot exist by Property 13.

Property 13 also states $N(e^2_\alpha)$ has a switch point only when e^2_α is a Type (12) square. Then, there is a unique $(k+1, k+2)$ switch point with x_2-coordinate above the intersection of the crossing and cusp loci. We show that a switch cannot occur at this point in any PFT. If this were to happen, the outgoing edge of the switch would be a $(k, k+2)$-flow line, γ, that begins at the switch point. By Property 10, γ cannot cross into the region T where $x_1 \geq 1/2$ and $x_2 \geq 1/2$. There are no critical points of $F_{k,k+2}$ in the part of $N(e^2_\alpha)$ with $F_{k,k+2} > 0$ outside of T, and S_k and S_{k+2} do not meet at a cusp edge. Thus, if it did not end at an internal vertex, γ would only be able terminate at the cusp or crossing locus, and would not be part of a valid PFT. Now, if γ ends at an internal vertex it can only be a Y_0 that occurs above the $(k+1, k+2)$-crossing locus. The two outgoing branches of the Y_0 will be a $(k, k+1)$-flow line and a $(k+1, k+2)$-flow line. However, the $(k+1, k+2)$-branch cannot be completed to a valid PFT. Indeed, Property 10 applies to show the flowline stays in the complement of T where there are no critical points of $F_{k+1,k+2}$ with $F_{k+1,k+2} > 0$, and there is no $(k+1, k+2)$-cusp edge. Thus, if it were part of a PFT, then this edge would have to end with an internal vertex. However, S_{k+1} and S_{k+2} have no sheets between them in the region where $F_{k+1,k+2} > 0$, so this edge cannot end at a Y_0- or Y_1-vertex. Moreover, the edge cannot end at the $(k+1, k+2)$-switch point, since the difference between z-coordinates of sheets strictly decreases along all non-constant edges of a PFT. □

Proposition 6.9. *For a square e^2_α of type (1)-(12), any GFT Γ starting at one of the generators $c_{i,j}$ or $\tilde{c}_{i,j}$ is rigid if and only if*

$$A - C + E = 0$$

where A and C denote the number of endpoints at generators of the form $a^{\pm,\pm}_{i,j}$ and $c_{i,j}$ or $\tilde{c}_{i,j}$ respectively, and E denotes the number of endpoints at e-vertices.

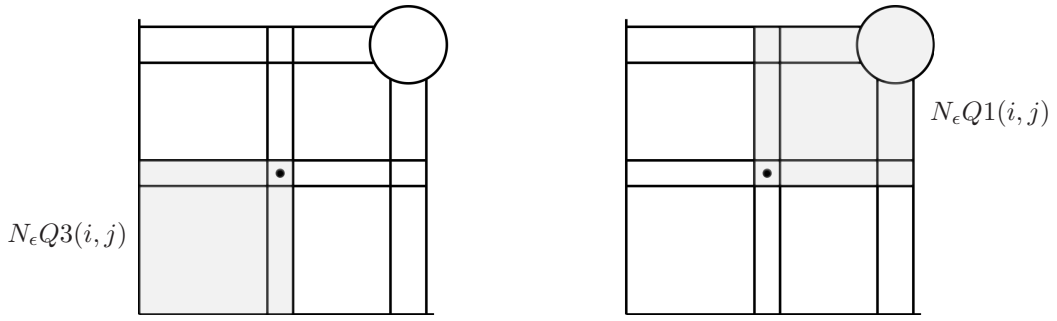

FIGURE 32. The enlarged first and third quadrants.

Proof. This follows from Proposition 6.8 and Proposition 2.9. □

6.4. **Rigid GFTs with at least one $c_{i,j}$ output.** The computation of $\partial c_{i,j}$, as stated in Theorem 6.5, is accomplished in two parts. In this section, we verify those terms in ∂C that correspond to rigid GFTs with at least one output at a c Reeb chord. Then, in 6.5 we identify the remaining terms in ∂C.

For $1 \leq i < j \leq n$, we introduce the notation

$$\partial_c c_{i,j} = \sum_{\Gamma} w(\Gamma)$$

where the sum is over those rigid GFTs, Γ, with an input at $c_{i,j}$ and having at least one output vertex at a Reeb chord of the form $c_{r,s}$ or $\tilde{c}_{r,s}$.

Theorem 6.10. *For a 2-cell e^2_α of type (1)-(12), and for any $1 \leq i < j \leq n$, we have*

$$\partial_c C = A^{+,+}C + CA^{-,-} + X_1 \tag{10}$$

where the matrices $C, A^{+,+}$, and $A^{-,-}$ are as in Theorem 6.5, and X_1 is a matrix whose entries belong to the 2-sided ideal generated by exceptional generators in $N(e^2_\alpha)$.

The proof of Theorem 6.10 is given below after the preliminary Lemmas 6.11 and 6.12.

6.4.1. *The First and Third Quadrant Lemmas.* Recall that we have coordinates $\widetilde{N}(e^2_\alpha) \subset [-1-1/32, 1+1/32] \times [-1-1/32, 1+1/32]$ where $\widetilde{N}(e^2_\alpha) \subset N(e^2_\alpha)$ is obtained by removing interiors of the $N(e^0_{\pm,\pm})$. Now, take the full upper right corner of $N(e^2_\alpha)$,

$$\{(x_1, x_2) \in \widetilde{N}(e^2_\alpha) \,|\, x_1 \geq 1/4,\ x_2 \geq 1/4\} \bigcup N(e^0_{+,+}),$$

and remove the vertical and horizontal bands

$$(\beta^U_{i,j} - \epsilon, \beta^U_{i,j} + \epsilon) \times [1/4, 1+1/32] \quad \text{and} \quad [1/4, 1+1/32] \times (\beta^R_{i,j} - \epsilon, \beta^R_{i,j} + \epsilon).$$

This results in four regions that we call the **(i,j)-quadrants** and denote by $Q1(i,j), Q2(i,j), Q3(i,j), Q4(i,j)$ where

$$Q1(i,j) \,=\, \{(x_1, x_2) \in \widetilde{N}(e^2_\alpha) \,\big|\, x_1 \geq \beta^U_{i,j} + \epsilon,\ x_2 \geq \beta^R_{i,j} + \epsilon\} \bigcup N(e^0_{+,+})$$

and the numeration proceeds in a counter-clockwise manner. In addition, let $N_\epsilon Q1(i,j)$ and $N_\epsilon Q3(i,j)$ denote thickened versions of $Q1(i,j)$ and $Q3(i,j)$ defined by

$$N_\epsilon Q1(i,j) \,=\, \{(x_1, x_2) \in \widetilde{N}(e^2_\alpha) \,\big|\, x_1 \geq \beta^U_{i,j} - \epsilon,\ x_2 \geq \beta^R_{i,j} - \epsilon\} \bigcup N(e^0_{+,+});$$

$$N_\epsilon Q3(i,j) \,=\, \{(x_1, x_2) \in \widetilde{N}(e^2_\alpha) \,\big|\, 1/4 \leq x_1 \leq \beta^U_{i,j} + \epsilon,\ 1/4 \leq x_2 \leq \beta^R_{i,j} + \epsilon\}\,.$$

See Figure 32.

Lemma 6.11 (First Quadrant Lemma)**.** *Let $i < m_1 \leq m_2 < j$. Any PFT, Γ, that begins with an (i, m_1)-flow line at a point in $N_\epsilon Q1(m_2, j)$ has all endpoints at $a^{+,+}$ generators. Moreover, the image of Γ is entirely contained in $N_\epsilon Q1(m_2, j)$.*

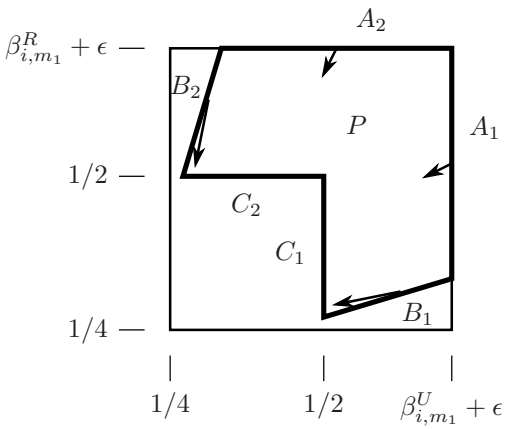

FIGURE 33. The polygonal region P and its bounding segments. The negative gradients $-\nabla F_{l_1,l_2}$ with $m_1 \le l_1 < l_2 \le j$ point into P along $A_1 \cup A_2 \cup B_1 \cup B_2$.

Proof. For any $i \le l_1 < l_2 \le m_1$, (5) implies that $N_\epsilon Q1(m_2, j) \subset Q1(l_1, l_2)$ Moreover, Properties 7 and 10 imply that an (l_1, l_2)-flow line that begins in $N_\epsilon Q1(m_2, j)$ cannot leave $N_\epsilon Q1(m_2, j)$ as t-increases (since $-\nabla F_{l_1,l_2}$ points inward along all portions of the boundary of $N_\epsilon Q1(m_2, j)$). Within $N_\epsilon Q_1(m_2, j)$, sheets appear in the same order that they are indexed, so any branch of the PFT tree that is below the initial (i, m_1)-flow line can only be an (l_1, l_2)-flow with $i \le l_1 < l_2 \le m_1$. (Any Y_0-vertices, including punctures, can only increase the first subscript and decrease the second.) The result then follows, since the only Reeb chord with upper and lower sheets S_{l_1} and S_{l_2} contained in $N_\epsilon Q1(m_2, j)$ is $a^{+,+}_{l_1,l_2}$. □

Lemma 6.12 (Third Quadrant Lemma)**.** *Suppose $i < m_1 \le m_2 < j$ and $x \in N_\epsilon Q3(i, m_1) \cap [1/2, 1] \times [1/2, 1]$.*

Then any PFT beginning with an (m_2, j)-flow at x has

1. *all endpoints at $a^{-,-}$'s and e-vertices, or*
2. *at least 1 endpoint at an exceptional generator.*

Proof. We begin by establishing the following Lemma.

Lemma 6.13. *Consider a PFT, Γ, that begins with a (m_2, j)-flow line at a point $x \in N_\epsilon Q3(i, m_1) \cap [1/2, 1] \times [1/2, 1]$, for some $i < m_1 \le m_2 < j$. Let γ be a path beginning at x and consisting of several consecutive edges of Γ, (each parametrized according to their orientation in Γ). The path γ must cross into $[1/4, 1/2] \times [1/4, 1/2]$ before leaving $N_\epsilon Q3(i, m_1)$.*

Proof of Lemma 6.13. Consider the (non-convex) hexagonal subset P of $N_\epsilon Q3(i, m_1)$ bounded by line segments $A_1, A_2, B_1, B_2, C_1, C_2$. Here, B_1 and B_2 are the segments from Property 12; A_1 is the vertical segment from $(\beta^U_{i,m_1} + \epsilon, \beta^U_{i,m_1} + \epsilon) = (\beta^R_{i,m_1} + \epsilon, \beta^R_{i,m_1} + \epsilon)$ to the right endpoint of B_1; and C_1 is the vertical segment from $(1/2, 1/2)$ to the left endpoint of B_1. The remaining segments A_2, B_2, C_2 are obtained from reflecting A_1, B_1, C_1 across $x_1 = x_2$. See Figure 33.

The region P satisfies

$$N_\epsilon Q3(i, m_1) \cap [1/2, 1] \times [1/2, 1] \subset P \subset N_\epsilon Q3(i, m_1) \cap [1/4, 1] \times [1/4, 1].$$

Therefore, the path γ which begins in $N_\epsilon Q3(i, m_1) \cap [1/2, 1] \times [1/2, 1]$ must leave P to leave $N_\epsilon Q3(i, m_1)$. Initially, γ is a (m_2, j)-flow line with $i < m_1 \le m_2 < j$. Moreover, until we leave $N_\epsilon Q3(i, m_1) \cap [1/4, 1] \times [1/4, 1]$ the only type of vertices that may appear in Γ are Y_0-vertices. [This is because the cusp locus is disjoint from $N_\epsilon Q3(i, m_1) \cap [1/4, 1] \times [1/4, 1]$.] Within $N_\epsilon Q3(i, m_1) \cap [1/2, 1] \times [1/2, 1]$ the sheets of $\tilde{L}$ appear in the order that they are indexed, thus after a Y_0, either outgoing edge is, for some $m_2 \le l_1 < l_2 \le j$, an (l_1, l_2)-flow line. In particular, the edges that constitute γ consist of such flows as long as γ remains in $N_\epsilon Q3(i, m_1) \cap [1/4, 1] \times [1/4, 1]$. Property 12 then shows that when leaving P the path γ cannot cross B_1 or B_2, and Property 10 shows γ cannot cross our of P along A_1 or A_2. Therefore, γ must leave P along one of the segments C_1 or C_2, and immediately afterward its image lies in $[1/4, 1/2] \times [1/4, 1/2]$. □

We return now to the proof of Lemma 6.12. Consider an endpoint of a partial flow tree Γ satisfying the stated hypothesis. Let γ denote the portion of the tree that travels from x to this endpoint. Applying Lemma 6.13, at some point y the path γ is in $[1/4, 1/2] \times [1/4, 1/2]$. The proof will now be completed by applying the following Lemma 6.14 to the PFT that consists of the subset of Γ below y. □

Lemma 6.14. *Any partial flow tree with initial point in* $[1/4, 1/2] \times [1/4, 1/2]$ *has*

(1) *all endpoints at* $a^{-,-}$*'s or e-vertices, or*
(2) *at least* 1 *endpoint at an exceptional generator.*

Proof. Let $L(1/2) = \{(x_1, x_2) \in \widetilde{N}(e^2_\alpha) \,|\, x_1 \leq 1/2\} \bigcup N(e^0_{-,+}) \bigcup N(e^0_{-,-})$ and $D(1/2) = \{(x_1, x_2) \in \widetilde{N}(e^2_\alpha) \,|\, x_2 \leq 1/2\} \bigcup N(e^0_{+,-}) \bigcup N(e^0_{-,-})$ so that $L(1/2) \cap D(1/2) = \{(x_1, x_2) \in \widetilde{N}(e^2_\alpha) \,|\, x_1 \leq 1/2,\, x_2 \leq 1/2, \} \bigcup N(e^0_{-,-})$.

We prove the stronger statement that any PFT with initial point in $L(1/2) \cap D(1/2)$ satisfies (1) or (2).

Claim 1. If sheets i, j with $i < j$ do not have a crossing arc on the R (resp. U) and do not meet at a cusp above the R (resp. U) edge, then $L(1/2)$ (resp. $D(1/2)$) is invariant for the (i, j)-flow, i.e. is $-\nabla F_{i,j}$ invariant in positive time.

This follows since together Properties 2, 3, 7, and 11 show that $-\nabla F_{i,j}$ points inward along all portions of the boundary.

Claim 2. Any partial flow tree starting with a (j, i)-flow line with $j > i$ has an endpoint at an exceptional generator.

At the first Y_0-vertex, the (j, i)-flow will split into edges that are (j, m)-flows and (m, i)-flows. Since $j > i$, we will have either $j > m$ or $m > i$. Proceeding inductively, we can then find an endpoint that limits to a Reeb chord whose upper endpoint is on a sheet with larger label than the lower endpoint. All such Reeb chords are exceptional.

Claim 3. Consider a square that has 2 crossings along the edge R, i.e. of type (5), (6), (8) or (12), so that along R sheet $k + 2$ crosses sheets $k + 1$ and k. [Sheets are labelled as they appear at $(+1, +1)$.] Then, any partial flow tree that begins with a $(k + 1, k + 2)$-flow in $D(1/2)$ has at least one endpoint at an exceptional Reeb chord.

From Claim 1, we see that $D(1/2)$ is $(k + 1, k + 2)$-invariant. [In any of the 12 squares, it is never the case that the same two sheets cross on both the edges R and U.] Observe that there are in fact no non-exceptional $(k + 1, k + 2)$ Reeb chords in $D(1/2)$ (and, in the case of a Type (12) square, no $(k + 1, k + 2)$ cusp edge). Thus, such a partial flow tree without Y_0-vertices would necessarily contain an exceptional generator. In all cases except for Type (8), sheets $k + 1$ and $k + 2$ are always adjacent in $D(1/2) \cap \{F_{k+1,k+2} > 0\}$, so no Y_0-vertex can occur. For a Type (8) square, the only portion of $D(1/2) \cap \{F_{k+1,k+2} > 0\}$ where a Y_0-vertex may occur in a $(k + 1, k + 2)$-flow is in the portion of the square where sheets appear in the order $z(S_{k+1}) > z(S_k) > z(S_{k+2})$. See Figure 34. One of the outgoing branches of such a Y_0-vertex would be a $(k + 1, k)$-flow, and Claim 2 would then imply that the tree has an endpoint at an exceptional generator.

With Claims 1-3 in hand, suppose that we are given a partial flow tree in a square of type (1)-(12) that begins with an (i, j)-flow at $x \in L(1/2) \cap D(1/2)$. In establishing the conclusion of the lemma, by Claim 2, we may assume $i < j$. We first treat all of the special cases in which the i and j sheets cross or meet at a cusp edge, and then address the remaining cases inductively. Note that an (i, j) crossing or cusp arc cannot have endpoints on both the R and U edge.

- Case 1: The (i, j) crossing arc does have a single endpoint on edge R or U. This includes the squares of type (2), (4)-(8), (10), (12) where (i, j) can correspond to any of the crossing arcs. Note that for any of the squares (5), (6), (12) with $(i, j) = (k + 1, k + 2)$, Claim 3 applies. The remaining cases are as follows:
  - Subcase 1: The square is any of (2), (4), (7), (10) with (i, j) any of the pictured arcs. First consider the case where the (i, j) crossing occurs on edge R. Then, from Claim 1, $D(1/2)$ is (i, j)-invariant. Moreover, in the subset of $D(1/2)$ where $F_{i,j} > 0$, the sheets

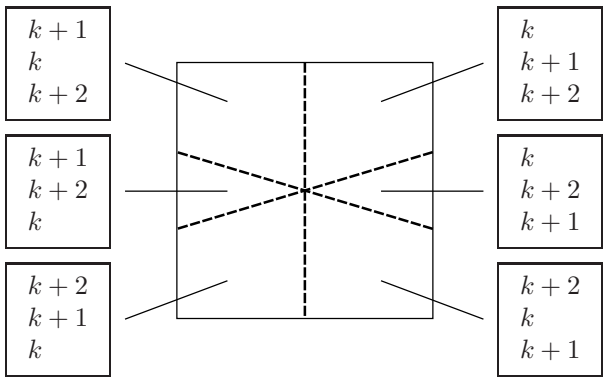

FIGURE 34. The order in which the 3 sheets that meet at a triple point appear in the 6 portions of a Type (8) square.

i and j are adjacent so that there are no possibilities for a partial flow starting at x to have Y_0-vertices. Finally, observe that the only non-exceptional (i,j) Reeb chord in $D(1/2) \cap \{F_{i,j} > 0\}$ is at $(-1,-1)$. [For a general square, the only non-exceptional (i,j) Reeb chords in $D(1/2)$ are $a^{-;-}_{i,j}, b^D_{i,j}$ and $a^{+;-}_{i,j}$, but in the present case there are no Reeb chords of the form $b^D_{i,j}$ and $a^{+;-}_{i,j}$ as they would necessarily on the other side of the (i,j) crossing arc.]

If the crossing occurs on edge U, a similar argument (reflected across $x_1 = x_2$) applies.

- Subcase 2: The square is (5), (6), or (12) with $(i,j) = (k, k+2)$. Again, $D(1/2)$ is $(k,k+2)$ invariant, and the only non-exceptional $(k,k+2)$ Reeb chord in $D(1/2)$ would have the form $a^{-;-}_{i,j}$. Thus, in the case there are no Y_0-vertices the result follows. If the flow tree has Y_0-vertices, then at the first Y_0-vertex the tree splits into a $(k,k+1)$-flow and a $(k+1,k+2)$-flow in the region above the $(k+1,k+2)$-crossing arc. Now, an application of Claim 3 shows that the flow tree must contain an exceptional generator.
- Subcase 3: The triple point square (8). The case $(i,j) = (k+1,k+2)$ is covered by Claim 3. For $(i,j) = (k,k+1)$, the partial flow tree must have an end point at an exceptional generator. This follows since $L(1/2)$ is (i,j)-invariant and contains no non-exceptional Reeb chords of type (i,j). The only possibility for a Y_0-vertex would produce an outgoing edge that is a $(k+2,k+1)$-flow to which we apply Claim 2. (See Figure 34.)

  Finally, consider $(i,j) = (k,k+2)$. The $(k,k+2)$-flow is $D(1/2)$-invariant with all (i,j) Reeb chords in $D(1/2)$ exceptional. If a Y_0-vertex occurs one out going edge will be a $(k+1,k+2)$-flow in $D(1/2)$ which must have an endpoint at an exceptional generator by Claim 3.

- Case 2: The (i,j) crossing arc has its endpoints on edges L and D. This only occurs in (3) with $(i,j) = (k,k+1)$. Here, Claim 1 gives that $L(1/2) \cap D(1/2)$ is $(k,k+1)$-invariant. In this region, sheets k and $k+1$ are adjacent and all $(k,k+1)$ Reeb chords are exceptional.
- Case 3: The (i,j) cusp edge has its endpoint on U or R. Supposing the cusp edge lies on U, Claim 1 shows that $L(1/2)$ is (i,j) invariant. As they are adjacently indexed, any Y_0 would produce an outgoing edge that is a (m,n)-flow with $m > n$, and Claim 2 would then produce an exceptional generator. Since there are no (i,j) Reeb chords in $L(1/2)$, if the PFT has no Y_0's, then the (i,j)-flow necessarily reaches an e-vertex.

With the special cases out of the way we handle the general case using induction on the number of Y_0-vertices in the partial flow tree. Since we can assume that the i,j sheets do not cross, Claim 1 shows that the quadrant $L(1/2) \cap D(1/2)$ is (i,j)-invariant. The only (i,j)-Reeb chord in $L(1/2) \cap D(1/2)$ is $a^{-;-}_{i,j}$, so in the case of no Y_0-vertices the result holds. For the inductive step, at the first Y_0-vertex, an (i,j)-flow line splits into a (i,l)-flow line and a (l,j)-flow line for some l. Since $L(1/2) \cap D(1/2)$ is (i,j) invariant, the inductive hypothesis applies to both partial flow trees below the Y_0-vertex. □

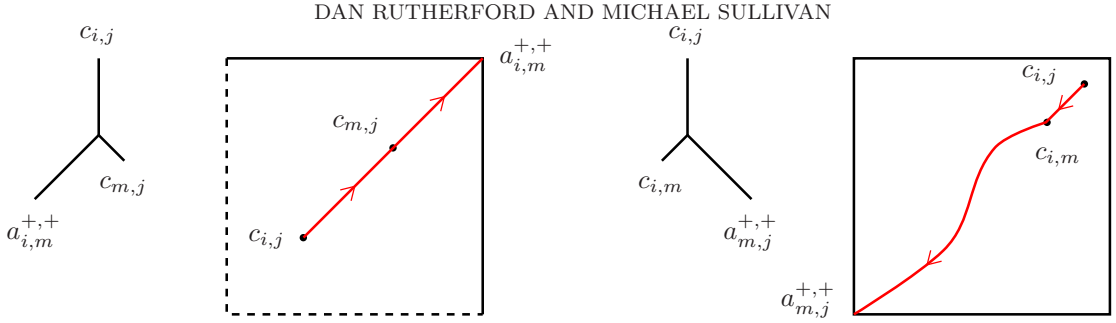

FIGURE 35. The domain and image (in red) of the trees from Terms 1 and 2. The short edges in the domain trees are constant when mapped into $N(e^2_\alpha)$.

Proof of Theorem 6.10. The matrix formula (10) is equivalent to the term-by-term formula

$$\partial_c c_{i,j} = \sum_{i<m<j} \left(a^{+,+}_{i,m} c_{m,j} + c_{i,m} a^{-,-}_{m,j} \right) + x \tag{11}$$

where any of the terms $a^{-,-}_{i,m}$ which correspond to Reeb chords that do not exist or are exceptional generators are replaced with 0, except that $a^{-,-}_{k,k+1}$ is replaced with 1 if S_k and S_{k+1} meet at a cusp edge in $N(e^2_\alpha)$; the x is an element of the ideal generated by exceptional generators in $N(e^2_\alpha)$. We show that, aside from x, each of the non-zero terms in (11) corresponds to an odd number of rigid GFTs beginning at $c_{i,j}$ and that any other rigid GFTs with an output at some $c_{r,s}$ or $\tilde{c}_{r,s}$ must have endpoints at exceptional generators.

For each of the (non-zero) quadratic terms of (11) we now observe a single GFT beginning at $c_{i,j}$ (and rigid by Proposition 6.9) whose word agrees with the given term.

Term 1: $a^{+,+}_{i,m} c_{m,j}$ for $i < m < j$.

Travel along the unique (i,j)-flow line beginning at $c_{i,j}$ that intersects $c_{m,j}$. Once this point is reached a puncture occurs. That is, a Y_0-vertex appears where the two outgoing edges are an (i,m)-flow line and the constant (m,j)-flow line at $c_{m,j}$. Since $c_{m,j} \in N_\epsilon Q1(m,j)$, the non-constant outgoing edge is an (i,m)-flow line that limits to an output vertex at $a^{+,+}_{i,m}$ by Lemma 6.11. See Figure 35.

Term 2: $c_{i,m} a^{-,-}_{m,j}$ for $i < m < j$. Travel along the (i,j)-flow line that hits $c_{i,m}$, and then puncture. Since $c_{i,m} \in N_\epsilon Q3(i,m)$, Lemma 6.12 shows that the outgoing (m,j)-flow line behaves as follows:

(1) It limits to $a^{-,-}_{m,j}$ as long as S_m and S_j do not cross and they both exist at $(x_1,x_2) = (-1,-1)$.
(2) If S_m and S_j cross, then if the crossing locus separates $c_{i,m}$ from $(-1,-1)$ the flow line runs into the crossing locus (and is not part of a valid GFT). In the case that the crossing locus does not separate $c_{i,m}$ from $(-1,-1)$, as can happen for Type (4) or (6) squares, the flow line may either run into the crossing locus or end at $a^{-,-}_{m,j}$. For such squares, $a^{-,-}_{m,j}$ is an exceptional generator so the precise behavior is not relevant.
(3) If S_m or S_j meets a third sheet in a cusp edge, then the (m,j)-flow line ceases to exist when the cusp edge is reached (and is not part of a valid GFT).
(4) If S_m and S_j meet one another at a cusp, then the flow line reaches an e-vertex at the cusp edge. In this case we do have a valid rigid GFT.

Note that the results described in (2) and (3) are consistent with the 0 entries that appear in $A^{-,-}$ as a result of crossings or cusps. Replacing the $(k,k+1)$-entry of $A^{-,-}$ with a 1 when S_k and S_{k+1} meet at a cusp edge is consistent with (4). See Figure 35.

Proof of uniqueness. We have thus identified a single rigid GFT for each of the (non-zero) terms in (11) aside from x. To complete the proof, we show that these are the only rigid GFTs beginning at $c_{i,j}$ with at least one output at some $c_{r,s}$ or $\tilde{c}_{r,s}$ and without any outputs at exceptional generators. We follow the outline indicated in Figure 36.

Let Γ be a rigid GFT that begins at some $c_{i',j'}$, $i' < j'$, without endpoints at exceptional generators and having at least one puncture at some $c_{r,s}$ or $\tilde{c}_{r,s}$. In the latter case, we are done since $\tilde{c}_{r,s}$ is an exceptional generator.

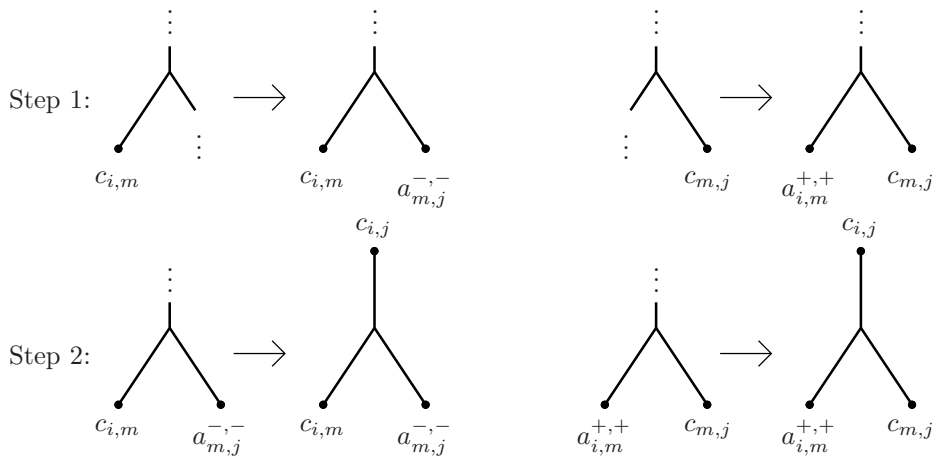

FIGURE 36. Steps 1 and 2 in the Proof of Uniqueness.

Step 1. If Γ has an (i,j)-edge that punctures at $c_{i,m}$ (resp. $c_{m,j}$), then there are no further internal vertices on the non-constant branch that follows the puncture. Thus, after the puncture Γ agrees with the GFT found in Step 1 (resp. Step 2).

The critical point $c_{i,m}$ is located in $N_\epsilon Q3(i,m) \cap [1/2,1] \times [1/2,1]$. Therefore, the PFT starting with the non-constant branch following the puncture begins with a (m,j)-flow in $N_\epsilon Q3(i,m) \cap [1/2,1] \times [1/2,1]$, and Lemma 6.12 implies all endpoints below the puncture must be at $a^{-,-}$ Reeb chords or e-vertices. A similar argument with Lemma 6.11 used in place of Lemma 6.12 shows that all endpoints below a puncture at $c_{k,j}$ must be at $a^{+,+}$ Reeb chords. Since Proposition 6.8 shows that any internal vertices of Γ must be Y_0's, the number of outputs of the PFT that starts below the puncture will be equal to the number of Y_0's plus 1. However, Proposition 6.9 states that the total number of outputs of Γ at a Reeb chords and e-vertices must be the same as the number of c outputs. Thus, there can be only one a or e-vertex below any c puncture, so after the puncture there are no Y_0-vertices and Step 1 follows.

In addition, Proposition 6.9 together with Step 1 show that:

(12) Any edge with its endpoint at an a or e-vertex must begin with a Y_0 that is a puncture at a c.

[As we have seen, any puncture at a c Reeb chord has its non-constant branch ending at an a or an e-vertex. This, gives an injection from the set of c endputs of Γ to the set of endpoints of Γ at a Reeb chords and at e-vertices. Proposition 6.9 shows that this injection is actually a bijection.]

Step 2. In (the domain of) Γ a puncture at a c cannot appear below any internal vertex, x.

By Proposition 6.8 the internal vertex x can only be a Y_0-vertex.

Case 1: Assume $i < j < l$, and an (i,l)-flow branches at x into the (i,j)-flow to some c and a (j,l)-flow.

- Subcase $c = c_{i,m}$: Introduce the notation
$$Sq(c_{i,m}, c_{i,j}) = [\beta^U_{i,m} - \epsilon, \beta^U_{i,j} + \epsilon] \times [\beta^R_{i,m} - \epsilon, \beta^R_{i,j} + \epsilon],$$
which may be approximately viewed as a square with lower left corner at $c_{i,m}$ and upper right corner $c_{i,j}$. See Figure 37. According to Property 10, $-\nabla F_{i,j}$ points outward along each of the edges of $Sq(c_{i,m}, c_{i,j})$. Therefore, as we follow the (i,j)-edge with decreasing t, from its end at $c_{i,m}$ towards its beginning at x, the edge cannot leave the square. Thus,
$$x \in Sq(c_{i,m}, c_{i,j}) \subset N_\epsilon Q3(i,j) \cap ([1/2,1] \times [1/2,1]),$$
and we apply Lemma 6.12 to the (j,l)-branch that starts at x to arrive at a contradiction of (12).
- Subcase $c = c_{m,j}$: A similar argument shows
$$x \in Sq(c_{i,j}, c_{m,j}) \subset N_\epsilon Q3(m,j) \cap ([1/2,1] \times [1/2,1]),$$
and we again apply Lemma 6.12 to the (j,l)-branch starting at x to deduce a contradiction.

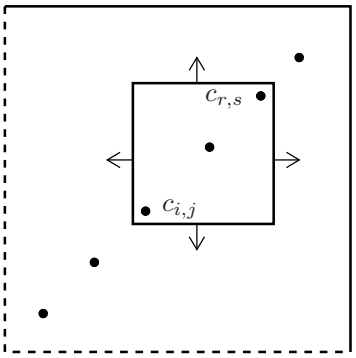

FIGURE 37. The square, $Sq(c_{i,j}, c_{r,s})$. For any (p,q) such that $(i,j) \preceq (p,q) \preceq (r,s)$ with respect to lexicographic order, $-\nabla F_{p,q}$ points outward along all edges of $Sq(c_{i,j}, c_{r,s})$.

Case 2: Assume $h < i < j$, and an (h,j)-flow branches at x into an (h,i)-flow and the (i,j)-flow to c.
An argument similar to that of Case 1 applies with Lemma 6.11 used in place of Lemma 6.12.

At this point, as a consequence of Steps 1 and 2, we see that Γ must be one of the trees identified in Terms 1 and 2 above. This completes the proof.

□

6.5. **Rigid GFTs without outputs at any $c_{i,j}$.** For $1 \leq i < j \leq n$, let

$$\partial_b c_{i,j} = \sum_{\Gamma} w(\Gamma)$$

where the sum is over rigid GFTs that do *not* have outputs at Reeb chords of the form $c_{r,s}$ or $\tilde{c}_{r,s}$.

Theorem 6.15. *For a 2-cell e^2_α of type (1)-(12), and for any $1 \leq i < j \leq n$, we have*

$$\partial_b C = (I + B_R)(I + B_D) + (I + B_U)(I + B_L) + X_2 \tag{13}$$

where the matrices C, and B_R, B_D, B_U, B_L are as in Theorem 6.5, while X_2 is a matrix whose entries belong to the 2-sided ideal generated by exceptional generators in $N(e^2_\alpha)$.

We prove Theorem 6.15 at the conclusion of this section after reducing the computation to a purely topological problem.

6.5.1. *b-trees.*

Lemma 6.16. *In $N(e^2_\alpha)$ where e^2_α has type (1)-(12), any rigid GFT starting at a $c_{i,j}$ and without outputs at Reeb chords of the form $c_{r,s}$ or $\tilde{c}_{r,s}$ must have*

1. *all outputs at Reeb chords of the form $b^X_{i,j}$ or $\tilde{b}^X_{i,j}$ with $X \in \{R, D, L, U\}$; and*
2. *all internal vertices are Y_0's.*

Proof. This is a consequence of Propositions 6.8 and 6.9. □

Definition 6.17. A **b-tree** is a PFT or GFT that satsifies conditions (1) and (2) from Lemma 6.16 and also has

3. no outputs at exceptional generators.

Define a **b^{LU}-tree** to be a b-tree with all endpoints at $b^L_{i,j}$ and/or $b^U_{i,j}$ Reeb chords. Define a **b^{RD}-tree** in a similar manner.

For $1 \leq i < j \leq n$, define a region $B^{LU}(i,j) \subset \widehat{N}(e^2_\alpha)$ to be the closed subset that is

- bounded on the right by $x_1 = \beta^U_{i,j} + \epsilon$;
- bounded below by (i) the horizontal segment from $(\beta^U_{i,j} + \epsilon, \beta^R_{i,j} - \epsilon)$ to the barrier B_2 from Property 12; (ii) the part of the barrier B_2 that lies between $x_2 = \beta^R_{i,j} - \epsilon$ and $x_2 = 1/2$; and (iii) the horizontal segment at $x_2 = 1/2$ from B_2 to the left boundary of $\widehat{N}(e^2_\alpha)$; and

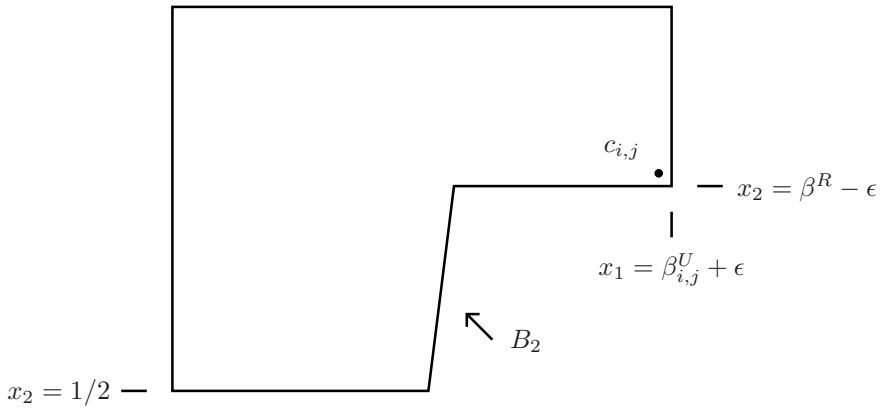

FIGURE 38. The region $B^{LU}(i,j)$. In the later Section 7.4.1, we will modify the definition of $B^{LU}(i,j)$ so that the segment B_2 from Property 12 is replaced with the Swallow Tail Barrier, P, from Property 16.

- bounded on the left and above by $\partial\widehat{N}(e^2_\alpha)$.

In addition, define regions $B^{RD}(i,j)$ to be the reflection of $B^{LU}(i,j)$ across the line $x_1 = x_2$. See Figure 38.

Lemma 6.18. *Any edge, γ, of a b^{LU}-tree (resp. a b^{RD}-tree) must*

1. *be an (i,j)-flow line for some $i < j$ and*
2. *have the intersection of its image with $\widehat{N}(e^2_\alpha)$ contained in the region $B^{LU}(i,j)$ (resp. $B^{RD}(i,j)$). Moreover, the image of γ is entirely in $\widehat{N}(e^2_\alpha)$ unless γ is part of a $b^X_{i,j}$-line for $X \in \{L,D,R,U\}$.*

(The terminology *$b^X_{i,j}$-line* from (2) is as in 6.3.2.)

Proof. First, in some cases, we need to focus on certain subsets $A^{LU}(i,j) \subset B^{LU}(i,j)$ defined by

1. $A^{LU}(i,j) = B^{LU}(i,j) \cap \{x_1 \geq 1/4\}$ if either S_i and S_j cross above e^1_U or meet one another at a cusp above e^1_U;
2. $A^{LU}(i,j) = B^{LU}(i,j) \cap \{x_1 \geq -3/8\}$ when exactly one of S_i and S_j ends at a cusp edge above e^1_U; and
3. $A^{LU}(i,j) = B^{LU}(i,j)$ in all other cases.

Observe that that $-\nabla F_{i,j}$ points outward along all segments of $\partial A^{LU}(i,j)$. [With $A^{LU}(i,j)$ as in (1), for boundary segments that are not part of $\partial\widehat{N}(e^2_\alpha)$, just use Properties 10, 11 and 12; as in (3) add Properties 11; as in (2) add Property 13.]

We prove the proposition by establishing the same result with each $B^{LU}(i,j)$ replaced with $A^{LU}(i,j)$ (this is a stronger statement) using induction on N, the number of Y_0's in the PFT beginning with γ. By Proposition 5.11, all of the $b^L_{i,j}$- and $b^U_{i,j}$-lines intersect $\partial\widehat{N}(e^2_\alpha)$ at a point in $\partial A^{LU}(i,j)$. [Note that if $A^{LU}(i,j)$ is as in (1) or (2) then there is no $b^L_{i,j}$-line.] It follows that as t decreases they must remain in $A^{LU}(i,j)$. Thus, the case $N = 0$ holds.

For the inductive step, consider the Y_0 at the end of γ. Both of the PFTs that begin with the outgoing edges of the Y_0 are themselves b^{LU}-trees. Thus, by the inductive hypothesis, this Y_0 has its image in $A^{LU}(i,m) \cap A^{LU}(m,j)$ for some m with $i < m < j$. [Note that the parts of the $b^L_{i,j}$- and $b^U_{i,j}$-lines that lie outside of $B^{LU}_{i,j}$ are contained in disjoint strips in e^1_L and e^1_U and cannot intersect one another.] Thus, the result follows once we verify that:

Claim. For any Type (1)-(12) square, e^2_α, for all $i < m < j$, we have $A^{LU}(i,m) \cap A^{LU}(m,j) \subset A^{LU}(i,j)$.

That

$$A^{LU}(i,m) \cap A^{LU}(m,j) \subset B^{LU}(i,m) \cap B^{LU}(m,j) \subset B^{LU}(i,j)$$

holds in general. [The second inclusion is easily verified using the lexicographic ordering of the $\beta_{i,j}$. See Figure 39.] Thus, when $A^{LU}(i,j) = B^{LU}(i,j)$ the Claim follows. Now, if $A^{LU}(i,j)$ is as in (2),

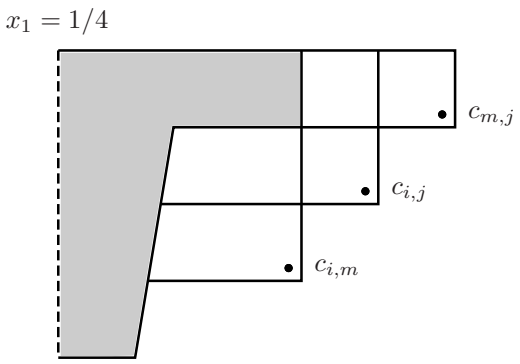

FIGURE 39. The regions $B^{LU}(i,m)$, $B^{LU}(m,j)$, and $B^{LU}(i,j)$ all agree to the left of $x_1 = 1/4$. There bordering segments are pictured, with $B^{LU}(i,m) \cap B^{LU}(m,j)$ shaded.

then at least one of the pairs (i,m) and (m,j) includes a sheet that ends at a cusp edge above e^1_U, and so at least one of $A^{LU}(i,m)$ or $A^{LU}(m,j)$ lies entirely to the right of $x_1 = -3/8$ so that

$$A^{LU}(i,m) \cap A^{LU}(m,j) \subset (B^{LU}(i,m) \cap B^{LU}(m,j)) \cap \{x_1 \geq -3/8\} \subset$$
$$B^{LU}(i,j) \cap \{x_1 \geq -3/8\} = A^{LU}(i,j).$$

Finally, if $A^{LU}(i,j)$ is as in (1), then the only way that there exists m with $i < m < j$ is when $\tilde{L}$ has two crossings, i.e. Type (2Cr), above $N(e^1_U)$, and $i = k, m = k+1, j = k+2$. Since sheets $k+1$ and $k+2$ also cross in this case, $A^{LU}(k+1,k+2)$ is also as in (1), and we see that

$$A^{LU}(k,k+1) \cap A^{LU}(k+1,k+2) \subset (B^{LU}(i,m) \cap B^{LU}(m,j)) \cap \{x_1 \geq 1/4\} \subset$$
$$B^{LU}(i,j) \cap \{x_1 \geq 1/4\} = A^{LU}(i,j).$$

□

Proposition 6.19. *Any b-tree is either a b^{LU}-tree or a b^{RD}-tree.*

Proof. Use induction on the number of Y_0's and Lemma 6.18. At the inductive step, note that the regions $B^{LU}(i,j)$ and $B^{RD}(i',j')$ are all disjoint except when $(i,j) = (i',j')$. □

6.5.2. *Topological preliminary.* Let D be a (region diffeomorphic to) a closed disk in $\mathbb{R}^2$. Suppose that we are given a collection of points $\{p_1, \ldots, p_M\} \subset \partial D$ and a collection of closed intervals $\{I_{i,j} \,|\, 1 \leq i < j \leq n\}$ with $I_{i,j} \subset \partial D$. In addition, suppose that

- the points p_m and intervals $I_{i,j}$ are all pairwise disjoint from one another, and
- each point p_m is assigned an **upper index** $i(p_m)$ and a **lower index** $j(p_m)$ that are integers with $1 \leq i(p_m) < j(p_m) \leq n$.

We refer to such a triple $(D, \{p_m\}, \{I_{i,j}\})$ as a **disk datum**.

Definition 6.20. A **generalized b-manifold** for the disk datum $(D, \{p_m\}, \{I_{i,j}\})$ is a collection $A = \bigsqcup_{r=1}^{n-1} A_r$ of (embedded) paths in D with the following properties:

(1) Each path $\gamma \in A_r$ has upper and lower indices, $1 \leq i(\gamma) < j(\gamma) \leq n$, satisfying $r = j(\gamma) - i(\gamma)$.
(2) For any $\gamma \in A$, the initial point of γ belongs to $I_{i(\gamma),j(\gamma)}$.
(3) For $r \geq 1$, paths in A_r are in bijection with (i) points p_m, with $r = j(p_m) - i(p_m)$, and (ii) triples (γ_1, γ_2, x) where $\gamma_1 \in A_{r_1}$, $\gamma_2 \in A_{r_2}$, $x \in \gamma_1 \cap \gamma_2$, that satisfy $r_1 + r_2 = r$, and $j(\gamma_1) = i(\gamma_2)$.
(4) A path $\gamma \in A_r$ corresponding to a point p_m as in (3) (i) has its endpoint at p_m and satisfies $(i(\gamma), j(\gamma)) = (i(p_m), j(p_m))$.
(5) A path $\gamma \in A_r$ corresponding to a triple (γ_1, γ_2, x) as in (3) (ii) has its endpoint at x and satisfies $(i(\gamma), j(\gamma)) = (i(\gamma_1), j(\gamma_2))$.
(6) All intersections between distinct $\gamma_1, \gamma_2 \in A$ are transverse. Moreover, the only case when intersections can occur at endpoints of a path, or when three paths meet at a common point is as specified in (5). There are no points where four or more paths intersect.

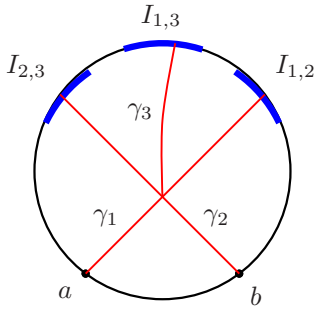

FIGURE 40. A generalized b-manifold, A, for the disk datum $(D, \{a, b\}, \{I_{1,2}, I_{1,3}, I_{2,3}\})$ with $(i(a), j(a)) = (1, 2)$ and $(i(b), j(b)) = (2, 3)$. Here, $A = A_1 \sqcup A_2$ with $A_1 = \{\gamma_1, \gamma_2\}$ and $A_2 = \{\gamma_3\}$. We have $\partial_A I_{1,2} = a$, $\partial_A I_{2,3} = b$, and $\partial_A I_{1,3} = ab$.

See Figure 40 for an example of a generalized b-manifold.

For each path $\gamma \in A$, we assign a **word**, $w(\gamma)$, that is a formal product of points from $\{p_1, \dots, p_M\}$, and a **sign**, $\sigma(\gamma) \in \{+1, -1\}$, as follows.

- For γ corresponding to a point p_m as in (3) (i), let $w(\gamma) = p_m$ and $\sigma(\gamma) = +1$.
- For γ corresponding to a triple (γ_1, γ_2, x) as in (3) (ii), let $w(\gamma) = w(\gamma_1) \cdot w(\gamma_2)$ and $\iota(\gamma_1, \gamma_2, x)\sigma(\gamma_1)\sigma(\gamma_2)$. Here, $\iota(\gamma_1, \gamma_2, x)$ is the intersection sign of $\gamma_1 \cap \gamma_2$ at x. (We assume an orientation on D is fixed.)

For $1 \leq i < j \leq n$, we define an element $\partial_A I_{i,j} \in \mathbb{Z}\langle p_1, \dots, p_M \rangle$ in the free associative $\mathbb{Z}$-algebra generated by $\{p_1, \dots, p_M\}$ by

$$\partial_A I_{i,j} = \sum_{\gamma} \sigma(\gamma) w(\gamma) \tag{14}$$

where the sum is over those $\gamma \in A$ that begin on $I_{i,j}$. (We introduce here a $\mathbb{Z}$-algebra instead of a $\mathbb{Z}_2$-algebra because we hope to generalize our main DGA computations to $\mathbb{Z}$-coefficients in a future paper. For this article, however, the reader can think of $\partial_A I_{i,j} \in \mathbb{Z}_2\langle p_1, \dots, p_M \rangle$.)

Main Example. Consider a Type (1)-(12) square, e^2_α, such that $\tilde{L}$ has n sheets above $N(e^2_\alpha)$. We let $D^{LU} \subset [-1, 1] \times [-1, 1]$ be obtained from $\bigcup_{1 \leq i < j \leq n} B^{LU}(i, j)$ by removing the small squares $Sq_{i,j} := (\beta^U_{i,j} - \epsilon, \beta^U_{i,j} + \epsilon) \times (\beta^R_{i,j} - \epsilon, \beta^R_{i,j} + \epsilon)$ that contain the $c_{i,j}$. Let $I_{i,j} \subset \partial D^{LU}$ be the upper and left sides of the closed square $\overline{Sq_{i,j}}$. By a slight abuse of notation, for $i < j$, we use $b^L_{i,j}$ and $b^U_{i,j}$ to denote the unique intersection point of the stable manifolds of these critical points with the boundary of $\widehat{N}(e^2_\alpha)$. (Note that $b^L_{i,j}$ is only defined for those $i < j$ such that S_i sits above S_j along the upper half of e^1_L.) The triple $(D^{LU}, \{b^L_{i,j}, b^U_{i,j}\}, \{I_{i,j}\})$ is a disk datum, where the upper and lower indices of the points $\{b^L_{i,j}, b^U_{i,j}\}$ are given by their subscripts. See Figure 41.

We will define a generalized b-manifold for the disk datum $(D^{LU}, \{b^L_{i,j}, b^U_{i,j}\}, \{I_{i,j}\})$. Suppose that $\widehat{\gamma}$ is the top branch of a GFT that is a b^{LU}-tree beginning at some $c_{i,j}$, and let $\gamma = \widehat{\gamma} \cap D^{LU}$. In addition, define upper and lower indices $1 \leq i(\gamma) < j(\gamma) \leq n$, so that γ is a trajectory for $-\nabla F_{i(\gamma), j(\gamma)}$, i.e. $S_{i(\gamma)}$ and $S_{j(\gamma)}$ are the sheets of $\widetilde{L}$ that correspond to $\widehat{\gamma}$ in the GFT that it belongs to.

Proposition 6.21. *Let $A = \bigsqcup_r A_r$ denote the collection of such paths γ with $i(\gamma)$ and $j(\gamma)$ as above. Then, A is a generalized b-manifold for the disk datum $(D^{LU}, \{b^L_{i,j}, b^U_{i,j}\}, \{I_{i,j}\})$. Moreover,*

$$\overline{\partial_A I_{i,j}} = \sum_{\Gamma} w(\Gamma)$$

where the sum on the right is over b^{LU}-trees that start at $c_{i,j}$, and $\overline{\partial_A I_{i,j}}$ denotes $\partial_A I_{i,j}$ with coefficients reduced mod 2.

An analogous result holds for b^{RD}-trees.

(Recall that the word, $w(\Gamma)$, of a GFT, Γ, was defined in Section 2.2.1.)

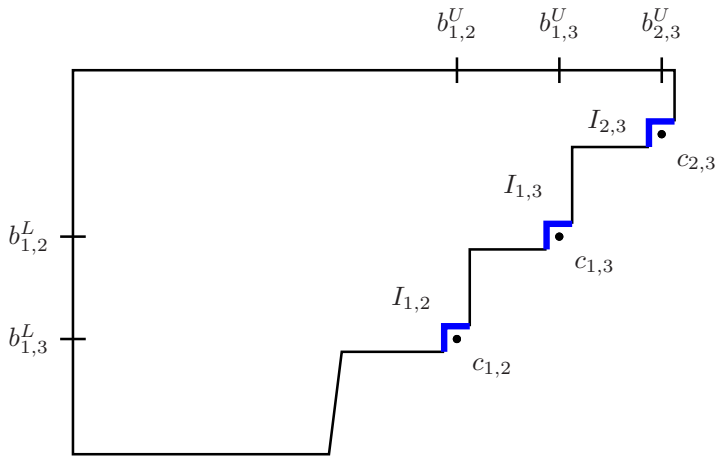

FIGURE 41. The disk datum $(D^{LU}, \{b^L_{i,j}, b^U_{i,j}\}, \{I_{i,j}\})$. In the pictured case the number of sheets is $n = 3$, and sheets 2 and 3 cross one another above e^1_U. Thus, $b^L_{2,3}$ does not exist.

Proof. The condition (1) in Definition 6.20 is clear. Condition (6) is one of the transversality conditions that is implied by $\tilde{L}$ being 1-regular.

The top most branch $\widehat{\gamma}$ of a b^{LU}-tree, Γ, must start at some $c_{i,j}$. Since $c_{i,j} \in Sq_{i,j}$, and $\gamma \subset B^{LU}(i,j)$ (by Lemma 6.18), we see that, as t increases from $-\infty$, $\widehat{\gamma}$ must enter D^{LU} along a unique point in $I_{i,j}$. [Uniqueness follows since $-\nabla F_{i,j}$ points outward along the entire boundary of $Sq_{i,j}$.] Thus, (2) holds.

Now, as $t \to +\infty$, $\widehat{\gamma}$ must either (a) limit to a critical point $b^L_{i,j}$ or $b^U_{i,j}$ or (b) end at a Y_0 that occurs at the intersection of two edges of Γ, γ_1 and γ_2, with $j(\gamma_1) = i(\gamma_2)$. Clearly, those γ satisfying (a) are in bijection with $\{b^L_{i,j}, b^U_{i,j}\}$ as in (3) (i) and satisfy (4). When γ satisfies (b), note that, when extended to allow $t \to -\infty$, the branches γ_1 and γ_2 are themselves the top branches of unique b^{LU}-trees. Thus, the γ satisfying (b) are in bijection with intersection points as in (3) (ii) and satisfy (5).

The equality $\overline{\partial_b I_{i,j}} = \partial_b c_{i,j}$ is clear since the word associated to a path $\gamma \in A$ that is a top branch of the b^{LU}-tree Γ is precisely the word $w(\Gamma)$. [This is verified by an obvious induction.]

□

The following key proposition will allow us to compute $\partial_b c_{i,j}$ without requiring detailed knowledge of the locations of b^X-lines.

Proposition 6.22. *For any disk datum $(D, \{p_m\}, \{I_{i,j}\})$, the sums $\partial_A I_{i,j}$ are independent of the choice of generalized b-manifold, A, associated to $(D, \{p_m\}, \{I_{i,j}\})$.*

Proof. We prove the following statement by induction on R with R decreasing from n to 1:

Inductive Statement: Let $A = \sqcup_{r=1}^{n-1} A_r$ and $A' = \sqcup_{r=1}^{n-1} A'_r$ be two generalized b-manifolds for $(D, \{p_m\}, \{I_{i,j}\})$ such that

$$A_r = A'_r \text{ for all } 1 \leq r < R.$$

Then, for all $1 \leq i < j \leq n$,

$$\partial_A I_{i,j} = \partial_{A'} I_{i,j}$$

where $\partial_A I_{i,j}$ and $\partial_{A'} I_{i,j}$ are elements of $\mathbb{Z}\langle p_1, \ldots, p_M \rangle$ as defined in (14).

The case $R = n$ is tautological. For the inductive step, suppose that the statement is known for larger values of R, and suppose $A_r = A'_r$ for $r < R$. Notice that paths in A_R and A'_R are in bijection, and have the same endpoints and indices. [The number of paths in A_R as well as their endpoints and indices are determined by the $\{p_m\}$ and intersections of paths in $\bigsqcup_{r<R} A_r$.] Thus, without loss of generality, we may assume that A_R and A'_R are identical except for a single pair of paths $\gamma \in A_R$ and $\gamma' \in A_R$ with the same endpoint and equal indices.

Since D is a topological disk, and γ and γ' are smoothly embedded arcs with the same endpoints, they are isotopic via an isotopy of arcs γ^t, $0 \leq t \leq 1$, with $\gamma^0 = \gamma$ and $\gamma^1 = \gamma'$ that preserves endpoints.

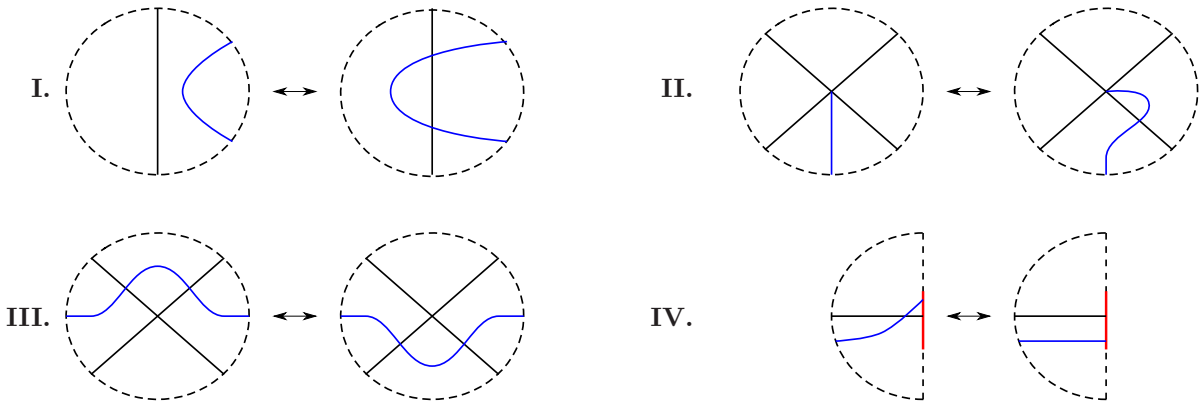

FIGURE 42. Moves I-IV. The blue path denotes γ^t while the black paths belong to X. In Move III, a third path from X may have an endpoint at the crossing of the two black curves. In Move IV, the red segment is part of the interval $I_{i,j} \subset \partial D$.

Set

$$X = \left(\bigsqcup_{r \leq R} A_r \right) \setminus \{\gamma\}.$$

By standard transversality results, after possibly modifying the isotopy γ^t, we may assume that there exist $0 = t_0 < t_1 < \ldots < t_T = 1$ such that, the γ^{t_s} are transverse to all paths in X, and for $1 \leq s \leq T$ either:

O. The paths in $X \cup \{\gamma^{t_s}\}$ are obtained from the corresponding paths in $X \cup \{\gamma^{t_{s-1}}\}$ by applying an orientation preserving diffeomorphism $\varphi : D \xrightarrow{\cong} D$.

Or, when $t_{s-1} < t < t_s$, γ^t remains fixed except in a small disk $D' \subset D$ where one of the following four moves occurs:

I. The disk $D' \subset D$ intersects a single path $\beta \in X$ in a properly embedded arc. For some $t_{s-1} < t < t_s$, γ^t has a tangential intersection with β that results in the creation or cancellation of two transverse intersections.

II. Suppose γ has its endpoint at a transverse crossing point, x, of paths $\beta_1, \beta_2 \in X$. The disk $D' \subset D$ contains x, and for some $t_{s-1} < t < t_s$, γ^t becomes tangent to either β_1 or β_2 at x resulting in the addition or removal of a single transverse intersection between γ^t and β_1 or β_2.

III. The disk $D' \subset D$ contains a crossing, x, of two paths $\beta_1, \beta_2 \in X$. Note that if β_1 and β_2 have a common upper and lower index, then x may be the endpoint of a third path $\beta_3 \in X$. Both $\gamma^{t_{s-1}}$ and γ^{t_s} have a single intersection point with β_1 in D', and these intersection points lie on opposite sides of x. The same holds for intersections of $\gamma^{t_{s-1}}$ and γ^{t_s} with β_2. If β_3 exists, then precisely one of $\gamma^{t_{s-1}}$ and γ^{t_s} intersects β_3 in D', and this intersection is unique.

IV. The disk $D' \subset D$ contains on its boundary part of the interval $I_{i,j}$ where γ has its initial point. For $t_{s-1} < t < t_s$ the endpoint of γ passes the location of the endpoint of another path $\beta \in X$ whose endpoint also lies on $I_{i,j}$. This creates or removes a crossing between γ and β.

See Figure 42 for a depiction of Moves I-IV.

Making use of the inductive hypothesis, it suffices to establish the following:

Claim. For any $1 \leq s \leq T$, there exist some generalized b-manifolds, C and C' for $(D, \{p_m\}, \{I_{i,j}\})$ such that $\partial_C I_{i,j} = \partial_{C'} I_{i,j}$;

$$\bigsqcup_{r \leq R} C_r = X \bigcup \{\gamma^{t_{s-1}}\}; \quad \text{and} \quad \bigsqcup_{r \leq R} C'_r = X \bigcup \{\gamma^{t_s}\}.$$

We prove the claim when $\gamma^{t_{s-1}}$ and γ^{t_s} are related by Moves O and I-III in a case-by-case manner.

Move O. Extend $X \cup \{\gamma^{t_{s-1}}\}$ to obtain a generalized b-manifold C as follows. Take $C_r = A_r$ for $r < R$, and $C_R = (A_R \setminus \{\gamma\}) \bigcup \{\gamma^{t_{s-1}}\}$. We then define C_r with $r > R$ inductively. With all $C_{r'}$ having $r' < r$ already defined, the required number of paths in C_r as well as their endpoints and indices are specified

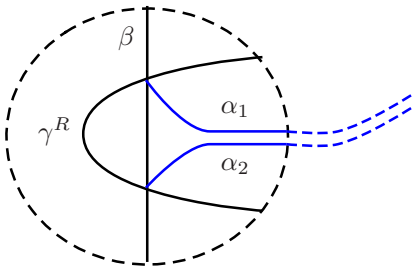

FIGURE 43. The paths α_1 and α_2 from C_1'.

by $\bigsqcup_{r'<r} C_{r'}$ and $\{p_m\}$ according to Definition 6.20. We then define C_r by choosing some collection of paths with the desired endpoints that are transverse to all paths in $\bigsqcup_{r'<r} C_{r'}$ and to one another. [Note that in order for Definition 6.20 to be met, any new intersection points $x \in \beta_1 \cap \beta_2$ with $\beta_1 \in C_r$ and $\beta_2 \in C_{r'}$, for some $r' \leq r$, and such that either $j(\beta_1) = i(\beta_2)$ or $i(\beta_1) = j(\beta_2)$ will have to be the endpoint of some path in $C_{r''}$ with $r'' = r + r'$. Since $r'' > r$, this will be arranged at a later step of the induction, and in particular will not require any modification of the already defined subsets $\bigsqcup_{r'\leq r} C_{r'}$.]

The construction of C is thus completed after finitely many such steps. We then arrive at C' by applying the diffeomorphism φ to each of the paths in C.

In considering Moves I-IV, we assume without loss of generality that $\gamma^{t_{s-1}}$ (resp. γ^{t_s}) corresponds to the diagram on the left (resp. right) as depicted in Figure 42. To simplify notation, we let γ^L and γ^R denote $\gamma^{t_{s-1}}$ and γ^{t_s} as they appear on the left and right side of Moves I-IV.

Move I. As in Move O., extend $X \cup \{\gamma^L\}$ to a generalized b-manifold C, but at the inductive step impose the additional requirement that all new paths are disjoint from D'. Unless $j(\beta) = i(\gamma)$ or $i(\beta) = j(\gamma)$, C' is obtained from C by simply replacing γ^L with γ^R.

Consider now the case where $j(\beta) = i(\gamma)$ or $i(\beta) = j(\gamma)$. Form C_0' from C by replacing γ^L with γ^R. We need to add two additional paths α_1 and α_2 to C_0' that end at the intersection points x_1 and x_2 of γ^R and β that appear on the right side of Move II. Do so by choosing a single path α from the right side of $\partial D'$ to $I_{i,j}$ (where i and j are as specified by the indices of γ^R and β). Then define α_1 and α_2 to travel from x_1 and x_2 to the initial point of α, and then follow parallel to α until they reach $I_{i,j}$. We take α_1 and α_2 to be close enough to one another so that their intersections with paths in C_0' are are in bijection with one another with the same signs, and are located in small neighborhoods of the intersection points of α. Set $C_1' = C_0' \cap \{\alpha_1, \alpha_2\}$. See Figure 43.

Now, the new paths α_1 and α_2 may have corresponding intersection points $y_1 \in \alpha_1 \cap \nu$ and $y_2 \in \alpha_2 \cap \nu$ with some $\nu \in C_1'$, such that for $p = 1, 2$, $i(\alpha_p) = j(\nu)$ or $j(\alpha_p) = i(\nu)$. For each such pair of intersections, we connect y_1 and y_2 to the appropriate $I_{i,j}$ using a pair of sufficiently close paths, and then denote the union of C_1' with all such pairs of paths as C_2'. We proceed inductively, and note that at each step the difference $j - i$ increases for all new paths. Thus, this process terminates after less than n steps, and we take C' to be the resulting generalized b-manifold.

To verify that $\partial_C I_{i,j} = \partial_{C'} I_{i,j}$, note that $(C \setminus \{\gamma^L\}) \subset (C' \setminus \{\gamma^R\})$. Now, $w(\gamma^L) = w(\gamma^R)$, and paths in $C' \setminus (C \cup \{\gamma^R\})$ that begin at $I_{i,j}$ come in pairs (as constructed in the previous paragraph), τ_1 and τ_2, such that $w(\tau_1) = w(\tau_2)$ and $\sigma(\tau_1) = -\sigma(\tau_2)$ (since the two intersections of γ^R with β have opposite signs). Such pairs cancel out in the sum from (14) that defines $\partial_{C'} I_{i,j}$.

Move II. Since the indices of the β_p, $p = 1, 2$, must be of the form (a, b) and (b, c) for some $a < b < c$, and $(i(\gamma), j(\gamma)) = (a, c)$, we have $i(\gamma) \neq j(\beta_p)$ and $j(\gamma) \neq i(\gamma)$. Thus, we can take C to be any extension of $X \cup \{\gamma^L\}$ with all new paths disjoint from D', and set $C' = (C \setminus \{\gamma^L\}) \cup \{\gamma^R\}$.

Move III. Let β_1, β_2 denote the two paths of X that cross in D'. In our figures we picture β_1 with negative slope and β_2 with positive slope. Label the intersection points in D' as $x \in \beta_1 \cap \beta_2$, $y^K \in \beta_1 \cap \gamma^K$, and $z^K \in \beta_2 \cap \gamma^K$ for $K \in \{L, R\}$. See Figure 44.

Introduce the following notation for indices:

$$(a, b) = (i(\beta_1), j(\beta_1)); \quad (c, d) = (i(\beta_2), j(\beta_2)); \quad \text{and} \quad (p, q) = (i(\gamma), j(\gamma)).$$

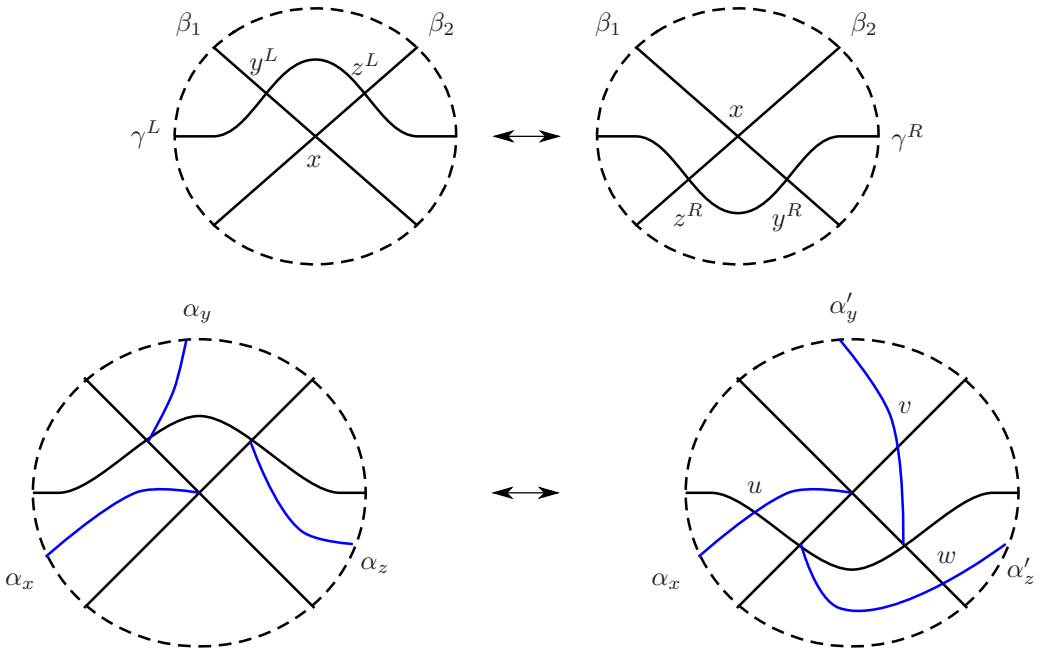

FIGURE 44. (top) The notations used for Move III. (bottom left) The paths α_x, α_y, and α_z are pictured in blue. (bottom right) The paths α_x, α'_y, and α'_z along with intersection points u, v, and w.

Recall that there may be an additional path $\beta_3 \in X$ that intersects D' and has its endpoint at x. If it exists, in D', β_3 intersects precisely one of γ^L and γ^R, and this intersection is in a single point. Without loss of generality we assume that, within D', β_3 is disjoint from γ^L and intersects γ^R precisely once. [If this is not the case, then interchange the left and right side of Move III and rotate the diagrams by 180°.]

To begin, choose an extension of $X \bigsqcup \{\gamma^L\}$ to a generalized b-manifold, C, so that any paths starting at x, y^L, and z^L (should they exist) are respectively disjoint from γ^L, β_2, and β_1. Denote these paths by α_x, α_y, α_z, and note that it may be the case that $\alpha_x = \beta_3$. See Figure 44.

To keep track of indices, it is convenient to assign a coefficient to each path $\nu \in C$, F_ν, that is the strictly upper triangular matrix $F_\nu = \sigma(\nu)E_{i(\nu),j(\nu)} \in Mat(n, \mathbb{Z})$ whose $(i(\nu), j(\nu))$-entry is $\sigma(\nu)$, and with other entries equal to 0. We then make the observation that if two paths $\nu, \nu' \in C$ intersect at a point w then Definition 6.20 specifies that the coefficient of the path in C that ends at w is

$$\iota(\nu, \nu', w)[F_\nu, F_{\nu'}] = \iota(\nu', \nu, w)[F'_\nu, F_\nu]$$

where if $[F_\nu, F_{\nu'}] = 0$, then no such path exists in C. Thus, we interpret a coefficient of 0 to indicate that the path is not part of C.

Above, $[\cdot, \cdot]$ is the commutator of matrices in $Mat(n, \mathbb{Z})$. Up to a sign, $[F_\nu, F_{\nu'}]$ has the form

$$[E_{i,j}, E_{k,l}] = \delta_{j,k}E_{i,l} - \delta_{l,i}E_{k,j}.$$

Note that since the subscripts satisfy $i < j$ and $k < l$, only one of the terms on the right can be non-zero. This implies the following:

Observation 1. Any iterated commutator of matrices of the form $E_{i,j}$ with $i < j$ again retains this form or is 0.

Note also that because a product of the form $E_{i,j}UE_{i,j}$ must be 0 when $i < j$ and U is upper triangular, we must have:

Observation 2. If the same $E_{i,j}$ appears more than once in such an iterated commutator, then the result is 0.

Abusing notation by writing ν for its coefficient F_ν, the coefficients of α_x, α_y, and α_z are respectively

$$\alpha_x = \iota(\beta_2, \beta_1, x)[\beta_2, \beta_1], \quad \alpha_y = \iota(\beta_1, \gamma^L, y^L)[\beta_1, \gamma^L], \quad \alpha_z = \iota(\gamma^L, \beta_2, z^L)[\gamma^L, \beta_2].$$

To construct C', start with C'_0 as follows. Take $\big(C \setminus \{\gamma^L\}\big) \cup \{\gamma^R\}$, but replace the paths α_y, α_z (if they exist) with new paths α'_y and α'_z that, outside of D', agree respectively with α_y and α_z. [Since the point x remains unchanged, we can retain the path α_x, which is the only one of the three that may belong to X.] We can arrange that α_x, α'_y, α'_z, respectively have unique intersection points in D' with γ^R, β_2, and β_1. Denote these intersection points as

$$u \in \gamma^R \cap \alpha_x; \quad v \in \beta_2 \cap \alpha'_y; \quad \text{and} \quad w \in \beta_1 \cap \alpha'_z.$$

Now, it may be the case that additional paths starting at u, v, and/or w must be added to C'_0 to form a generalized b-manifold. Whether such paths are necessary, and what their indices should be are determined by the coefficients associated to these intersection points. They are

$$\begin{array}{rc} \text{Coeff. of } u\text{:} & \iota(\alpha_x, \gamma^L, u)\iota(\beta_2, \beta_1, x)\left[[\beta_2, \beta_1], \gamma^L\right]; \\ \text{Coeff. of } v\text{:} & \iota(\alpha'_y, \beta_2, v)\iota(\beta_1, \gamma^L, y^L)\left[[\beta_1, \gamma^L], \beta_2\right]; \\ \text{Coeff. of } w\text{:} & \iota(\alpha'_z, \beta_1, w)\iota(\gamma^L, \beta_2, z^L)\left[[\gamma^L, \beta_2], \beta_1\right]. \end{array}$$

[Note that at the level of coefficients, $\alpha_y = \alpha'_y$, $\alpha_z = \alpha'_z$, and $\gamma^L = \gamma^R$.] Moreover, the initial signs are all equal

$$\iota(\alpha_x, \gamma^L, u)\iota(\beta_2, \beta_1, x) = \iota(\alpha'_y, \beta_2, v)\iota(\beta_1, \gamma^L, y^L) = \iota(\alpha'_z, \beta_1, w)\iota(\gamma^L, \beta_2, z^L).$$

[To verify this, note that α_x, α'_y, and α'_z are all oriented toward their endpoints which appear in D'. Moreover, reversing the orientation of any one of $\beta_1, \beta_2, \gamma^L$ changes all three quantities by a sign. Therefore, it is enough to check the equality for a single choice of orientation of $\beta_1, \beta_2, \gamma^L$. If we orient these three curves to the right as pictured, the three products become

$$(-1)(-1) = (+1)(+1) = (+1)(+1). \quad]$$

Therefore, by the Jacobi identity, the sum of these three coefficients is

$$u + v + w = 0 \in Mat(n, \mathbb{Z}).$$

Since each of them is either 0 or a single matrix of the form $\pm E_{i,j}$ with $i < j$ (by Observation 1), we have two possibilities:

(1) **All three coefficients are** 0**.** This means that no additional paths are necessary, so $C' = C'_0$ is a generalized b-manifold with the desired properties.
(2) **One coefficient is** 0 **and the other two are negatives of one another.** This means that we need to add two paths starting at two of the points u, v, and w and with the same indices but opposite signs. We choose these paths so that outside of D' they are small shift of a single path from the $\partial D'$ to the appropriate $I_{i,j}$. Note that the coefficients of any intersection points in D' between these two new paths and existing paths must be 0 because of the Observation 2. Then, proceeding as in Move I, we construct C' inductively so that all paths not corresponding to paths in C cancel in pairs when computing $\partial_{C'} I_{i,j}$.

Move IV. Since $(i(\gamma), j(\gamma)) = (i(\beta), j(\beta))$, Move IV may be treated as in Move II.

□

Proof of Theorem 6.15. From Propositions 6.19, 6.21, and 6.22 we have

$$\partial_b c_{i,j} = \overline{\partial_{A^{LU}} I_{i,j}} + \overline{\partial_{A^{RD}} I_{i,j}} + X$$

where A^{LU} (resp. A^{RD}) is any generalized b-manifold associated to the disk datum $(D^{LU}, \{b^L_{i,j}, b^U_{i,j}\}, \{I_{i,j}\})$ (resp. $(D^{RD}, \{b^R_{i,j}, b^D_{i,j}\}, \{I_{i,j}\})$).

Thus, Theorem 6.15 follows from:

Claim. There exists generalized b-manifolds A^{LU} and A^{RD} for the above disk data such that

$$\overline{\partial_{A^{LU}} I_{i,j}} = b^U_{i,j} + b^L_{i,j} + \sum_{i<m<j} b^U_{i,m} b^L_{m,j}; \quad \text{and} \quad \overline{\partial_{A^{RU}} I_{i,j}} = b^R_{i,j} + b^D_{i,j} + \sum_{i<m<j} b^R_{i,m} b^D_{m,j}.$$

(Here, any of the $b^L_{i,j}$ or $b^D_{i,j}$ that do not exist are replaced with 0.)

We construct A^{LU} as the construction of A^{RD} is identical after reflecting across $x_1 = x_2$.

(1) Connect each $b^U_{i,j}$ to $I_{i,j}$ with a vertical (i.e. slope ∞) line segment, $\gamma^U_{i,j}$.

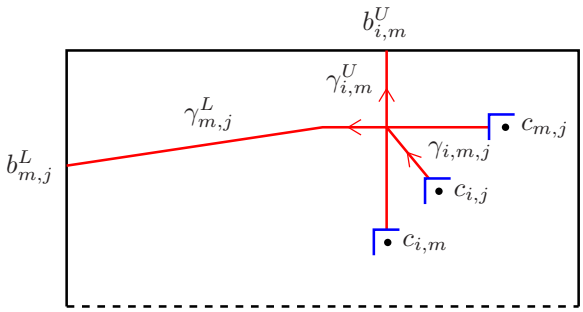

FIGURE 45. The paths $\gamma^U_{i,m}$, $\gamma^L_{m,j}$, and $\gamma_{i,m,j}$.

(2) Connect each $b^L_{i,j}$ to $I_{i,j}$ by a piecewise linear segment (smoothed at the corner), $\gamma^L_{i,j}$, consisting of (i) the line segment from $b^L_{i,j}$ to $(0, \beta^R_{i,j})$, followed by (ii) the horizontal segment (i.e. slope 0) from $(0, \beta^R_{i,j})$ to $I_{i,j}$.
(3) For each $1 \leq i < m < j \leq n$ such that $b^L_{m,j}$ exists, the paths $\gamma^U_{i,m}$ and $\gamma^L_{m,j}$ intersect in a unique point. (This follows from the location of the intervals $I_{i,j}$.) Connect this intersection point to $I_{i,j}$ via a straight line segment, $\gamma_{i,m,j}$.

See Figure 45.

It is clear from definitions that $\overline{\partial_{A^{LU}} I_{i,j}}$ has the desired form, so to complete the proof we only need to verify that A^{LU} is in fact a generalized b-manifold. To this end, it suffices to check that the only intersections between paths $\gamma_1, \gamma_2 \in A^{LU}$ for which

$$j(\gamma_1) = i(\gamma_2) \tag{15}$$

are as in (3).

Clearly, all the $\gamma^U_{i,j}$ are disjoint from one another. When $x_1 > 0$, the $\gamma^L_{i,j}$ are horizontal lines, so because of the relative positioning of the $I_{i,j}$ (lexicographically ordered along the diagonal, $x_1 = x_2$) $\gamma^U_{m,j}$ and $\gamma^L_{i,m}$ are disjoint.

To see that $\gamma_{i,m,j}$ is disjoint from any path with lower index i, note that any path of the form $\gamma^U_{h,i}, \gamma^L_{h,i}$ or $\gamma_{h,g,i}$ is, at least when $x_1 > 0$, entirely above $x_2 = \beta^R_{h,i} - \epsilon$ and to the left of $x_1 = \beta^U_{h,i} + \epsilon$. However, $\gamma_{i,m,j}$ is entirely to the right of $x_1 = \beta^U_{i,m} - \epsilon$ and below $x_2 = \beta^R_{m,j} + \epsilon$. These regions are disjoint (since (h,i) preceds both (i,m) and (m,j) lexicographically). A similar argument shows that $\gamma_{i,m,j}$ is disjoint from paths with upper index j.

Finally, we show that for any $i < m < j$, $\gamma^L_{i,m} \cap \gamma^L_{m,j} = \emptyset$ (provided both of these paths exist). As in (2) (i), the first half of the $\gamma^L_{i,j}$ are line segments that, for all $i < j$, begin and end at on a common pair of vertical lines. [Recall that, by Property (2) of 3 the left side of $\partial \widehat{N}(e^2_\alpha)$ is a vertical line when $1/2 \leq x_2 \leq 3/4$.] Two such segments intersect if and only if the ordering of their x_2-coordinates is opposite along the verical lines where the left and right endpoints sit. The left endpoint of $\gamma^L_{i,j}$ satisfies $\beta^L_{i,j} - \epsilon \leq x_2 \leq \beta^L_{i,j} + \epsilon$, while the right endpoint is at $x_2 = \beta^R_{i,j} = \beta_{i,j}$. Now, $\beta^L_{i,j} = \beta_{\sigma_L(i),\sigma_L(j)}$ where $\sigma_L(i)$ is the position of the sheet S_i above $(-1,1)$. Thus, in order for $\gamma^L_{i,m}$ and $\gamma^L_{m,j}$ to cross we would need to have $(\sigma_L(m), \sigma_L(j)) \prec (\sigma_L(i), \sigma_L(m))$ with respect to lexicographic order. Since $\sigma_L(m) \neq \sigma_L(i)$ this would mean that $\sigma_L(m) < \sigma_L(i)$ which can only happen if sheets S_i and S_m cross above e^1_U. However, in this case $b^L_{i,m}$ doesn't exist.

□

Proof of Theorem 6.5. As $\partial C = \partial_c C + \partial_b C$, the result follows from Theorems 6.10 and 6.15. □

7. Computation of LCH, Part 3: 2-cells with swallowtail singularities

In this section, we compute in Theorem 7.4 the sub-DGAs $(\mathcal{A}_{LCH}(e^2_\alpha), \partial)$ when e^2_α is a square of type (13) or (14). A key feature of the Type (13) and (14) squares is that some rigid GFTs contain

switch vertices. This results in a differential that departs substantially from the common formula from Theorem 6.5 that applies to squares of type (1)-(12).

7.0.3. *Upward and downward swallowtails.* Recall from Section 3.2 that the Type (13) square contains a single upward swallowtail point while the Type (14) contains a single downward swallowtail point. The projections of the crossing and cusp locus in Type (13) and (14) squares are identical.

To simplify exposition, we consider only the case of the Type (13) square in detail while an analogous construction and computation holds for a Type (14) square. (See Remark 7.3 for more about translating the discussion of the Type (13) square to the case of a Type (14) square.)

7.0.4. *Labeling of sheets and Reeb chords above the Type (13) and (14) squares.* Let e^2_α be a 2-cell of type (13). Near $(x_1, x_2) = (+1, +1)$ we label the sheets of L above e^2_α as $S_1, \dots, S_n$ with descending z-coordinate, so that S_k, S_{k+1}, S_{k+2} denote the three sheets that all meet at the swallowtail point. The sheets S_{k+1} and S_{k+2} that cross one another near the swallow tail point both correspond to the same sheet to the left of the cusp locus, so we cannot extend this labelling to the entire square. Instead, we use the following:

Convention 7.1.
(1) For $m \notin \{k+1, k+2\}$, we let S_m denote the entire sheet that sits in position m at $(+1, +1)$. Note that S_k only exists to the right of the cusp locus.
(2) We use S_{k+1} and S_{k+2} to denote only the closed subset of the sheets with position $k+1$ and $k+2$ at $(+1, +1)$ that lies on or to the right of the cusp locus. More precisely, the base projections of S_{k+1} and S_{k+2} lie on or to the right of the cusp locus.
(3) We use $\widetilde{S}_k$ to denote the sheet with base projection on or to the left of the cusp locus that extends to agree with S_{k+2} (resp. S_{k+1}) when x_2 is above (resp. below) the swallowtail point; denote the defining function of $\widetilde{S}_k$ by $\widetilde{F}_k$.

Thus, to the left of the cusp locus the sheets appear with decreasing z-coordinate in the order $S_1, \dots, S_{k-1}, \widetilde{S}_k, S_{k+3}, \dots, S_n$.

The Reeb chords above the neighborhoods of the boundary edges and corners of e^2_α are specified by Properties 2 and 3. Reeb chords above $\widehat{N}(e^2_\alpha)$, and their locations are as in Properties 8 and 9:

- For all $1 \leq i < j \leq n$, there is a Reeb chord $c_{i,j}$ with
$$c_{i,j} \in (\beta^U_{i,j} - \epsilon, \beta^U_{i,j} + \epsilon) \times (\beta^R_{i,j} - \epsilon, \beta^R_{i,j} + \epsilon).$$
- Sheets S_{k+1} and S_{k+2} cross, so there is a Reeb chord $\tilde{c}_{k+2,k+1}$ with
$$\tilde{c}_{k+2,k+1} \in (\beta^D_{k+2,k+1} - \epsilon, \beta^D_{k+2,k+1} + \epsilon) \times (\tilde{\beta}^R_{k+2,k+1} - \epsilon, \tilde{\beta}^R_{k+2,k+1} + \epsilon).$$

As long as neither endpoint of a Reeb chord lies on $\widetilde{S}_k$ we follow our earlier Convention 5.7 so that $a^{\pm,\pm}_{i,j}$, $b^L_{i,j}$, $b^D_{i,j}$, $b^U_{i,j}$, $b^R_{i,j}$, and $c_{i,j}$ denote Reeb chords above the various vertices, edges, and interior of the square with upper endpoint on S_i and lower endpoint on S_j. There are two Reeb chords $\tilde{b}^R_{k+2,k+1}$ and $\tilde{c}_{k+2,k+1}$ that are decorated with tildes. They respectively lie in the lower half of the right edge and in the lower right portion of $\widehat{N}(e^2_\alpha)$.

Convention 7.2. If a Reeb chord has an endpoint on the sheet $\widetilde{S}_k$, then we use $k+2$ for the corresponding subscript when $x_2 > 0$, i.e. for the the b^L and $a^{-,+}$ Reeb chords, and $k+1$ when $x_2 < 0$, i.e. for the $a^{-,-}$ Reeb chords.

Remark 7.3. A similar enumeration of sheets and Reeb chords applies to the Type (14) square. There the roles of the swallowtail sheets are reversed, so that exposition of the computation of GFTs for the Type (14) square would require translating considerations applied to the sheets $\tilde{S}_k$, S_k, S_{k+1}, and S_{k+2} from the Type (13) square to considerations for sheets of the form $\tilde{S}_l, S_l, S_{l-1}$, and S_{l-2}. In particular, for Reeb chords in a Type (14) square with endpoints on $\tilde{S}_l$, we use the subscript $l-2$ when $x_2 > 0$, and $l-1$ when $x_2 < 0$.

7.0.5. *Statement of the differential.* We form matrices containing Reeb chords in $N(e^2_\alpha)$ where e^2_α has type (13). Let $A_{+,+}$, $A_{-,-}$, B_X for $X \in \{L, D, R, U\}$, and C denote strictly upper triangular matrices with (i,j)-entries, for $i < j$, given by the corresponding Reeb chord provided that it exists. For example, take $a^{+,+}_{i,j}$ for the (i,j)-entry of $A_{+,+}$ when $i < j$. In view of Convention 7.2, there are no $a^{-,-}$ Reeb chords with k or $k+2$ as a subscript. We set the $(k, k+2)$-entry of $A_{-,-}$ to be 1, while all remaining entries in rows and columns k and $k+2$ are set to 0. Convention 7.2 also shows that there are no b^L Reeb chords with subscript k or $k+1$, and we set all entries of the k and $k+1$ rows and columns of B_L to be 0. We also place a 0 in the $(k+1, k+2)$-entry of B_D. The Reeb chords $b^D_{k+2,k+1}, \tilde{b}^R_{k+2,k+1}, \tilde{c}_{k+2,k+1}$ do not appear in any of these matrices.

A similar procedure is applied to form matrices from the Reeb chords of a Type (14) square. In this case, $A_{-,-}$ has $(l-2, l)$ entry 1, while all remaining entries in the $l-2$ and l rows and columns are 0; B_L has 0 entries in the l and $l-1$ rows and columns.

Recall that $E_{i,j}$ denotes the matrix with (i,j)-entry 1 and all other entries 0.

Theorem 7.4. *For a 2-cell e^2_α of type (13), in $(\mathcal{A}_{LCH}(e^2_\alpha), \partial)$ we have*

$$\begin{aligned}\partial C = \;& A_{+,+}C + C(I + E_{k+2,k+1})A_{-,-}(I + E_{k+2,k+1}) + \\ & (I + B_U)(I + B_L)(I + A_{-,-}E_{k+1,k} + E_{k+1,k+2}) + (I + B_R)(I + B_D + B_D E_{k+2,k+1}) + X,\end{aligned}$$

where X denotes a strictly upper triangular matrix with entries in the ideal generated by $\tilde{b}^R_{k+2,k+1}, \tilde{c}_{k+2,k+1}$. In particular, the Reeb chord $b^D_{k+2,k+1}$ does not appear in the differential of any of the $c_{i,j}$.

For a 2-cell e^2_α of Type (14), in $(\mathcal{A}_{LCH}(e^2_\alpha), \partial)$ we have

$$\begin{aligned}\partial C = \;& A_{+,+}C + C(I + E_{l-1,l-2})A_{-,-}(I + E_{l-1,l-2}) + \\ & (I + B_U)(I + B_L)(I + E_{l,l-1}A_{-,-} + E_{l-2,l-1}) + (I + B_R)(I + B_D + B_D E_{l-1,l-2}) + X,\end{aligned}$$

where X denotes a strictly upper triangular matrix with entries in the ideal generated by $\tilde{b}^R_{l-1,l-2}, \tilde{c}_{l-1,l-2}$. In particular, the Reeb chord $b^D_{l-1,l-2}$ does not appear in the differential of any of the $c_{i,j}$.

Theorem 7.4 is proved at the conclusion of this section as a consequence of Theorem 7.15 and Propositions 7.27 and 7.36. In the remainder of this section we present only the case of a Type (13) square, i.e. an upward swallowtail, as the Type (14) square is analogous.

7.1. **Properties of gradients.** In the following we continue to use the terminology (i,j)-*flow line* to denote a flow line for $-\nabla F_{i,j}$, while $(\tilde{k}, j)$-*flow line* or $(i, \tilde{k})$-*flow line* refers to a flow line of $-\nabla(\tilde{F}_k - F_j)$ or $-\nabla(\tilde{F}_k - F_j)$ respectively. Notice that a single edge of a GFT may change, for instance, from being an $(i, k+2)$-flow line to an $(i, \tilde{k})$-flow line if its image crosses the upper half of the cusp locus.

Many of the properties of squares of type (1)-(12) stated in Section 6 continue to hold for the Type (13) square. Specifically, as previously discussed, Properties 8 and 9 hold. In addition, Property 12 continues to hold as stated. The statements from Property 10 also hold and apply as well to difference functions $F_i - \tilde{F}_k$ and $\tilde{F}_k - F_j$ provided $\beta^L_{i,k+2}$ and $\beta^L_{k+2,j}$ are used when providing the restrictions on x_2 that appear in the statements of these properties. (This is consistent with the Convention 7.2.)

Lemma 7.5. *The Lemmas 6.11, and 6.13 continue to hold for the Type (13) square.*

Proof. The proofs of these Lemmas use only Properties 10 and 12 from Section 6, and do not depend on the precise form of the singular set above $N(e^2_\alpha)$. □

Property 11 requires the following modification, and strengthening. Recall the notation $\nabla F = (\delta_{x_1} F, \delta_{x_2} F)$.

Property 14 (Monotonicity in half spaces, Type (13) square)**.** The defining functions in a Type (13) square satisfy:

- Suppose that $1 \le i < j \le n$, and $\{i, j\} \not\subset \{k, k+1, k+2\}$. Then, (where defined)
$$-\delta_{x_2} F_{i,j} < 0, \quad \text{when } x_2 = 1/2.$$
Moreover, for $i < k$ and $k+2 < j$, we also have (where defined)
$$-\delta_{x_2}(F_i - \widetilde{F}_k) < 0 \text{ and } -\delta_{x_2}(\widetilde{F}_k - F_j) < 0, \text{ when } x_2 = 1/2.$$

- Suppose that $1 \leq i < j \leq n$, and $(i,j) \neq (k+1, k+2)$. Then, for $(x_1, x_2) \in \widehat{N}(e^2_\alpha)$ we have

$$-\delta_{x_1} F_{i,j}(x_1, x_2) < 0, \quad \text{whenever } x_1 \in \Big[1/4,\ \mathrm{Min}\{\beta^U_{i,j}, \beta^D_{i,j}\} - \epsilon\Big], \text{ and} \tag{16}$$

$$-\delta_{x_1} F_{i,j}(x_1, x_2) > 0, \quad \text{whenever } x_1 \in \Big[\mathrm{Max}\{\beta^U_{i,j}, \beta^D_{i,j}\} + \epsilon, 3/4\Big]. \tag{17}$$

Remark 7.6. Since sheets S_{k+1} and S_{k+2} cross above e^1_R, we have $\beta^D_{i,j} = \beta^U_{\sigma_D(i),\sigma_D(j)}$ where σ_D transposes $k+1$ and $k+2$. Compare with Remark 6.1.

On the other hand, Property 13 requires a serious modification for Type (13) squares. This leads to many new rigid gradient flow trees.

Property 15 (Existence and uniqueness of switch points)**.** Let O_1 denote the closed disk centered at $(-3/8, 0)$ with radius $R_1 = 1/16$, and let $\Sigma \subset N(e^2_\alpha)$ denote (the base projection of) the cusp locus within a Type (13) square. The projection of Σ to the x_2-coordinate is injective. The swallowtail point, Q, is located within O_1 along the horizontal line $x_2 = 0$ at a point with $-7/16 < x_1 < -3/8$. At Q two branches of Σ meet at a semi-cubical cusp, where the x_1-coordinate is minimized along Σ. For $x_2 \geq 0$ sheets S_k and S_{k+1} meet along Σ, while for $x_2 \leq 0$ sheets S_k and S_{k+2} meet along Σ. For $|x_2| \leq 1/32$, the $(k, k+1)$-cusp locus and $(k, k+2)$-cusp locus each project injectively to the x_1-axis. Outside of O_1, Σ agrees with the vertical line $x_2 = -3/8$.

The defining functions F_i satisfy the following.

(1) For any $i < k$, there is a unique (i,k)-switch point along Σ. This switch point has $x_2 > 0$.
(2) For any $k+2 \leq j$, there is a unique $(k+1, j)$-switch point in $\Sigma \cap \{x_2 \geq 0\}$.
(3) For any $k+2 < j$, there are no $(k+2, j)$-switch points in $\Sigma \cap \{x_2 \leq 0\}$.
(4) There is a unique $(k+2, k+1)$-switch point in $\Sigma \cap \{x_2 \leq 0\}$.

Moreover, all of these switch points are non-degenerate and are located in O_1 with $|x_2| \leq 1/32$.

Definition 7.7. We refer to the portion of the cusp locus with $x_2 > 0$ (resp. $x_2 < 0$) where sheets S_k and S_{k+1} (resp. S_k and S_{k+2}) meet as the $(k, k+1)$**-cusp locus** (resp. the $(k, k+2)$**-cusp locus**).

Corollary 7.8. (1) *For $(r,s) = (i,k)$, or $(r,s) = (k+1, j)$, with $i < k$, $k+1 < j$, $-\nabla F_{r,s}$ is transverse to the $(k, k+1)$-cusp locus at all points besides the (r,s)-switch point, P. Moreover, between P and Q (the swallowtail point), $-\nabla F_{r,s}$ points in the direction where the number of sheets increases, while at all other points $-\nabla F_{r,s}$ points in the direction where the number of sheets decreases.*

(2) *For $(r,s) = (i,k)$, or $(r,s) = (k+2, j)$, with $i < k$, $j > k+2$, $-\nabla F_{r,s}$ is transverse to the $(k, k+2)$-cusp locus everywhere and points in the direction where the number of sheets increases. The same statement applies for $(r,s) = (k+2, k+1)$ except between the $(k+2, k+1)$-switchpoint, P, and the swallowtail point Q where $-\nabla F_{k+2,k+1}$ points in the direction where the number of sheets increases.*

See Figure 46.

Proof. As we precede along the $(k, k+1)$- or $(k, k+2)$-cusp locus, the direction of transversality of $-\nabla F_{r,s}$ to Σ changes exactly when either $-\nabla F_{r,s}$ becomes tangent to the cusp locus; for (r,s) as in the statement of the Corollary, such points of tangency are exactly at the (r,s)-switch points. [The direction of transversality *must* change at a switch point because all switch points are non-degenerate.] Moreover, when x_2 is near ± 1, the direction of transversality for all positive difference functions is from right to left, by Property 7. The result follows. □

7.1.1. *Additional monotonicity properties for squares containing swallowtails.* The following Properties 16-19 provide more detailed constraints on the direction of gradient vector fields. They are used at various places during the course of the proof of Theorem 7.4.

Property 16 (The Swallowtail Barrier)**.** For the Type (13) square, there is a polygonal path $P = P_1 \cup P_2$ that satisfies the following.

(1) The subset P_1 is a single line segment that starts on $x_2 = -3/8$; ends on $x_2 = 3/4$; and is entirely contained in $(1/4, 1/2) \times [-3/8, 3/4]$.

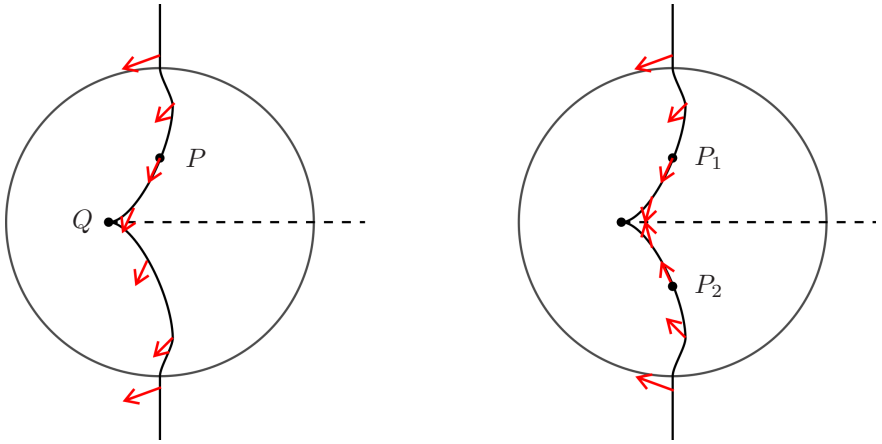

FIGURE 46. (left) The (r,s)-switch point P for $(r,s) = (i,k)$ with $i < k$ or $(r,s) = (k+1,j)$ with $k+2 < j$. The vector field $-\nabla F_{r,s}$ is schematically pictured in red. (right) The $(k+1,k+2)$-switch point, P_1, and the $(k+2,k+1)$-switch point, P_2. The vector field $-\nabla F_{k+1,k+2}$ (resp. $-\nabla F_{k+2,k+1}$) is pictured along the $(k,k+1)$-cusp locus (resp. along the $(k,k+2)$-cusp locus).

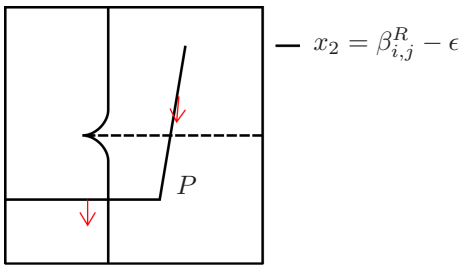

FIGURE 47. The Swallowtail Barrier, P. For $i < j$, $-\nabla F_{i,j}$, pictured in red, points to the region below and to the right along P when $x_2 \leq \beta^R_{i,j} - \epsilon$.

(2) For all $1 \leq i < j \leq n$ and for all $(x_1,x_2) \in P_1$ with $-3/8 \leq x_2 \leq \beta^R_{i,j} - \epsilon$,
$$-\nabla F_{i,j}(x_1,x_2) \text{ points transversally into the region to the right of } P_1.$$
(3) The subset P_2 has monotonic x_1-coordinate with its right endpoint at the lower endpoint of P_1 and its left endpoint on the left boundary of $N(e^2_\alpha)$. Moreover, $P_2 \subset [-1-1/32, 1/2] \times [-3/8, -1/4]$.
(4) For all $(x_1,x_2) \in P_2$, and $(i,j) \neq (k+2,k+1)$ such that $F_{i,j}(x_1,x_2) > 0$,
$$-\nabla F_{i,j}(x_1,x_2) \text{ points transversally into the region below } P_2.$$
(We include the case of $-\nabla(F_i - \widetilde{F}_k)$ and $-\nabla(\widetilde{F}_k - F_j)$.)

See Figure 47.

Property 17 (Barrier at $x_1 = -17/64$)**.** For any $i < k$, we have $-\delta_{x_1} F_{i,k} < 0$, $-\delta_{x_1} F_{i,k+1} < 0$, and $-\delta_{x_1} F_{i,k+2} < 0$ at all points along $x_1 = -17/64$.

Property 18 (Downward gradients when $x_2 \leq -1/4$)**.** For $i < k$ and $j > k+2$, we have $-\delta_{x_2}(F_i - w)(x_1,x_2) < 0$ and $-\delta_{x_2}(w - F_j)(x_1,x_2) < 0$ for all $(x_1,x_2) \in (\text{domain of } w) \cap \{(x_1,x_2) \in \widetilde{N}(e^2_\alpha) \,|\, x_1 \leq -1/4 \text{ and } -1/4 \leq x_2 \leq 1/4\}$ where w is any of F_k, F_{k+1}, F_{k+2} or $\widetilde{F}_k$. Moreover, at points with $x_1 \leq -1/4$ that belong to the crossing locus, $-\nabla(F_i - w)$ points into the region where $F_{k+2} > F_{k+1}$.

Property 19 (Switch point barriers)**.** There exists a line segment $L_{k+1,k+2}$ contained entirely in O_1 with upper endpoint at the $(k+1,k+2)$-switch point and lower endpoint on the $(k,k+2)$ cusp locus such that

- $-\nabla F_{k+1,k+2}$ points from right to left at all points of $L_{k+1,k+2}$ above or on the crossing locus; and

- $-\nabla F_{k,k+2}$ points from right to left along all of $L_{k+1,k+2}$ except for the endpoint on the $(k,k+2)$ cusp edge.

Similarly, there is a line segment $L_{k+2,k+1}$ contained in O_1 with endpoints at the $(k+2,k+1)$-switch point and on the $(k,k+1)$ cusp edge such that

- $-\nabla F_{k+2,k+1}$ points from right to left at all points of $L_{k+2,k+1}$ below or on the crossing locus; and
- $-\nabla F_{k,k+1}$ points from right to left along all of $L_{k+2,k+1}$ except for the endpoint on the $(k,k+2)$ cusp edge.

See Figure 48.

7.1.2. *The (i,k), $(k+1,k+2)$, and $(k+2,k+1)$ switch flow lines and GFTs.* Flow lines that end at switch points play a role in the Type (13) square that is similar to the stable manifolds of b Reeb chords. In this subsection, we examine the flow lines ending at the (i,k)-, $(k+1,k+2)$-, and $(k+2,k+1)$-switch points.

For each (r,s)-switch point identified in Property 15, we call the (unique) (r,s)-flow line that ends at the switch point the (r,s)**-switch flow line**.

Lemma 7.9. (1) *The $(k+1,k+2)$-switch flow line (resp. $(k+2,k+1)$-switch flow line) limits to $c_{k+1,k+2}$ (resp. $\tilde{c}_{k+2,k+1}$) as $t \to -\infty$.*

(2) *The $(k,k+2)$-flow line (resp. $(k,k+1)$-flow line) starting at the $(k+1,k+2)$-switch point (resp. the $(k+2,k+1)$-switch point) ends at an e-vertex at a point on the $(k,k+2)$-cusp locus (resp. $(k,k+1)$-cusp locus).*

Proof. For (1), recall that any flow line must either limit to a Reeb chord or terminate at the cusp edge as $t \to -\infty$. (See the discussion around Proposition 5.11.) If the $(k+1,k+2)$-switch flow line were to terminate at the cusp edge as t decreases, it could only do so at a point of the $(k,k+1)$-cusp edge where $-\nabla F_{k+1,k+2}$ points in the direction where the number of sheets increases. From Corollary 7.8, such a point must be located between the $(k+1,k+2)$-switch point, P, and the swallow tail point, Q. However, Property 19 prevents the $(k+1,k+2)$-switch flow line from passing to the left of $L_{k+1,k+2}$ as t decreases, and the portion of the cusp locus between P and Q lies entirely to the left of $L_{k+1,k+2}$. Thus, as $t \to -\infty$, the $(k+1,k+2)$-switch flow line limits to a $(k+1,k+2)$-Reeb chord in $\widehat{N}(e_\alpha^2)$; the only such Reeb chord is $c_{k+1,k+2}$.

A similar argument (using the statement about $-\nabla F_{k+2,k+1}$ and the segment $L_{k+2,k+1}$ in Property 19) applies to show the $(k+2,k+1)$-switch flow line begins at $\tilde{c}_{k+2,k+1}$.

For (2), consider only the $(k,k+1)$-flow line starting at the $(k+2,k+1)$-switch point as a similar proof will establish the statement about the $(k,k+2)$-flow line. Along the segment, $L_{k+2,k+1}$, that starts at the $(k+2,k+1)$-switch point, $-\nabla F_{k,k+1}$ points to the left (by Property 19). Therefore, as t increases, the flow must exit the triangle-like region formed by $L_{k+2,k+1}$ and the cusp edge somewhere along the cusp edge. Along the lower half of the cusp locus, to the left of the $(k+2,k+1)$-switch point, $-\nabla F_{k,k+1}$ points across the cusp edge from the side with fewer sheets to the side with more sheets. [This follows from Corollary 7.8 since $\nabla F_{k,k+1}$ and $\nabla F_{k+2,k+1}$ agree along the $(k,k+2)$-cusp edge.] Thus, as t increases the flow line can only reach the upper half of the cusp edge (which is part of the $(k,k+1)$-cusp locus) where it ends at an e-vertex. See Figure 48 (left). □

The flow lines identified in (1) and (2) of Lemma 7.9 fit together in pairs to produce gradient flow trees starting at $c_{k+1,k+2}$ and $c_{k+2,k+1}$ respectively. Both of these GFTs contain a single switch as an internal vertex and have a single output at an e-vertex. See Figure 48. We refer to these gradient flow trees as the $(k+1,k+2)$**- and** $(k+2,k+1)$**-switch GFTs**.

We will make use of the following constraint on the image of the $(k+1,k+2)$-switch flow line. Let $R(sw_{k+1,k+2}) \subset \widehat{N}(e_\alpha^2)$ denote the region bounded

(1) on the left by $L_{k+1,k+2}$ and the $(k,k+1)$-cusp locus;

(2) below by a path constructed from left to right from (i) the $(k+1,k+2)$ crossing locus from $L_{k+1,k+2}$ to the Swallowtail Barrier P (from Property 16); (ii) the part of P below $x_2 = \beta^R_{k+1,k+2} - \epsilon$; and (iii) the part of the line segment $\{x_2 = \beta^R_{k+1,k+2} - \epsilon\}$ between P and $x_1 = \beta^U_{k+1,k+2} + \epsilon$;

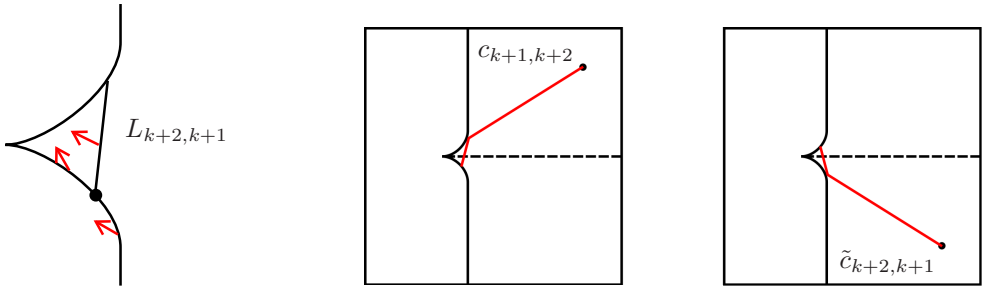

FIGURE 48. (left) The $(k+2,k+1)$-switch point appears as a dot. Arrows indicate the direction of $-\nabla F_{k,k+1}$ along the lower half of the cusp locus and the line segment $L_{k+2,k+1}$ as used in Proof of Lemma 7.9. (right) The images of the GFTs resulting from Lemma 7.9.

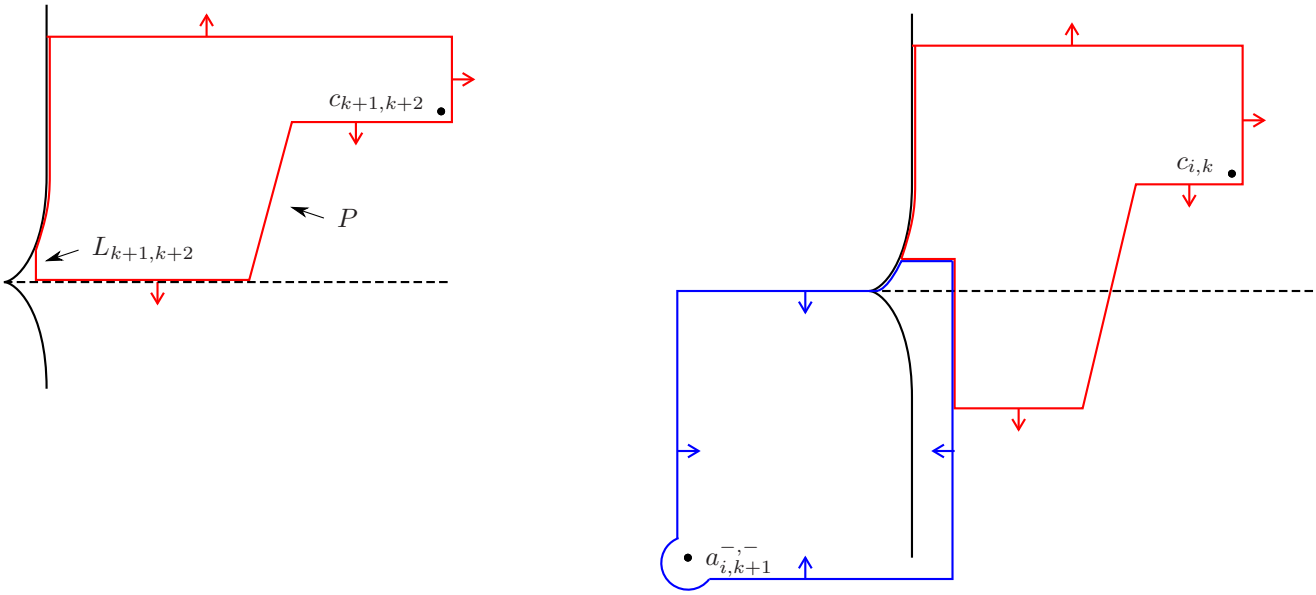

FIGURE 49. (left) The region $R(sw_{k+1,k+2})$. (right) The regions $R(sw_{i,k})$ (in red) and $C_{i,k}$ (in blue).

(3) on the right by $\{x_1 = \beta^U_{k+1,k+2} + \epsilon\}$;
(4) and above by $\partial\widehat{N}(e^2_\alpha)$.

See Figure 49.

Lemma 7.10. *The $(k+1,k+2)$-switch flow line is entirely contained in $R(sw_{i,k})$.*

Proof. Note that $-\nabla F_{k+1,k+2}$ points outward along all segments of the boundary of $R(sw_{i,k})$. [Working clockwise from $L_{k+1,k+2}$, use Property 19, Corollary 7.8, 3, Property 10 (twice), Property 16, and that $F_{k+1,k+2}$ goes from being positive to being negative when we pass the crossing locus.] Since the $(k+1,k+2)$-switch flow line begins at the upper endpoint of $L_{k+1,k+2}$ it will remain within $R(sw_{i,k})$ as t decreases. □

Next, we study the (i,k)-switch flow line. Define a closed region $R(sw_{i,k}) \subset \widehat{N}(e^2_\alpha)$ to be bounded by the curve that, beginning at the (i,k)-switch point and proceeding clock-wise, consists of

(1) the upper part of the $(k,k+1)$-cusp locus;
(2) part of the upper boundary of $\widehat{N}(e^2_\alpha)$;
(3) the vertical line $\{x_1 = \beta^U_{i,k} + \epsilon\}$;
(4) the horizontal line segment $\{x_2 = \beta^R_{i,k} - \epsilon\}$;
(5) the part of the Swallowtail Barrier, P, with $x_2 \leq \beta^R_{i,k} - \epsilon$ and $x_1 \geq -17/64$;
(6) the vertical segment $\{x_1 = -17/64\}$ from P to the x_2-coordinate of the (i,k)-switch point; and

(7) the horizontal segment from the (i,k)-switch point to $x_1 = -17/64$.

See Figure 49.

Lemma 7.11. *For $i < k$,*

(1) *the (i,k)-flow line ending at the (i,k)-switch point (i.e. the (i,k)-switch flow line) is entirely contained in $R(sw_{i,k})$ and limits to $c_{i,k}$ as $t \to -\infty$;*
(2) *the $(i,k+1)$-flow line beginning at the (i,k)-switch point limits to $a^{-,-}_{i,k+1}$.*

Proof. Along each of the boundary segments (1)-(7) of $R(sw_{i,k})$ we have that $-\nabla F_{i,k}$ points outward. [Verify with Corollary 7.8, Property 3, Property 10 (used twice), then Properties 16, 17, and 18.] Thus, as t decreases the (i,k)-switch flow line remains in $R(sw_{i,k})$ and can therefore only limit to $c_{i,k}$.

To verify the claim concerning the $(i,k+1)$-flow line, γ, that begins at the (i,k)-switch point, we consider a region $C_{i,k}$ bounded by:

(1) the horizontal segment from the (i,k)-switch point to $x_1 = -17/64$;
(2) the vertical segment $x_1 = -17/64$ from the x_2-coordinate of the (i,k)-switch point to the lower boundary of $N(e^2_\alpha)$;
(3) the portion of $\partial N(e^2_\alpha)$ running clock-wise from the bottom side at $x_1 = -17/64$ to the left side at $x_2 = 0$;
(4) the horizontal segment from the left side of $\partial N(e^2_\alpha)$ at $x_2 = 0$ to the swallowtail point Q; and
(5) the portion of the $(k,k+1)$-cusp locus between Q and the (i,k)-switch point.

Note that $-\nabla F_{i,k+1}$ and $-\nabla(F_i - \widetilde{F}_k)$ point inward along those parts of $\partial C_{i,k}$ where they are defined. [Verify along (1)-(5) using Properties 18, 17, 3, 18 (again), and Corollary 7.8.] Thus, even though γ may change from being an $(i,k+1)$-flow line to an $(i,\tilde{k})$ flow line if it crosses the $(k,k+2)$-cusp locus, as t increases γ must be entirely contained in $C_{i,k}$. The only Reeb chord in $C_{i,k}$ with upper endpoint on S_i and lower endpoint on S_{k+1} or $\widetilde{S}_k$ is $a^{-,-}_{i,k+1}$ (which in fact has its lower endpoint on $\widetilde{S}_k$). Thus, γ must limit to $a^{-,-}_{i,k+1}$ as $t \to +\infty$. □

We refer to the gradient flow tree obtained by appending the flow lines from (1) and (2) together at a switch vertex as the (i,k)**-switch GFT**.

7.1.3. *The $(k+1,k+2)$ and $(k+2,k+1)$ partial flow trees.* Partial flow trees beginning with certain $(k+1,k+2)$- or $(k+2,k+1)$-flow lines serve as a base case for inductive arguments used later in the section. In this subsection we establish some preliminary results about such PFTs.

Lemma 7.12. *The only non-constant PFTs starting with a $(k+2,k+1)$-flow at a point in $\widehat{N}(e^2_\alpha)$ (to the right of the cusp edge and below the crossing locus) are*

(1) *PFTs consisting of a single edge with output vertex limiting to $b^D_{k+2,k+1}$ or $\tilde{b}^R_{k+2,k+1}$. These flow trees are subsets of unique flow lines that exist from $\tilde{c}_{k+2,k+1}$ to $b^D_{k+2,k+1}$ or $\tilde{b}^R_{k+2,k+1}$, and are respectively contained in the vertical strip*

$$V = \{(x_1,x_2) \in \widetilde{N}(e^2_\alpha) \,\Big|\, x_1 \in (\beta^D_{k+2,k+1} - \epsilon, \beta^D_{k+2,k+1} + \epsilon) \text{ and } x_2 \leq \tilde{\beta}^R_{k+2,k+1} + \epsilon\}$$

or the horizontal strip

$$H = \{(x_1,x_2) \in \widetilde{N}(e^2_\alpha) \,\Big|\, x_1 \geq \beta^D_{k+2,k+1} - \epsilon \text{ and } x_2 \in (\tilde{\beta}^R_{k+2,k+1} - \epsilon, \tilde{\beta}^R_{k+2,k+1} + \epsilon)\}.$$

(2) *PFTs consisting of a single edge with output at $a^{+,-}_{k+2,k+1}$. These PFTs are contained entirely in*

$$\{(x_1,x_2) \in \widetilde{N}(e^2_\alpha) \,\Big|\, x_1 \geq \beta^D_{k+2,k+1} - \epsilon \text{ and } x_2 \leq \tilde{\beta}^R_{k+2,k+1} + \epsilon\} \bigcup N(e^0_{+,-}).$$

(3) *PFTs that form some subset of $(k+2,k+1)$-switch GFT.*

Proof. First, we show that any PFT, Γ, without internal vertices and beginning with a $(k+2,k+1)$ flow in $\widehat{N}(e^2_\alpha)$ must be as in (1) or (2). Since Γ does not have internal vertices it must simply be a portion of a flow line that limits to a Reeb chord as $t \to +\infty$. [Ending at an e-vertex is impossible since there is no $(k+1,k+2)$-cusp edge.] The only $(k+2,k+1)$ Reeb chords are $\tilde{c}_{k+2,k+1}, \tilde{b}^R_{k+2,k+1}, b^D_{k+2,k+1}$,

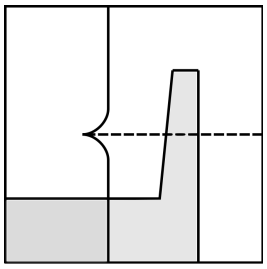

FIGURE 50. The region A.

and $a^{+,-}_{k+2,k+1}$, so Γ must begin on a point belonging to the stable manifolds of one of these Reeb chords. The stable manifolds of $b^D_{k+2,k+1}$ and $\tilde{b}^R_{k+2,k+1}$ must be contained in the strips V and H respectively, by Properties 10 and 7 (and therefore both limit to $\tilde{c}_{k+2,k+1}$ respectively as claimed). On the other hand, a point in the intersection of the stable manifold of $a^{+,-}_{k+2,k+1}$ with $\widehat{N}(e^2_\alpha)$ must be in the region bounded by the stable and unstable manifolds of $b^D_{k+2,k+1}$ and $\tilde{b}^R_{k+2,k+1}$, since flow lines cannot cross.

It remains to show that the only PFTs starting with a $(k+2,k+1)$-flow in $\widehat{N}(e^2_\alpha)$ and having internal vertices are as in (3). Consider the first internal vertex of such a PFT, Γ. Since sheets S_{k+2} and S_{k+1} are adjacent in the entire region where S_{k+2} is above S_{k+1}, it follows that this vertex cannot be a Y_1 or Y_0-vertex. Therefore, the vertex can only be a switch at the unique $(k+2,k+1)$-switch point, so it follows that the initial edge of the PFT is indeed a subset of the $(k+2,k+1)$-switch flow line. The edge of Γ that begins after the switch vertex is the $(k,k+1)$-flow line that begins at the $(k+2,k+1)$-switch point. We need to show that an internal vertex cannot occur along this edge.

Suppose instead that Γ has a second internal vertex occurs after the switch point. The only possibility is a Y_0 vertex where the $(k,k+1)$-flow splits into a $(k,k+2)$ flow and a $(k+2,k+1)$-flow. Furthermore, the image of this Y_0 vertex must be located below the $(k+1,k+2)$-crossing locus (otherwise there are no intermediate sheets between S_k and S_{k+1}), and to the left of $L_{k+2,k+1}$ (since by Property 19 $-\nabla F_{k,k+1}$ points to the left side of $L_{k+2,k+1}$). However, the outgoing branch of the Y_0 that is a $(k+2,k+1)$-flow line cannot be completed to a PFT since we have already seen that the only PFTs starting with a $(k+2,k+1)$-flows must have their initial point either with $x_1 \geq \beta^D_{k+2,k+1} - \epsilon$ or somewhere along the $(k+2,k+1)$-switch flow line. Moreover, by Property 19 the $(k+2,k+1)$-switch flow line is contained entirely to the right of $L_{k+2,k+1}$ except at its endpoint. □

Recall the notations $D(1/2) = \{(x_1,x_2) \in \widetilde{N}(e^2_\alpha) \,|\, x_2 \leq 1/2\} \bigcup N(e^0_{-,-}) \bigcup N(e^0_{+,-})$ and $L(1/2) = \{(x_1,x_2) \in \widetilde{N}(e^2_\alpha) \,|\, x_1 \leq 1/2\} \bigcup N(e^0_{-,-}) \bigcup N(e^0_{-,+})$.

Lemma 7.13. *The only PFTs starting with a $(k+1,k+2)$-flow in $D(1/2) \cup L(1/2)$ are subsets of the $(k+1,k+2)$-switch GFT.*

Proof. Any $(k+1,k+2)$-flow line that starts in $D(1/2) \cup L(1/2)$ must remain in $D(1/2) \cup L(1/2)$ since Property 10 shows that $-\nabla F_{k+1,k+2}$ points inward along the boundary segments $\{(x_1,x_2) \,|\, x_1 \geq 1/2, x_2 = 1/2\}$ and $\{(x_1,x_2) \,|\, x_1 = 1/2, x_2 \geq 1/2\}$. There are no $(k+1,k+2)$ Reeb chords in $D(1/2) \cup L(1/2)$. Thus any such PFT must have an internal vertex. Since S_{k+1} and S_{k+2} are always adjacent the first vertex can only be a switch at the unique $(k+1,k+2)$-switch point. After the switch, an argument similar to that used in Lemma 7.12 shows that the outgoing $(k,k+2)$-flow line cannot end at an internal vertex. □

7.1.4. *The invariant region A.* Let A denote the subset of $D(1/2) \cap L(1/2)$ obtained by removing those points that lie strictly above and to the left of the Swallowtail Barrier P. Note that the boundary of A consists of:

(1) the vertical segment $\{x_1 = 1/2\} \cap \{x_2 \leq 1/2\}$;
(2) the segment of $\{x_2 = 1/2\}$ with endpoints on P and $x_1 = 1/2$;
(3) the portion of P below $x_2 = 1/2$;
(4) the portion of $\partial N(e^2_\alpha)$ that sits below P and to the left of $\{x_1 = 1/2\}$.

See Figure 50.

Lemma 7.14. *Suppose $(i,j) \neq (k+1,k+2)$, and $(i,j) \neq (k+2,k+1)$. Any (i,j)-flow line that begins in A remains in A as t increases (as long as it is defined). This statement includes $(i,\tilde{k})$- and $(\tilde{k},j)$-flow lines.*

Proof. This follows since $-\nabla F_{i,j}$ points into A along all segments comprising the boundary of A. [Check with Property 14 for (1) and (2), Property 16 for (3), and Properties 2 and 3 for (4).] □

7.2. **Enumeration of flow trees with at least one $c_{i,j}$ output.** For a Type (13) square, e^2_α, we again write

$$\partial_c c_{i,j} = \sum_\Gamma w(\Gamma) \tag{18}$$

with the sum over rigid GFTs that begin at $c_{i,j}$ and contain at least one puncture at a Reeb chord of the form $c_{r,s}$ or $\tilde{c}_{k+2,k+1}$.

Recall that we have labeled the Reeb chords in $N(e^0_{-,-})$ with the index $k+1$ used for chords that begin or end on $\tilde{S}_k$.

Theorem 7.15. *We have*

$$\partial_c c_{i,j} = \sum_{i<m<j} a^{+,+}_{i,m} c_{m,j} + \sum_{i<m<j} c_{i,m} y_{m,j} + x \tag{19}$$

where $y_{m,j}$ denotes the (m,j)-entry of the matrix $(I+E_{k+2,k+1})A_{-,-}(I+E_{k+2,k+1})$ from Theorem 7.4 and x belongs to the two-sided ideal generated by $\tilde{c}_{k+2,k+1}$ and $\tilde{b}^R_{k+2,k+1}$. That is,

- *for $\{m,j\} \cap \{k,k+2\} = \emptyset$, $y_{m,j} = a^{-,-}_{m,j}$;*
- *$y_{k,k+2} = 1$;*
- *$y_{k,k+1} = 1$;*
- *for $k+2 < j$, $y_{k+2,j} = a^{-,-}_{k+1,j}$;*
- *all remaining $y_{m,j}$ are zero.*

The proof of Theorem 7.15 consists of two parts. In Section 7.2.2, we identify an odd number of rigid GFTs corresponding to each of the terms in the sum. Then, in Section 7.2.3, after some preliminary results, we show that any rigid GFT with a puncture at a $c_{r,s}$ must be one of the GFTs from our list.

7.2.1. *Degree of a partial flow tree.* Rigid GFTs can be identified by the following criterion.

Lemma 7.16. *Let e^2_α be a Type (13) square. A GFT Γ in $N(e^2_\alpha)$ that begins at some $c_{i,j}$ or $\tilde{c}_{k+2,k+1}$ is rigid if and only if*

$$A - C + E - Y_1 - SW = 0$$

where A (resp. C) denotes the number of endpoints at Reeb chords of the form $a^{\pm,\pm}_{m,n}$ (resp. $c_{m,n}$ or $\tilde{c}_{k+2,k+1}$); E denotes the number of endpoints at e-vertices; Y_1 denotes the number of Y_1-vertices; and SW denotes the number of switch vertices.

(Recall from Theorem 2.7, that since $\tilde{L}$ is 1-regular all vertices of $\tilde{L}$ are either inputs, outputs, e-, Y_0-, Y_1-, or sw-vertices.)

Proof. This is just Proposition 2.9 since all a, b, and c Reeb chords are respectively local minima, saddles, and local maxima. □

We make the following definition to help identify PFTs that may appear as part of some rigid GFT.

Definition 7.17. For a PFT, Γ, contained in $N(e^2_\alpha)$ we define the **degree of** Γ to be

$$D(\Gamma) = A - C + E - Y_1 - SW$$

with A, C, E, Y_1, and SW as in Lemma 7.16.

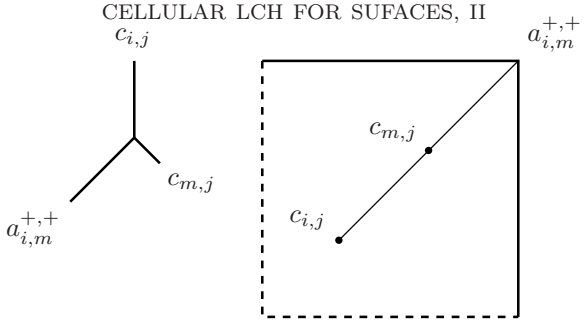

FIGURE 51. The domain and image of the trees from Term 1.

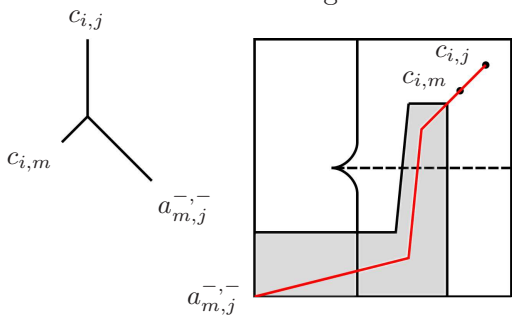

FIGURE 52. The domain and image (in red) of the trees from Term 2.

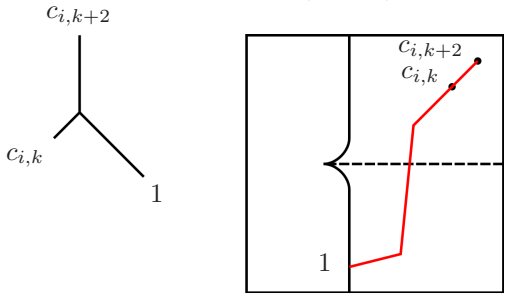

FIGURE 53. The domain and image (in red) of the trees from Term 3.

7.2.2. *List of rigid GFTs with punctures at c's.* For each term in the formula for $\partial_c c_{i,j}$ given in Theorem 7.15 we identify an odd number of corresponding rigid GFTs.

Term 1: $a^{+,+}_{i,m} c_{m,j}$ **for** $i < m < j$**.** The GFT begins by following the unique (i,j)-flow line that limits to $c_{i,j}$ as $t \to -\infty$ and passes the location of $c_{m,j}$. When the flowline reaches $c_{m,j}$ a puncture (Y_0-vertex) occurs. The non-constant branch after the puncture is the (i,m)-flow line beginning at $c_{m,j}$. In view of the lexicographic ordering of the $c_{i,j}$ along the diagonal $x_1 = x_2$, (this follows from Properties 8 and 6), we have $c_{m,j} \in N_\epsilon Q1(i,m)$, i.e. $c_{m,j}$ is to the right and above $c_{i,m}$. Therefore, by Lemma 6.11 (see also Lemma 7.5), this flowline limits to $a^{+,+}_{i,m}$ as $t \to +\infty$. See Figure 51.

Term 2: $c_{i,m} a^{-,-}_{m,j}$ **for** $i < m < j$ **with** $\{m,j\} \cap \{k, k+2\} = \emptyset$**.** Begin by following the unique (i,j)-flow line from $c_{i,j}$ to $c_{i,m}$. When the flow line reaches $c_{i,m}$ a puncture occurs. After the puncture the non-constant branch is the (m,j)-flow line starting at $c_{i,m}$. As stated in Lemma 7.5, the Lemma 6.13 is applicable in this situation, and it shows that this flow line will pass into $[1/4, 1/2] \times [1/4, 1/2] \subset A$ where A is the region from Lemma 7.14. Once this occurs, Lemma 7.14 shows that the limit of this flow line can only be the Reeb chord $a^{-,-}_{m,j}$ as this is the only (m,j)-Reeb chord in A. [Note that because of the restriction $\{m,j\} \cap \{k, k+2\} = \emptyset$, neither the m or j sheet has a cusp locus in A. If one of m or j is $k+1$, then the Convention 7.2 is relevant since the S_{k+1} sheet becomes $\tilde{S}_k$ when the flow line crosses the $(k, k+2)$-cusp locus.] See Figure 52.

Term 3: $c_{i,k} \cdot 1$ **for** $i < k < j = k+2$**.** Begin with the unique $(i, k+2)$-flow line from $c_{i,k+2}$ to $c_{i,k}$, and then puncture at $c_{i,k}$. By Lemma 6.13 and Lemma 7.14, the $(k, k+2)$-flow line that begins at $c_{i,k}$ must then enter and remain in A where it can only end at an e-vertex along the lower half of the cusp edge where sheets S_k and S_{k+2} meet; this produces a flow tree as in Figure 53.

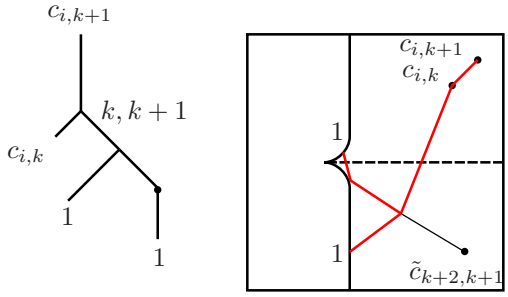

FIGURE 54. A tree from Term 4. More intersections between the $(k, k+1)$-flow line starting at $c_{i,k}$ and the $(k+2, k+1)$-switch flow line may occur, resulting in an even number of additional trees.

Term 4: $c_{i,k} \cdot 1$ **for** $i < k < j = k+1$**.**

Again by Lemmas 6.13 and Lemma 7.14, the $(k, k+1)$-flow line γ,that starts at $c_{i,k}$ enters and remains in A where it can only terminate at the $(k, k+2)$-cusp locus.

Consider the closed subset $D \subset N(e^2_\alpha)$, consisting of the part of $N(e^2_\alpha)$ that sits to the right of the cusp locus with the upper right corner removed just below and to left of $c_{i,k}$, and the lower right corner removed just above and to left of $\tilde{c}_{k+1,k+2}$. More precisely, remove

$$\{(x_1, x_2) \in \widetilde{N}(e^2_\alpha) \,|\, x_1 > \beta^U_{i,k} - \epsilon,\ x_2 > \beta^R_{i,k} - \epsilon\} \bigcup N(e^0_{+,+}),$$

and

$$\{(x_1, x_2) \in \widetilde{N}(e^2_\alpha) \,|\, x_1 > \beta^D_{k+2,k+1} - \epsilon,\ x_2 < \tilde{\beta}^R_{k+2,k+1} + \epsilon\} \bigcup N(e^0_{+,-}).$$

Now, D is homeomorphic to D^2, and the intersection of γ and the $(k+2, k+1)$-switch flow line, λ, with D are closed intervals with their endpoints on ∂D. [That the intersections of these flow lines with D consist of single arcs follows from Property 10.] Moreover, the endpoints of γ, A_1, A_2, and the endpoints of λ, B_1, B_2, appear cyclically in the order $A_i B_k A_j B_l$. As γ and λ intersect transversally (by the 1-regularity of $\tilde{L}$), standard differential topology shows that they intersect in an odd number of points, $w_1, \ldots, w_{2r+1}$.

To produce an odd number of GFTs: Begin with the $(i, k+1)$-flow line from $c_{i,k+1}$ to $c_{i,k}$, and puncture at $c_{i,k}$. Follow γ until it reaches one of the w_i. At w_i, a Y_0-vertex occurs so that the outgoing edges are a $(k, k+2)$-flow line, γ_a, and a $(k+2, k+1)$-flow line, γ_b. Since $w_i \in A$, γ_a must remain in A and will thus terminate at an e-vertex along the $(k, k+2)$-cusp edge; γ_b ends at a switch vertex at the $(k+2, k+1)$-switch point that is followed by a $(k, k+1)$-flow line that terminates at the cusp edge.

See Figure 54.

Term 5: $c_{i,k+2} a^{-,-}_{k+1,j}$ **for** $i < k+2 < j$**.**

We identify an odd number of GFTs, each of which has initial branch consisting of the (i, j)-flow line from $c_{i,j}$ to $c_{i,k+2}$. The $(k+2, j)$-flow line beginning at $c_{i,k+2}$ will enter A (by Lemma 6.13). Next, by Lemma 7.14 this flow line will proceed to terminate at a point on the $(k, k+2)$-cusp locus. Along its way it will intersect the $(k+2, k+1)$ switch line transversally in an odd number of points, $w_1, \ldots, w_{2r+1}$. [The reasoning is as in Term 4.] To construct GFTs $\Gamma_1, \ldots, \Gamma_{2r+1}$, after the puncture we follow the $(k+2, j)$-flow line starting at $c_{i,k+2}$ to one of the w_s where a Y_0 occurs. The branch that is a $(k+1, j)$ flow will then proceed to $a^{-,-}_{k+1,j}$ (again by Lemma 7.14), so a GFT of the form pictured in Figure 55 results.

Note that by Lemma 7.16, the GFTs identified in Terms 1-5 are all rigid.

7.2.3. *Establishing uniqueness.* The following Lemmas 7.18 and 7.20 serve as a replacement for the 3-rd Quadrant Lemma.

Lemma 7.18. *Any PFT, Γ, beginning at a point in A satisfies $D(\Gamma) \geq 0$. Moreover, equality holds only for those PFTs that are subsets of the $(k+2, k+1)$- switch GFT beginning at a point on the initial edge, i.e. beginning with part of the $(k+2, k+1)$- switch flow line.*

Proof. Note that the cases of a PFT beginning with a (i, j)-flow in A where $(i, j) = (k+2, k+1)$ or $(i, j) = (k+1, k+2)$ are covered by Lemmas 7.12 and 7.13. [Note that the PFTs identified in (1) and

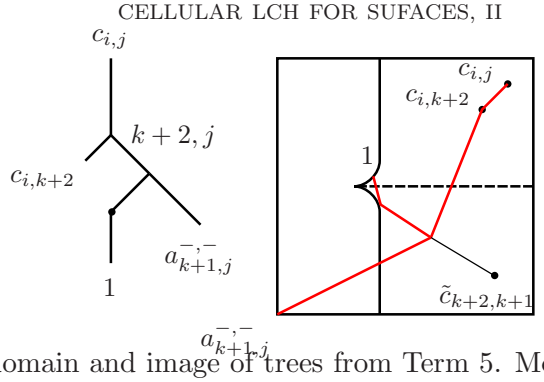

FIGURE 55. The domain and image of trees from Term 5. More intersections between the $(k+2,j)$-flow line starting at $c_{i,k+2}$ and the $(k+2,k+1)$-switch flow line may occur, resulting in an even number of additional trees.

(2) of Lemma 7.12 are entirely disjoint from A, and the $(k+1,k+2)$-switch flow line is disjoint from A via Lemma 7.10.]

Thus, we consider the case of a PFT, Γ, beginning with an (i,j)-flow starting in A with $(i,j) \neq (k+1,k+2)$ and $(i,j) \neq (k+2,k+1)$, and we use induction on the number of Y_0-vertices in Γ.

The initial edge of Γ remains in A (by Lemma 7.14), so the first internal vertex of Γ can only be a Y_0-vertex by the following:

Lemma 7.19. *No Y_1 or switch vertex can have its image in A.*

Proof. The only portion of the cusp locus that intersects A is along the vertical segment $\{x_1 = -3/8\}$ below the Swallowtail Barrier P. For $i < k$ and $j = k+1$ or $j \geq k+3$, so that S_i and S_j are respectively above and below the $(k,k+2)$-cusp locus, Corollary 7.8 gives $-\delta_{x_1} F_{i,k} < 0$ and $-\delta_{x_1} F_{k+2,j} < 0$, so that no switches are possible. Moreover, since F_k and F_{k+2} agree to first order along the $(k,k+2)$-cusp edge, we have

$$-\delta_{x_2} F_{i,j} = -\delta_{x_2} F_{i,k} - \delta_{x_2} F_{k+2,j} < 0$$

so that no Y_1 is possible. □

Now, in the base case where Γ has no Y_0 vertices, we have that Γ has no internal vertices at all and can only limit to an (i,j)-Reeb chord within A or end at an e-vertex. (If i or j is $k+1$, this Reeb chord will have an endpoint on $\widetilde{S}_k$.) The only (i,j)-Reeb chord in A is $a^{-,-}_{i,j}$, so we have $D(\Gamma) = A - C + E - Y_1 - SW = 1$. For the inductive step, assume Γ has at least one Y_0-vertex, and let Γ_1 and Γ_2 denote the PFTs that begin with the two branches of Γ that immediately follow the first vertex. The image of this vertex must lie in A by Lemma 7.14, so the inductive hypothesis applies to both Γ_1 and Γ_2. Therefore, we have $D(\Gamma_i) \geq 0$ for $i = 1,2$. It is impossible that we have equality in both cases since at most one of the Γ_i can begin with the $(k+2,k+1)$-switch flow line. Therefore, $D(\Gamma) = D(\Gamma_1) + D(\Gamma_2) > 0$. □

Lemma 7.20. *Let $i < m_1 \leq m_2 < j$. Any PFT Γ that begins with an (m_2,j)-flow line starting at a point $x \in N_\epsilon Q3(i,m_1) \cap [1/2,1] \times [1/2,1]$ satisfies $D(\Gamma) > 0$.*

Proof. Applying Lemma 6.13, repeatedly if necessary, we can locate some number of points $x_1, \ldots, x_r$ in the domain of Γ with the following properties.

(1) For some $m_2 = s_0 < s_1 < \ldots < s_r = j$, the branch of the tree that x_i sits on parametrizes an (s_{i-1}, s_i)-flow.
(2) The image of each x_i is in $[1/4,1/2] \times [1/4,1/2]$.
(3) We have $\Gamma = \gamma_0 \sqcup \Gamma_1 \sqcup \cdots \sqcup \Gamma_r$ where Γ_i denotes the PFT consisting of the portion of Γ starting at and below x_i and γ_0 is some portion of the tree that does not have any output vertices and has image contained in $N_\epsilon Q3(i,m_1) \cap [1/4,1] \times [1/4,1]$.

Note in particular that γ_0 can only have Y_0 vertices because the cusp locus is disjoint from $[1/4,1]^2$. See Figure 56. [One locates the x_i as follows. Suppose the initial branch of Γ leaves $N_\epsilon Q3(i,m_1)$. Then, we apply Lemma 6.13 to locate a suitable point x_1 with image in $[1/4,1/2]^2$, and take $r = 1$. If the initial branch of the tree does not leave $N_\epsilon Q3(i,m_1)$, then it can only end at a Y_0-vertex. In this case, we treat the two outgoing branches of the tree at the Y_0 inductively.]

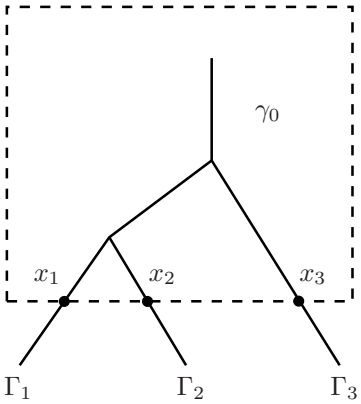

FIGURE 56. Decomposing the partial flow tree $\Gamma' = \gamma_0 \sqcup \Gamma_1 \sqcup \cdots \sqcup \Gamma_r$.

Since $x_i \in [1/4, 1/2] \times [1/4, 1/2] \subset A$, we can now apply Lemma 7.18 to each of the Γ_i to conclude that for all i, $D(\Gamma_i) > 0$. [None of the Γ_i begins with the $(k+2, k+1)$-switch flow line since we are above the crossing locus.] Thus, we have $D(\Gamma') = \sum_i D(\Gamma_i) \geq 1$ as desired.

□

Conclusion of Proof of Theorem 7.15. Let Γ be a rigid GFT beginning at $c_{i,j}$ that contains at least one puncture at a Reeb chord of the form $c_{r,s}$. (If Γ instead contains a puncture at $\tilde{c}_{k+2,k+1}$, then its contribution to $\partial_c c_{i,j}$ is absorbed into the term x from (19)). By Lemma 7.16,

$$D(\Gamma) = A - C + E - Y_1 - SW = 0.$$

We will show that Γ is one of the GFTs identified in Terms 1-5.

First, choose one of the punctures of Γ at a Reeb chord of the form $c_{r,s}$ and consider the PFT, Γ', consisting of the portion of Γ beginning just below this puncture.

Step 1. The PFT, Γ', has $D(\Gamma') \geq 1$ with equality if and only if Γ' agrees with the portion of one of the trees described in Terms 1-5 that follows the puncture.

We verify Step 1 in two cases.

Case 1. For some $i < r < s$, an (i, s)-flow becomes an (i, r)-flow at the puncture.

In this case, the 1-st Quadrant Lemma applies (see Lemmas 7.5 and 6.11). This lemma states that the image of Γ' is contained in $N_\epsilon Q1(r, s)$, so all internal vertices of Γ' must be Y_0's. Thus, $D(\Gamma')$ agrees with the number of endpoints of Γ'. If Γ' has only one endpoint, then it is simply a portion of the (i, r)-flow line from $c_{r,s}$ to $a_{i,r}^{+,+}$. In this case, Γ' agrees with the post-puncture part of a tree from Term 1.

Case 2. For some $r < s < j$, an (r, j)-flow becomes an (s, j)-flow at the puncture.

Lemma 7.20 applies to show $D(\Gamma') \geq 1$.

It remains to establish the claim about equality in Step 1. Suppose that $D(\Gamma') = 1$. As in Proof of Lemma 7.20, we can write $\Gamma' = \gamma_0 \sqcup \Gamma_1 \sqcup \cdots \sqcup \Gamma_p$, where the decomposition has the properties discussed in Proof of Lemma 7.20. Again, we can now apply Lemma 7.18 to each of the Γ_i to conclude that for all i, $D(\Gamma_i) > 0$. Thus, we must have $p = 1$ so the initial edge of Γ' is in $[1/4, 1/2]^2$ at the image of x_1.

First, **suppose Γ' has no internal vertices**. Then, Γ' is a single (s, j)-flow line. It must be the case that $(s, j) \neq (k+1, k+2)$ (by Lemma 7.13), so Γ_1 has image contained in A (by Lemma 7.14). Since this flow line, Γ_1, is an actual PFT, it must end at a Reeb chord or at an e-vertex.

- If Γ_1 ends at a Reeb chord, the only possible Reeb chord in A is $a_{s,j}^{-,-}$. Therefore, it must be that $\{s, j\} \cap \{k, k+2\} = \emptyset$ because otherwise $a_{s,j}^{-,-}$ does not exist. Thus, Γ' agrees with the post-puncture part of a tree from Term 2 (as ordered in Section 7.2.2).
- If Γ_1 ends at an e-vertex, then Γ_1 must be a $(k, k+2)$-flow line terminating somewhere along the $(k, k+2)$-cusp edge. [The $(k, k+1)$-cusp locus is disjoint from A.] In this case, Γ' agrees with the post-puncture part of a tree from Term 3.

Next, **suppose that Γ' has at least 1 internal vertex**. The first internal vertex is located somewhere on the initial edge of Γ_1 which is an (s,j)-flow line with $(s,j) \neq (k+1,k+2)$ (by Lemma 7.13). Thus, the vertex is located somewhere in A (by Lemma 7.14) and is a Y_0 (by Lemma 7.19).

Consider the PFTs Γ_a and Γ_b that begin with the branches of Γ' that follow this first Y_0 vertex, labeled so the lower sheet of Γ_a agrees with the upper sheet of Γ_b. By Lemma 7.18, it is the case that $D(\Gamma_a) \geq 0$ (resp. $D(\Gamma_b) \geq 0$) with equality only if Γ_a (resp. Γ_b) is a subset of the $(k+2,k+1)$-switch GFT starting on the $(k+2,k+1)$-switch flow line. Since $1 = D(\Gamma') = D(\Gamma_a) + D(\Gamma_b)$, one of the following two cases holds:

Case: Γ_a is a subset of the $(k+2,k+1)$-switch flow. Then, we have $s = k+2$ and $j > k+2$, and Γ_b would begin with a $(k+1,j)$-flow line, starting in the part of A that is below the crossing locus. We claim that there cannot be any internal vertices in Γ_b. [*Proof:* Suppose this is not the case and consider the first such vertex, z, which (due to the location of the image in A) must also be a Y_0. Now, Lemma 7.18 shows that the PFTs, $\Gamma_{z,1}$ and $\Gamma_{z,2}$, beginning with the outgoing edges at z both have $D(\Gamma_{z,i}) \geq 1$. (Neither one can start with a $(k+2,k+1)$-flow line since Γ_b began with a $(k+1,j)$-flow line.) This implies

$$D(\Gamma') = D(\Gamma_a) + D(\Gamma_b) = D(\Gamma_a) + D(\Gamma_{z,1}) + D(\Gamma_{z,2}) \geq 0 + 1 + 1 = 2,$$

which contradicts that $D(\Gamma') = 1$.]

Therefore, Γ_b must be a single flow line that can only end at $a^{-,-}_{k+1,j}$. It follows that Γ' agrees with the post-puncture portion of a flow tree from Term 5.

Case: Γ_b is a subset of the $(k+2,k+1)$-switch flow. Then, Γ_a would have to begin with an $(s,k+2)$-flow line for $s \leq k$.

First, **suppose Γ_a has no internal vertices.** Then, by Lemma 7.14 the $(s,k+2)$-flow line would have to end at the $(k,k+2)$-cusp edge, and could only be part of a PFT if $s = k$. Then, the initial branch of Γ' that precedes Γ_a and Γ_b would be the $(k,k+1)$-flow line that starts at $c_{r,k}$. Thus, Γ' would agree with the post-puncture part of a GFT from Term 4.

Finally, **suppose Γ_a has at least one internal vertex.** Applying Lemmas 7.14 and 7.19, we conclude that the first internal vertex of Γ_a must be a Y_0 in A. Neither outgoing branch of this Y_0 could begin with a $(k+2,k+1)$-flow line (since the incoming branch is an $(s,k+2)$-flow line), so Lemma 7.18 would give $D(\Gamma') > 1$, a contradiction.

Step 2. Above the puncture at $c_{r,s}$, Γ must consist of a single edge that limits to $c_{i,j}$.

This is similar to Step 2 from the uniqueness proof of Theorem 6.5, although the implementation is more involved.

Consider the path, β, within the domain of Γ, that starts just above the puncture at $c_{r,s}$ and follows edges in a manner that is reverse to their orientation until the the input vertex (assumed to be at $c_{i,j}$) is reached. In other words, β, consists of several consecutive edges $B_1, \ldots, B_N$ of Γ so that, with respect to the orientation of Γ, the endpoint of B_1 is at $c_{r,s}$; the initial point of B_i is the endpoint of B_{i+1} for $1 \leq i \leq N-1$; and B_N limits to $c_{i,j}$ as $t \to -\infty$. Let $y_1, \ldots, y_{N-1}$ denote the internal vertices where B_i and B_{i+1} meet for $1 \leq i \leq N-1$. See Figure 57.

Lemma 7.21. *The following properties hold:*

1. *The image of each B_i is contained in $[1/2,3/4] \times [1/2,3/4]$.*
2. *Each y_i is a Y_0-vertex.*
3. *At each y_i for $1 \leq i \leq N-1$, let Γ_i denote the PFT that begins with the edge of Γ at y_i that is not B_i or B_{i+1}. Then, $D(\Gamma_i) \geq 1$.*

Proof of Lemma 7.21. Recall the notation

$$Sq(c_{m_1,n_1}, c_{m_2,n_2}) = N_\epsilon Q1(m_1,n_1) \cap N_\epsilon Q3(m_2,n_2).$$

We establish the following statement:

Suppose that for some $1 \leq i \leq n-1$, B_i satisfies the following.

(A) There exists l, l', m, m' satisfying $l < l' \leq m$, and $l \leq m' < m$ such that B_i is an (l,m)-flow line and has its endpoint in $Sq(c_{l,l'}, c_{m',m})$.

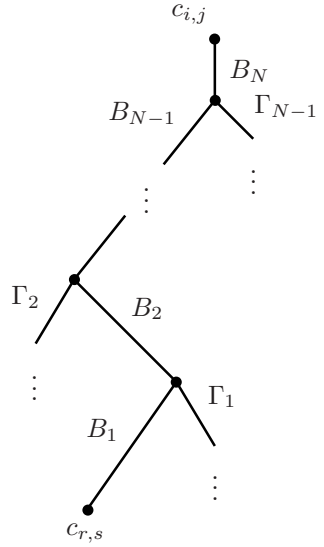

FIGURE 57. The sequence of edges $B_1, B_2, \ldots, B_N$ and the partial flow trees $\Gamma_1, \ldots, \Gamma_{N-1}$.

Then, (1), (2), and (3) hold for B_i, y_i and Γ_i, and B_{i+1} also satisfies (A).

It is straightforward that B_1 satisfies (A). [The endpoint of B_1 is at $c_{r,s}$, and B_1 is either an (r_1, s)-flow or a (r, s_1) for some $r_1 < r$ or $s < s_1$. In the first case, put $l = r_1$, $m' = r$, and $l' = m = s$; in the second case, put $m' = l = r$, $l' = s$, and $m = s_1$.] Thus we can apply the statement repeatedly to deduce the Lemma.

To prove the statement, observe that $-\nabla F_{l,m}$ points outward along all four edges of $Sq(c_{l,l'}, c_{m',m})$ by Property 10 (since (l, m) is between (l, l') and (m', m) with respect to lexicographic order). Thus, if the endpoint of B_i is in $Sq(c_{l,l'}, c_{m',m})$, then B_i remains there as t decreases. Thus, (1) holds since $Sq(c_{l,l'}, c_{m',m}) \subset [1/2, 3/4]^2$. Next, (2) holds since the cusp locus is disjoint from $[1/2, 3/4]^2$. Now, consider cases

Case 1. Γ_i begins with a (m, p)-flow line for some $m < p$. Since $Sq(c_{l,l'}, c_{m',m}) \subset N_\epsilon Q3(m', m)$, we can apply Lemma 7.20 to deduce that $D(\Gamma_i) \geq 1$. Moreover, B_{i+1} then begins with an (l, p)-flow line in $Sq(c_{l,l'}, c_{m',m}) \subset Sq(c_{l,l'}, c_{m',p})$, so B_{i+1} satisfies (A).

Case 2. Γ_i begins with a (h, l)-flow line for some $h < l$. Since $Sq(c_{l,l'}, c_{m',m}) \subset N_\epsilon Q1(l, l')$, we can apply Lemmas 6.11 and 7.5 to deduce that $D(\Gamma_i) \geq 1$ (all endpoints are at $a^{+,+}$ Reeb chords and, since the image of $D(\Gamma_i)$ is contained in a region that is disjoint from the cusp locus, all internal vertices of Γ_i are Y_0's). Moreover, B_{i+1} then begins with an (h, m)-flow line in $Sq(c_{l,l'}, c_{m',m}) \subset Sq(c_{h,l'}, c_{m',m})$, so B_{i+1} satisfies (A).

□

We now deduce Step 2 from Lemma 7.21. Using Step 1, we can compute

$$\begin{aligned} 0 = D(\Gamma) &= D(\Gamma') - 1 + \sum_{i=1}^{N-1} D(\Gamma_i) \\ &\geq 1 - 1 + (N-1), \end{aligned}$$

Thus, we must have $N = 1$ so that the edge B_1 runs from $c_{r,s}$ to its limit at $c_{i,j}$ without internal vertices. This is Step 2. Moreover, we see that $D(\Gamma') = 1$ must hold, so that Step 1 and Step 2 together show that the portions of Γ below and above the puncture at $c_{r,s}$ agree with a particular GFT from Terms 1-5. This completes the proof of Theorem 7.15.

□

7.3. **Flow trees without punctures at $c_{i,j}$'s.** With $\partial_c c_{i,j}$ understood, we turn now to the remaining terms in $\partial c_{i,j}$. To this end, let

$$\partial_b c_{i,j} = \sum_{\Gamma} w(\Gamma)$$

with the sum over rigid GFTs beginning at $c_{i,j}$ that do not have any outputs at Reeb chords of the form $c_{r,s}$ or $\tilde{c}_{k+2,k+1}$. In the remainder of 7.3, we work to obtain a characterization of these GFTs that

will allow computation of $\partial_b c_{i,j}$. See Proposition 7.27. The computation of $\partial_b c_{i,j}$ is then carried out in Section 7.4.

Lemma 7.22. *No edge in a partial flow tree can have both of its endpoints at switch vertices.*

Proof. Note that by Property 15 edges that end at a switch vertex can only be either (i,k)-, $(k+1,j)$-, $(k+1,k+2)$-, or $(k+2,k+1)$-flow lines for some $i<k$ or $k+2<j$; edges that begin at a switch point can only be $(i,k+1)$-, (k,j)-, $(k,k+2)$-, and $(k,k+1)$-flow lines. Recall, that within a Type (13) square, a single edge of a PFT may change from being an (i,j)-flow line to an (i',j')-flow line if it has an endpoint on $\tilde{S}_k, S_{k+1}$, or S_{k+2} and crosses the portion of the cusp locus where these sheets are identified. Thus, an index that begins as $k+1$ or $k+2$ could possibly become $k+2$ or $k+1$ during the course of the edge. However, even with this point in mind, considering the indices of edges that may begin or end with a switch vertex shows that no edge can both begin and end with a switch vertex. □

Lemma 7.23. *For $\{i,j\}\subset\{k,k+1,k+2\}$, any PFT, Γ, starting with an (i,j)-flow in $L(1/2)$ satisfies $D(\Gamma)\geq 0$. Moreover, equality holds only for those PFTs that are subsets of the $(k+1,k+2)$- or $(k+2,k+1)$- switch GFT beginning at a point on the initial edge, i.e. beginning with part of the $(k+1,k+2)$- or $(k+2,k+1)$- switch flow line.*

Proof. We establish the result by induction on the number of Y_0-vertices in the flow tree.

For PFTs beginning with a $(k+1,k+2)$ or $(k+2,k+1)$-flow line starting in $L(1/2)$ the result follows from Lemmas 7.12 and 7.13.

Thus, we can consider a PFT, Γ, beginning with a $(k,k+1)$- or $(k,k+2)$- flow line in $L(1/2)$. Note that along the initial edge no Y_1 or switch vertices are possible because the upper sheet of the flow is the upper sheet of the cusp locus. In the base case where there are no Y_0's, Γ can only terminate at the cusp edge since its image is contained in $L(1/2)$ (by Property 14) and there are no $(k,k+1)$- or $(k,k+2)$- Reeb chords in $L(1/2)$. In this case,

$$D(\Gamma)=A-C+E-Y_1-SW=0-0+1-0-0=1.$$

For the inductive step, suppose Γ has at least one Y_0. At the first Y_0, which is located in $L(1/2)$ (by Property 14), the initial $(k,k+1)$-flow line (resp. $(k,k+2)$-flow line), splits into a $(k,k+2)$-flow line and a $(k+2,k+1)$-flow line (resp. a $(k,k+1)$-flow line and a $(k+1,k+2)$-flow line). Let Γ_1 and Γ_2 denote the two PFTs consisting of the portion of Γ that begins with these two branches of the tree. The inductive hypothesis gives $D(\Gamma_1)>0$, and $D(\Gamma_2)\geq 0$. Thus, $D(\Gamma)=D(\Gamma_1)+D(\Gamma_2)>0$. □

Let $B=D(1/2)\cap L(1/2)$.

Lemma 7.24. *Any PFT Γ starting in B satisfies $D(\Gamma)\geq 0$. Moreover, equality holds only for trees with a single internal vertex at a switch. Any such partial flow tree can be described in one of the following ways:*

1. *A subset of the (i,k)-switch GFT beginning on the branch that precedes the switch.*
2. *A subset of the $(k+1,k+2)$-switch GFT beginning on the branch that precedes the switch.*
3. *A subset of the $(k+2,k+1)$-switch GFT beginning on the branch that precedes the switch.*

(By the definition of PFT (see Definition 2.3), in (1)-(3) Γ contains the entire portion of the appropriate switch GFT that follows the initial point of Γ, including the switch vertex and the last edge of the GFT.)

Proof. First, note that for PFTs beginning with an (i,j)-flow line with $\{i,j\}\subset\{k,k+1,k+2\}$, the result follows from Lemma 7.23.

We now assume Γ begins in B with an (i,j)-flow line with $\{i,j\}\not\subset\{k,k+1,k+2\}$, and prove the Lemma by induction on the sum of the number of Y_0 and Y_1 vertices in Γ. (We do allow the possibility that Γ begins with a flowline involving the sheet $\tilde{S}_k$.)

For the **base case**, suppose that Γ has no Y_0's and Y_1's. The tree must have precisely one output vertex possibly preceded by a switch vertex. Since $\{i,j\}\not\subset\{k,k+1,k+2\}$, the Property 14 shows that the entire image of Γ is in the region B. As B does not contain $b_{i,j}$ or $c_{i,j}$ Reeb chords, the output must be at an $a^{-,-}$ Reeb chord or at an e-vertex, so we have

$$1=A-C+E.$$

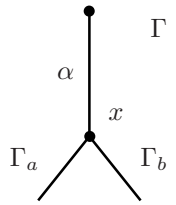

FIGURE 58. The PFT Γ begins in B and has its first Y_0- or Y_1-vertex at $x \in B$. The segment α begins with the initial edge of Γ and may possibly contain a 2-valent switch vertex.

Since there are no Y_1 vertices, and Γ can have at most one switch by Lemma 7.22, the inequality

$$D(\Gamma) = A - C + E - SW - Y \geq 0$$

follows. Those PFTs that contain exactly one switch will produce equality. We claim that without Y_0's or Y_1's, there are no such trees with a switch at the $(k+1, j)$-switch point for $k+2 < j$. Thus, in view of Property 15, trees without Y_0's and Y_1's and with $D(\Gamma) = 0$ match the description given in (1)-(3) of the statement of Lemma 7.24. [To verify the claim, note that the (k, j)-flowline that we are left with after a switch at the $(k+1, j)$-switch point must remain in B. However, there are no (k, j) Reeb chords in B, and sheets k and j do not meet at any cusp edge.]

For the **inductive step**, suppose that Γ has at least one Y_0- or Y_1-vertex. Consider the first Y_0- or Y_1-vertex, x, that is encountered when traveling away from the initial point of Γ. A priori, the part of the tree, $\alpha \subset \Gamma$, that connects x to the start of Γ may contain switches. However, Lemma 7.22 implies that α can have at most one such switch.

Let Γ_a and Γ_b denote the PFTs that begin with the two branches of Γ that follow x, notated so that, for some i, j, m, l, (some of which may be equal to $\tilde{k}$), the incoming edge is a (i, j)-flow line at x, Γ_a begins with an (i, m)-flow line, and Γ_b begins with an (l, j)-flow. Note that i and j used here may be different from their values at the initial point of Γ, due to α crossing the boundary between sheets $\widetilde{S}_k$ and one of S_{k+1} or S_{k+2}, or due to a switch occurring along α. However, note that at all points of α we still have $\{i, j\} \not\subset \{k, k+1, k+2\}$, so that the image of α is entirely contained in B (by Property 14). Thus, the inductive hypothesis applies to both Γ_a and Γ_b. See Figure 58.

Case 1: The vertex x is a Y_1.

First, **suppose that α does not contain a switch**. Supposing the Y_1 is along the $(k, k+1)$-cusp edge, Γ_a and Γ_b would respectively begin with $(i, k+1)$- and (k, j)- flow lines, and we must have $i < k$ and $k+1 < j$. If instead the Y_1 occurs along the $(k, k+2)$-cusp edge, Γ_a and Γ_b would respectively begin with $(i, k+2)$- and (k, j)- flow lines with $i < k$ and $j \in \{k+1, k+3, \ldots\}$. Note that none of the degree 0 PFTs listed in (1), (2), (3) of the statement begin with an edge that is a $(i, k+1)$-, $(i, k+2)$-, or (k, j)-flow line for $i < k, j \geq k+1$. As Γ_a and Γ_b both begin with edges of one of these types, the inductive hypothesis shows that $D(\Gamma_a) \geq 1$ and $D(\Gamma_b) \geq 1$, and we can estimate

$$D(\Gamma) = D(\Gamma_a) + D(\Gamma_b) - 1 \geq 1 + 1 - 1 = 1.$$

Next, **suppose that α does contain a switch**. We will show that this case cannot actually occur. The only possibility is that the switch occurs at the (i, k)-switch point with the incoming edge an (i, k)-flow line and the outgoing edge initially an $(i, k+1)$-flow line. [For the other possible switch vertices identified in Property 15, the outgoing edge must be either a $(k, k+1)$-, $(k, k+2)$-, or (k, j)-flow line for some $k+2 < j$. However, the internal vertex that occurs at the end of this edge was assumed to be the Y_1 at x. This is impossible since the entire edge must have S_k as the upper sheet, and the incoming edge at a Y_1 vertex must have its upper sheet above the sheets that meet at the cusp edge.]

Thus, the outgoing edge at the switch is the $(i, k+1)$-flow line, ν, that begins at the (i, k)-switch point. Recall that in the proof of Lemma 7.11, a region $C_{i,k}$ was defined (see Figures 49 and 59) and shown to satisfy the following:

Claim A. For $i < k$, the $(i, k+1)$-flow line, ν, beginning at the (i, k)-switch point has its entire image contained in $C_{i,k}$. (The parts of ν that lie to the left of the $(k, k+2)$-cusp locus are $(i, \tilde{k})$-flow lines and are also contained in $C_{i,k}$.)

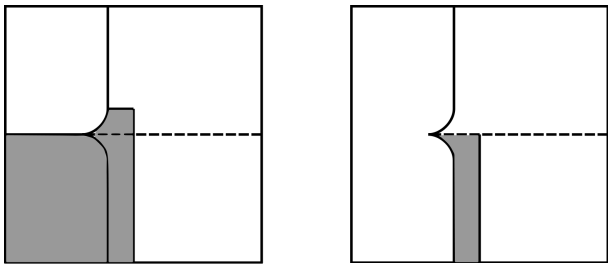

FIGURE 59. The regions $C_{i,k}$ and C' from Claims A and B.

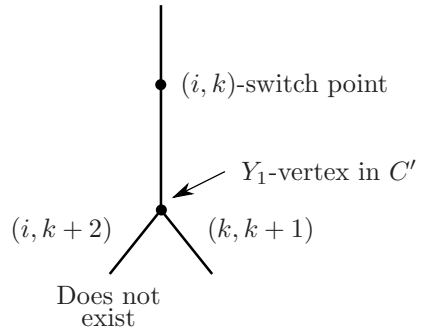

FIGURE 60. Summary of reasoning applied for the inductive step in Case 1 when the initial branch of Γ ends at a switch.

Thus, the Y_1 vertex that occurs at x could only be located somewhere on the $(k,k+2)$ cusp edge since the incoming edge must be either a $(i,k+1)$- or $(i,\tilde{k})$-flow line contained in $C_{i,k}$. After the Y_1, the outgoing edges are an $(i,k+2)$-flow line and a $(k,k+1)$-flow line. We show that the PFT beginning with the edge that is the $(i,k+2)$-flow line cannot exist. (Our line of reasoning is summarized in Figure 60.)

Claim B. For $i<k$, there are no PFTs that begin with an $(i,k+2)$-flow line starting in the region C' that lies below the crossing locus; to the right of the $(k,k+2)$-cusp locus; and to the left of $x_1=-17/64$.

Proof of Claim B. The region C' is pictured in Figure 59. Suppose such a PFT does exist. The $(i,k+2)$-flow line cannot leave C' (by Properties 17 and 18, and the fact that the flow line would terminate if it reaches the $(k,k+2)$ cusp edge since $i<k$.) Thus, since there are no $(i,k+2)$-Reeb chords in C', and S_i and S_{k+2} do not meet at a cusp edge in C', this edge must end at an internal vertex which can only be a Y_0. The outgoing edges will be a (i,i')-flow line and a $(i',k+2)$-flowline for some $i<i'\leq k$. If $i'<k$, then we repeat this argument with the $(i',k+2)$-edge to locate another Y_0. If $i'=k$, then the (i,k)-edge must remain in C' (by the same reasoning that shows the $(i,k+2)$-flow line cannot leave). Then, we can apply a similar argument to see that this edge must end at a Y_0. (Note, that the edge cannot end at the (i,k)-switch point which does not belong to C'.) One of the outgoing edges at this Y_0 would be an (i'',k)-flow line with $i<i''<k$ beginning in C', and so we could repeat the same argument to find yet another Y_0. However, this process cannot go on indefinitely since there are only finitely many numbers between i and k, so we reach a contradiction.

Case 2: The vertex x is a Y_0.

First, **suppose that α does not contain a switch**. Then,

$$D(\Gamma)=D(\Gamma_a)+D(\Gamma_b).$$

The inductive hypothesis gives $D(\Gamma_a)\geq 0$ and $D(\Gamma_b)\geq 0$. Note that because Γ_a and Γ_b must respectively start with an (i,m)-flow line and an (m,j)-flow line, it is impossible that they are both degree 0 PFTs as described in (1), (2), (3) in the statement of this Lemma. Thus, $D(\Gamma_a)>0$ or $D(\Gamma_b)>0$, so $D(\Gamma)\geq 1$ holds.

Finally, **suppose that α does contain a single switch**, y, so that

$$D(\Gamma) = D(\Gamma_a) + D(\Gamma_b) - 1.$$

We do not need to consider the case where y is at the $(k+1,k+2)$- or $(k+2,k+1)$-switch point (since Γ does not begin with an (i,j)-flow line with $\{i,j\} \subset \{k,k+1,k+2\}$), so we are left to consider two cases.

Subcase A: The vertex y is an (i,k)-switch point with $i < k$. Then, the edge of the tree that directly follows y and precedes x begins is the $(i,k+1)$-flow line, ν, starting at the switch.

In view of Claim A, the incoming edge at x is a flow line in $C_{i,k}$ with lower sheet either $\tilde{S}_k$ or S_{k+1}, so we see that either

(a) Γ_a begins with an (i,m)-flow line and Γ_b begins with an $(m,k+1)$-flow line for some m such that sheet S_m lies between sheets S_i and S_{k+1} at the image of x, or

(b) Γ_a begins with an (i,m)-flow line and Γ_b begins with an $(m,\tilde{k})$-flow line (i.e. a flow line for $-\nabla(F_m - \tilde{F}_k)$) for some m such that sheet S_m lies between sheets S_i and $\widetilde{S}_k$ at the image of x.

Here, (a) occurs if x is to the right of the cusp locus and (b) occurs if x is to the left of the cusp locus. By the description of degree 0 PFTs found in (1)-(3) of this Lemma, we know from the inductive hypothesis that both Γ_a and Γ_b have degree strictly greater than 0 in all cases except possibly when (a) occurs and $m = k$ or $m = k+2$. We address these exceptional cases separately.

- If $m = k$, note that x cannot occur at a point belonging to the (i,k)-switch flow line that precedes the (i,k)-switch point. [A switch at the (i,k) switch point, y, has already occured in the edge from y to x, and the difference functions $F_{i,j}$ strictly decrease along all edges of a PFT and when passing a Y_0 vertex.] Thus, Γ_a and Γ_b both have strictly positive degree so that $D(\Gamma) \geq 1$ holds.
- The case $m = k+2$ cannot actually occur.
  As $F_{k+2,k+1}$ is only positive below the crossing locus, and Γ_b begins with a $(k+2,k+1)$-flow, it must be the case that the image of x which is in $C_{i,k}$ (by Claim A) lies below the crossing locus and right of the cusp locus, i.e. in the region C' from Claim B. However, the PFT Γ_a then starts with an $(i,k+2)$-flow line in C', with $i < k$, and cannot exist by Claim B.

Subcase B: The vertex y is a $(k+1,j)$-switch point with $k+2 < j$. The edge that follows y and ends at x is then a (k,j)-flow line. Thus, Γ_a and Γ_b will begin respectively with (k,l)- and (l,j)-flow lines for some $k < l$. The characterization of degree 0 PFTs from (1)-(3) applies to show that both $D(\Gamma_a) \geq 1$ and $D(\Gamma_b) \geq 1$, and $D(\Gamma) \geq 1$ follows.

□

Lemma 7.25. *Let Γ be a PFT with $D(\Gamma) = 0$ and without endpoints at Reeb chords of the form $c_{i,j}$ or $\tilde{c}_{k+2,k+1}$. Then,*

(1) *Γ has no Y_1 vertices,*
(2) *any edge that starts with a switch vertex ends at a Reeb chord or e-vertex, and*
(3) *all endpoints of Γ occur either at b Reeb chords or at the end of an edge that starts with a switch at either the (i,k)-, $(k+1,k+2)$-, or $(k+2,k+1)$-switch point.*

Proof. Let $y_1, \ldots, y_m$ denote a collection of Y_1 and switch vertices of Γ such that

(1) the PFTs $\Gamma_1, \ldots, \Gamma_m$ that begin just above the y_i are disjoint from one another (as subsets of the domain of Γ), and
(2) all Y_1 and switch vertices of Γ are contained in the union of the Γ_i.

See Figure 61. [To construct such a collection $y_1, \ldots, y_m$, note that if two PFTs intersect (in the domain of Γ) than one is contained in the other. Begin by listing all the switches and Y_1 vertices as $z_1, \ldots, z_M$. Start with $y_1^1 = z_1$, and build collections $\{y_1^i, \ldots, y_{m_i}^i\}$ inductively for $1 \leq i \leq M$ so that at the i-th step (1) holds and all vertices $z_1, \ldots, z_i$ are contained in the PFTs starting above $y_1^i, \ldots, y_{m_i}^i$. For the inductive step, if z_{i+1} is already contained in the union of PFTs starting at $y_1^i, \ldots, y_{m_i}^i$, then do not change the collection. Else, add z_{i+1} to the $y_1^i, \ldots, y_{m_i}^i$ and throw out all y_j^i that are contained in the PFT starting at z_{i+1}.]

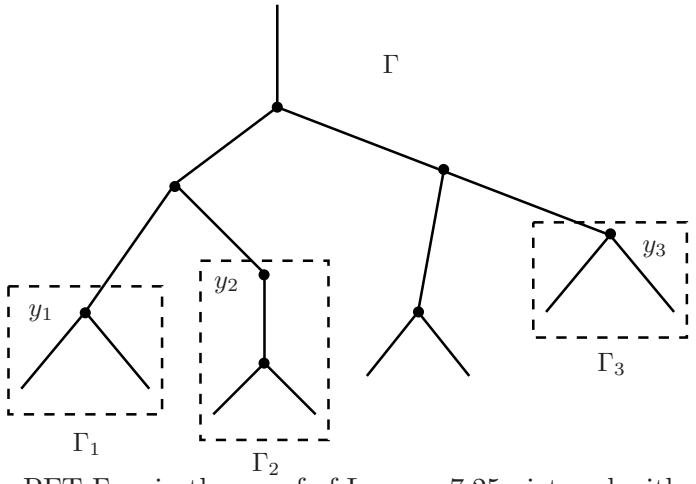

FIGURE 61. The PFT Γ as in the proof of Lemma 7.25 pictured with $m = 3$. The vertices $y_1, \dots, y_m$ are Y_1- and sw- vertices chosen so that all vertices outside of $\Gamma_1, \dots, \Gamma_m$ are Y_0's.

Since Γ was assumed to not have punctures at $c_{i,j}$'s, we then have

$$0 = D(\Gamma) = \sum_i D(\Gamma_i) + A' + E', \tag{20}$$

where A' and E' respectively denote the number of output vertices at $a_{i,j}$'s and at e-vertices that are located in $\Gamma \setminus (\bigcup_i \Gamma_i)$.

Each of the Γ_i starts in B. [Property 10 shows that Y_1's cannot occur where $x_2 \geq 1/2$ since, for all S_i and S_j that are above and below the cusp edge, $-\nabla F_{i,j}$ points to the side of the cusp locus with fewer sheets. In addition, all switch points are located in B.] Thus, by Lemma 7.24 each Γ_i has $D(\Gamma_i) \geq 0$. Therefore, all terms on the right hand side of (20) are non-negative, and we can conclude that they all vanish. Consequently, all of the y_i must be switches with the flow trees Γ_i as described in (1)-(3) of Lemma 7.24. It follows that Γ has no Y_1-vertices, and there are no other switches in Γ. Since $A' = E' = 0$, all endpoints of Γ that do not follow switches are at $b_{i,j}$ generators.

□

7.4. **Enumeration of b-trees.** With Lemma 7.25 in hand, we can now compute $\partial_b c_{i,j}$ using a method that is parallel to that of Section 6.5. We begin by modifying some of the terminology from 6.5 to our current setting.

Definition 7.26. In a Type (13) square, a **b-tree** is a PFT or GFT that satisfies the conclusions (1)-(3) of Lemma 7.25 and also

(4) does not have any endpoints at $\tilde{b}^R_{k+2,k+1}$.

Let

$$\partial_b c_{i,j} = \sum w(\Gamma) \tag{21}$$

where the summation is over b-trees that begin with a positive puncture at $c_{i,j}$.

The following is an immediate consequence of Lemma 7.25.

Proposition 7.27. *For any $1 \leq i < j \leq n$,*

$$\partial c_{i,j} = \partial_c c_{i,j} + \partial_b c_{i,j} + x$$

where x denotes a term belonging to the two-sided ideal generated by $\tilde{b}^R_{k+2,k+1}$.

Note that branches of a b-tree that follow switches must be as in the (i,k)-, $(k+1,k+2)$-, and $(k+2,k+1)$-switch GFTs, and in particular are uniquely determined by the switch point. In these three cases the branch that follows the switch is the flow line that starts at the switch point and respectively limits to $a^{-,-}_{i,k+1}$, ends at an e-vertex on the $(k,k+2)$-cusp edge, or ends at an e-vertex on the $(k,k+1)$-cusp edge. (See Lemmas 7.9 and 7.11.) When such a switch occurs in a b-tree, we will refer to the switch and the following edge as a **switch output** at $sw_{i,k}$, $sw_{k+1,k+2}$, or $sw_{k+2,k+1}$.

We consider two types of b-trees as follows. Define a b^{LU}**-tree** to be a b-tree that has all outputs at Reeb chords of the form $b^L_{i,j}$, $b^U_{i,j}$ or at switch outputs of the form $sw_{i,k}, sw_{k+1,k+2}$. Define a b^{RD}**-tree** to be a b-tree that has all outputs at Reeb chords of the form $b^R_{i,j}$, $b^D_{i,j}$, or at switch outputs of the form $sw_{k+2,k+1}$. We write $\partial_{b^{LU}} c_{i,j}$ and $\partial_{b^{RD}} c_{i,j}$ respectively for the portion of the sum (21) arising from b^{LU}-trees and b^{RD}-trees.

In the Type (13) square, the role of b^{LU}-trees and b^{RD}-trees are no longer entirely symmetric. Consequently, we compute $\partial_{b^{LU}} c_{i,j}$ and $\partial_{b^{RD}} c_{i,j}$ separately in 7.4.1 and 7.4.2, respectively.

The following observations follow from the definition of b-tree.

Lemma 7.28. (i) *Aside from the switches at $sw_{i,j}$-outputs, all other internal vertices in a b-tree must be Y_0's.*

(ii) *For any Y_0 in a b-tree, b^{LU}-tree, or b^{RU}-tree, both of the PFTs that start with the outgoing edges of the Y_0 are themselves b-trees, b^{LU}-trees, or b^{RU}-trees, respectively.*

7.4.1. *b^{LU}-trees.* For $1 \leq i < j \leq n$, we again define regions $B^{LU}(i,j)$. The definition is as in Section 6.5, except that we **replace all uses of the segment B_2 that appear in the definition from Section 6.5 with the Swallowtail Barrier** P, see Figure 38. Recall $R(sw_{i,j})$ from Figure 49.

Lemma 7.29. *Any edge, γ, of a b^{LU}-tree that does not start with a switch must*

(1) *be an (i,j)-flow line for some $i < j$ and*

(2) *have the intersection of its image with $\widehat{N}(e^2_\alpha)$ contained in the region*

$$B^{LU}(i,j), \text{ if } (i,j) \text{ does not have the form } (k+1,k+2) \text{ or } (i,k) \text{ with } i<k;$$

$$R(sw_{i,j}), \text{ if } (i,j) = (k+1,k+2) \text{ or } (i,j)=(i,k) \text{ with } i<k.$$

Moreover, the image of γ is entirely in $\widehat{N}(e^2_\alpha)$ unless γ is part of a $b^X_{i,j}$-line for $X \in \{L,U\}$.

Proof. We consider slightly smaller regions $A^{LU}(i,j)$, defined by

(1) $A^{LU}(i,j) = R(sw_{i,j})$, if $(i,j) = (i,k)$ or $(i,j) = (k+1,k+2)$;
(2) $A^{LU}(i,j) = B^{LU}(i,j) \cap \{x_1 \geq 1/4\}$, if $(i,j) = (k,k+1)$ or $(i,j) = (k,k+2)$;
(3) $A^{LU}(i,j) = B^{LU}(i,j) \cap \{x_1 \geq -3/8\}$, if $\{i,j\} \cap \{k,k+1\} \neq \emptyset$, and (i,j) is not $(i,k), (k+1,k+2), (k,k+1)$, or $(k,k+2)$.
(4) $A^{LU}(i,j) = B^{LU}(i,j)$, if $\{i,j\} \cap \{k,k+1\} = \emptyset$.

Note that for any $i<j$, $-\nabla F_{i,j}$ points outwards along all parts of $\partial A^{LU}(i,j)$, with $-\nabla(F_i - \widetilde{F}_k)$ or $-\nabla(\widetilde{F}_k - F_j)$ pointing outward as well when $i = k+2$ or $j = k+2$. [For $A^{LU}(i,j)$ as in (1), this is shown in Lemmas 7.10 and 7.11; as in (2), use Properties 10, 16, and 3; as in (4), add Property 14 and 2; as in (3), add Corollary 7.8.]

We prove a slightly stronger version of the proposition, where the $B^{LU}(i,j)$ are replaced with the $A^{LU}(i,j)$, by induction on the number of Y_0's in the PFT that starts with γ. In the base case, Lemma 7.28 (i) implies the only b^{LU}-trees without Y_0's are the $b^L_{i,j}$-lines (here $\{i,j\} \cap \{k,k+1\} = \emptyset$); the $b^U_{i,j}$-lines, and the (i,k)- and $(k+1,k+2)$-switch GFTs. By Proposition 5.11, we see that the $b^L_{i,j}$- and $b^U_{i,j}$-lines all enter $\widehat{N}(e^2_\alpha)$ along $\partial A^{LU}(i,j)$, and that the parts of their images that lie outside of $\widehat{N}(e^2_\alpha)$ are all pairwise disjoint. Lemma 7.10 and Lemma 7.11 show that the branchs of the (i,k)- and $(k+1,k+2)$-switch GFTs that do not start with switches are contained in $A^{LU}(i,k)$ and $A^{LU}(k+1,k+2)$.

For the inductive step, Lemma 7.28 implies that if the PFT starting with γ contains at least 1 Y_0, then γ itself must end at a Y_0. Moreover, the inductive hypothesis applies to the two outgoing edges at the Y_0, so, for some $i<m<j$, they must be (i,m) and (m,j)-flow lines with the Y_0 point located in $A^{LU}(i,m) \cap A^{LU}(m,j)$. Since we have seen that $-\nabla F_{i,j}$ points out along $\partial A^{LU}(i,j)$, the argument is completed by the following.

Claim. For any $i<m<j$, $A^{LU}(i,m) \cap A^{LU}(m,j) \subset A^{LU}(i,j)$.

To verify the claim, note that it is impossible that both (i,m) and (m,j) are of the forms (i,k) or $(k+1,k+2)$. Thus, $A^{LU}(i,m) \cap A^{LU}(m,j) \subset \{x_2 \geq 1/2\}$, so we show $\widehat{A}^{LU}(i,m) \cap \widehat{A}^{LU}(m,j) \subset A^{LU}(i,j)$ where $\widehat{A}^{LU}(i,j) = A^{LU}(i,j) \cap \{x_2 \geq 1/2\}$. Moreover, $\widehat{A}^{LU}(i,j) \cap \{x_1 \geq 1/4\} = B^{LU}(i,j) \cap \{x_1 \geq 1/4\}$,

and just as in Section 6.5, the lexicographic ordering of the $\beta_{i,j}$ easily shows $B^{LU}(i,m)\cap B^{LU}(m,j)\subset B^{LU}(i,j)$. (See Figure 39.) It only remains to check that

$$\left(\widehat{A}^{LU}(i,m)\cap\widehat{A}^{LU}(m,j)\right)\cap\{x_1<1/4\}\subset A^{LU}(i,j)\cap\{x_1<1/4\}. \tag{22}$$

Note that each $\widehat{A}^{LU}(i,j)\cap\{x_1<1/4\}=\{(x_1,x_2)\in\widehat{N}(e^2_\alpha)\,|\,\alpha_{i,j}\le x_1<1/4, 1/2\le x_2\}$ where

$$\alpha_{i,j}=\begin{cases}-1, & \text{if } \{i,j\}\cap\{k,k+1\}=\emptyset,\\ -3/8, & \text{if } \{i,j\}\cap\{k,k+1\}\neq\emptyset \text{ and } (i,j)\neq(k,k+1),(k,k+2),\\ 1/4, & \text{if } (i,j)=(k,k+1) \text{ or } (i,j)=(k,k+2).\end{cases}$$

Thus, (22) is equivalent to $Max\{\alpha_{i,m},\alpha_{m,j}\}\ge\alpha_{i,j}$ for all $i<m<j$. This is easily verified by cases. [It's clear when $\alpha_{i,j}=-1$. When $\alpha_{i,j}=-3/8$, since $\{i,j\}\cap\{k,k+1\}\neq\emptyset$, we also have $\{i,m,j\}\cap\{k,k+1\}\neq\emptyset$. When $\alpha_{i,j}=1/4$, we can only have $(i,m,j)=(k,k+1,k+2)$, and $\alpha_{k,k+1}=\alpha_{k,k+2}=1/4$.] □

Next, we define a disk datum $(D^{LU},\{b^L_{i,j},b^U_{i,j},sw_{i,k},sw_{k+1,k+2}\},\{I_{i,j}\})$. Let $R\subset\widehat{N}(e^2_\alpha)$ denote the region below $x_2=1/2$ that is above and to the left of the Swallowtail Barrier P and to the right of the cusp locus. We define

$$D^{LU}=\left(\bigcup_{1\le i<j\le n}B^{LU}_{i,j}\bigcup R\right)\setminus\left(\bigcup_{1\le i<j\le n}Sq_{i,j}\right)$$

where the $Sq_{i,j}=(\beta^U_{i,j}-\epsilon,\beta^U_{i,j}-\epsilon)\times(\beta^R_{i,j}-\epsilon,\beta^R_{i,j}-\epsilon)$ are small squares containing $c_{i,j}$. We use $b^L_{i,j},b^U_{i,j}$ to denote (by slight abuse of notation) the unique intersection points of the $b^L_{i,j}$- and $b^U_{i,j}$-lines with ∂D^{LU}, and use $sw_{i,k},sw_{k+1,k+2}$ to denote the (i,k)- and $(k+1,k+2)$-switch points which also lie on ∂D. In all cases, the upper and lower indices agree with the subscripts. The intervals $I_{i,j}$ are given by the upper and left edges of the closure $\overline{Sq}_{i,j}$.

There is a generalized b-manifold $A=\sqcup_r A_r$ given by paths γ that are the intersection with $\widehat{N}(e^2_\alpha)$ of the top branch of a GFT that is a b^{LU}-tree beginning at some $c_{i,j}$. (Note that except for the ends of the $b^L_{i,j}$- and $b^R_{i,j}$-lines all such top branches are in fact entirely contained in $D^{LU}\cup Sq_{i,j}$, by Lemma 7.29.) Upper and lower indices $i(\gamma)<j(\gamma)$ are assigned to each $\gamma\in A$ so that γ is an $(i(\gamma),j(\gamma))$-flow line (or an $(i,\tilde{k})$- or $(\tilde{k},j)$-flow line if $j(\gamma)=k+2$ or $i(\gamma)=k+2$). (Note that this definition of $(i(\gamma),j(\gamma))$ is well defined: All γ have there image in D^{LU} and, in particular, may not cross the $(k,k+2)$-cusp locus. Thus, crossing the cusp locus *cannot* cause, γ, to change from an $(i,\tilde{k})$-flow line to an $(i,k+1)$-flow line, or from a $(\tilde{k},j)$-flow line to a $(k+1,j)$-flow line.)

Lemma 7.30. *Let $A=\bigsqcup_r A_r$ denote the collection of such paths γ with $i(\gamma)$ and $j(\gamma)$ as above. Then, A is a generalized b-manifold for the disk datum $(D^{LU},\{b^L_{i,j},b^U_{i,j},sw_{i,k},sw_{k+1,k+2}\},\{I_{i,j}\})$. Moreover, for $1\le i<j\le n$,*

$$\varphi(\partial_A I_{i,j})=\partial_{b^{LU}}c_{i,j} \tag{23}$$

where the sum on the right is over b^{LU}-trees that start at $c_{i,j}$, and

$$\varphi:\mathbb{Z}/2\langle b^L_{i,j},b^U_{i,j},sw_{i,k},sw_{k+1,k+2}\rangle\to\mathcal{A}_{LCH}(e^2_\alpha)$$

is the $\mathbb{Z}/2$-algebra homomorphism determined by

$$\varphi(b^L_{i,j})=b^L_{i,j};\quad \varphi(b^U_{i,j})=b^U_{i,j};\quad \varphi(sw_{i,k})=a^{-,-}_{i,k+1};\quad \varphi(sw_{k+1,k+2})=1.$$

Proof. That $A=\sqcup A_r$ is indeed a generalized b-manifold is verified as in the proof of Proposition 6.21. Items (1) and (6) from Definition 6.20 are verified exactly as in Proposition 6.21, while in the verification of (2) we need to use Lemma 7.29 instead of Lemma 6.18. Finally, to check items (3)-(5) concerning the endpoints of paths, we note that if $\widehat{\gamma}$ is the top most branch of a b^{LU}-tree, Γ, then Lemma 7.28 shows that when $t\to+\infty$, $\widehat{\gamma}$ must either (a.) limit to some $b^L_{i,j}$ or $b^U_{i,j}$, (b.) end at a Y_0 such that the outgoing edges are themselves top branches of b^{LU}-trees, or (c.) end at a switch vertex at either $sw_{i,k}$ or $sw_{k+1,k+2}$. Thus, paths in $A=\sqcup A_r$ indeed correspond to (i) the

points $\{b^L_{i,j}, b^U_{i,j}, sw_{i,k}, sw_{k+1,k+2}\} \subset \partial D^{LU}$ and (ii) triples (γ_1, γ_2, x) with $\gamma_1, \gamma_2 \in A$, $x \in \gamma_1 \cap \gamma_2$, and $j(\gamma_1) = i(\gamma_2)$.

To verify (23), let γ be the top of a b^{LU}-tree Γ that starts at $c_{i,j}$. Then, verify using induction on the number of Y_0's in Γ that

$$\varphi(w(\gamma)) = w(\Gamma)$$

where on the left $w(\gamma)$ is the word associated to $\gamma \in A$. In the base case, Lemmas 7.9 and 7.11 give that $w(\Gamma_{k+1,k+2}) = 1$ and $w(\Gamma_{i,k}) = a^{-}_{i,k+1}$ when $\Gamma_{k+1,k+2}$ and $\Gamma_{i,k}$ are respectively the $(k+1,k+2)$- and (i,k)-switch GFTs. The inductive step is an immediate consequence of equation (14) and the definitions of $w(\gamma)$ (defined right after Definition 6.20) and $w(\Gamma)$. □

Proposition 7.31. *For any $1 \le i < j \le n$, $\partial_{b^{LU}} c_{i,j}$ is equal to the (i,j)-entry of the matrix*

$$(I + B_U)(I + B_L)(I + A_{-,-}E_{k+1,k} + E_{k+1,k+2})$$

where the matrices B_U, B_L and $A_{-,-}$ are as in Theorem 7.4.

Proof. From Lemma 7.30 and Proposition 6.22, we see that

$$\partial_{b^{LU}} c_{i,j} = \varphi(\partial_A I_{i,j})$$

where A is *any* generalized b-manifold associated to the disk datum $(D^{LU}, \{b^L_{i,j}, b^U_{i,j}, sw_{i,k}, sw_{k+1,k+2}\}, \{I_{i,j}\})$.

We construct an explicit generalized b-manifold $A = \sqcup A_r$ in several steps that we call *levels*. At Level 0, we will begin by choosing paths to connect each of the points $\{b^L_{i,j}, b^U_{i,j}, sw_{i,k}, sw_{k+1,k+2}\}$ to the appropriate $I_{i,j}$. Then, at Level 1 we identify all intersections between paths that share a common upper and lower index, and choose paths to connect each of these intersection points to the required $I_{i,j}$. The construction is completed once we reach a Level where no new intersections arise.

We say that an intersection of paths $\gamma_1, \gamma_2 \in A$ is **A-relevant** if $j(\gamma_1) = i(\gamma_2)$ and A-irrelevant otherwise.

Level 0

(1) Connect each $b^U_{i,j}$ to $I_{i,j}$ by a straight vertical segment, $\gamma^U_{i,j}$.
(2) Connect each $b^L_{i,j}$ to $I_{i,j}$ by a piecewise linear path, $\gamma^L_{i,j}$, (smoothed at the corner) consisting of (i) the segment from $b^L_{i,j}$ to $(-1/2, \beta^R_{i,j})$, then (ii) the straight horizontal segment from $(-1/2, \beta^R_{i,j})$ to $I_{i,j}$. Here, $\{i,j\} \cap \{k, k+1\} = \emptyset$.
(3) For $(i,j) = (i,k)$ or $(i,j) = (k+1, k+2)$, connect $sw_{i,j}$ to $I_{i,j}$ by a piecewise linear path, $\gamma^{sw}_{i,j}$, (smoothed at the corners) consisting of (i) a horizontal segment from $sw_{i,j}$ to $x_1 = -1/4$, then (ii) the straight vertical segment from this point to $(-1/4, \beta^R_{i,j})$, then (iii) the straight horizontal segment from $(-1/4, \beta^R_{i,j})$ to $I_{i,j}$. The second segment (ii) is identical for different values of $(i,j) = (i,k), (k+1, k+2)$, so we shift the segments slightly in the horizontal direction. [The precise manner that this is done is irrelavent, since intersections between any two $\gamma^{sw}_{i,j}$ are A-irrelevant.]

Note that the contribution to $\varphi(\partial_A I_{i,j})$ from paths constructed at Level 0 is the (i,j)-entry of the matrix

$$B_U + B_L + A_{-,-}E_{k+1,k} + E_{k+1,k+2}.$$

Level 1

The A-relevant intersections between paths defined at Level 0 are as follows:

(1) For $i < m < j$, with $\{m,j\} \cap \{k, k+1\} = \emptyset$, $\gamma^U_{i,m}$ intersects $\gamma^L_{m,j}$ in an ϵ-neighborhood of $(\beta^U_{i,m}, \beta^R_{m,j})$.
(2) For $i < m < j$, with $(m,j) = (m,k)$ or $(m,j) = (k+1, k+2)$, $\gamma^U_{i,m}$ intersects $\gamma^{sw}_{m,j}$ in an ϵ-neighborhood of $(\beta^U_{i,m}, \beta^R_{m,j})$.
(3) For $i < m < j$, with $(m,j) = (m,k)$ or $(m,j) = (k+1, k+2)$, $\gamma^L_{i,m}$ intersects $\gamma^{sw}_{m,j}$ at $(-1/4, \beta^R_{i,m})$.

All of these intersections are unique.

Now, for each of the A-relevant intersection points we add a path to A as follows:

(1) For $i < m < j$, with $\{m,j\} \cap \{k, k+1\} = \emptyset$, use a straight (negatively sloped) line segment from $x \in \gamma^U_{i,m} \cap \gamma^L_{m,j}$ to $I_{i,j}$. Call this segment $\gamma^L_{i,m,j}$.

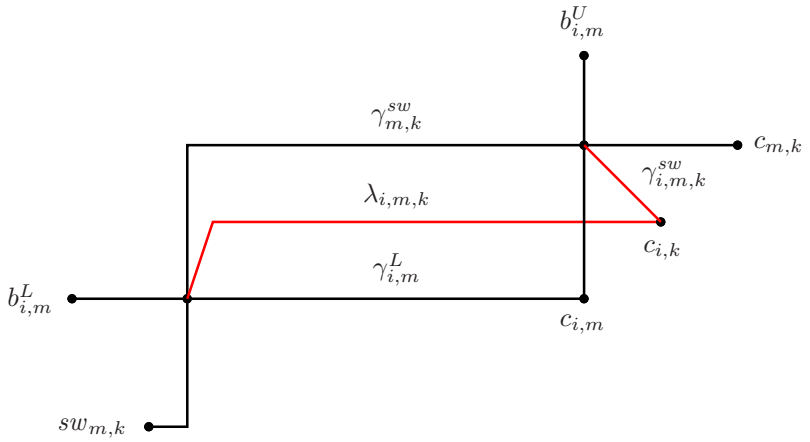

FIGURE 62. Several of the paths created at Levels 0 and 1.

(2) For $i < m < j$, with $(m, j) = (m, k)$ or $(m, j) = (k + 1, k + 2)$, also use a straight (negatively sloped) line segment from $x \in \gamma^U_{i,m} \cap \gamma^{sw}_{m,j}$ to $I_{i,j}$. We call these segments $\gamma^{sw}_{i,m,j}$.
(3) For $i < m < j$, with $(m, j) = (m, k)$ or $(m, j) = (k + 1, k + 2)$, we use a piece-wise linear path, $\lambda_{i,m,j}$, from $x \in \gamma^L_{i,m} \cap \gamma^{sw}_{m,j}$ to $I_{i,j}$. Define $\lambda_{i,m,j}$ as (i) a vertical segment from x up to $x_2 = \beta^R_{i,j}$ followed by (ii) a horizontal segment to $I_{i,j}$. Note that this agrees precisely with part of the previously defined $\gamma^{sw}_{i,j}$, so we can shift $\lambda_{i,m,j}$ slightly to make it disjoint from $\gamma^{sw}_{i,j}$ except at its endpoint. [This is not so important, as intersections between these two paths are A-irrelevant.]

See Figure 62.

Note that since

$$w(\gamma^L_{i,m,j}) = b^U_{i,m} b^L_{m,j}; \quad w(\gamma^{sw}_{i,m,j}) = b^U_{i,m} sw_{m,j}; \quad \text{and} \quad w(\gamma^{sw}_{i,m,j}) = b^L_{i,m} sw_{m,j},$$

the contribution to $\varphi(\partial_A I_{i,j})$ from paths constructed at Level 1 is the (i, j)-entry of the matrix

$$B_U B_L + B_U(A_{-,-}E_{k+1,k} + E_{k+1,k+2}) + B_L(A_{-,-}E_{k+1,k} + E_{k+1,k+2}).$$

Level 2 The only A-relevant intersections involving at least one path created at Level 1 are:

(1) For $i < h < m < j$ with $(m, j) = (m, k)$ or $(m, j) = (k + 1, k + 2)$, $\lambda_{h,m,j}$ intersects $\gamma^U_{i,h}$ at a unique point in an ϵ-neighborhood of $(\beta^U_{i,j}, \beta^R_{h,j})$.

[The diagonal segments $\gamma^L_{i,m,j}$ and $\gamma^{sw}_{i,m,j}$ are seen to be disjoint from all other segments with lower index i or upper index j using the lexicographic ordering of the $c_{i,j}$ along $x_1 = x_2$. This is as in Proof of Theorem 6.15.]

We complete the construction of A by adding, straight line segments, $\gamma_{i,h,m,j}$, from $x \in \gamma^U_{i,h} \cap \lambda_{h,m,j}$ to $I_{i,j}$ for each such $i < h < m < j$. These diagonal segments have no A-relevant intersections with other paths in A (again using the lexicographic ordering of the $c_{i,j}$), and they contribute the (i, j)-entry of the matrix

$$B_U B_L(A_{-,-}E_{k+1,k} + E_{k+1,k+2})$$

to $\varphi(\partial_A I_{i,j})$.

To complete the proof, simply sum the contributions to $\varphi(\partial_A I_{i,j})$ that were identified at Levels 0-2. The result is the (i, j) entry of $(I + B_U)(I + B_L)(I + A_{-,-}E_{k+1,k} + E_{k+1,k+2})$. □

7.4.2. *b^{RD}-trees.* We turn now to b^{RD}-trees which were defined to be b-trees with all outputs at $b^R_{i,j}$ or $b^D_{i,j}$ Reeb chords (including possibly $b^D_{k+2,k+1}$, but not $\tilde{b}^R_{k+2,k+1}$) or at $sw_{k+2,k+1}$. Due to the presence of $(k + 2, k + 1)$-flow lines as edges in b^{RD}-trees, we require a bit more preliminary work than usual before reaching a situation where we can apply Proposition 6.22.

Recall the definition of regions $B^{RD}(i, j) \subset \widehat{N}(e^2_\alpha)$ for $1 \le i < j \le n$ from Section 6.5 (as in Figure 38, but reflected across $x_1 = x_2$). We use the same definition here.

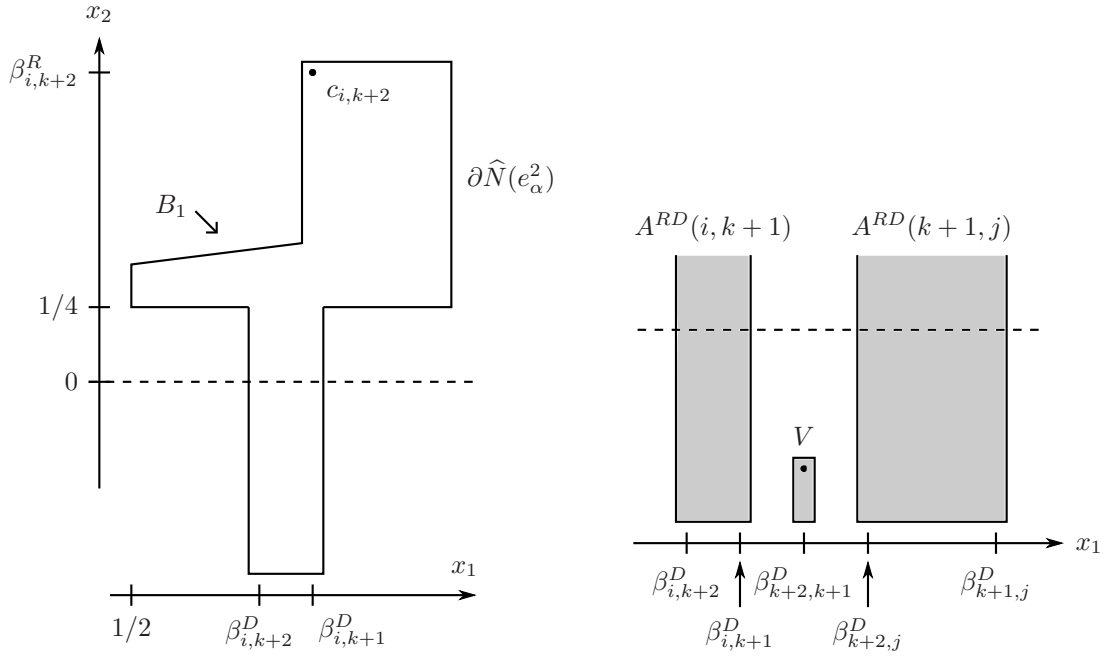

FIGURE 63. (left) The region $A^{RD}(i,k+2)$. The $(k+1,k+2)$-crossing locus is pictured as a dotted line, and the segment B_1 is from Property 12. Note that $\beta^D_{i,k+2} = \beta^U_{i,k+1}$ and $\beta^D_{i,k+1} = \beta^U_{i,k+2}$ with the β^U appearing in lexicographical order. (right) Below $x_2 = 1/4$, the regions $A^{RD}(i,k+1)$ and $A^{RD}(k+1,j)$ agree with $A^{RD}(i,k+2)$ and $A^{RD}(k+2,j)$, for $i < k+1$ and $k+2 < j$. These regions are disjoint from the strip V that contains $\tilde{c}_{k+2,k+1}$.

Next, for $i < j$, with $(i,j) \neq (k+1,k+2)$, let

$$A^{RD}(i,j) = \left(B^{RD}(i,j) \cap \{x_2 \geq 1/4\}\right) \bigcup$$

$$\left\{(x_1,x_2) \in \widehat{N}(e^2_\alpha) \,|\, Min(\beta^U_{i,j},\beta^D_{i,j}) - \epsilon \leq x_1 \leq Max(\beta^U_{i,j},\beta^D_{i,j}) + \epsilon,\, x_2 \leq 1/4\right\},$$

while

$$A^{RD}(k+1,k+2) = B^{RD}(k+1,k+2) \cap \{x_2 \geq 1/4\}.$$

See Figure 63.

Lemma 7.32. *Any edge, γ, of a b^{RD}-tree that does not begin with a switch either*

1. *has $i < j$, and the intersection of its image with $\widehat{N}(e^2_\alpha)$ is in $A^{RD}(i,j)$, or*
2. *is the $(k+2,k+1)$-switch flow line, or*
3. *is the $b^D_{k+2,k+1}$-line which is contained in the strip*

$$V = [\beta^D_{k+2,k+1} - \epsilon, \beta^D_{k+2,k+1} + \epsilon] \times [-1 - 1/32, \tilde{\beta}^R_{k+2,k+1} + \epsilon].$$

Moreover, the image of γ is entirely in $\widehat{N}(e^2_\alpha)$ unless γ is part of a $b^X_{i,j}$-line for $X \in \{R,D\}$.

Proof. As a preliminary, note that the $b^D_{k+2,k+1}$-line is indeed contained in the strip V, since $-\nabla F_{k+2,k+1}$ points out along the left, right, and upper boundaries of V (by Property 10). Moreover, V contains the portion of $N(e^1_D)$ where $b^D_{k+2,k+1}$ is located, and the $b^D_{k+2,k+1}$-line cannot cross the lower boundary of $\partial N(e^1_D)$ (by Proposition 5.11).

In addition, note that for all $1 \leq i < j \leq n$, $-\nabla F_{i,j}$ points out along all boundary segments of $A^{RD}(i,j)$. [Along boundary segments shared with $B^{RD}(i,j) \cap \{x_2 \geq 1/4\}$, this follows from Properties 3, 10, and 12. Along the vertical lines $x_1 = Min(\beta^U_{i,j},\beta^D_{i,j}) - \epsilon$ and $x_1 = Max(\beta^U_{i,j},\beta^D_{i,j}) + \epsilon$, this is from Property 14.]

Now, we prove the Proposition using induction on the number of Y_0's in the PFT that begins with the edge γ. In the base case, γ must be either the $(k+2,k+1)$-switch flow line or one of the $b^R_{i,j}$- or $b^D_{i,j}$-lines. In the latter case, the claimed bound on the location holds since, for $i < j$, as t decreases

from $+\infty$ these lines enter $\widehat{N}(e_\alpha^2)$ at a point on $\partial A^{RD}(i,j)$ (as specified by Proposition 5.11). Note that the segments of the $b^R_{i,j}$- or $b^D_{i,j}$-lines that lie outside of $\widehat{N}(e_\alpha^2)$ are all pairwise disjoint.

Suppose now that the PFT starting with γ has at least one Y_0. From Lemma 7.28, γ must end with a Y_0, and the two PFTs starting with the outgoing branches are themselves b^{RD}-trees. These outgoing branches, γ_1 and γ_2, are respectively (i,m)- and (m,j)-flow lines for some i,m,j. We need to show that $i<j$ and that $\gamma \subset A^{RD}(i,j)$.

Case 1: One of (i,m) and (m,j) is equal to $(k+2,k+1)$.

Consider the case where $(i,m)=(k+2,k+1)$; the other case is similar. By the inductive hypothesis, γ_1 must be either the $(k+2,k+1)$-switch flow line or the $b^D_{k+2,k+1}$-line. The latter case is impossible, since the strip V is disjoint from all $A^{RD}(i,j)$. [See Figure 63 (right).] Thus, γ_1 is the $(k+2,k+1)$-switch flow line. Of course, $(m,j)=(k+1,k+2)$ is not possible, since all $(k+2,k+1)$- and $(k+1,k+2)$-flow lines are disjoint from one another. Thus, $(m,j)=(k+1,j)$ with $k+2<j$, so $(i,j)=(k+2,j)$ satisfies $i<j$. The Y_0 is located in $A^{RD}(k+1,j)$, below the crossing locus. Note that below the crossing locus $A^{RD}(k+1,j)$ and $A^{RD}(k+2,j)$ coincide (because $\{\beta^U_{k+1,j},\beta^D_{k+1,j}\}=\{\beta^D_{k+2,j},\beta^U_{k+2,j}\}$), so the edge γ has its end point in $A^{RD}(k+2,j)$ as required. [Since $-\nabla F_{k+2,j}$ points out along $\partial A^{RD}(k+2,j)$, γ remains in $A^{RD}(i,j)$ as t decreases.]

Case 2: Neither of (i,m) or (m,j) are equal to $(k+2,k+1)$.

Then, the inductive hypothesis shows that $i<m<j$, and the Y_0 at the end of γ is in $A^{RD}(i,m)\cap A^{RD}(m,j)$. To complete the proof we show that $A^{RD}(i,m)\cap A^{RD}(m,j)\subset A^{RD}(i,j)$.

First, we have

$$A^{RD}(i,m)\cap A^{RD}(m,j)\cap\{x_2\geq 1/4\}=B^{RD}(i,m)\cap B^{RD}(m,j)\cap\{x_2\geq 1/4\}\subset$$

$$B^{RD}(i,j)\cap\{x_2\geq 1/4\}=A^{RD}(i,j)\cap\{x_2\geq 1/4\}.$$

To check that

$$A^{RD}(i,m)\cap A^{RD}(m,j)\cap\{x_2<1/4\}=\emptyset\subset A^{RD}(i,j)\cap\{x_2<1/4\},$$

note that for $(i,m),(m,j)\neq(k+1,k+2)$, the intervals $[Min(\beta^U_{i,m},\beta^D_{i,m})-\epsilon, Max(\beta^U_{i,m},\beta^D_{i,m})+\epsilon]$ and $[Min(\beta^U_{m,j},\beta^D_{m,j})-\epsilon, Max(\beta^U_{m,j},\beta^D_{m,j})+\epsilon]$ are disjoint. □

Corollary 7.33. *Any b-tree is either a b^{LU}- or b^{RD}-tree.*

Proof. This is verified using induction on the number of Y_0's. At the inductive step, Lemmas 7.29 and 7.32 show that except for possibly branches that are (i,k)- $(k+1,k+2)$- or $(k+2,k+1)$-flow lines, all edges of b^{LU}-trees are disjoint from all edges of b^{RD}-trees. No Y_0 can occur between two flow lines with indices of the form $(i,k),(k+1,k+2)$, or $(k+2,k+1)$. □

Consider the set X of ordered pairs (x,Γ) where Γ is a PFT that is a b^{RD}-tree starting on the line $x_2=1/4$ with initial point $x=(x_1,1/4)$. As we will see in Lemma 7.34 the elements (x,Γ) of X are described as follows:

(1) For $i<j$, $(i,j)\neq(k+1,k+2)$, the portion of the $b^D_{i,j}$-line beginning at its unique intersection point with $x_2=1/4$.
(2) For $i<k+1$, the $(k+2,k+1)$-switch flow line intersects the $b^D_{i,k+2}$-line in an *odd* number of points, $q_1,\dots,q_{2r+1}$. [This is because the endpoints of the $(k+2,k+1)$-switch flow line are at $\tilde{c}_{k+2,k+1}$ and the $(k+2,k+1)$-switch flow line, and these lie on opposite sides of the portion of the $b^D_{i,k+2}$-line that is below the crossing locus. See Figure 64.] For each such intersection point q_s, there is a unique PFT $\Gamma^s_{i,k+2,k+1}$ whose top edge is the $(i,k+1)$-flow line starting at $x_2=1/4$ and ending at q_s. [The $(i,k+1)$-flow line through q_s has a unique intersection with $x_2=1/4$, since it is contained in $A^{RD}(i,k+1)$ and, in $A^{RD}(i,k+1)$, $-\nabla F_{i,k+1}$ points down along $x_2=1/4$.] The PFT $\Gamma^s_{i,k+2,k+1}$ then has a Y_0 with the outgoing edges limiting to $b^D_{i,k+2}$, and following the remainder of the $(k+2,k+1)$-switch GFT.

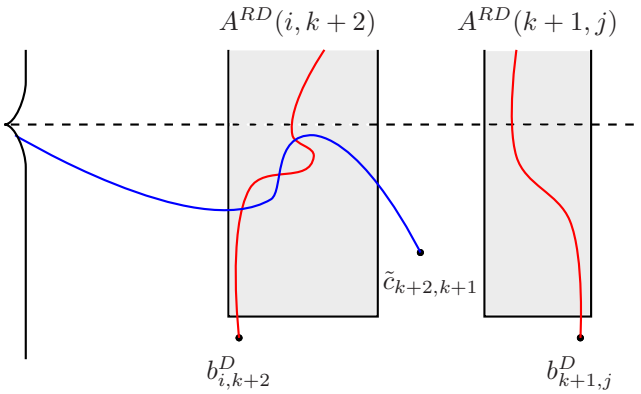

FIGURE 64. Topological considerations show that the $b^D_{i,k+2}$-line and the $b^D_{k+1,j}$-line (red) intersect the $(k+2,k+1)$-switch flow line (blue) in an odd and even number of points respectively.

(3) For $k+2<j$, the $(k+2,k+1)$-switch flow line intersects the $b^D_{k+1,j}$-line in an *even* number of points, $q_1,\dots,q_{2r}$, where it is possible that $r=0$. [This is because the endpoints of the $(k+2,k+1)$-switch flow line both sit to the left of the portion of the $b^D_{k+1,j}$-line that is below the crossing locus.] For each such intersection point q_s, there is a unique PFT $\Gamma^s_{k+2,k+1,j}$ whose top edge is the $(k+2,j)$-flow line starting at $x_2=1/4$ and ending at q_s. [This flow line has a unique intersection with $x_2=1/4$.] The PFT $\Gamma^s_{k+2,k+1,j}$ then has a Y_0 with the outgoing edges limiting to $b^D_{k+1,j}$, and following the remainder of the $(k+2,k+1)$-switch GFT.

Lemma 7.34. *These are the only PFT b^{RD}-trees starting along $x_2=1/4$.*

Proof. Verify by induction on, N, the number of Y_0's in Γ with $(x,\Gamma)\in X$. In the base case, the only b^{RD}-trees without Y_0's are subsets of the $b^R_{i,j}$-lines, $b^D_{i,j}$-lines, and the $(k+2,k+1)$-switch GFT. Only the $b^D_{i,j}$ lines with $i<j$ intersect $x_2=1/4$, and each one of them does indeed intersect $x_2=1/4$ in a unique point.

Now, suppose that $(x,\Gamma)\in X$ is such that Γ has $N\geq 1$ Y_0-vertices.

Using Lemma 7.32, we notice that for $(x,\Gamma)\in X$, the entire image of Γ lies strictly below $x_2=1/4$, except for at the initial point, x. [For all $i<j$, $-\nabla F_{i,j}$ points down along $\{x_2=1/4\}\cap A^{RD}_{i,j}$, and any $(k+2,k+1)$-branches of Γ lie below the crossing locus.] Also, note that any edge of Γ, that is not part of the $(k+2,k+1)$-switch GFT or the $b^D_{k+2,k+1}$-line would limit to $c_{i,j}$ if extended to allow $t\to-\infty$. Thus, the PFTs Γ_1 and Γ_2 that begin with the outgoing edges at the first Y_0 of Γ are themselves subsets of PFTs that are b^{RD}-trees starting along $x_2=1/4$, or are subsets of the $(k+2,k+1)$-switch GFT or the $b^D_{k+2,k+1}$-line. When $x_2<1/4$, the regions $A^{RD}(i,m)$ and $A^{RD}(m,j)$ are all disjoint and are disjoint from the $b^D_{k+2,k+1}$-line. Thus, the only possibility is that one of Γ_1 or Γ_2 begins with the $(k+2,k+1)$-switch flow line and the other Γ_i begins with either a $(i,k+2)$ or $(k+1,j)$-flow line and has $N-1$ Y_0 vertices. [No PFT starting with the $(k+2,k+1)$-switch flow line can have any Y_0-vertices by Lemma 7.12.] By the inductive hypothesis, the other Γ_i that begins with a $(i,k+2)$ or $(k+1,j)$-flow can only be (a subset of) one of the PFTs from X as in (1)-(3) above. It cannot be that the top branch of this Γ_i is as in (2) or (3) since then the outgoing branches of the Y_0 would be either a $(k+2,k+1)$- and $(i,k+1)$-flow line or a $(k+2,k+1)$- and $(k+2,j)$-flow line. Thus, Γ_i must be as in (1), and so Γ must be as in (2) or (3). □

Now, we have a disk datum $\left(D,\{b^R_{i,j}\}\cup\{x\,|\,(x,\Gamma)\in X\},I_{i,j}\right)$ where D is $\bigcup B^{RD}(i,j)\cap\{x_2\geq 1/4\}$ with the squares $Sq_{i,j}$ that contain the $c_{i,j}$ removed, and the points x with $(x,\Gamma)\in X$ are assigned upper and lower indices that agree so that the first branch of Γ is an $(i(x),j(x))$-flow line. As usual, the $I_{i,j}$ are the lower and right edges of $\overline{Sq_{i,j}}$.

We associate a generalized b-manifold, A, to this disk datum consisting of paths γ that are the intersection with D of the top branches of GFTs that are b^{RD}-trees.

Lemma 7.35. *Defined as above, A is a generalized b-manifold for $\left(D, \{b^R_{i,j}\} \cup \{x \,|\, (x,\Gamma) \in X\}, I_{i,j}\right)$. Moreover,*

$$\varphi(\partial_A I_{i,j}) = \partial_{b^{RD}} c_{i,j}$$

where φ is the $\mathbb{Z}/2$-algebra homomorphism defined by $\varphi(b^R_{i,j}) = b^R_{i,j}$ and $\varphi(x) = w(\Gamma)$ for $(x,\Gamma) \in X$.

Proof. That A is a generalized b-manifold follows as usual, since if the top edge, γ, of a b^{RD}-tree, Γ, intersects D, then it starts at some $c_{i,j}$ and either ends at a Y_0 within $D \cap \{x_2 \geq 1/4\}$ or leaves this region at one of the points in $\{b^R_{i,j}\} \cup \{x \,|\, (x,\Gamma) \in X\}$. That $\varphi(w(\gamma)) = w(\Gamma)$ follows from induction on the number of Y_0's that Γ has with image in $D \cap \{x_2 \geq 1/4\}$, where the base case is arranged by the definition of φ. □

Proposition 7.36. *For all $1 \leq i < j \leq n$, $\partial_{b^{RD}} c_{i,j}$ agrees with the (i,j)-entry of the matrix*

$$(I + B_R)(I + B_D + B_D E_{k+2,k+1})$$

with B_R and B_D as in Theorem 7.4.

Proof. From Lemma 7.35 and Proposition 6.22, we see that $\varphi(\partial_A I_{i,j}) = \partial_{b^{RD}} c_{i,j}$ for *any* generalized b-manifold associated to the disk datum $\left(D, \{b^R_{i,j}\} \cup \{x \,|\, (x,\Gamma) \in X\}, I_{i,j}\right)$. Construct a generalized b-manifold $A = \sqcup A_r$ as follows:

Level 0

(1) Connect each $b^R_{i,j}$ to $I_{i,j}$ via a straight horizontal segment, $\gamma^R_{i,j}$.
(2) For each $(x,\Gamma) \in X$, connect x to the appropriate $I_{i,j}$ by a path, γ_x, that is (i) a line segment from $x = (x_1, 1/4)$ to $(y, 3/8)$ with $y \in (\beta^U_{i(x),j(x)} - \epsilon, \beta^U_{i(x),j(x)} + \epsilon)$, then (ii) a straight vertical segment connecting $(y, 3/8)$ to $I_{i(x),j(x)}$.

Notice that any intersections between the paths γ_x are not A-relevant, since all endpoints of γ_x have x_1-coordinate in the interval $J_{i,j} := [Min(\beta^U_{i,j}, \beta^D_{i,j}) - \epsilon, Max(\beta^U_{i,j}, \beta^D_{i,j}) + \epsilon]$ where $i = i(x)$ and $j = j(x)$; as we have already observed, for $i < m < j$, $J_{i,m} \cap J_{m,j} = \emptyset$.

Recall that above Lemma 7.34 we divided all $(x,\Gamma) \in X$ into three families (1)-(3). The paths corresponding to $(x,\Gamma) \in X$ as in (1) contribute a $b^D_{i,j}$ term to $\varphi(\partial_A I_{i,j})$; as in (2) contribute an *odd* number of $b^D_{i,k+2} \cdot 1$ terms to $\varphi(\partial_A I_{i,k+1})$ for $i < k+1$; as in (3) contribute an *even* number of $1 \cdot b^D_{k+1,j}$ terms to $\varphi(\partial_A I_{k+2,j})$ for $k+2 < j$. As we use $\mathbb{Z}/2$-coefficients, for $i < j$, the total contribution to $\varphi(\partial_A I_{i,j})$ from paths defined at Level 0 is the (i,j)-entry of the matrix

$$B_R + B_D + B_D E_{k+2,k+1}.$$

Level 1

For each $i < m < j$ with $(m,j) \neq (k+1, k+2)$, every path γ_x with $(i(x), j(x)) = (m,j)$ intersects every $\gamma^R_{i,m}$ exactly once at a point in $[\beta^U_{m,j} - \epsilon, \beta^U_{m,j} + \epsilon] \times [\beta^R_{i,m} - \epsilon, \beta^R_{i,m} + \epsilon]$. Connect each of these points to $I_{i,j}$ using a straight line segment. An earlier argument (see the proof of Theorem 6.15) based on the lexicographic ordering of the $\beta_{i,j}$ shows that none of the segments constructed at Level 1 has any A-relevant intersections with other paths from A. Thus, the construction of A is complete.

Keeping in mind the $\mathbb{Z}/2$ coefficients, the contribution to $\varphi(\partial_A I_{i,j})$ from paths defined at Level 1 is the (i,j)-entry of the matrix

$$B_R(B_D + B_D E_{k+2,k+1}).$$

Thus, in total $\varphi(\partial_A I_{i,j})$ is the (i,j)-entry of the matrix $(I + B_R)(I + B_D + B_D E_{k+2,k+1})$. □

Proof of Theorem 7.4. Using Proposition 7.27 followed by Corollary 7.33, we compute

$$\partial C = \partial_c C + \partial_b C + X = \partial_c C + \partial_{b^{LU}} C + \partial_{b^{RD}} C + X$$

where X has entries in the ideal generated by $\tilde{c}_{k+2,k+1}$ and $\tilde{b}^R_{k+2,k+1}$. Substituting the computations established in Theorem 7.15 and Propositions 7.31 and 7.36, this becomes

$$A_{+,+}C + C(I + E_{k+2,k+1})A_{-,-}(I + E_{k+2,k+1}) +$$
$$(I + B_U)(I + B_L)(I + A_{-,-}E_{k+1,k} + E_{k+1,k+2}) + (I + B_R)(I + B_D + B_D E_{k+2,k+1}).$$

[Note that the two I terms cancel out, so that the entries on and below the main diagonal are all zero, just as in ∂C.] This establishes the formula for ∂C as stated in Theorem 7.4. □

8. Isomorphism between the cellular DGA and LCH

In the preceding three sections, we have computed, at least up to terms involving the exceptional generators, the sub-DGAs $(\mathcal{A}_{LCH}(e^d_\alpha),\partial)$ of $(\mathcal{A}_{LCH},\partial)$ generated by Reeb chords located in the neighborhood of a single 0, 1, or 2-cell, e^d_α, of the square decomposition $\mathcal{E}_\Cap$. In the present section, we combine these local computations to give a computation of $(\mathcal{A}_{LCH},\partial)$ up to stable tame isomorphism (in Proposition 8.6), and then use this result to show that $(\mathcal{A}_{LCH},\partial)$ is equivalent to the Cellular DGA of L (in Proposition 8.7).

8.0.3. *Local vs. global computation of* $(\mathcal{A}_{LCH},\partial)$. In computing the sub-DGAs $(\mathcal{A}_{LCH}(e^d_\alpha),\partial)$, we have used different notations for the same Reeb chords depending on which cell was under consideration. To address this ambiguity, we take the following formal approach when considering the entire DGA of L, $(\mathcal{A}_{LCH},\partial)$.

For a d-cell e^d_α of $\mathcal{E}_\Cap$, where $d=0,1$, or 2, we write

$$(x,e^d_\alpha)$$

to indicate the Reeb chord that is notated by x when considered in the context of the neighborhood $N(e^d_\alpha)$. Here, x has one of the forms $a_{i,j}$, $b_{i,j}$, or $c_{i,j}$ possibly decorated with super-scripts and/or a tilde. Such a notation then specifies a well-defined generator of $(\mathcal{A}_{LCH},\partial)$. However, the same generator may have several different notations. For example, suppose that a 1-cell e^1_α has intial vertex $e^0_{\beta_0}$ and terminal vertex $e^0_{\beta_1}$, and that $\tilde{L}$ has a single crossing above e^1_α, i.e. the 1-cell is of type (1Cr), with the crossing involving sheets S_k and S_{k+1} as labelled above $x=+1$. Then, for $i<k$, we have equalities

$$(a_{i,k},e^0_{\beta_0})=(a^-_{i,k+1},e^1_\alpha);\quad (a_{i,k},e^0_{\beta_1})=(a^+_{i,k},e^1_\alpha);\quad \text{and}\quad (a_{k,k+1},e^0_{\beta_0})=(a^-_{k+1,k},e^1_\alpha).$$

If a Type (13) 2-cell, e^2_α has boundary 1-cells e^1_X with location indicated by $X\in\{L,D,R,U\}$, and boundary 0-cells $e^0_{\pm,\pm}$, then, for $i<k$,

$$(b^D_{i,k+1},e^2_\alpha)=(b_{i,k+2},e^1_D);\quad (b^L_{i,k+2},e^2_\alpha)=(b_{i,k},e^1_L);\quad \text{and}\quad (a^{-,-}_{i,k+1},e^2_\alpha)=(a_{i,k},e^0_{-,-}).$$

[Here, we recall the Convention 7.2.]

Consequently, the generators of $\mathcal{A}_{LCH}$ should be viewed as equivalence classes of pairs (x,e^d_α) with x a generator for $\mathcal{A}_{LCH}(e^d_\alpha)$, such that two pairs are equivalent if they correspond to the same Reeb chord of $\tilde{L}$. Often, the cell e^d_α that we consider a generator of $\mathcal{A}_{LCH}$ in will be clear from context, and then we simply write x for (x,e^d_α).

Remark 8.1. In categorical language, for each cell e^d_α of $\mathcal{E}_\Cap$, we have an algebra $\mathcal{A}(e^d_\alpha)$ generated by symbols (x,e^d_α). The cells of $\mathcal{E}_\Cap$ form a category $\mathcal{C}$ with a unique morphism $e^d_\beta\to e^{d'}_\alpha$ whenever $e^d_\beta\subset\overline{e^{d'}_\alpha}$. Moreover, there is a functor from $\mathcal{C}$ to DGAs that assigns to morphisms the resulting inclusions $\mathcal{A}(e^d_\beta)\hookrightarrow\mathcal{A}(e^{d'}_\alpha)$ obtained from identifying the different notations for common Reeb chords. We have thus constructed an inductive system of DGAs. As all of these DGAs include into $(\mathcal{A}_{LCH},\partial)$, and any generator of $(\mathcal{A}_{LCH},\partial)$ belongs to one of the $\mathcal{A}(e^d_\alpha)$, it is immediate that the direct limit of this system is the DGA of $\tilde{L}$, $(\mathcal{A}_{LCH},\partial)$.

This can be viewed as a refinement of the push-out square (Seifert-Van Kampen Theorem) proved for $\mathcal{A}_{LCH}$ for one-dimensional Legendrian knots [17] and two-dimensional Legendrian surfaces [14].

8.1. **The differential ideal I.** Let I denote the ideal generated by

- $(b^D_{k+2,k+1};e^2_\alpha)+1$ for all Type (13) squares e^2_α;
- $(b^D_{l-1,l-2};e^2_\alpha)+1$ for all Type (14) squares e^2_α; and
- all other Reeb chords that are exceptional generators (for at least one 2-cell).

(Recall the definition of *exceptional generator* from Definition 6.2.)

Theorem 8.2. *The ideal $I\subset\mathcal{A}_{LCH}$ satisfies $\partial(I)\subset I$ so that $(\mathcal{A}_{LCH}/I,\partial)$ is a semi-free DGA with generating set given by the non-exceptional Reeb chords of $\tilde{L}$. Moreover, $(\mathcal{A}_{LCH}/I,\partial)$ is stable tame isomorphic to $(\mathcal{A}_{LCH},\partial)$.*

The proof of Theorem 8.2 is given at the end of this subsection. In preparation for the proof, we examine the exceptional generators more closely (a square-by-square list appears below) and compute some of their differentials.

8.1.1. *Differential of exceptional generators in the* 1*-skeleton.* First, we consider generators of the form $\tilde{b}_{i,j}$. These generators are always exceptional, and they occur only in 1-cells of type (1Cr) and (2Cr).

Lemma 8.3. (1Cr) *Let e^1_α be a 1-cell of type (1Cr) so that sheets S_k and S_{k+1} cross above $N(e^1_\alpha)$. In $\mathcal{A}_{LCH}$, we have*

$$\partial \tilde{b}_{k+1,k} = a^-_{k+1,k}.$$

(2Cr) *Let e^1_α be a 1-cell of type (2Cr) so that sheet S_{k+2} crosses S_{k+1} and then S_k as we follow e^1_α from its terminal point to its initial point. The exceptional generators $\tilde{b}_{k+2,k}$ and $\tilde{b}_{k+2,k+1}$ satisfy*

$$\partial \tilde{b}_{k+2,k} = a^-_{k+2,k}; \quad \textit{and}$$

$$\partial \tilde{b}_{k+2,k+1} = a^-_{k+2,k+1} + X \tag{24}$$

where X denotes a term belonging to the ideal generated by $\tilde{b}_{k+2,k}, a^-_{k+2,k}$.

Proof. In the (1Cr) case, note that the sheets S_{k+1} and S_k are adjacent above the portion of $N(e^1_\alpha)$ where $F_{k+1,k} > 0$, so there is no possibility for a GFT starting at $\tilde{b}_{k+1,k}$ to have internal vertices. Moreover, the $(k+1,k)$-descending manifold of $\tilde{b}_{k+1,k}$ has two non-constant flowlines. One of them limits to $a^-_{k+1,k}$ while the other terminates at the crossing locus. [This is verified as in the proof of Proposition 5.11 (1): If the two flowlines in the unstable manifold of $\tilde{b}_{k+1,k}$ either both limit to $a^-_{k+1,k}$ or both reach the crossing locus, then one of the flow lines from the stable manifold would have to start at a local maximum of $F_{k+1,k}$ in $N(e^1_\alpha)$.]

In the (2Cr) case, the first formula is verified as in the (1Cr) case. To verify the second formula, note that the only opportunity for a $(k+2,k+1)$-flow starting at $\tilde{b}_{k+2,k+1}$ to have a Y_0-vertex is if it splits into a $(k+2,k)$-flow and a $(k,k+1)$-flow somewhere in the region where S_k lies between S_{k+2} and S_{k+1}. The edge that is a $(k+2,k)$-flow must end either at $\tilde{b}_{k+2,k}$ or $a^-_{k+2,k}$ by considerations as in the (1Cr) case above. □

8.1.2. *Exceptional generators in* 2*-cells.*

Lemma 8.4. *The exceptional generators in $N(e^2_\alpha)$ for a 2-cell e^2_α of type (1)-(14) are as indicated in the following table. Note that we use the notation $b_{k+2,\{k+1,k\}}$ to denote a pair of generators of the form $b_{k+2,k+1}$ and $b_{k+2,k}$. Moreover, the differentials of exceptional generators of the form $\tilde{c}_{i,j}$ are as indicated.*

Square Type	*Exceptional Generators*	*Differentials*
(1)	$\emptyset$	*N/A*
(2)	$\begin{matrix}\tilde{b}^U_{k+1,k} & \tilde{b}^D_{k+1,k} & \tilde{c}_{k+1,k}\\ a^{-,+}_{k+1,k} & a^{-,-}_{k+1,k} & b^L_{k+1,k}\end{matrix}$	$\partial\tilde{c}_{k+1,k} = \tilde{b}^U_{k+1,k} + \tilde{b}^D_{k+1,k} + b^L_{k+1,k}$
(3)	$\begin{matrix}\tilde{b}^L_{k+1,k} & \tilde{c}_{k+1,k}\\ a^{-,-}_{k+1,k} & \tilde{b}^D_{k+1,k}\end{matrix}$	$\partial\tilde{c}_{k+1,k} = \tilde{b}^L_{k+1,k} + \tilde{b}^D_{k+1,k}$
(4)	$\begin{matrix}\tilde{b}^R_{k+1,k} & \tilde{b}^D_{k,k+1} & \tilde{c}_{k+1,k}\\ a^{+,-}_{k+1,k} & a^{-,-}_{k,k+1} & b^D_{k+1,k}\end{matrix}$	$\partial\tilde{c}_{k+1,k} = \tilde{b}^R_{k+1,k} + b^D_{k+1,k}$
(5)	$\begin{matrix}\tilde{b}^L_{k+2,\{k+1,k\}} & \tilde{b}^R_{k+2,\{k+1,k\}} & \tilde{c}_{k+2,\{k+1,k\}}\\ a^{-,-}_{k+2,\{k+1,k\}} & a^{+,-}_{k+2,\{k+1,k\}} & b^D_{k+2,\{k+1,k\}}\end{matrix}$	$\partial\tilde{c}_{k+2,k} = \tilde{b}^L_{k+2,k} + \tilde{b}^R_{k+2,k} + b^D_{k+2,k};$ $\partial\tilde{c}_{k+2,k+1} = \tilde{b}^L_{k+2,k+1} + \tilde{b}^R_{k+2,k+1} + b^D_{k+2,k+1} + O(k+2,k);$
(6)	$\begin{matrix}\tilde{b}^R_{k+2,\{k+1,k\}} & \tilde{b}^L_{k+2,k+1} & \tilde{b}^D_{k,k+2} & \tilde{c}_{k+2,\{k+1,k\}}\\ a^{+,-}_{k+2,\{k+1,k\}} & a^{-,-}_{k+2,k+1} & a^{-,-}_{k,k+2} & b^D_{k+2,\{k+1,k\}}\end{matrix}$	$\partial\tilde{c}_{k+2,k} = \tilde{b}^R_{k+2,k} + b^D_{k+2,k};$ $\partial\tilde{c}_{k+2,k+1} = \tilde{b}^R_{k+2,k+1} + b^D_{k+2,k+1} + \tilde{b}^L_{k+2,k+1} + O(k+2,k);$
(7)	*[Similar to (2)]* $\times 2$	
(8)	$\left\{\begin{matrix}\tilde{b}^L_{k+2,\{k+1,k\}} & \tilde{b}^R_{k+2,\{k+1,k\}} & \tilde{b}^U_{k+1,k}\\ a^{-,-}_{k+2,\{k+1,k\}} & a^{+,-}_{k+2,\{k+1,k\}} & a^{-,+}_{k+1,k}\\ \\ \tilde{b}^D_{k+1,k} & \tilde{c}_{k+2,\{k+1,k\}} & \tilde{c}_{k+1,k}\\ a^{-,-}_{k+1,k} & b^D_{k+2,\{k+1,k\}} & b^L_{k+1,k}\end{matrix}\right\}$	$\partial\tilde{c}_{k+2,k} = b^D_{k+2,k} + X;$ $\partial\tilde{c}_{k+1,k} = b^L_{k+1,k} + Y$ $\partial\tilde{c}_{k+2,k+1} = b^D_{k+2,k+1} + Z;$
(9)	$\emptyset$	*N/A*
(10)	*Similar to (2)*	
(11)	$\emptyset$	*N/A*
(12)	$\begin{matrix}\tilde{b}^R_{k+2,\{k+1,k\}} & \tilde{c}_{k+2,\{k+1,k\}}\\ a^{+,-}_{k+2,\{k+1,k\}} & b^D_{k+2,\{k+1,k\}}\end{matrix}$	$\partial\tilde{c}_{k+2,k} = \tilde{b}^R_{k+2,k} + b^D_{k+2,k};$ $\partial\tilde{c}_{k+2,k+1} = \tilde{b}^R_{k+2,k+1} + b^D_{k+2,k+1} + O(k+2,k).$
(13)	$\begin{matrix}\tilde{b}^R_{k+2,k+1} & \tilde{c}_{k+2,k+1}\\ a^{+,-}_{k+2,k+1} & b^D_{k+2,k+1}\end{matrix}$	$\partial\tilde{c}_{k+2,k+1} = b^D_{k+2,k+1} + \tilde{b}^R_{k+2,k+1} + 1;$
(14)	$\begin{matrix}\tilde{b}^R_{l-1,l-2} & \tilde{c}_{l-1,l-2}\\ a^{+,-}_{l-1,l-2} & b^D_{l-1,l-2}\end{matrix}$	$\partial\tilde{c}_{l-1,l-2} = b^D_{l-1,l-2} + \tilde{b}^R_{l-1,l-2} + 1.$

In the squares (5), (6), and (12), $O(k+2,k)$ denotes an element of the ideal generated by those exceptional Reeb chords with upper endpoint on S_{k+2} and lower endpoint on S_k. In square (8), the terms X, Y, Z respectively belong to the 2-sided ideals generated by

$$\begin{aligned} E_X &= E \setminus \{\tilde{c}_{k+2,\{k+1,k\}}, b^D_{k+2,\{k+1,k\}}, \tilde{c}_{k+1,k}, b^L_{k+1,k}\},\\ E_Y &= E_X \cup \{\tilde{c}_{k+2,k}\}\\ E_Z &= E_Y \cup \{b^D_{k+2,k}\}\end{aligned}$$

where E denotes the set of all exceptional generators of the square.

Proof. The verification for the differentials of the $\tilde{c}$ depends on the square type.

1. *For squares of type (2)-(4), (7) and (10).*

The sheets S_{k+1} and S_k that form the upper and lower endpoint of $\tilde{c}_{k+1,k}$ never have another sheet between them in the region where $F_{k+1,k} > 0$. Therefore, no interval vertices are possible in a GFT that begins at $\tilde{c}_{k+1,k}$. A flow tree without internal vertices is rigid if and only if it is simply a flow line from $\tilde{c}_{k+1,k}$ to one of the $b_{k+1,k}$ or $\tilde{b}_{k+1,k}$ Reeb chords (by Proposition 6.9). There is a unique such flow line for each $b_{k+1,k}$ and $\tilde{b}_{k+1,k}$ in $N(e_\alpha^2)$. [In the terminology from 6.3.2, these flow lines are the $b_{k+1,k}$- and $\tilde{b}_{k+1,k}$-lines. That they indeed limit to $\tilde{c}_{k+1,k}$ as $t \to -\infty$ was established in Lemma 6.7.]

2. *For squares of type (5), (6), and (12).*

The formulas for $\partial\tilde{c}_{k+2,k}$ are derived as in 1., as sheets S_{k+2} and S_k are adjacent in the region where $F_{k+2,k} > 0$. All terms besides $O(k+2,k)$ in $\partial\tilde{c}_{k+2,k+1}$ correspond to GFTs without internal vertices, and these correspond to the unique flow lines from $\partial\tilde{c}_{k+2,k+1}$ to each of the $b_{k+2,k+1}$ and $\tilde{b}_{k+2,k+1}$ Reeb chords in $N(e_\alpha^2)$. We claim that any other rigid GFT starting at $\tilde{c}_{k+2,k+1}$ must have an endpoint at a Reeb chords with upper sheet S_{k+2} and lower sheet S_k, and thus is accounted for in the $O(k+2,k)$ term. [Indeed, for a GFT starting at $\tilde{c}_{k+2,k+1}$, the first internal vertex must be a Y_0 (by Proposition 6.8) where the initial $(k+2,k+1)$-flow line splits into a $(k+2,k)$-flow line and a $(k,k+1)$-flow line (because S_k is the only sheet that is ever between S_{k+2} and S_{k+1}). The $(k+2,k)$-branch has no possibility for further Y_0-vertices below it, and hence terminates at one of the $(k+2,k)$ Reeb chords.]

3. *For the Type (8) square.*

First observe that the rigid GFTs without internal vertices that start at the $\tilde{c}$ account for the given term or belong to the appropriate ideal. Next, assume that we have a rigid GFT Γ starting at one of the $\tilde{c}$ with at least one Y_0-vertex. We claim that we can find a path γ within the domain of Γ from the input at $\tilde{c}$ to an output Reeb chord such that all edges that appear along γ are flow lines for some $F_{i,j}$ with $i > j$. [To see this, start at $\tilde{c}$ and work down. When a Y_0-vertex is reached, if the edge oriented into the vertex is a flowline for $F_{i,j}$ with $i > j$, then the outputs must be flow lines for $F_{i,h}$ and $F_{h,j}$ for some h. If it were the case that $i < h$ and $h < j$ then $i < j$ would hold also, so at least one of the output edges satisfies the desired inequality. Note that here, as usual, we consider punctures at c's as being special cases of Y_0-vertices where one outgoing edge is a constant flowline.]

All Reeb chords for which the subscripts i, j satisfy $i > j$ belong to the collection E. Therefore, the endpoint of γ must belong to E, and we just need to show that it belongs to the appropriate one of E_X, E_Y, or E_Z. This follows from the following sequence of statements:

- The endpoint of γ cannot be a puncture at $\tilde{c}_{k+1,k}$ or $\tilde{c}_{k+2,k+1}$. This is because of the ordering of sheets at these points: there is no way the branch of the path above the puncture could be a flow for $F_{i,j}$ with $i > j$. See Figure 34.
- The endpoint of γ cannot be at $b^D_{k+2,k+1}$ or $b^L_{k+1,k}$. In the first case, the branch of the flow tree immediately above such an endpoint would be a portion of the $b^D_{k+2,k+1}$-line from $b^D_{k+2,k+1}$ to $\tilde{c}_{k+2,k+1}$, and this flow line is contained entirely in the corner $C_{R,D}$. [The notation is as in Property 10. By Property 10, the $b^D_{k+2,k+1}$-line is contained in a vertical strip of width 2ϵ and centered at $x_1 = \beta^D_{k+2,k+1}$ that lies below $x_2 = \tilde{\beta}^R_{k+2,k+1} + \epsilon$.] In $C_{R,D}$, the z-coordinates of sheets satisfy $S_{k+2} > S_k > S_{k+1}$ so again a branch of the path above a Y_0-vertex along this flow line would violate the $i > j$ condition. Similarly, the flow line from $b^L_{k+1,k}$ to $\tilde{c}_{k+1,k}$ belongs entirely to $C_{L,U}$ where $S_{k+1} > S_k > S_{k+2}$, so the Y_0-vertex preceding the edge would be impossible.
- If the endpoint of γ is a puncture at $\tilde{c}_{k+2,k}$, then the initial vertex of Γ cannot also be $\tilde{c}_{k+2,k}$. This is because the difference between z-coordinates of sheets decreases along all edges of a GFT.
- If the endpoint of γ is at $b^D_{k+2,k}$, then the initial vertex would have to be at $\tilde{c}_{k+2,k+1}$. To verify, note that the point x on the $b^D_{k+2,k}$-line from $b^D_{k+2,k}$ to $\tilde{c}_{k+2,k}$ where the Y_0 above $b^D_{k+2,k}$ occurs must belong to $T = \{(x_1,x_2) \in \tilde{N}(e_\alpha^2) \,|\, x_1 \geq 1/4, \text{ and } x_2 \leq -1/4\}$. [Since the entire $b^D_{k+2,k}$-line remains in this region by Property 10.] Thus, the edge in the path γ that precedes this edge

is a $(k+2, k+1)$-flow line. Again, using Property 10, this flow line from x to $\tilde{c}_{k+2,k+1}$ must remain in T as t decreases. Above T, we have $S_{k+2} > S_k > S_{k+1}$, so another Y_0 is impossible since the edge above the Y_0 could not be an (i,j)-flow with $i > j$. Thus, this edge must limit to $\tilde{c}_{k+2,k+1}$, so the initial vertex of the tree is indeed $\tilde{c}_{k+2,k+1}$ as desired.

4. *For squares of type (13) and (14).*
The formula for $\partial\tilde{c}_{k+2,k+1}$ follows from Lemmas 7.12 and 7.16.

□

Proof of Theorem 8.2. For each square type the exceptional generators are divided into pairs according to the way they are listed in columns of 2 in the table from Lemma 8.4. We order these pairs of generators for squares of type (2)-(4), (7), and (10) as they appear from left to right. For squares of type (5), (6), (8), and (12) the columns with subscripts of the form $k+2, \{k+1, k\}$ represent two distinct pairs of generators. In this case, order pairs of generators by proceeding from left to right using $k+2, k$ subscripts everywhere, and then listing the remaining $k+2, k+1$ generators as they appear from left to right. For example, in the neighborhood of a Type (6) 2-cell there are 6 pairs of exceptional generators ordered as:

$$\begin{array}{cccccc} \tilde{b}^R_{k+2,k} & \tilde{b}^L_{k+2,k+1} & \tilde{b}^D_{k,k+2} & \tilde{c}_{k+2,k} & \tilde{b}^R_{k+2,k+1} & \tilde{c}_{k+2,k+1} \\ a^{+,-}_{k+2,k} & a^{-,-}_{k+2,k+2} & a^{-,-}_{k,k+2} & b^D_{k+2,k} & a^{+,-}_{k+2,k+1} & b^D_{k+2,k+1} \end{array}$$

Lemma 8.5. *Let x and y denote a pair of exceptional generators in $N(e^2_\alpha)$ with x appearing above y in the table from Lemma 8.4. Then, in a quotient of $(\mathcal{A}_{LCH}, \partial)$ in which all of the previous pairs of exceptional generators of the square (with respect to the ordering just described) have been set to zero we have $\partial x = y$, unless either e^2_α has type (13) and $x = \tilde{c}_{k+2,k+1}$ or e^2_α has type (14) $x = \tilde{c}_{l-1,l-2}$. In these latter two cases, we have*

$$\partial\tilde{c}_{k+2,k+1} = b^D_{k+2,k+1} + 1; \text{ and } \partial\tilde{c}_{l-1,l-2} = b^D_{l-1,l-2} + 1.$$

Proof. This is easily verified from the formulas for differentials established in Lemmas 8.3 and 8.4. □

Using Lemma 8.5, we can apply Theorem 2.1 from [15] multiple times to see that the quotient of $(\mathcal{A}_{LCH}, \partial)$ by the ideal generated by those generators of I that lie in a single $N(e^2_\alpha)$ is stable tame isomorphic to $(\mathcal{A}_{LCH}, \partial)$. [Apply Theorem 2.1 from [15] to cancel the exceptional generators of $N(e^2_\alpha)$ one pair at a time, in the order previously specified. Lemma 8.5 shows that the result of this procedure is indeed $\mathcal{A}_{LCH}$ quotiented by the ideal generated by those generators of I that lie in $N(e^2_\alpha)$.] However, to see that the quotient of $(\mathcal{A}_{LCH}, \partial)$ by all of I is stable tame isomorphic to $\mathcal{A}_{LCH}$ we need to be slightly more careful about the order in which we cancel exceptional generators in distinct squares for the following reason: After cancelling all exceptional generators in a given square, one could worry that when considering a neighboring square some of the generators from the 1-skeleton that are necessary to carry out the cancellation process may be missing. Conditions (A2)-(A4) in the construction of $\mathcal{E}_{\pitchfork}$ are designed to prevent this from happening.

The procedure to globally cancel all exceptional generators using repeated applications of Theorem 2.1 from [15] is as follows:

Step 1. Cancel all exceptional generators in squares of type (3).

The property (A3) of Proposition 3.2 states that no two Type (3) squares of $\mathcal{E}_{\pitchfork}$ can border one another. Therefore, there is no overlap among the generators from different squares that should be cancelled in Step 1.

Step 2. For all (1Cr) 1-cells e^1_α that do not border a Type (3) square, cancel $\tilde{b}_{k+1,k}$ with $a^-_{k+1,k}$; for all (2Cr) 1-cells e^1_α cancel $\tilde{b}_{k+2,k}$ with $a^-_{k+2,k}$ and then cancel $\tilde{b}_{k+2,k+1}$ with $a^-_{k+2,k+1}$. (Note that Lemma 8.3 shows that in the (2Cr) case, once $\tilde{b}_{k+2,k}$ and $a^-_{k+2,k}$ are equal to 0, $\partial\tilde{b}_{k+2,k+1} = a^-_{k+2,k+1}$ so that Theorem 2.1 from [15] applies.)

For carrying out Step 2, we need to choose some ordering of the (1Cr) and (2Cr) 1-cells before proceeding. This choice of order is irrelevant. However, since a single 0-cell e^0_α can appear as the initial vertex of more than one 1-cell, it is important to verify the cancelling procedure does not specify that a single Reeb chord $a_{i,j} \in N(e^0_\alpha)$ should be cancelled more than once. This holds since the

property (A2) of $\mathcal{E}_{\Cap}$ (from Proposition 3.2) shows that the only way this can happen is when e^0_α is at the lower left corner of a Type (3) square, e^2_β, where sheets k and $k+1$ cross, and the Reeb chord is $(a_{k,k+1}, e^0_\alpha) = (a^{-,-}_{k+1,k}, e^2_\beta)$. However, these Reeb chords and the $\tilde{b}$ Reeb chords that lie on the left and down edges of type (3) 2-cells have already been cancelled in Step 1, and cancelling them is not part of the Step 2 procedure.

Step 3. Choose some ordering of the non-Type (3) squares and cancel all remaining exceptional generators one 2-cell at a time.

At the conclusion of Step 2., all exceptional generators of the form $\tilde{b}$ together with the a generators that appear immediately below them in Lemma 8.4 have already been cancelled. [Note that in all cases the generator y that appears below a $\tilde{b}$ Reeb chord in Lemma 8.4 is precisely the a Reeb chord between the same two sheets and above the initial vertex of the edge of $\tilde{b}$. These are precisely the Reeb chords that the $\tilde{b}$ were cancelled with in Step 2.] Therefore, we can cancel the exceptional generators in a given 2-cell by applying Theorem 2.1 from [15] repeatedly to the pairs of exceptional generators in $N(e^2_\alpha)$ in the order described above, and skipping those (already cancelled) pairs that begin with a $\tilde{b}$ generator.

During Step 3., the only Reeb chords to be cancelled that belong to neighborhoods of more than one 2-cell are Reeb chords of the form $b^X_{i,j}$ (without a tilde). Such a Reeb chord is exceptional in $N(e^2_\alpha)$ if and only if a segment of the (i,j)-crossing locus of e^2_α is homotoped to sit above the boundary 1-cell e^X_1 during the procedure defined in Section 3.4. Property (A4) from Proposition 3.2 states that no crossing arcs from distinct 2-cells are homotoped to the same 1-cell. Thus, there is no overlap among Reeb chords in distinct 2-cells that need to be cancelled at Step 3.

At this point, we have obtained $(\mathcal{A}_{LCH}/I, \partial)$ from $(\mathcal{A}_{LCH}, \partial)$ by repeated applications of Theorem 2.1 from [15], so it follows that these DGAs are stable tame isomorphic. □

8.2. **Isomorphism between $(\mathcal{A}_{LCH}/I, \partial)$ and the Cellular DGA.** For easier comparison with the cellular DGA, we record here the presentation of $(\mathcal{A}_{LCH}/I, \partial)$ determined by the computations from Sections 5-7. Recall the procedure introduced in Section 3.4 for homotoping the cusp and crossing loci of $\tilde{L}$ into the 1-skeleton of $\mathcal{E}_{\Cap}$.

Proposition 8.6. *The DGA $(\mathcal{A}_{LCH}/I, \partial)$ has the following generators.*

For each 0-cell; 1-cell; or 2-cell, e^d_α, of $\mathcal{E}_{\Cap}$ we respectively have generators

$$a^\alpha_{i,j}, \quad b^\alpha_{i,j}, \quad \text{or } c^\alpha_{i,j}$$

for each i, j such that

- *$1 \le i < j \le n$ where n is the number of sheets above e^d_α, and*
- *the crossing locus between sheets S_i and S_j (as notated above e^d_α) is not placed above (the interior of) e^α_d when it is homotoped to sit above the 1-skeleton as in Section 3.4.*

Supposing L is equipped with an $\mathbb{Z}/m(L)$-valued Maslov potential, μ, the grading of generators is

$$|a^\alpha_{i,j}| = \mu(S_i) - \mu(S_j) - 1; \quad |b^\alpha_{i,j}| = \mu(S_i) - \mu(S_j); \quad |c^\alpha_{i,j}| = \mu(S_i) - \mu(S_j) + 1. \tag{25}$$

Moreover, with the exception of Type (13) and (14) squares, and some Type (9) squares, the differentials are computed using the process defined in Section 3.6 of [15]*:*

- *For a 0-cell e^0_α, form the strictly upper triangular matrix with (i,j)-entry $a^\alpha_{i,j}$, if it exists, and 0 otherwise. We have*

$$\partial A = A^2. \tag{26}$$

- *Suppose there are n sheets above the 1-cell e^1_α with 0-cells e^0_γ and e^0_β at $x = -1$ and $x = +1$. Form $n \times n$ matrices B, A_-, A_+ as in Section 3.6 of* [15]*. That is, the columns and rows of A_- and A_+ in which the a^γ_{ij} and a^β_{ij} appear are determined by identifying the sheets above e^0_β and e^0_γ with a subset of the sheets above e^1_α. All remaining entries are 0 except when sheets k and $k+1$ of e^1_α meet in a cusp in which case a 1 is placed in the $(k, k+1)$ entry of A_-.*

  We have

$$\partial B = A_+(I + B) + (I + B)A_-. \tag{27}$$

- *Consider a 2-cell e^2_α with L, D, R, U edges given by the 1-cells $e^1_{\beta_L}, e^1_{\beta_D}, e^1_{\beta_R}, e^1_{\beta_U}$ and 0-cells $e^0_{\gamma_0}$ and $e^0_{\gamma_1}$ at $(x_1, x_2) = (-1, -1)$ and $(x_1, x_2) = (+1, +1)$. Define upper triangular matrices C, B_L, B_D, B_R, B_U, $A_{-,-}$ and $A_{+,+}$ whose entries are respectively the Reeb chords $c^\alpha_{i,j}$, $b^{\beta_L}_{i,j}$, $b^{\beta_D}_{i,j}$, $b^{\beta_R}_{i,j}$, $b^{\beta_U}_{i,j}$, $a^{\gamma_0}_{i,j}$, and $a^{\gamma_1}_{i,j}$. The placement of the $b_{i,j}$ and $a_{i,j}$ generators in rows and columns of the B_X and $A_{\pm,\pm}$ is determined as in Section 3.6 of* [15] *by identifying sheets above boundary cells with the sheets of e^2_α whose closure they belong to. Remaining entries are 0 except that the $(k, k+1)$ entry of $A_{-,-}$ is 1 whenever sheets k and $k+1$ of e^2_α meet at a cusp above e^2_α.*

  We have

$$\partial C = A_{+,+}C + CA_{-,-} + (I + B_U)(I + B_L) + (I + B_R)(I + B_D). \tag{28}$$

The above holds for a square of type (9), e^2_α, as well, with the following exception. Suppose that after the singular set $\pi_x(\Sigma)$ is homotoped into the 1-skeleton, a swallowtail point sits above the initial point of the edge $e^1_{\beta_X}$ and the crossing arc that ends at the swallowtail point sits above $e^1_{\beta_X}$ (as in Figure 66 below). Then, (28) holds provided that we take the (i, j)-entry of B_X to be 1 if sheets S_i and S_j (as labeled above e^2_α) cross above $e^1_{\beta_X}$.

For squares of type (13) or (14) recall that we have decomposed those sheets above e^2_α that contain the swallowtail point in their closure into subsets S_k, S_{k+1}, S_{k+2}, and $\tilde{S}_k$ (resp. S_l, S_{l-1}, S_{l-2}, and $\tilde{S}_l$). Form matrices C, B_X and $A_{\pm,\pm}$ by making the convention that generators $b^L_{i,j}$ whose upper (resp. lower) sheet is a portion of $\tilde{S}_k$ (resp. $\tilde{S}_l$) are placed in row $k+2$ (resp. column $l-2$) of B_L while generators $a^{-,-}_{i,j}$ whose upper (resp. lower) sheet is a portion of $\tilde{S}_k$ (resp. $\tilde{S}_l$) are placed in row $k+1$ (resp. column $l-1$) of $A_{-,-}$. All remaining entries are 0 except for the $(k, k+2)$-entry (resp. column $(l-2, l)$-entry) of $A_{-,-}$ which is 1.

We have

$$\begin{aligned}\partial C = \;& A_{+,+}C + C(I + E_{k+2,k+1})A_{-,-}(I + E_{k+2,k+1}) + \\ & (I + B_U)(I + B_L)(I + A_{-,-}E_{k+1,k} + E_{k+1,k+2}) + (I + B_R)(I + B_D + B_D E_{k+2,k+1}).\end{aligned}$$

Proof. By construction, the generating set of $(\mathcal{A}_{LCH}/I, \partial)$ is obtained from the generating set of $(\mathcal{A}_{LCH}, \partial)$ by removing all exceptional Reeb chords. That the remaining generators are as stated follows from the definition of exceptional generator (in Definition 6.2). Note that in the statement of the Proposition, when providing subscripts for generators, we used the ordering of sheets above the unique 0-cell, e^0_α, containing $a^\alpha_{i,j}$, above the unique 1-cell, e^1_α, containing $b^\alpha_{i,j}$, and above the unique 2-cell, e^2_α, containing $c^\alpha_{i,j}$. That is,

$$a^\alpha_{i,j} := (a^\alpha_{i,j}, e^0_\alpha); \quad b^\alpha_{i,j} := (b^\alpha_{i,j}, e^1_\alpha); \quad \text{and} \quad c^\alpha_{i,j} := (c^\alpha_{i,j}, e^2_\alpha).$$

The mod $m(L)$ grading of generators is computed as in equation (2).

The formulas for differentials follow from Propositions 5.9, 5.10, Theorem 6.5, and Theorem 7.4.

In elaborating, we first discuss cases other than Type (13) or Type (14) squares. In the computations from Sections 5-7, when computing the sub-DGA generated by Reeb chords above $N(e^d_\alpha)$, subscripts were determined using the labelling of sheets above e^d_α (at the terminal vertex if $d = 1$ and above the upper-right corner if $d = 2$). Moreover, when it is a Reeb chord, the (i, j)-entry for any of the "boundary matrices" B_X, $A_\pm$ or $A_{\pm,\pm}$ has subscripts i and j. That is, the Reeb chords in the boundary matrices are placed so that if the upper and lower sheets of the Reeb chord above the boundary cell belong to the closure of sheet i and j as labeled above e^d_α, then that Reeb chord appears in row i and column j. This is precisely the way we place generators in the boundary matrices in the statement of the current Proposition 8.6. Moreover, the appearance of 0's and 1's in these matrices is identical as well. Indeed, by the definition of I, with a single exception in each Type (13) and (14) squares all exceptional generators equal 0 in $\mathcal{A}_{LCH}/I$. The single exceptional generator that is set to 1 in Type (13) and (14) squares is reflected by the 1 placed in the (i, j) entry of B_X whenever $e^1_{\beta_X}$ is an edge of a Type (9) square that sits under a crossing arc between sheets S_i and S_j with swallowtail endpoint. [This Reeb chord $b^X_{i,j}$ is equal to the Reeb chord notated $b^D_{k+2,k+1}$ or $b^D_{l-1,l-2}$ in the neighboring Type (13) or Type (14) square.] Moreover, the extra terms, x and X, that appear in Proposition 5.10 and Theorem 6.5 vanish in $\mathcal{A}_{LCH}/I$, so that the formulas from the statement of Proposition 8.6 agree precisely with the corresponding formulas from Propositions 5.9, 5.10, and Theorem 6.5.

Finally, we consider the differentials in a Type (13) square, e^2_α, as similar considerations apply to the Type (14) squares. The X term in Theorem 7.4 belongs to the ideal generated by exceptional generators of e^2_α other than $b^D_{k+2,k+1}$, and hence is 0 in $\mathcal{A}_{LCH}/I$. Moreover, the matrices B_X and $A_{\pm,\pm}$ agree precisely with the matrices from Theorem 7.4 since the manner in which generators are placed in the statement of Proposition 8.6 is consistent with placement of generators in the matrices of Theorem 7.4. In particular, the placement of generators whose upper or lower sheet is $\tilde{S}_k$ is consistent with Convention 7.2.

□

8.2.1. *The cellular DGA* $(\mathcal{A}_{||}, \partial)$. The presentation of $(\mathcal{A}_{LCH}/I, \partial)$ from Proposition 8.6 looks quite similar to the definition of the cellular DGA. To realize an isomorphism between $(\mathcal{A}_{LCH}/I, \partial)$ and the cellular DGA of L, we make use of the L-compatible polygonal decomposition $\mathcal{E}_{||}$.

Recall the construction of $\mathcal{E}_{||}$ from Section 3.6 as well as its relation to $\mathcal{E}_{\pitchfork}$ as stated in Proposition 3.4. The differential of the cellular DGA (as defined in Section 3 of [15]) associated to $\mathcal{E}_{||}$ relies on a few choices which we make as follows:

- Orient 1-cells to agree with the orientation of edges of corresponding squares in $\mathcal{E}_{\pitchfork}$. There are also some extra 1-cells added to squares of type (5), (6), (8), and (12) that do not correspond to subsets of edges of squares in $\mathcal{E}_{\pitchfork}$. We orient these 1-cells from left to right when viewed using the parametrizations of squares from $\mathcal{E}_{\pitchfork}$.
- For each 2-cell of $\mathcal{E}_{||}$ that is also a square of $\mathcal{E}_{\pitchfork}$, choose the initial and terminal vertices v_0 and v_1 for the 2-cell to be the lower left and upper right vertices of the square respectively. Each Type (5), (6), (8), and (12) square of $\mathcal{E}_{\pitchfork}$ contains a pair of 2-cells of $\mathcal{E}_{||}$. (See Section 3.6 and Figure 65.) For each of these 2-cells use the lower left (or just the left vertex if the 2-cell is a triangle) and upper right vertex for v_0 and v_1 respectively.
- For each swallowtail point, assign the decorations S and T so that the S corresponds to a corner of a Type (13) or (14) square, and the T is a corner of the Type (9) square that has the bottom edge of the Type (13) or (14) square as a border. In the Type (9) squares containing T decorations, we shift the initial vertex, v_0, so that it lies at the border of the T edge and the left border of the square. (See Figure 66 below.)

Denote the cellular DGA associated to $\mathcal{E}_{||}$ with the above choices by $(\mathcal{A}_{||}, \partial)$.

8.2.2. *Outline of equivalence of* $(\mathcal{A}_{LCH}/I, \partial)$ *and* $(\mathcal{A}_{||}, \partial)$. In comparing, $(\mathcal{A}_{LCH}/I, \partial)$ as presented in Proposition 8.6 with the cellular DGA $(\mathcal{A}_{||}, \partial)$ we notice the following key differences:

(1) The cellular DGA has more generators associated to the Type (5), (6), (8), and (12) squares of $\mathcal{E}_{\pitchfork}$, since each of these squares is subdivided into two 2-cells of $\mathcal{E}_{||}$. In addition, in $(\mathcal{A}_{LCH}/I, \partial)$ the bottom edges of the Type (5), (6), (8), and (12) squares have matrices B_D with two above diagonal entries equal to 0, specifically the $(k+1, k+2)$ and $(k, k+2)$ entries. This does not occur in any of the B matrices used in defining $(\mathcal{A}_{||}, \partial)$.
(2) The differentials in $(\mathcal{A}_{||}, \partial)$ of generators associated to the squares of $\mathcal{E}_{||}$ that contain the swallowtail decorations S or T appear somewhat different than the differentials of corresponding generators of $(\mathcal{A}_{LCH}/I, \partial)$.

To address (1), we produce a stable tame isomorphic quotient $(\mathcal{A}_{||}/J, \partial)$ whose generators are in precise correspondence with those of $(\mathcal{A}_{LCH}/I, \partial)$. We then give a (tame) DGA isomorphism between $(\mathcal{A}_{||}/J, \partial)$ and $(\mathcal{A}_{LCH}/I, \partial)$. For most squares, the isomorphism simply identifies generators, but, as may be expected from (2), the isomorphism is more involved for squares that contain S or T decorations.

Proposition 8.7. *There exists a stable tame isomorphic quotient of* $(\mathcal{A}_{||}, \partial)$ *that is tame isomorphic to* $(\mathcal{A}_{LCH}/I, \partial)$.

Proof. **Constructing the quotient $\mathcal{A}_{||}/J$.**

All cells of $\mathcal{E}_{||}$ were obtained from cells of $\mathcal{E}_{\pitchfork}$ by applying a homeomorphism of the base surface S and then subdividing some of the cells of $\mathcal{E}_{\pitchfork}$. Let us set notation for the cells that appear during the subdivision process (which is summarized in Proposition 3.4).

First, for each $\mathcal{E}_{\pitchfork}$ square, e^2_α, of type (5), (6), (8), and (12), the right edge of the square is subdivided into two 1-cells by adding a new 0-cell at the intersection of the (upper) crossing arc with the edge.

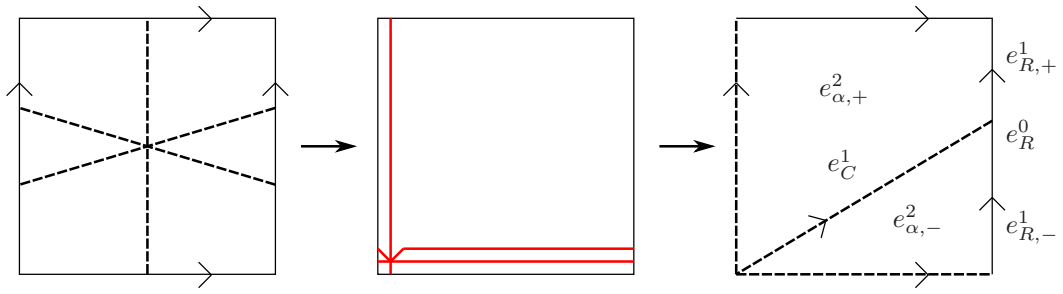

FIGURE 65. Subdividing a Type (8) cell of $\mathcal{E}_{\pitchfork}$ to form $\mathcal{E}_{||}$.

Denote the new 0-cell by e^0_R and the 1-cells that constitute the upper and lower half of this edge by $e^1_{R,+}$ and $e^1_{R,-}$. If e^2_α is a Type (6) square then we also subdivide the left edge to produce cells e^0_L, $e^1_{L,+}$ and $e^1_{L,-}$. (Note that some of these edges are shared with neighboring cells, in a manner that is visible in Figures 12 and 13. We caution that the "left" and "right" edges that we refer to are with respect to the parametrizations by $[-1,1]\times[-1,1]$, and not with respect to the appearance in Figures 12 and 13.)

Secondly, a new 1-cell is added that connects either $e^0_{-,-}$ to e^0_R, in the case of Type (5), (8), and (12) squares, or e^0_L to e^0_R, in the case of a Type (6) square. Denote this new cell by e^1_C, and the 2-cells that respectively form the upper and lower half of e^2_α as $e^2_{\alpha,+}$ and $e^2_{\alpha,-}$. See Figure 65.

To form the quotient $\mathcal{A}_{||}/J$, we will apply Theorem 2.1 from [15] to cancel many generators in these squares. The hypothesis of Theorem 2.1 from [15] requires an ordering of the generating set of $\mathcal{A}_{||}$ for which the differential is triangular. Such orderings for the cellular DGA are discussed in Section 4.1 of [15].

Cancellation 1. Label sheets of all cells that belong to the closure of $e^2_{\alpha,-}$ in the order they appear above $e^2_{\alpha,-}$. With generators associated to a cell placed into matrices with the same subscripts as the cell, we have

$$\partial B_{R,-} = A_R[I+B_{R,-}] + [I+B_{R,-}]A_{+,-}.$$

Where the $(k+1,k+2)$ entry of A_R is 0 and the $(k,k+1)$-entry of $A_{+,-}$ is 0. [The $k, k+1$, and $k+2$ sheets above e^1_R in $\mathcal{E}_{\pitchfork}$ appear as in Figure 5 (2Cr), so above $e^1_{R,-}$ in $\mathcal{E}_{||}$ they appear as in the region between the two crossings in Figure 5 (2Cr).]

First, since

$$\partial\boxed{b^{R,-}_{k+1,k+2}} = \boxed{a^{+,-}_{k+1,k+2}}$$

we can quotient by the 2-sided ideal generated by $b^{R,-}_{k+1,k+2}$ and $\partial b^{R,-}_{k+1,k+2}$ which we notate as $I(b^{R,-}_{k+1,k+2}, \partial b^{R,-}_{k+1,k+2})$. Theorem 2.1 from [15] tells us that the quotient with the boxed generators removed from the generating set is stable tame isomorphic to $(\mathcal{A}_{||},\partial)$.

Next, quotient by $I(b^{R,-}_{i,j}, \partial b^{R,-}_{i,j})$ inductively for all remaining $i<j$, so that $|i-j|$ is non-increasing during the inductive process. When we quotient by $I(b^{R,-}_{i,j}, \partial b^{R,-}_{i,j})$, we already have that $b^{R,-}_{i,k} = 0 = b^{R,-}_{k,j}$ for all $i<k<j$, so that

$$\partial\boxed{b^{R,-}_{i,j}} = \boxed{a^R_{i,j}} + a^{+,-}_{i,j}$$

for $(i,j)\neq(k,k+1)$, and

$$\partial\boxed{b^{R,-}_{k,k+1}} = \boxed{a^R_{k,k+1}}.$$

Thus, Theorem 2.1 from [15] implies that (removing boxed generators from the generating set) the result is stable tame isomorphic to $(\mathcal{A}_{||},\partial)$.

After the inductive process is complete, the new generating set contains no generators associated to e^0_R or $e^1_{R,-}$ and has only the generators $a^{+,-}_{i,j}$ such that S_i and S_j do not cross above e^1_R; i.e. with $(i,j)\neq(k+1,k+2)$ and $(i,j)\neq(k,k+1)$. We have relations

$$a^{+,-}_{i,j} = a^R_{i,j} \quad \text{for } (i,j)\notin\{(k,k+1),(k+1,k+2)\}; \quad a^{+,-}_{k+1,k+2}=0; \quad a^R_{k,k+1}=0. \tag{29}$$

Perform this same process on the generators associated to the generators of $\mathcal{A}_{||}$ associated to e^0_L, $e^1_{L,+}$ and $e^1_{L,-}$ cells in Type (6) squares.

Cancellation 2. The generators associated to $e^2_{\alpha,-}$ satisfy

$$\partial C \doteq A_{-,-}C + CA_R + [I + B_D] + [I + B_C] \tag{30}$$

where $\doteq$ denotes equality in the currently considered quotient. [Note that in $(\mathcal{A}_{||}, \partial)$ there may be other factors of the form $[I + B_{L,-}]$ or $[I + B_{R,-}]$ in the final two terms of ∂C. However, $B_{L,-} \doteq B_{R,-} \doteq 0$ after the first cancellation procedure.]

First, cancel

$$\partial \boxed{c^{\alpha,-}_{k+1,k+2}} = \boxed{b^D_{k+1,k+2}}.$$

Then, inductively cancel the remaining $c^{\alpha,-}_{i,j}$ with the $b^C_{i,j}$ in an order so that $|i-j|$ is non-decreasing. As we proceed, we can verify

$$\partial \boxed{c^{\alpha,-}_{i,j}} \doteq \boxed{b^C_{i,j}} + b^D_{i,j} \text{ for } (i,j) \notin \{(k,k+1),(k+1,k+2)\}, \text{ and } \partial \boxed{c^{\alpha,-}_{k,k+1}} = \boxed{b^C_{k,k+1}},$$

so that Theorem 2.1 from [15] implies the result is equivalent to $(\mathcal{A}_{||}, \partial)$. [Any $a^{-,-}_{i,m}c_{m,j}$ or $c_{i,m}a^R_{m,j}$ terms that may appear in $\partial c_{i,j}$ are already equal to 0 in the quotient, since $|m-j| < |i-j|$.]

After the inductive process is complete, the new generating set contains no generators associated to e^1_C or $e^2_{\alpha,-}$ and has only the generators $b^D_{i,j}$ such that S_i and S_j do not cross above e^1_D when the crossing locus of e^2_α is homotoped into the one skeleton; i.e. with $(i,j) \neq (k+1,k+2)$ and $(i,j) \neq (k,k+1)$. We have relations

$$b^C_{i,j} = b^D_{i,j} \quad \text{for } (i,j) \notin \{(k,k+1),(k+1,k+2)\}; \quad b^D_{k+1,k+2} = 0; \quad b^C_{k,k+1} = 0. \tag{31}$$

Once Cancellation 2 is completed in all Type (5), (6), (8), and (12) squares, we let $J \subset \mathcal{A}_{||}$ denote the resulting ideal so that stable tame isomorphic quotient that we have constructed is $(\mathcal{A}_{||}/J, \partial)$.

Correspondence between generators. We have completely removed all generators associated to the cells of $\mathcal{E}_{||}$ that do not correspond to cells of $\mathcal{E}_{\pitchfork}$ from the generating set. In fact, every remaining generator of $\mathcal{A}_{||}/J$ corresponds to a cell of $\mathcal{E}_{\pitchfork}$ and a pair of sheets S_i and S_j above that cell that do not meet when the crossing locus is homotoped into the 1-skeleton. [In particular, it was noted during the construction of J that this holds for the 0- and 1-cells along the bottom edges of Type (5), (6), (8), and (12) squares.]

In the remainder of the argument, we use this correspondence to identify the underlying algebras,

$$\mathcal{A}_{||}/J \cong \mathcal{A}_{LCH}/I.$$

Note that the grading of generators coincides; see (25) and equation (1) in Section 3.4 of [15].

Claim: Let e^2_α be a 2-cell of $\mathcal{E}_{\pitchfork}$ that is not one of those Type (13), (14) and (9) squares that correspond to a square of $\mathcal{E}_{||}$ containing an S or T decoration. Then, the differentials from $\mathcal{A}_{||}/J$ and $\mathcal{A}_{LCH}/I$ agree when applied to generators associated to cells in the closure of e^2_α.

Proof of Claim. For generators associated to 0 and 1-cells, note that the formulas (2) and (3) from [15] used to define the differential on the Cellular DGA are identical to the formulas (26) and (27) and the formulas are identical. Moreover, the entries of matrices that appear in these formulas coincide. [Here, we note that in $(\mathcal{A}_{||}, \partial)$, for the matrices $A_\pm$ and B used for the bottom edge of a Type (5), (6), (8) and (12) square the two entries that correspond to the sheets that cross are both replaced with 0 in $\mathcal{A}_{||}/J$ due to the relations (29) and (31).]

For 2-cells of $\mathcal{E}_{||}$ such that the cell decomposition of the entire 2-cell coincides with the decomposition of an entire square of $\mathcal{E}_{\pitchfork}$, the formulas (4) from [15] and (28) give identical differentials. This relies on our having chose the initial and terminal vertices in $\mathcal{E}_{||}$ to coincide with the lower left and upper right corners of squares from $\mathcal{E}_{\pitchfork}$.

There may be some squares, e^2_α, not of type (5), (6), (8) or (12) that none-the-less have one of their boundary edges subdivided when we form $\mathcal{E}_{||}$ from $\mathcal{E}_{\pitchfork}$. [Specifically, this can happen for squares that share an edge with a Type (5), (6), (8) or (12) square.] We discuss the case where the edge D is

subdivided, although, similar considerations apply if other edges are subdivided. Then, (4) from [15] gives that in $(\mathcal{A}_{||}, \partial)$

$$\partial C = A_{+,+}C + CA_{-,-} + [I + B_U][I + B_L] + [I + B_R][I + B_{D,+}][I + B_{D,-}]$$

where $B_{D,\pm}$ contain generators associated to the two halfs of the subdivided edge. When we formed the quotient $\mathcal{A}_{||}/J$, all generators associated to $B_{D,-}$ became 0. Thus, in $\mathcal{A}_{||}/J$, the desired formula

$$\partial C = A_{+,+}C + CA_{-,-} + [I + B_U][I + B_L] + [I + B_R][I + B_{D,+}]$$

holds for e^2_α.

Finally, consider a Type (5), (6), (8), or (12) square, e^2_α. For Type (5), (8), (12) the generators of $\mathcal{A}_{||}$ associated to $e^2_{\alpha,+}$ (which are the ones identified with generators of e^2_α under the isomorphism $\mathcal{A}_{||}/J \cong \mathcal{A}_{LCH}/I$) have their differential in $(\mathcal{A}_{||}, \partial)$ given by

$$\partial C = A_{+,+}C + CA_{-,-} + [I + B_U][I + B_L] + [I + B_{R,+}][I + B_C].$$

For Type (6), they satisfy

$$\partial C = A_{+,+}C + CA_L + [I + B_U][I + B_{L,+}] + [I + B_{R,+}][I + B_C].$$

In $\mathcal{A}_{||}/J$, the relations (29) and (31) identify the entries of the matrices B_C and B_D, as well as A_L and $A_{-,-}$ in the Type (6) case. Note that the location of entries in the matrices B_C and A_L may be different here than in (30) (in fact, the $k+1$ and $k+2$ rows and columns are transposed). However, the relations (29) and (31) preserve the the upper and lower sheet associated to generators, thus the previous formula is indeed equivalent to

$$\partial C = A_{+,+}C + CA_{-,-} + [I + B_U][I + B_L] + [I + B_R][I + B_D]$$

that holds in $(\mathcal{A}_{LCH}/I, \partial)$. [Recall that it is the entries of $B_{R,+}$ and $B_{L,+}$ that are associated to the e^1_R and e^1_L generators of $\mathcal{A}_{LCH}/I$ under the isomorphism $\mathcal{A}_{||}/J \cong \mathcal{A}_{LCH}/I$.] □

The isomorphism $\Phi : (\mathcal{A}_{LCH}/I, \partial) \to (\mathcal{A}_{||}/J, \partial)$.

Adding subscripts 1 and 2 to distinguish the notation for differentials, we will define an isomorphism $\Phi : (\mathcal{A}_{LCH}/I, \partial_1) \to (\mathcal{A}_{||}/J, \partial_2)$. On all generators belonging to the closure of a square without a swallowtail decoration S or T, Φ simply identifies generators of $\mathcal{A}_{LCH}/I$ and $\mathcal{A}_{||}$. In defining Φ on the S and T squares, we consider only the case of a Type (13) square (upward swallowtail) such that the swallowtail involves sheets $k, k+1$, and $k+2$, as the other case is similar.

We fix matrices containing generators from cells belonging to the closure of squares that have S and T decorations. The S and T squares, as they appear in $\mathcal{E}_{\Cap}$ and $\mathcal{E}_{||}$, are pictured in Figure 66 where matrices associated to each cell are indicated. Supposing there are n sheets to the right of the cusp edge, all matrices are $n \times n$ except for A which is $(n-2) \times (n-2)$. The matrices $B_0, B_1, B_2, B_3, A_1, A_2$, and C_1 always have generators placed so that the ordering of rows and columns corresponds to the ordering of sheets of $\tilde{L}$ in the T square, and B_1 has all entries in rows and columns k and $k+1$ equal to 0. Note that the $(k+1, k+2)$ entry of B_0 is 0. The matrices B_4, B_5, B_6, A_3, and C_2 use the ordering of sheets above S, and B_4 also has 0's in rows and columns k and $k+1$.

As in [15, Section 3.11], we let $\widehat{A}_{k,k+1}$ (resp. $\widehat{A}_{k,k+2}$) denote A with two rows and columns added in positions k and $k+1$ (resp. k and $k+2$) with all entries 0 except the $(k, k+1)$-entry (resp. the $(k, k+2)$-entry) which is 1. In addition, let $T = I + E_{k+1,k+2}$ and $S = I + \widehat{A}_{k,k+1}E_{k+2,k} + E_{k+1,k+2}$, as in equation (7) from Section 3.11 of [15].

We complete the definition of Φ by setting

$$\Phi(C_1) = C_1; \quad \Phi(C_2) = C_2; \text{ and}$$
$$\Phi(B_0) = B_0[I + E_{k+1,k+2}].$$

[All other generators belong to cells lying in the closure of squares without S or T decorations.] Since $[I + E_{k+1,k+2}]$ is upper triangular, it is easy to verify that Φ is a *tame* isomorphism. [For more details, compare with the proof of tameness given for the map ψ from Theorem 4.5 from [15].] Observe the formula

$$\Phi(I + B_0 + E_{k+1,k+2}) = (I + B_0)(I + E_{k+1,k+2}). \tag{32}$$

From Proposition 8.6 and the definition of the Cellular DGA, we have the following formulas:

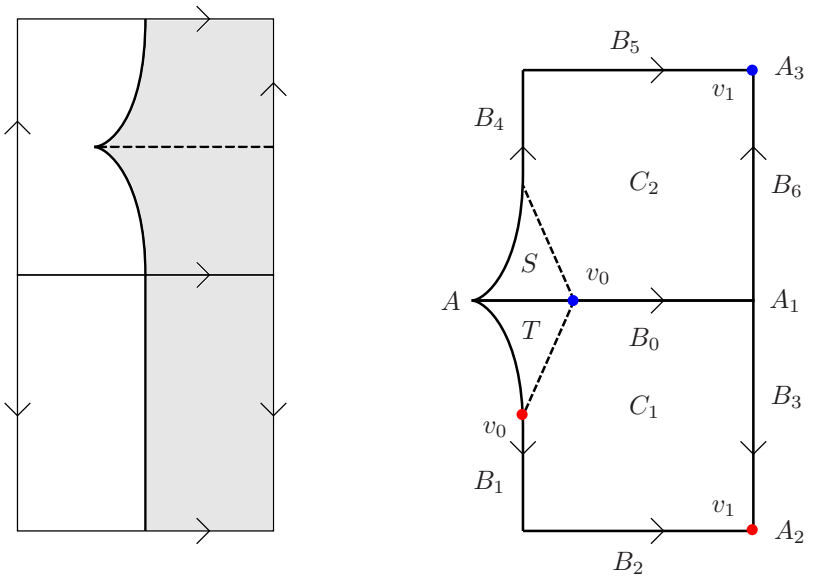

FIGURE 66. Two squares of $\mathcal{E}_{\pitchfork}$ and $\mathcal{E}_{||}$ near a swallowtail point. The dotted edges labelled S and T in the right are considered when computing the cellular differential, but are not 1-cells of $\mathcal{E}_{||}$. Initial and terminal vertices of the C_1 and C_2 squares are depicted in blue and red respectively.

$$\begin{aligned}\partial_1 B_0 = &\quad A_1[I + B_0 + E_{k+1,k+2}] + [I + B_0 + E_{k+1,k+2}]\widehat{A}_{k,k+1}\\ \partial_2 B_0 = &\quad A_1[I + B_0] + [I + B_0][I + E_{k+1,k+2}]\widehat{A}_{k,k+1}[I + E_{k+1,k+2}]\end{aligned}$$

[The $E_{k+1,k+2}$ terms appear in $\partial_1 B_0$ because the B_0 Reeb chord between the $k+1, k+2$ sheets of the T square is the exceptional generator $b^D_{k+2,k+1}$ from the Type (13) square that satisfies $b^D_{k+2,k+1} = 1$ in $\mathcal{A}_{LCH}/I$.]

$$\begin{aligned}\partial_1 C_1 = &\quad A_2 C_1 + C_1\widehat{A}_{k,k+1} + [I + B_2][I + B_1] + [I + B_3][I + B_0 + E_{k+1,k+2}]\\ \partial_2 C_1 = &\quad A_2 C_1 + C\widehat{A}_{k,k+1} + [I + B_2][I + B_1] + [I + B_3][I + B_0]T\end{aligned}$$

$$\begin{aligned}\partial_1 C_2 = &\quad A_3 C_2 + C_2(I + E_{k+2,k+1})\widehat{A}_{k,k+2}(I + E_{k+2,k+1}) +\\ &[I + B_5][I + B_4][I + \widehat{A}_{k,k+2}E_{k+1,k} + E_{k+1,k+2}] + [I + B_6][I + QB_0Q + QB_0QE_{k+2,k+1}]\\ \partial_2 C_2 = &\quad A_3 C_2 + C_2(I + E_{k+2,k+1})\widehat{A}_{k,k+2}(I + E_{k+2,k+1}) +\\ &[I + B_5][I + B_4]S + [I + B_6][I + QB_0Q].\end{aligned}$$

where Q denotes the permutation matrix of the trasposition $(k+1\ k+2)$. [All occurences of B_0 are conjugated by Q because the order of the $k+1$ and $k+2$ sheets is opposite above the S square and the T square.]

The verification of $\Phi \circ \partial_1 = \partial_2 \circ \Phi$ on generators is as follows. When applied to a generator not appearing in B_1, C_1, or C_2, the equality follows from the Claim. For the remaining generators, we compute using (32)

$$\begin{aligned}\Phi \circ \partial_1(B_0) =& A_1\Phi(I + B_0 + E_{k+1,k+2}) + \Phi(I + B_0 + E_{k+1,k+2})\widehat{A}_{k,k+1} =\\ &\left(A_1[I + B_0] + [I + B_0][I + E_{k+1,k+2}]\widehat{A}_{k,k+1}[I + E_{k+1,k+2}]\right)[I + E_{k+1,k+2}] =\\ &\partial_2(B_0[I + E_{k+1,k+2}]) = \partial_2 \circ \Phi(B_0);\end{aligned}$$

and

$$\Phi \circ \partial_1(C_1) = A_2 C_1 + C_1\widehat{A}_{k,k+1} + [I + B_2][I + B_1] + [I + B_3]\Phi(I + B_0 + E_{k+1,k+2}) = \partial_2 \circ \Phi(C_1).$$

Finally, observe that $[I + \widehat{A}_{k,k+2}E_{k+1,k} + E_{k+1,k+2}] = [I + \widehat{A}_{k,k+1}E_{k+2,k} + E_{k+1,k+2}] = S$, so that all terms in $\partial_1 C_2$ and $\partial_2 C_2$ that do not involve B_0 are identical. Thus, showing that $\Phi \circ \partial_1(C_2) = \partial_1 \circ \Phi(C_2)$ reduces to the computation

$$\Phi(I + QB_0Q + QB_0QE_{k+2,k+1}) = Q\Phi(I + B_0[I + E_{k+1,k+2}])Q = Q(I + B_0)Q = I + QB_0Q.$$

□

Proof of Theorem 1.1. Stable tame isomorphism has the properties of an equivalence relation. Thus, since $(\mathcal{A}_{||}/J, \partial)$ is stable tame isomorphic to the Cellular DGA of L, and $(\mathcal{A}_{LCH}/I, \partial)$ is stable tame isomorphic to the Legendrian contact homology DGA of L, it follow that the Cellular DGA is stable tame isomorphic to the LCH DGA. □

9. Proof of Theorem 5.1 Part 1: Construction of squares without swallowtails

The remaining four sections of the paper concern the proof of Theorem 5.1. We need to establish the existence of a Legendrian $\tilde{L}$ satisfying the (many) stated properties. This task is carried out in two parts. In Sections 9-11, we construct an initial approximation, $\tilde{L}_0$,to $\tilde{L}$ that satisfies all of the requirements of Theorem 5.1 except that $\tilde{L}_0$ is not necessarily 1-regular. Then, in Section 12 we show that by applying an appropriate perturbation to $\tilde{L}_0$ we may obtain the 1-regular condition while preserving the other requirements of Theorem 5.1.

The construction of $\tilde{L}_0$ is carried out in a fairly explicit manner using local coordinates on S associated to the transverse square decomposition, $\mathcal{E}_{\pitchfork}$. Recall that above each of the squares of $\mathcal{E}_{\pitchfork}$, the singular set of L (topologically) matches one of the types (1)-(14), and that above each 1-cell the singular set has one of the four types (PV), (1Cr), (2Cr), and (Cu). For each square type, we will produce a collection of functions defined on (subsets of) $[-1,1]\times[-1,1]$ whose 1-jets define $\tilde{L}_0$ above squares of that type. These *defining functions* have a standard form near each boundary edge of $[-1,1]\times[-1,1]$ that only depends on the type of the edge, and this will allow us to verify that the pieces of $\tilde{L}_0$ fit together to produce a smooth Legendrian.

The construction of defining functions for squares of type (1)-(12) is done in a uniform manner and is carried out in the remainder of Section 9. In Sections 9.1-9.2 we construct functions over $[-1,1]$ that match the four possible 1-cell types. Then, in Section 9.3 we define two-variable functions for the Type (1)-(12) squares as a suitable sum of interpolations between the one-variable functions associated to the boundary edges. The construction of the Type (13) and (14) squares is more involved due to the presence of swallowtail points, and is the topic of Section 10. The verification that the singular set of the resulting Legendrian has the proper form above each square is deferred until Section 11 where all of the properties of Theorem 5.1 are verified, except for 1-regularity.

9.0.3. *Preliminaries.* Fix the Legendrian $L \subset J^1(S)$ and transverse square decomposition $\mathcal{E}_{\pitchfork}$ from the statement of Theorem 5.1. Let N denote the maximal number of sheets of the front projection of L over any point in S.

We can assume without loss of generality that above all squares of $\mathcal{E}_{\pitchfork}$ the lower most and upper most sheet of L do not meet any other sheets at singular points, i.e. crossings, cusps, and swallowtail points. If this is not the case, then we simply take the union of L with the 1-jets of a pair of constant functions with sufficiently large negative and positive value. After constructing the resulting Legendrian, suitable defining functions for the original L arise from discarding the two new components.

For the constructions, we fix a constant $0 < \epsilon_1 < 1$ such that

$$\epsilon_1 < \left(\frac{1}{10N}\right)^{10}. \tag{33}$$

Later in the construction we will fix additional, even smaller constants ϵ_2 and ϵ_3.

Remark 9.1. No explicit relation is assumed between $\epsilon_1, \epsilon_2, \epsilon_3$ and the constant ϵ that appears in some of the Properties from Sections 5-7, such as Property 6.

The possible (topological) appearance of the front projection of L above any edge $e \cong [-1,1]$ of $\mathcal{E}_{\pitchfork}$ is determined by

(i) the number of sheets, n, of L above $[-1,1]$;
(ii) the nature of the singular set above $[-1,1]$ which must be one of (PV), (1Cr), (2Cr), (Cu); and
(iii) the location of crossing and cusp sheets which are specified in the (1Cr) and (Cu) case by a pair of consecutive integers $1 < k < k+1 < n$, and in the (2Cr) by $1 < k < k+1 < k+2 < n$.

We refer to the data (i)-(iii) as an **edge type**.

In Sections 9.1-9.2, we construct 1-variable defining functions for 1-dimensional Legendrians matching all possible edge types with $1 \leq n \leq N$. Following the convention from Section 5.4, when considering a particular edge type we label the sheets of the Legendrian above $[-1,1]$ as $S_1, \ldots, S_n$ with descending z-coordinate at $x = +1$. We will notate the corresponding defining functions as $f_1, \ldots, f_n : [-1,1] \to \mathbb{R}$. (For (Cu) edges, the defining functions f_k and f_{k+1} will have proper subsets of $[-1,1]$ as their domain.) For $1 \leq i, j \leq n$, we notate *difference functions* as

$$f_{i,j} := f_i - f_j.$$

Our constructions often make use of the following (probably standard) technical lemma.

Lemma 9.2. *Suppose we are given smooth functions f and g such that $g : [a,b] \to \mathbb{R}$ satisfies $0 < g'(x)$ for all $x \in [a,b]$, and for some $\delta > 0$, $f : [a, a+\delta] \cup [b-\delta, b] \to \mathbb{R}$ satisfies*

$$\begin{array}{ll} 0 < f'(x) < g'(x), & \text{for all } x \in [a, a+\delta] \cup [b-\delta, b], \text{ and} \\ 0 < f(b) - f(a) < g(b) - g(a). & \end{array}$$

Then, there exists $0 < \delta' < \delta$ and $\tilde{f} : [a,b] \to \mathbb{R}$ such that

$$\begin{array}{ll} 0 < \tilde{f}'(x) < g'(x) & \text{for all } x \in [a,b], \text{ and} \\ \tilde{f}(x) = f(x) & \text{for all } x \in [a, a+\delta'] \cup [b-\delta', b]. \end{array} \tag{34}$$

Proof. By continuity, we can choose $a < a' < a + \delta$ and $b - \delta < b' < b$ so that

$$0 < f(b') - f(a') < g(b') - g(a')$$

continues to hold. Start by defining $\widehat{f} : [a,b] \to \mathbb{R}$ via

$$\widehat{f}(x) = \begin{cases} f(x), & x \in [a,a'] \cup [b',b], \\ f(a') + \alpha \int_{a'}^{x} d_x g(s)\, ds, & x \in [a',b'], \end{cases}$$

where

$$\alpha = \frac{f(b') - f(a')}{g(b') - g(a')} \qquad \text{satisfies } 0 < \alpha < 1.$$

Note that $\widehat{f}$ is continuous everywhere and is smooth at points other than $x = a'$ and $x = b'$. It is easy to verify that $0 < d_x \widehat{f}(x) < d_x g(x)$ holds for all $x \in [a,b]$ including for the right and left derivatives of $\widehat{f}$ when $x = a'$ and $x = b'$. Therefore, we can produce $\tilde{f}$ by choosing sufficiently small neighborhoods of a' and b' and smoothing $\widehat{f}$ within these neighborhoods in a manner that retains the inequality $0 < d_x \tilde{f}(x) < d_x g(x)$. □

In typical applications of Lemma 9.2, with g already defined, and f defined on $[a,b] \cup [c,d]$ satisfying $0 < f'(x) < g'(x)$ and $0 < f(c) - f(b) < g(c) - g(b)$, we extend f to $[a,d]$ in a manner that preserves the derivative inequalities. This is accomplished with Lemma 9.2 by first choosing some extension of f to $[a, b+\delta]$ and $[c-\delta, d]$ and taking δ small enough so that the hypothesis of the Lemma are satisfied. We will often make such extensions without explicit reference to Lemma 9.2.

9.1. 1-dimensional defining functions in $[1/2, 3/4]$.

Proposition 9.3. *There exists a collection of smooth functions,*

$$h_i : [1/2 - \epsilon_1, 3/4 + \epsilon_1] \to \mathbb{R}, \quad \text{for } i = 1, \ldots N,$$

satisfying:

1. *For all $1 \leq i < j \leq N$, $h_i(1/2) = h_i(3/4) = 0$, and $h_i(x) > h_j(x)$, for all $x \in (1/2, 3/4)$.*
2. *For all $1 \leq i \leq N$, $||h_i||_{C^0} < \epsilon_1/6$.*
3. *For all $1 \leq i < j \leq N$, $h_{i,j}$ has a unique critical point, $\eta_{i,j} \in [1/2 - \epsilon_1, 3/4 + \epsilon_1]$, that is a non-degenerate local maximum in $(1/2, 3/4)$. Moreover, the $\eta_{i,j}$ appear in lexicographic order: For any other $i' < j'$,*

$$i' < i, \text{ or } i' = i \text{ and } j' < j \quad \Rightarrow \quad \eta_{i',j'} < \eta_{i,j}. \tag{35}$$

Proof. Inductively select points $p_N, p_{N-1}, \ldots, p_1$ in $(1/2, 3/4) \times (0, +\infty)$ so that for all $1 \leq i < N$, we have

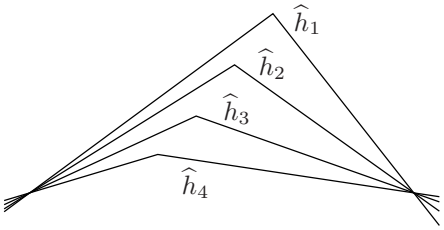

FIGURE 67. Graphs of the piecewise linear functions $\widehat{h}_i$.

(i) $x(p_i) > x(p_{i+1})$, and
(ii) p_i lies above the line through $(1/2, 0)$ and p_{i+1}.

Define $\widehat{h}_i : [1/2 - \epsilon_1, 3/4 + \epsilon_1] \to \mathbb{R}$ to be piece-wise linear agreeing with the line ℓ_i through $(1/2, 0)$ and p_i on $[1/2 - \epsilon_1, x(p_i)]$ and with the line ℓ_i' through p_i and $(3/4, 0)$ on $[x(p_i), 3/4 + \epsilon_1]$. See Figure 67. Next, produce $\widetilde{h}_i$ from $\widehat{h}_i$, by smoothing in a small neighborhood of $x = x(p_i)$ in a manner so that $d_x\tilde{h}_i$ decreases monotonically, and $d_x^2\tilde{h}_i$ is non-zero where $\tilde{h}_i$ is non-linear. It follows easily from (i) and (ii) that the critical points of $\tilde{h}_{i,j}$ are as required in item (3). Finally, put $h_i = \alpha\tilde{h}_i$ where $\alpha > 0$ is an overall constant chosen to be small enough so that item (2) holds. □

Let

$$\epsilon_\eta = \frac{1}{3}\text{Min}\{|\eta_{i,j} - \eta_{i',j'}| \,:\, (i,j) \neq (i',j')\}, \tag{36}$$

so that ϵ_η-balls centered around the $\eta_{i,j}$ are all disjoint. Let

$$M = \text{Min}_{i<j}\left(\inf\{|d_x f_{i,j}(x)| \,:\, x \in [1/2, 3/4] \setminus (\eta_{i,j} - \epsilon_\eta, \eta_{i,j} + \epsilon_\eta)\}\right) > 0. \tag{37}$$

Choose $\epsilon_2 > 0$ such that

$$\epsilon_2 < \min\left\{\frac{\epsilon_1^{10}}{(10N)^{10}}, \frac{4M\epsilon_1}{N}\right\}. \tag{38}$$

9.2. **1-dimensional defining functions.** For an arbitrary edge type with $1 \leq n \leq N$, we fix defining functions

$$f_1, \ldots, f_n : [-1, 1] \to \mathbb{R}$$

[Although the edge type is not indicated in the notation for the f_i, no relation is assumed between f_i corresponding to distinct edge types.]

We let $\sigma_-(i)$ denote the ordering that sheet S_i appears in above $x = -1$, where in the (Cu) case we put $\sigma_-(k) = \sigma_-(k+1) = k - 0.5$ when S_k and S_{k+1} meet at the left cusp. Explicitly, for edges of type (PV), (1Cr), and (2Cr), σ_- is respectively given by permutations id, $(k\ k+1)$ and $(k\ k+1\ k+2)$ while in the (Cu) case we have

$$\sigma_-(i) = \begin{cases} i, & i < k; \\ k - 0.5, & i = k, k+1; \\ i - 2, & i > k+1. \end{cases}$$

Note that σ_- uniquely determines the edge type. For $i < j$, sheets S_i and S_j cross if and only if $\sigma_-(i) > \sigma_-(j)$. In addition, put $\sigma_+(i) := i$ for $1 \leq i \leq n$.

For each edge type, we fix $y_{i,i+1}$, $i = 1, \ldots, n-1$, that will correspond approximately to the maximum values of the $f_{i,i+1}$ as follows:

(PV) and (Cu): Set all $y_{i,i+1} = 1$.

(1Cr): Set $y_{i,i+1} = 1$, $i \neq k-1, k, k+1$, and

$$y_{k-1,k} = 1.5, \quad y_{k,k+1} = 0, \quad y_{k+1,k+2} = 1.5.$$

(2Cr): Set $y_{i,i+1} = 1$, $i \neq k-1, k, k+1, k+2$, and

$$\begin{aligned} y_{k-1,k} = 1.125, \quad y_{k,k+1} = 0.625, \quad y_{k+1,k+2} = 0.125, \\ y_{k+2,k+3} = (k+3) - (k-1) - \textstyle\sum_{\eta=k-1}^{k+1} y_{\eta,\eta+1} = 2.125. \end{aligned} \tag{39}$$

Finally, for $1 \le i \le j \le n$, put $y_{i,j} = \sum_{l=i}^{j-1} y_{l,l+1}$.

Proposition 9.4. *For any (PV), (1Cr), or (2Cr) edge type, functions f_i, $1 \le i \le n$, can be constructed so that for all $1 \le i < j \le n$ the following properties hold:*

(1) *If $\sigma_-(i) < \sigma_-(j)$, then $f_{i,j}(x) > 0$, $\forall x \in [-1,1]$.*
If $\sigma_-(i) > \sigma_-(j)$, then $f_{i,j}$ has a unique non-degenerate 0 located at $x = 0$ in the (1Cr) case, and located in $[1/4, 1/4+\epsilon_1]$ in the (2Cr) case.

(2) *For all $x \in [1/2, 3/4]$,*
$$d_x f_{i,j}(x) = d_x h_{i,j}(x),$$
and for all $x \in [1/4, 3/4]$,
$$|f_{i,j}(x) - y_{i,j}| < N\epsilon_1.$$
In particular, $f_{i,j}$ has a non-degenerate local maximum at $\eta_{i,j}$.
If $\sigma_-(i) < \sigma_-(j)$, then $\eta_{i,j}$ is the only critical point of $f_{i,j}$ in $(-1,1)$.
If $\sigma_-(i) > \sigma_-(j)$, then the only critical points of $f_{i,j}$ in $(-1,1)$ are $\eta_{i,j}$ and a non-degenerate local minimum, $\tilde{\eta}_{j,i} \in [-3/4, -1/2]$.

(3) *For $x \in [-1, -1/4]$,*
$$|f_{i,i+1}(x)| < \epsilon_1.$$

(4) *For $|x - (\pm 1)| \le 1/8$,*
$$f_{i,i+1}(x) = (\sigma_\pm(i+1) - \sigma_\pm(i))Q_\pm(x)$$
where
$$Q_\pm(x) := \epsilon_2(x - (\pm 1))^2 + \epsilon_2.$$

(5) *The restriction of $f_{i,i+1}$ to $[-1/4, 1/4]$ is linear with slope*
$$|d_x f_{i,i+1} - 2y_{i,i+1}| < \epsilon_1.$$

(6) *For $x \in [1/3 - \epsilon_1, 1/3 + \epsilon_1]$, $d_x f_{i,i+1}(x) = \epsilon_2$.*

Proof. We construct the f_i by setting $f_n = 0$ and specifying $f_{i,i+1} = f_i - f_{i+1}$ for $1 \le i \le n-1$.

To begin, fix a smooth function $g : [-1, -1/4 - \epsilon_1] \to \mathbb{R}$ with the following properties:

(G1) For $x \in [-1, -7/8]$, $g(x) = Q_-(x)$.
(G2) For all $x \in (-1, -1/4 - \epsilon_1]$, $\quad g'(x) > 0$.
(G3) We have $g(-3/4) = .06\epsilon_1$, $g(-1/2) = .07\epsilon_1$, $g(-3/8) = .08\epsilon_1$, and $g(-1/4 - \epsilon_1) = .09\epsilon_1$.
(G4) For all $x \in [-3/8 - \epsilon_2, -3/8 + \epsilon_2]$, $g'(x) = 1$.

It is possible to construct such a function using Lemma 9.2 since

$$g(-7/8) = \epsilon_2 65/64 < g(-3/4) < g(-1/2) < g(-3/8 - \epsilon_2) < g(-3/8 + \epsilon_2) < g(-1/4 - \epsilon_1).$$

(We use the Lemma to verify that $g'(x) > 0$ is attainable with no upper bound on g' required. Thus, we just need to check that $g(b) - g(a) > 0$ holds on the intervals $[a, b]$ that we extend g over.)

Defining $f_{i,i+1}$ when $\sigma_-(i) < \sigma_-(i+1)$: In all cases where $\sigma_-(i) < \sigma_-(i+1)$, we define $f_{i,i+1}$ in the following steps.

Let $\sigma(i, i+1) := \sigma_-(i+1) - \sigma_-(i)$.

Step 1. Begin by making the partial definition

$$f_{i,i+1}(x) = \begin{cases} \sigma(i,i+1) \cdot g, & x \in [-1, -1/4 - \epsilon_1], \\ .1\epsilon_1 \cdot \sigma(i,i+1) + 2y_{i,i+1}(x + 1/4), & x \in [-1/4, 1/4], \\ y_{i,i+1} + (2/3)\epsilon_1 + h_{i,i+1}(x), & x \in [1/2, 3/4], \\ Q_+(x). & x \in [7/8, 1]. \end{cases} \tag{40}$$

Step 2. On the remaining portions of $[-1,1]$, smoothly interpolate in a manner that produces the conditions

$$\begin{array}{ll} f'_{i,i+1}(x) > 0, & x \in (-1, 1/2]; \\ f'_{i,i+1}(x) < 0, & x \in [3/4, 1); \text{ and} \\ f'_{i,i+1}(x) = \epsilon_2, & x \in [1/3 - \epsilon_1, 1/3 + \epsilon_1]. \end{array} \tag{41}$$

[The first two conditions required in (41) are obtainable since the inequalities already hold on intervals where $f_{i,i+1}$ was defined in (40), and (keeping in mind that $\sigma(i,i+1) \leq 3$)

$$f_{i,i+1}(-1/4-\epsilon_1) = .09\epsilon_1 \cdot \sigma(i,i+1) < f_{i,i+1}(-1/4) = .1\epsilon_1 \cdot \sigma(i,i+1);$$
$$f_{i,i+1}(1/4) = y_{i,i+1} + .1\epsilon_1 \cdot \sigma(i,i+1) < y_{i,i+1} + (2/3)\epsilon_1 = f_{i,i+1}(1/2);$$
$$f_{i,i+1}(3/4) = y_{i,i+1} + (2/3)\epsilon_1 > (65/64)\epsilon_2 = f_{i,i+1}(7/8).$$

The third condition is obtainable since the total change to $f_{i,i+1}$ that it requires on the interval $[1/3-\epsilon_1, 1/3+\epsilon_1]$ is much smaller in magnitude than $f_{i,i+1}(1/2) - f_{i,i+1}(1/4)$ from (38).]

Next, we define $f_{i,i+1}$ in the two special cases where $\sigma_-(i) > \sigma_-(i+1)$.

Defining $f_{k,k+1}$ for a (1Cr) edge: Set

$$f_{k,k+1}(x) = \begin{cases} \sigma(k,k+1)g(x) = (-1)g(x), & x \in [-1,-3/4]; \\ -.05\epsilon_1 + .2\epsilon_1(x+1/4), & x \in [-1/4,1/4]; \\ (5/6)\epsilon_1 + h_{k,k+1}(x), & x \in [1/2,3/4]; \\ Q_+(x), & x \in [7/8,1], \end{cases} \tag{42}$$

then (using Lemma 9.2) complete the definition by smoothly interpolating in a manner that arranges

- $d_x f_{k,k+1}$ has a unique 0 at some $\tilde{\eta}_{k+1,k} \in (-3/4,-1/2)$ and satisfies $d_x f_{k,k+1}(x) \geq -d_x g(x)$ for $x \in (-3/4,-1/2)$;
- $d_x f_{k,k+1} > 0$ on $[-1/2,1/2]$; $\quad d_x f_{k,k+1} < 0$ on $[3/4,7/8]$; and
- $d_x f_{k,k+1} = \epsilon_2$ on $[1/3-\epsilon_1, 1/3+\epsilon_1]$.

[The first condition is obtained by choosing a small interval within $(-3/4,-1/2)$ to interpolate $d_x f_{k,k+1}$ between $-d_x g(x)$ and a small positive constant. We can then arrange that $d_x f_{k,k+1} > 0$ continues to hold up to $x = -1/4$ since the local minimum value will satisfy

$$f_{k,k+1}(\tilde{\eta}_{k+1,k}) < f_{k,k+1}(-3/4) = -g(-3/4) = -.06\epsilon_1 < -.05\epsilon_1 = f_{k,k+1}(-1/4).$$

The 2-nd and 3-rd conditions are obtainable using Lemma 9.2 since

$$f_{k,k+1}(1/4) = .05\epsilon_1 < (5/6)\epsilon_1 = f_{k,k+1}(1/2), \quad f_{k,k+1}(3/4) = (5/6)\epsilon_1 > (65/64)\epsilon_2 = f_{k,k+1}(7/8),$$
$$\text{and} \quad f_{k,k+1}(1/2) - f_{k,k+1}(1/4) > 2\epsilon_1\epsilon_2.]$$

Defining $f_{k+1,k+2}$ for a (2Cr) edge: Set

$$f_{k+1,k+2}(x) = \begin{cases} \sigma(k+1,k+2)g(x) = (-2)g(x), & x \in [-1,-3/4]; \\ -.11\epsilon_1 + 2y_{k+1,k+2}(x+1/4), & x \in [-1/4,1/4]; \\ y_{k+1,k+2} + h_{k+1,k+2}(x), & x \in [1/2,3/4]; \\ Q_+(x), & x \in [7/8,1], \end{cases} \tag{43}$$

then complete the definition by smoothly interpolating in a manner that arranges

- $d_x f_{k+1,k+2}$ and $d_x(g + f_{k+1,k+2})$ both have unique 0's in $(-3/4,-1/2)$ that we denote $\tilde{\eta}_{k+2,k+1}$ and $\tilde{\eta}_{k+2,k}$. In addition, $d_x f_{k+1,k+2}(x) \geq -2d_x g(x)$ for $x \in (-3/4,-1/2)$;
- $d_x f_{k+1,k+2} > 0$ on $[-1/2,1/2]$; $\quad d_x f_{k+1,k+2} < 0$ on $[3/4,7/8]$; and
- $d_x f_{k+1,k+2} = \epsilon_2$ on $[1/3-\epsilon_1, 1/3+\epsilon_1]$.

[The uniqueness of the 0 of $d_x(g + f_{k+1,k+2})$ is arranged by taking the 2-nd derivative of $f_{k+1,k+2}$ to be sufficiently large when we interpolate $d_x f_{k+1,k+2}$ between $-2d_x g$ and a small positive constant in a small subinterval of $(1/2,3/4)$. To see that $d_x f_{k+1,k+2}$ may remain positive in $(\tilde{\eta}_{k+2,k+1}, -1/4]$ and that the 2-nd and 3-rd conditions are obtainable (using Lemma 9.2), note that

$$f_{k+1,k+2}(\tilde{\eta}_{k+2,k+1}) < f_{k+1,k+2}(-3/4) = -2g(-3/4) = -.12\epsilon_1 < -.11\epsilon_1 = f_{k+1,k+2}(-1/4),$$
$$f_{k+1,k+2}(1/4) = -.11\epsilon_1 + y_{k+1,k+2} < y_{k+1,k+2} = f_{k+1,k+2}(1/2),$$
$$f_{k+1,k+2}(3/4) = y_{k+1,k+2} > (65/64)\epsilon_2 = f(7/8),$$
$$\text{and} \quad f_{k+1,k+2}(1/2) - f_{k+1,k+2}(1/4) > 2\epsilon_1\epsilon_2.]$$

With the definition of all $f_{i,i+1}$ complete, we verify properties (1)-(6).

Items (3)-(6): These items all follow from (40), (42), and (43) together with the additional itemized requirements imposed during the interpolation process. Item (3) follows from verifying the inequality at $x = -1$ and $x = -1/4$, and at the critical point $\tilde{\eta}_{i+1,i}$ if it exists. [Keep in mind that in all cases,

$|\sigma(i,i+1)| \leq 3$.] Item (4) follows from (G1). Item (5) is explicit in the definitions of $f_{i,i+1}$. Item (6) was arranged during the interpolation step of the constructions of the $f_{i,i+1}$.

Item (2): For $1 \leq i < j \leq n$,

$$f_{i,j} = \sum_{l=i}^{j-1} f_{l,l+1}. \tag{44}$$

Thus, for $x \in [1/2, 3/4]$,

$$f_{i,j}(x) = \sum_{l=i}^{j-1}(C_l + h_{l,l+1}(x)) = \left(\sum_{l=i}^{j-1} C_l\right) + h_{i,j}(x),$$

where each C_l is a non-negative constant satisfying $|C_l - y_{i,j}| \leq (5/6)\epsilon_1$. [See (40), (42), and (43).] That $d_x f_{i,j}(x) = d_x h_{i,j}(x)$ follows, and using Proposition 9.3 (2), we have

$$|f_{i,j}(x) - y_{i,j}| \leq \sum_{l=i}^{j-1} |C_i - y_{i,i+1}| + |h_{i,j}(x)| < \left(\sum_{l=i}^{j-1}(5/6)\epsilon_1\right) + \epsilon_1/6 \leq N\epsilon_1. \tag{45}$$

Note that $f_{i,j}(x)$ is increasing on $[1/4, 1/2]$, so to verify that the inequality (45) continues to hold on $[1/4, 1/2]$ it is enough to check that $|f_{i,i+1}(x) - y_{i,i+1}| \leq \epsilon_1$ holds at $x = 1/4$. This is explicitly seen from (40), (42), and (43).

Within $[1/2, 3/4]$ the only critical point of $f_{i,j}(x)$ is $\eta_{i,j}$ (from Proposition 9.3 (3)), and in $[-1/2, 1/2]$ (resp. $[3/4, 1)$) we have $d_x f_{i,i+1} > 0$ (resp. $d_x f_{i,i+1} < 0$) for all i, so that $d_x f_{i,j} > 0$ (resp. $d_x f_{i,j} < 0$) follows from (44). Thus, to establish the claim about the critical points of $f_{i,j}$ we are left to consider $x \in (-1, -1/2]$.

Note that when $x \in (-1, -1/2]$, the constructions give

$$d_x f_{i,i+1}(x) \geq \sigma(i, i+1) d_x g(x),$$

so we can estimate

$$d_x f_{i,j}(x) = \sum_{l=i}^{j-1} d_x f_{l,l+1} \geq \sum_{l=i}^{j-1} \sigma(l, l+1) d_x g(x) = (\sigma_-(j) - \sigma_-(i))\, d_x g(x).$$

Thus, when $\sigma_-(i) < \sigma_-(j)$,

$$d_x f_{i,j}(x) > 0, \quad \text{for } x \in (-1, -1/2]$$

follows from (G2), so $\eta_{i,j}$ is the only critical point of $f_{i,j}$ in $(-1, 1)$. In the three cases where $\sigma_-(i) > \sigma_-(j)$, the existence of a unique critical point in $(-1, -1/2)$, denoted $\tilde{\eta}_{j,i}$, follows from the construction. [In the case of a (2Cr) edge with $(i,j) = (k, k+2)$, $f_{k,k+2} = -g(x)$ holds in $(-1, -3/4]$; in $[-3/4, -1/2]$, $f_{k,k+2} = g(x) + f_{k+1,k+2}$, and the existence of a unique 0 of $d_x(g(x) + f_{k+1,k+2})$ in $[-3/4, -1/2]$ was required in the definition of $f_{k+1,k+2}$.]

Item (1): When $\sigma_-(i) < \sigma_-(j)$, $f_{i,j} > 0$ follows since it holds when $x = \pm 1$ (by Item (4)), and the unique critical point of $f_{i,j}$ in $(-1, 1)$ is a local maximum.

The three cases where $\sigma_-(i) > \sigma_-(j)$ are $f_{k,k+1}$ for a (1Cr) edge, and $f_{k,k+2}$ and $f_{k+1,k+2}$ for a (2Cr) edge. All three of these functions are negative at -1 and $-1/4$ with a single local min in $(-1, -1/4)$. [For $f_{k,k+2}$ use Item (4), and compute

$$f_{k,k+2}(-1/4) = .1\epsilon_1 + (-.11\epsilon_1) = -.01\epsilon_1 < 0.]$$

Moreover, all three are positive at $1/4$ and 1 with a single local max in $(1/4, 1)$. We conclude that all three are negative (resp. positive) on $[-1, -1/4]$ (resp. $[1/4, 1]$). Each function has a unique 0 on the interval $[-1/4, 1/4]$ that can be explicitly found using (40), (42), and (43) with the location as specified in the statement.

□

With defining functions now fixed for all (PV), (1Cr), and (2Cr) edge types, we let

$$K = \inf\{d_x f_{i,j}^{(1Cr)}(x)\}.$$

The infimum is taken over all (1Cr) difference functions where we allow for any number of sheets $n \leq N$ and all locations of the crossing sheets k and $k+1$; in addition, we require $i < j$ and $-3/8 \leq x \leq \eta_{i,j} - \epsilon_\eta$

(where ϵ_η was defined in (36)). Note that since the collection of functions involved is finite, compactness gives $K > 0$.

Next, fix $\epsilon_3 > 0$ to satisfy

$$\epsilon_3 < \min\left\{\epsilon_2, \frac{16\epsilon_1}{9N}\cdot\min\{K, 1/5\}\right\}. \tag{46}$$

Proposition 9.5. *For any (Cu) edge type, we can construct functions*

$$f_i : [-1,1] \to \mathbb{R}, \quad 1 \le i \le n,\ i \notin \{k, k+1\}, \quad \text{and} \quad f_k, f_{k+1} : [-3/8, 1] \to \mathbb{R},$$

so that for all $1 \le i < j \le n$ the items (1)-(5) of Proposition 9.4 hold provided that we impose the additional hypothesis that x belongs to the domain of the function under consideration. In place of item (6), we have

(6') *For $x \in [1/3 - \epsilon_1, 1/3 + \epsilon_1]$, $d_x f_{i,i+1} = \epsilon_3$.*

In addition, we have

(7') *The function $f_{k-1,k+2}$ satisfies*

$$\begin{array}{ll} f_{k-1,k+2} = Q_-(x), & \forall\, x \in [-1, -7/8]; \\ d_x f_{k-1,k+2} > 0, & \forall\, x \in (-1, -3/8]; \\ |f_{k-1,k+2}(x)| \le \epsilon_1, & \forall\, x \in [-1, -3/8]. \end{array}$$

(8') *For $x \in [-3/8 - \epsilon_2, -3/8 + \epsilon_2]$ the functions f_i with $i \notin \{k, k+1\}$ are linear with slopes satisfying*

$$\begin{array}{l} d_x f_{i,j}(x) = j - i, \qquad \text{for } \{i,j\} \cap \{k, k+1\} = \emptyset. \\ d_x f_{k-1,k}(-3/8) = d_x f_{k+1,k+2}(-3/8) = 1.5. \end{array}$$

For $x \in [-3/8, -3/8 + \epsilon_2]$,

$$\begin{array}{l} f_k(x) = L(x) + (x + 3/8)^{3/2}, \\ f_{k+1}(x) = L(x) - (x + 3/8)^{3/2}, \end{array}$$

where $L(x)$ is a linear function. In particular, the sheets k and $k+1$ meet in a semicubical cusp point at $x = -3/8$. The function $f_{k,k+1}$ satisfies

$$f_{k,k+1}(x) > 0, \quad x \in (-3/8, 1],$$

and $\eta_{k,k+1}$ is the only critical point of $f_{k,k+1}$ in $(-3/8, 1)$.

Proof. For $i \neq k-1, k, k+1$, we define $f_{i,i+1}$ as in the proof of Proposition 9.4 with the modification that on the interval $[1/3 - \epsilon_1, 1/3 + \epsilon_1]$ we now require that $d_x f_{i,i+1} = \epsilon_3$.

To construct the f_i, we will define $f_{k-1,k}$, $f_{k,k+1}$, and $f_{k+1,k+2}$, which all have domain $[-3/8, +1]$. In addition, we will define $f_{k-1,k+2}$ in $[-1, -3/8 + \epsilon_2]$. Then, we set $f_n = 0$, and

$$f_i := \sum_{l=i}^{n-1} f_{i,i+1} \quad \text{for } k \le i \le n$$

where when $i = k, k+1$ we restrict the domain of all functions in the summation to $[-3/8, 1]$. For $1 \le i \le k-1$, we set

$$f_i(x) := \begin{cases} \displaystyle\sum_{l=k+2}^{n-1} f_{l,l+1}(x) + f_{k-1,k+2}(x) + \sum_{l=k-2}^{i} f_{l,l+1}(x), & x \in [-1, -3/8 + \epsilon_2] \\ \displaystyle\sum_{l=i}^{n-1} f_{l,l+1}(x), & x \in [-3/8, +1], \end{cases} \tag{47}$$

and check that $f_{k-1,k+2} = f_{k-1,k} + f_{k,k+1} + f_{k+1,k+2}$ holds on $[-3/8, -3/8 + \epsilon_2]$ to verify well-definedness.

Define $f_{k-1,k+2}|_{[-1,-3/8+\epsilon_2]}$ to have

$$f_{k-1,k+2}(x) = \begin{cases} Q_-(x), & x \in [-1, -7/8], \\ 3g(x), & x \in [-3/4, -3/8 + \epsilon_2], \end{cases}$$

(where $g(x)$ is from the proof of Proposition 9.4), and to satisfy

$$d_x f_{k-1,k+2}(x) > 0, \quad \text{for } x \in (-1, -3/8 + \epsilon_2].$$

[This is possible since $f_{k-1,k+2}(-7/8) = (65/64)\epsilon_2 < f_{k-1,k+2}(-3/4) = .18\epsilon_1$.]

Next, define $f_{k+1,k+2}$, $f_{k,k+1}$ and $f_{k-1,k}$ on $[-3/8, -3/8+\epsilon_2]$ by

$$f_{k+1,k+2}(x) = .12\epsilon_1 + 1.5(x+3/8) - (x+3/8)^{3/2}, \quad f_{k,k+1}(x) = 2(x+3/8)^{3/2}, \quad \text{and}$$
$$f_{k-1,k}(x) = f_{k-1,k+2}(x) - f_{k,k+1}(x) - f_{k+1,k+2}(x), \qquad \text{for } x \in [-3/8, -3/8+\epsilon_2]. \tag{48}$$

Note that for $x \in [-3/8, -3/8+\epsilon_2]$,

$$\begin{aligned} d_x f_{k+1,k+2}(x) &= 1.5 - (3/2)(x+3/8)^{1/2} \geq 1.5 - (3/2)\epsilon_2^{1/2} > 0, \\ d_x f_{k,k+1}(x) &= 3(x+3/8)^{1/2} > 0, \quad \text{for } x \in (-3/8, -3/8+\epsilon_2], \quad \text{and} \\ d_x f_{k-1,k}(x) &= 3d_x g(x) - d_x f_{k+1,k+2}(x) - d_x f_{k+1,k+2}(x) = 3 - 1.5 - (3/2)(x+3/8)^{1/2} > 0 \end{aligned}$$

where in the last equality we used the property (G4) of $g(x)$. Moreover,

$$f_{k+1,k+2}(-3/8) = .12\epsilon_1, \quad f_{k,k+1}(-3/8) = 0, \quad \text{and} \tag{49}$$
$$f_{k-1,k} = 3g(-3/8) - .12\epsilon_1 = .12\epsilon_1.$$

[We used properties (G2) and (G3) of $g(x)$.] Note that $f_{k-1,k+2} = f_{k-1,k} + f_{k,k+1} + f_{k+1,k+2}$ holds on $[-3/8, -3/8+\epsilon_2]$ as required.

We now complete the definition of $f_{k+1,k+2}$, $f_{k,k+1}$ and $f_{k-1,k}$ by requiring, for $i = k-1, k$, and $k+1$,

$$f_{i,i+1}(x) = \begin{cases} .2\epsilon_1 + 2y_{k-1,k}(x+1/4), & x \in [-1/4, 1/4], \\ y_{k-1,k} + (2/3)\epsilon_1 + h_{i,i+1}, & x \in [1/2, 3/4], \\ Q_+(x), & x \in [7/8, 1]; \end{cases}$$

and by interpolating on the remaining intervals so that

$$d_x f_{i,i+1} > 0 \text{ for } x \in (-3/8, 1/2]; \quad d_x f_{i,i+1} < 0 \text{ for } x \in [3/4, 1); \text{ and}$$
$$d_x f_{i,i+1} = \epsilon_3, \quad \text{for } x \in [1/3 - \epsilon_1, 1/3 + \epsilon_1].$$

[This is possible since we have verified above that $d_x f_{i,i+1} > 0$ at $x = -3/8 + \epsilon_2$, and $f_{i,i+1}(-3/8+\epsilon_2) < .2\epsilon_1$. Moreover, $f_{i,i+1}(1/4) < f_{i,i+1}(1/2)$, $f_{i,i+1}(3/4) > f_{i,i+1}(7/8)$, and $f_{i,i+1}(1/2) - f_{i,i+1}(1/4) > 2\epsilon_1\epsilon_3$ are all easily verified.]

With the definitions complete we verify items (1)-(5) from Proposition 9.4 and (6')-(8').

The properties stated in items (3)-(5) and (6')-(7') and most of the conditions of (8') all follow immediately from the construction. To verify, that in $[-3/8 - \epsilon_2, -3/8 + \epsilon_2]$ the f_i with $i \neq k, k+1$ are linear use induction. By definition, $f_n = 0$; at the inductive step we use that (G4) states that $g(x)$ is linear with slope 1 in $[-3/8 - \epsilon_2, -3/8 + \epsilon_2]$, and observe that $f_{i,i+1} = g(x)$ for $i \geq k+2$ and $i \leq k-2$, and $f_{k-1,k+2} = 3g(x)$ hold in $[-3/8 - \epsilon_2, -3/8 + \epsilon_2]$. That f_k and f_{k+1} have the required form in $[-3/8 - \epsilon_2, -3/8 + \epsilon_2]$ then follows from the definition of $f_{k+1,k+2}$ and $f_{k,k+1}$.

Item (2): Verify as in the proof of Proposition 9.4. Note that when checking $d_x f_{i,j} > 0$ in $(-1, 1/2]$ it is important that this property holds for $f_{k-1,k+2}$ and $f_{i,i+1}$, $i = k-1, k, k+1$ (aside from $d_x f_{k,k+1}(-3/8) = 0$).

Item (1): Follows from from the corresponding statement for $(i,j) = (i, i+1)$ or $(k-1, k+2)$. In all cases, we check positivity (strict except when $(i,j) = (k, k+1)$) at the endpoints of the interval of definition. This follows from items (4) and (7') together with equation (49). Checking endpoints suffices since, in the interior of its interval of definition, each $f_{i,j}$ has only a single critical point that is a local maximum by (2).

□

Corollary 9.6. *For any edge type, and any $1 \leq i < j \leq n$, the following properties hold for all x belonging to the domain of $f_{i,j}$. (The numbering follows Proposition 9.4.)*

(3) *If $x \in [-1, -1/4]$, then*

$$|f_{i,j}(x)| < N\epsilon_1.$$

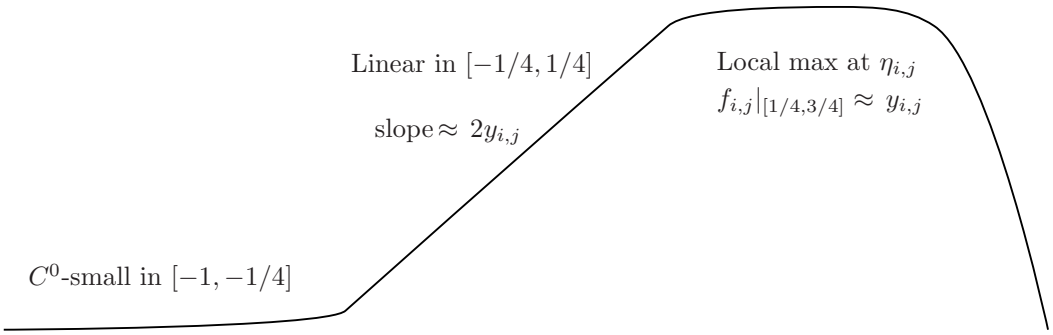

FIGURE 68. The key features of the difference functions $f_{i,j}$.

(4) *If* $|x - (\pm 1)| \leq 1/8$, *then*

$$f_{i,j}(x) = (\sigma_\pm(j) - \sigma_\pm(i))\, Q_\pm(x),$$

and

$$f_i(x) = (n_\pm - \sigma_\pm(j))Q_\pm(x)$$

where $n_\pm$ *is the number of sheets defined above* $x = \pm 1$.

(5) *The restriction of* $f_{i,j}$ *to* $[-1/4, 1/4]$ *is linear with slope*

$$|d_x f_{i,j} - 2y_{i,j}| < N\epsilon_1.$$

(6) *If* $x \in [1/3 - \epsilon_1, 1/3 + \epsilon_1]$, *then*

$$0 < d_x f_{i,j}(x) \leq N\epsilon_2 \qquad (\textit{resp. } 0 < d_x f_{i,j}(x) \leq N\epsilon_3)$$

for (PV), (1Cr), and (2Cr) edge types (resp. for (Cu) edge types).

Proof. For (PV), (1Cr), and (2Cr) edge types, we have $f_{i,j} = \sum_{l=i}^{j-1} f_{l,l+1}$. Thus, (3)-(6) follow from the corresponding properties in Proposition 9.4 using induction and the triangle inequality. For (Cu), $f_{i,j}$ is determined via the $f_{i,i+1}$ and $f_{k-1,k+2}$ as in (47), so to apply induction we use Proposition 9.5 including item (7'). The second equation in (4) follows from the first since $f_n = 0$. □

A summary of the properties of the difference functions $f_{i,j}$ appears in Figure 68.

9.3. **Two-skeleton.** We now turn to constructing functions over $[-1, 1] \times [-1, 1]$ for squares with type (1)-(12) as numbered in Section 3. In this section, when we refer to a Legendrian *square type* we mean a specification of the singular set as one of the squares (1)-(12), together with the number of sheets n with $1 < n \leq N$ and the location of sheets that correspond to the crossing arcs and cusp edges. Fixing a square type specifies edge types for the edges U, R, D, L of $[-1, 1] \times [-1, 1]$ which are respectively $[-1, 1] \times \{1\}, \{1\} \times [-1, 1], [-1, 1] \times \{-1\}$, and $\{-1\} \times [-1, 1]$, and we note that this (ordered) collection of edge types uniquely determines the square type. Denote the 1-dimensional functions associated to each of the edge types as f_i^U, f_i^R, f_i^D, and f_i^L.

In (64), we construct a defining function $F_i : [-1, 1] \times [-1, 1] \to \mathbb{R}$ for each sheet S_i of a given square type, as a sum of interpolations of 1-dimensional functions determined by the location of S_i above each of the four boundary edges. However, due to the presence of cusp edges, some sheets may not exist above all four edges of $[-1, 1] \times [-1, 1]$. In response, we create, in the next Lemma, some 'artificial' 1-dimensional functions $f_{k-.5}^L$ (resp. $f_{k-.5}^D$) for the cases where S_i terminates at a cusp edge above U (resp. above R). They will possess properties similar to those of Proposition 9.4. We focus our notation on the construction of $f_{k-.5}^L$ functions, while the construction of $f_{k-.5}^D$ is carried out in an identical manner.

Label sheets above $[-1, 1] \times [-1, 1]$ as $S_1, \ldots, S_n$ with descending z-coordinate at $(+1, +1)$. For integers i, j let $y_{i,j}^L$ denote $y_{i,j}$ as defined above Proposition 9.4 based on whether edge L is (PV) as in squares (9) or (12), (1Cr) as in square (10) or (Cu) as in square (11). Edge L will never be (2Cr).

Lemma 9.7. *Consider a (9)-(12) square type such that S_k and S_{k+1} meet at a cusp above the U edge. There exists $f^L_{k-.5} \in C^\infty([-1,1])$ such that for all $1 \leq i < k-.5 < j \leq n-2$ the following properties hold (with the hypothesis that x belongs to the domain of the functions in question always imposed).*

(1) *For all $x \in [-1,1]$, $f^L_{i,k-.5}(x) > 0$ and $f^L_{k-.5,j}(x) > 0$, except in the case of a Type (12) square when $j = k$. For the Type (12) square, $f^L_{k-.5,k}$ has a unique non-degenerate 0 in $(-1/4, 0)$.*

(2) *For all $x \in (-1, 1/2]$, $d_x f_{i,k-.5} > 0$ and $d_x f_{k-.5,j} > 0$, except in the case of a Type (12) square when $j = k$. For the Type (12) square, $f^L_{k-..5,k}$ has a unique critical point in $(-1, 1/2]$ that is a local minimum located in $(-3/4, -1/2)$.*
For all $x \in [3/4, 1)$, $d_x f_{i,k-.5} < 0$ and $d_x f_{k-.5,j} < 0$.
For all $x \in [1/4, 3/4]$,
$$|f_{i,k-.5}(x) - C_{i,k-.5}| < N\epsilon_1, \quad \text{and} \quad |f_{k-.5,j}(x) - C_{k-.5,j}| < N\epsilon_1$$
for constants $C_{i,k-.5} \in \{y^L_{i,k-1}, y^L_{i,k}\}$ and $C_{k-.5,j} \in \{y^L_{k-1,j}, y^L_{k,j}\}$.

(3) *For $x \in [-1, -1/4]$,*
$$|f^L_{i,k-.5}(x)| < N\epsilon_1, \quad \text{and} \quad |f^L_{k-.5,j}(x)| < N\epsilon_1.$$

(4) *Let σ_+ and σ_- be associated to the functions f^L_i, so that $\sigma_\pm(i)$ specifies the ordering of the $f^L_i(\pm 1)$ with descending z-coordinate.*[1] *In addition, set $\sigma_+(k-.5) = k-.5$, and $\sigma_-(k-.5) = l-.5$ where along D sheets S_k and S_{k+1} meet at a cusp between the sheets that appear in positions $l-1$ and l above $(-1,-1)$. For $|x - (\pm 1)| \leq 1/16$,*
$$f^L_{k-.5,j}(x) = (\sigma_\pm(j) - \sigma_\pm(k-.5))Q_\pm(x), \quad \text{and} \quad f^L_{i,k-.5}(x) = (\sigma_\pm(k-.5) - \sigma_\pm(i))Q_\pm(x). \tag{50}$$

(5) *$f^L_{i,k-.5}$ and $f_{k-.5,j}$ are linear when restricted to $[-1/4, 1/4]$ with slopes*
$$|df^L_{i,k-.5} - 2C_{i,k-.5}| < N\epsilon_1, \quad \text{and} \quad |df^L_{k-.5,j} - 2C_{k-.5,j}| < N\epsilon_1.$$

Proof. First we construct $f^L_{k-.5}$ for **squares of type (9)-(11)**. Consider the sheets S_{k-1} and S_{k+2} that appear directly above or below the cusping sheets along edge U. For any square of type (9)-(11) it is the case that at least one of S_{k-1} or S_{k+2} does not meet another sheet at a crossing or cusp anywhere above $[-1,1] \times [-1,1]$ which leads to cases:

Case 1. S_{k-1} is disjoint from all other sheets above $[-1,1] \times [-1,1]$. Note that since S_{k-1} is directly above S_k and S_{k+1} above both the U and D edge, we have
$$\sigma_+(k-.5) = k-.5 = \sigma_+(k-1) + .5, \quad \text{and} \quad \sigma_-(k-.5) = \sigma_-(k-1) + .5. \tag{51}$$

Let $f^{PV}_{1,2}$ denote the difference function for the (PV) edge type with 2 sheets. (Actually, taking any $f_{i,i+1}$ of any (PV) edge type would work, but we consider $f^{PV}_{1,2}$ for concreteness.) We seek to define $f^L_{k-.5}$ by requiring that
$$f^L_{k-.5}(-1) = f^L_{k-1}(-1) - .5 f^{PV}_{1,2}(-1), \tag{52}$$
and that
$$d_x f^L_{k-.5} = d_x f^L_{k-1} - \beta d_x f^{PV}_{1,2} \tag{53}$$
where $\beta : [-1,1] \to \mathbb{R}$ is an even function satisfying
$$0 < \delta \leq \beta(x) \leq 1/2; \quad \beta(x) = 1/2, \text{ when } |x - (\pm 1)| \leq 1/16; \quad \text{and} \quad \beta(x) = \delta, \text{ when } x \in [-7/8, 7/8].$$

Case 2: S_{k-1} is not disjoint from all other sheets. Then, S_{k+2} must be disjoint from the others. In this case we define $f^L_{k-.5}$ to satisfy
$$f^L_{k-.5}(-1) = f^L_k(-1) + .5 f^{PV}_{1,2}(-1),$$
and
$$d_x f^L_{k-.5} = d_x f^L_k + \beta d_x f^{PV}_{1,2}. \tag{54}$$

[1]Here, we can take $\sigma_-(l)$ to be undefined if -1 is not in the domain of f^L_i as may occur for an (11) square type.

We show that the required conditions (1)-(5) are satisfied provided that $\delta > 0$ is chosen sufficiently small. We present the proof when $f^L_{k-.5}$ is defined as in Case 1. With obvious modifications, the proof applies equally well in Case 2.[2]

Lemma 9.8. *For all sufficiently small $\delta > 0$,*

$$||f^L_{k-1} - f^L_{k-.5}||_{C^0([-1,1])} < 2\epsilon_2.$$

Proof. Note that the combination of (52) and (53) gives

$$f^L_{k-.5}(x) = f^L_{k-1}(x) - .5f^{PV}_{1,2}(-1) - \int_{-1}^{x} \beta(x) \cdot d_x f^{PV}_{1,2}(x)\, dx.$$

As $-.5f^{PV}_{1,2}(-1) = -.5\epsilon_2$, this allows us to estimate for $x \in [-1, 1]$

$$|f^L_{k-1}(x) - f^L_{k-.5}(x)| \le .5\epsilon_2 + |\int_{-1}^{x} \beta(x) \cdot d_x f^{PV}_{1,2}(x)\, dx| \le .5\epsilon_2 + \int_{-1}^{1} \beta(x)|d_x f^{PV}_{1,2}(x)|\, dx. \tag{55}$$

Now, since $\beta \le 1/2$ is even and $d_x f^{PV}_{1,2}(-x) = -d_x f^{PV}_{1,2}(x)$ for $x \in [-1, -7/8]$, we have

$$\int_{7/8}^{1} \beta(x)|d_x f^{PV}_{1,2}(x)|\, dx = \int_{-1}^{-7/8} \beta(x)|d_x f^{PV}_{1,2}(x)|\, dx \le$$

$$.5\int_{-1}^{-7/8} d_x f^{PV}_{1,2}(x)\, dx = .5[f^{PV}_{1,2}(-7/8) - f^{PV}_{1,2}(-1)] = \epsilon_2/128.$$

Thus, for small enough $\delta > 0$, we have

$$\int_{-1}^{1} \beta(x)|d_x f^{PV}_{1,2}(x)|\, dx < 2(\epsilon_2/128) + \delta \int_{-7/8}^{7/8} |d_x f^{PV}_{1,2}(x)|\, dx < \epsilon_2,$$

In conjunction with (55), this results in

$$|f^L_{k-1} - f^L_{k-.5}(x)| \le .5\epsilon_2 + \epsilon_2 < 2\epsilon_2.$$

□

Item (4): Note that in view of Corollary 9.6 (4), since $f^L_{i,k-.5} = f^L_{i,k-1} + f^L_{k-1,k-.5}$ and $f^L_{k-.5,j} = f^L_{k-1,j} - f^L_{k-1,k-.5}$, it suffices to establish the case of $f^L_{k-1,k-.5}$. We have that for $|x - (\pm 1)| \le 1/16$,

$$d_x f^L_{k-1,k-.5}(x) = .5d_x f^{PV}_{1,2}(x) = .5d_x Q_{\pm}(x) = d_x\left[(\sigma_-(k - .5) - \sigma_-(k-1))Q_{\pm}(x)\right] \tag{56}$$

where we used (51). In addition, we have

$$f^L_{k-1,k-.5}(-1) = .5f^{PV}_{1,2}(-1) = (\sigma_-(k - .5) - \sigma_-(k-1))Q_-(-1),$$

so it follows that (50) holds when $x \in [-1, -15/16]$. At $x = 1$ we have

$$f^L_{k-1,k-.5}(1) = f^L_{k-1,k-.5}(-1) + \int_{-1}^{1} \beta d_x f^{PV}_{1,2}\, dx \tag{57}$$

Note that using Proposition 9.4 (4), we have

$$\int_{-1}^{1} \beta d_x f^{PV}_{1,2}\, dx = \int_{-1}^{-7/8} \beta d_x f^{PV}_{1,2}\, dx + \int_{7/8}^{1} \beta d_x f^{PV}_{1,2}\, dx + \int_{-7/8}^{7/8} \delta d_x f^{PV}_{1,2}\, dx =$$

$$\int_{-1}^{-7/8} \beta(x) \cdot \epsilon_2 2(x+1)\, dx + \int_{7/8}^{1} \beta(x) \cdot \epsilon_2 2(x-1)\, dx + \delta\left(f^{PV}_{1,2}(7/8) - f^{PV}_{1,2}(-7/8)\right) =$$

$$\int_{1}^{7/8} \beta(-x) \cdot \epsilon_2 2(-x+1)\,(-1) dx + \int_{7/8}^{1} \beta(x) \cdot \epsilon_2 2(x-1)\, dx + 0 = 0.$$

[2]The change from $-$ to $+$ that occurs between equations (53) and (54) is to arrange that in Case 1 $d_x f^L_{k-1,k-.5} = \beta d_x f^{PV}_{1,2}$ and in Case 2 $d_x f^L_{k-.5,k} = \beta d_x f^{PV}_{1,2}$ so that these derivatives share their sign with $d_x f^{PV}_{1,2}$. In verifying properties of derivatives for the other $f^L_{i,k-.5}$ and $f^L_{k-.5,j}$, the $\beta d_x f^{PV}_{1,2}$ terms are dominated in absolute value by remaining terms, so that the difference between the $-$ and the $+$ is irrelevant.

(In the last two equalities, we substituted $u = -x$, and used that β is even.) Thus, (57) becomes

$$f^L_{k-1,k-.5}(1) = f^L_{k-1,k-.5}(-1) = .5Q_-(-1) = .5Q_+(-1) = (\sigma_+(k-.5) - \sigma_+(k-1))Q_+(-1)$$

where we used (51). When combined with (56), this shows that item (4) holds for $x \in [15/16, 1]$.

In the remaining items note that for $i < k - .5 < j$, we set $C_{i,k-.5} = y^L_{i,k-1}$ and $C_{k-.5,j} = y^L_{k-1,j}$.

Item (2): For $x \in [1/4, 3/4]$, using Lemma 9.8 and item (2) of Propositions 9.4 and 9.5 we have

$$|f^L_{i,k-.5}(x) - C_{i,k-.5}| \leq |f^L_{k-1,k-.5}(x)| + |f^L_{i,k-1}(x) - y^L_{i,k-1}| < 2\epsilon_2 + (k-1-i)\epsilon_1 < N\epsilon_1,$$

and $|f^L_{k-.5,j}(x) - C_{k-.5,j}| < N\epsilon_1$ holds similarly.

To address the remaining inequalities required in (2), note that

$$d_x f^L_{i,k-.5} = d_x f^L_{i,k-1} + \beta d_x f^{PV}_{1,2}, \quad \text{and} \quad d_x f^L_{k-.5,j} = d_x f^L_{k-1,j} - \beta d_x f^{PV}_{1,2}.$$

When $i = k-1$ the inequalities required of $d_x f^L_{k-1,k-.5} = \beta d_x f^{PV}_{1,2}$ follow from the properties of $d_x f^{PV}_{1,2}$ (as in Proposition 9.4 (2)). Thus, we may assume $i < k-1$. For $0 < |x - (\pm 1)| \leq 1/8$ we use the explicit form (as in Corollary 9.6 (4)) of the $f^L_{i,k-1}$, $f^L_{k-1,j}$, and $f^{PV}_{1,2}(x)$ to verify

$$d_x f^L_{i,k-.5}(x) = [\sigma_\pm(k-1) - \sigma_\pm(i) + \beta(x)]\, d_x Q_\pm(x) \quad \text{and} \tag{58}$$

$$d_x f^L_{k-.5,j}(x) = [\sigma_\pm(j) - \sigma_\pm(k-1) - \beta(x)]\, d_x Q_\pm(x).$$

Since sheet S_{k-1} does not meet any crossing or cusp above the edge L, and $i < k-1 < j$, we have

$$\sigma_\pm(k-1) - \sigma_\pm(i) \geq 1, \quad \text{and} \quad \sigma_\pm(j) - \sigma_\pm(k-1) \geq 1.$$

As $0 < \beta \leq 1/2$, we see from (58) that $d_x f^L_{i,k-.5}(x)$ and $d_x f^L_{k-.5,j}(x)$ have the same sign as $d_x Q_\pm(x)$ as required.

Now for $x \in [-7/8, 1/2] \cup [3/4, 7/8]$, we have

$$d_x f^L_{i,k-.5} = d_x f^L_{i,k-1} + \delta d_x f^{PV}_{1,2}(x), \quad \text{and} \quad d_x f^L_{k-.5,j} = d_x f^L_{k-1,j} - \delta d_x f^{PV}_{1,2}(x).$$

Thus, as long as $\delta > 0$ is small enough so that for all $i < k-1 < j$,

$$\delta\, ||d_x f^{PV}_{1,2}||_{C^0} < \inf_{x \in [-7/8,1/2]\cup[3/4,7/8]} \{\, |d_x f^L_{i,k-1}(x)|\,,\, |d_x f^L_{k-1,j}(x)|\,\},$$

it follows that $d_x f^L_{i,k-.5}$ and $d_x f^L_{k-.5,j}$ have the same sign as $d_x f^L_{i,k-1}$ and $d_x f^L_{k-1,j}$. [The infimum is positive since sheet S_{k-1} does not meet other sheets at crossings or cusps, so that $f^L_{i,k-1}$ and $f^L_{k-1,j}$ have no critical points in $[-7/8, 1/2] \cup [3/4, 7/8]$ by Proposition 9.4 (2).]

Item (3): For $x \in [-1, 1/4]$ we have

$$|f^L_{i,k-.5}(x)| \leq |f^L_{i,k-1}(x)| + ||f^L_{k-1,k-.5}||_{C^0} \leq (k-1-i)\epsilon_1 + 2\epsilon_2 \leq N\epsilon_1.$$

[We used Lemma 9.8 and Proposition 9.4 (3).] A similar argument applies for $f^L_{k-.5,j}$.

Item (5): For $x \in [-1/4, 1/4]$, $d_x f^L_{i,k-.5} = d_x f^L_{i,k-1} + \delta d_x f^{PV}_{1,2}$. Both terms are constant, and we have

$$|d_x f^L_{i,k-.5} - 2C_{i,k-.5}| \leq |d_x f^L_{i,k-1} - 2y^L_{i,k-1}| + \delta |d_x f^{PV}_{1,2}| < (k-1-i)\epsilon_1 + \delta(2+\epsilon_1) \leq N\epsilon_1$$

where the 2nd inequality used Proposition 9.4 (5) and the 3rd requires us to take $\delta < \epsilon_1/4$.

Item (1): To verify $f^L_{i,k-.5} > 0$ and $f^L_{k-.5,j} > 0$, first check that the inequality holds at the endpoints of the domain of definition of these functions. [This follows from item (4) in all cases except when edge L is a (Cu) edge. In this case, we use that from Lemma 9.8 $f^L_{k-.5}(-3/8)$ is within $2\epsilon_2$ from $f^L_{k-1}(-3/8)$ and this is much smaller than the difference in values between the functions that define the cusp sheets and either of the adjacent sheets–in (49) that distance is computed to be $.12\epsilon_1$.] Then, (2) shows that these functions remain positive on $[-1, 1/2]$ and $[3/4, 1]$. In all the cases where $C_{i,k-.5}$ (resp. $C_{k-.5,j}$) is non-zero the C^0 bound from (2) shows that $f^L_{i,k-.5}$ (resp. $f^L_{k-.5,j}$) cannot vanish in $[1/2, 3/4]$ and hence must remain positive there. The only case where this argument does not apply is when $C_{i,k-.5} = C_{k-1,k-.5} = 0$. Then, $d_x f^L_{k-1,k-.5} = \delta d_x f^{PV}_{1,2}$ in $[1/2, 3/4]$ which has a unique critical point in $[1/2, 3/4]$ that is local max, and since $f^L_{k-1,k-.5}$ has already been shown to be positive at $1/2$ and $3/4$ it follows that positivity must hold on $[1/2, 3/4]$ as well.

The Type (12) square:

Recall that during the proof of Proposition 9.4, for the (1Cr) edge types the difference functions for the crossing sheets $f_{k,k+1}$ were constructed in a manner that is independent of n and k on $[-1,1/4]$. Denote the restriction of these difference functions to $[-1,1/4]$ by $f^{(1Cr)}$. Recall that $f^{(1Cr)}$ has a unique critical point in $(-1,1/4)$ that is a local minimum located at some $\tilde{\eta}\in(-3/4,-1/2)$.

Choose α with $\tilde{\eta}<\alpha<-1/2$ and to be close enough to $\tilde{\eta}$ so that

$$.5f^{(1Cr)}(\alpha)<.5f^{(1Cr)}(-3/4)=-.03\epsilon_1 \tag{59}$$

and

$$0<.5d_xf^{(1Cr)}(x)<d_xf^L_{k-1,k}(x),\quad \text{for } x\in(\tilde{\eta},\alpha]. \tag{60}$$

Note also that since $-g(x)\leq f^{(1Cr)}$ holds in $[-1,-1/2]$ with g increasing (here g is the function fixed in the proof of Proposition 9.4, specifically (G1)-(G4)), we have the lower bound

$$-.035\epsilon_1=-.5g(-1/2)<-.5g(\alpha)\leq .5f^{(1Cr)}(\alpha). \tag{61}$$

Recall h_i defined in Proposition 9.3. Define

$$f^L_{k-.5,k}(x)=\begin{cases}.5f^{(1Cr)}(x), & x\in[-1,\alpha],\\ -.02\epsilon_1+\epsilon_1(x+1/4), & x\in[-1/4,1/4],\\ .5\epsilon_1+.5h_{k-1,k}, & x\in[1/2,3/4],\\ .5Q_+(x), & x\in[7/8,1],\end{cases}$$

and then extend $f^L_{k-.5,k}$ to satisfy

$$\begin{aligned}&0<d_xf^L_{k-.5,k}(x)<d_xf^L_{k-1,k}(x), && x\in(\tilde{\eta},1/2],\\ &d_xf^L_{k-1,k}(x)<d_xf^L_{k-.5,k}(x)<0, && x\in[3/4,1).\end{aligned} \tag{62}$$

To verify that such an extension is possible using Lemma 9.2, note that the L edge is (PV), so $f^L_{k-1,k}$ is defined as in (40). Explicit comparison of $d_xf_{k-.5,k}$ with $d_xf_{k-1,k}$ in $[-1/4,1/4]$ and $[7/8,1]$ together with the inequality (60) in $(-\tilde{\eta},\alpha]$, show that the inequalities already hold in these regions. Thus, existence of such an extension follows from a check of the inequalities

$$\begin{aligned}&0<f^L_{k-.5,k}(-1/4)-f^L_{k-.5,k}(\alpha)<f^L_{k-1,k}(-1/4)-f^L_{k-1,k}(\alpha),\\ &0<f^L_{k-.5,k}(1/2)-f^L_{k-.5,k}(1/4)<f^L_{k-1,k}(1/2)-f^L_{k-1,k}(1/4),\\ &f^L_{k-1,k}(7/8)-f^L_{k-1,k}(3/4)<f^L_{k-.5,k}(7/8)-f^L_{k-.5,k}(3/4)<0,\end{aligned}$$

by consulting the following table of values obtained from (59) and (61) and the definitions of $f^L_{k-1,k}$ and $f^L_{k-.5,k}$.

x	$f^L_{k-.5,k}(x)$	$f^L_{k-1,k}$
α	$-.035\epsilon_1<f^L_{k-.5,k}(\alpha)<-.03\epsilon_1$	$.06\epsilon_1<f^L_{k-1,k}(\alpha)<.07\epsilon_1$
$-1/4$	$-.02\epsilon_1$	$.1\epsilon_1$
$1/4$	$.48\epsilon_1$	$1+.1\epsilon_1$
$1/2$	$.5\epsilon_1$	$1+(2/3)\epsilon_1$
$3/4$	$.5\epsilon_1$	$1+(2/3)\epsilon_1$
$7/8$	$.5(65/64)\epsilon_2$	$(65/64)\epsilon_2$

With $f^L_{k-.5,k}$ defined we set $f^L_{k-.5}=f^L_{k-.5,k}+f^L_k$.

To conclude the proof we check items (1)-(5), taking $C_{i,k-.5}=y_{i,k}$ and $C_{k-.5,j}=y_{k,j}$.

Item (2): In $[1/4,3/4]$, $f^L_{k-.5}(x)$ is within $.5\epsilon_1+.5||h_{k,k+1}||_{C^0([1/2,3/4])}<\epsilon_1$ of f^L_k (see Proposition 9.3 (2)), and it easily follows that $|f^L_{i,k-.5}(x)-C_{i,k-.5}|$ and $|f^L_{k-.5,j}(x)-C_{k-.5,j}|$ satisfy the required bound.

The inequalities (62), imply

$$d_xf^L_{k-.5,k}>0, d_xf^L_{k-1,k-.5}>0\quad\text{on } (\tilde{\eta},1/2],\text{ and }\quad d_xf^L_{k-.5,k}<0, d_xf^L_{k-1,k-.5}<0\quad\text{on } [3/4,1),$$

and it follows (using Proposition 9.4 (2)) that for any $i\leq k-1$ and $k\leq j$, the required inequalites hold for $d_xf^L_{i,k-.5}=d_xf^L_{i,k-1}+d_xf^L_{k-1,k-.5}$ and $d_xf^L_{k-.5,j}=d_xf^L_{k,j}+d_xf^L_{k-.5,k}$ on these intervals. Finally

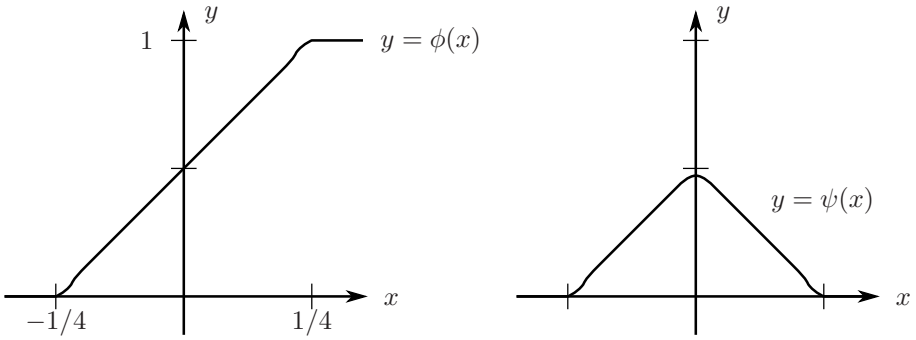

FIGURE 69. Schematic graphs of ϕ and ψ (defined in Section 10.2). The smoothings at $-1/4$ and $1/4$ are actually carried out in the very small intervals $[-1/4, -1/4+\epsilon_1]$ and $[1/4-\epsilon_1, 1/4]$.

(using properties of $f^{(1Cr)}$), the unique critical point for $f^L_{k-.5,k}$ in $(-1, 1/2]$ is the local minimum $\tilde{\eta}$, and for $x \in (-1, \tilde{\eta}]$ we can estimate

$$d_x f^L_{k-.5,k+1}(x) = d_x f^L_{k-.5,k}(x) + d_x f^L_{k,k+1}(x) \geq -.5 d_x g(x) + d_x g(x) > 0,$$

and (using that $d_x f^L_{k-.5,k}$ is non-positive in $(-1, \tilde{\eta})$)

$$d_x f^L_{k-1,k-.5}(x) = d_x f^L_{k-1,k}(x) - d_x f^L_{k-.5,k}(x) > 0.$$

It follows that $d_x f^L_{i,k-.5}(x) > 0$ and $d_x f^L_{k-.5,j}$ holds in $(-1, 1/2]$ for any $i \leq k-1$, $k+1 \leq j$.

Item (1): The unique non-degenerate 0 of $f^L_{k-.5,k}$ in $(-1/4, 0)$ is clear from the construction. Positivity of remaining $f^L_{i,k-.5}$ and $f^L_{k-.5,j}$ follows as usual from item (2) and from checking positivity at endpoints.

Item (3): Follows, since $|f^L_{k-.5,k}(x)| < \epsilon_1$ in $[-1, -1/4]$.

Item (4): Above the edge U (resp. D) the cusping sheets S_k and S_{k+1} are directly above (resp. below) S_{k+2}. Therefore, we have

$$\sigma_+(k-.5) = k-.5, \quad \text{and} \quad \sigma_-(k-.5) = k+.5.$$

For $|x-(-1)| < 1/8$, we have

$$f^L_{k-.5,k}(x) = .5 f^{(1Cr)}(x) = -.5 Q_-(x),$$

and for $|x-1| < 1/8$ we have $f^L_{k-.5,k}(x) = .5 Q_+(x)$. Thus, the result follows.

Item (5): Note that $f^L_{k-.5,k}$ is linear with slope ϵ_1 in $[-1/4, 1/4]$. Since $C_{i,k-.5} = y_{i,k}$ and $C_{k-.5,j} = y_{k,j}$, the result follows easily.

□

Given any (1)-(12) square type, recall we impose the global labeling of sheets over the square $[-1,1]_{x_1} \times [-1,1]_{x_2}$ consistent with the labeling of sheets over the top right corner $\{+1\} \times \{+1\}$, and use $f^U_i, f^R_i, f^D_i, f^L_i$ for functions associated to the edge types along the boundary.

Let $\sigma_L(i)$ denote the ordering of S_i as it appears over the up left corner $\{-1\} \times \{+1\}$, and $\sigma_D(i)$ denotes its ordering as it appears over the down right corner $\{+1\} \times \{-1\}$. If sheets S_k and S_{k+1} meet at a cusp edge above U (resp. R) then we set $\sigma_L(k) = \sigma_L(k+1) = k-.5$ (resp. $\sigma_D(k) = \sigma_D(k+1) = k-.5$).

Let $\phi : [-1,1] \to [0,1]$ be a smooth non-decreasing function such that:

$$\begin{gathered} \text{for } -1/4+\epsilon_1 < x < 1/4-\epsilon_1, \ \ \phi(x) = 2(x+1/4); \\ \text{for } -1/4 < x < 1/4, \ \ 0 < d_x\phi(x) < 2+\epsilon_2; \\ \phi^{-1}(0) = [-1, -1/4]; \ \ \phi^{-1}(1) = [1/4, 1]; \\ \text{for } 1/4-\epsilon_1 \leq x \leq 1/4, \ \ \phi(x) \geq 2(x+1/4); \\ \text{and } \phi(x) - 1/2 \text{ is an odd function.} \end{gathered} \tag{63}$$

See Figure 69. Define

$$\begin{aligned} F_i(x_1,x_2) &= \phi(x_2)f_i^U(x_1) + (1-\phi(x_2))f^D_{\sigma_D(i)}(x_1) \\ &+ \phi(x_1)f_i^R(x_2) + (1-\phi(x_1))f^L_{\sigma_L(i)}(x_2). \end{aligned}$$

$$\begin{aligned} F_{i,j} = F_i - F_j &= \phi(x_2)f_{i,j}^U(x_1) + (1-\phi(x_2))f^D_{\sigma_D(i),\sigma_D(j)}(x_1) \\ &+ \phi(x_1)f_{i,j}^R(x_2) + (1-\phi(x_1))f^L_{\sigma_L(i),\sigma_L(j)}(x_2). \end{aligned} \tag{64}$$

10. Proof of Theorem 5.1 Part 2: Construction of squares with swallowtails

For the construction of the (13) and (14) square types, we fix concentric, closed disks O_1 and O_2 centered at $(-3/8, 0)$ with radii $R_1 = 1/16$ and $R_2 = 3/32$. The construction then has a different character within each of the 3 regions O_1, $O_2 \setminus O_1$, and $[-1,1]^2 \setminus O_2$. Within O_1 a suitably scaled and shifted version of a standard coordinate model for the swallowtail is used; see Section 10.1 below. Outside of the disk O_2 defining functions of a similar nature to those of squares (1)-(12) are employed; see Section 10.2. Section 10.3 combines the models in a single formula that carries out an interpolation in the annulus between O_1 and O_2.

As in Section 7 we consider only the case of a Type (13) (upward) swallowtail in detail. A similar construction applies for the (14) square types that contain downward swallotail points.

We maintain Convention 7.1, and label the sheets of a (13) square type as $S_1, \dots, S_n, \widetilde{S}_k$ where the sheets $S_k, S_{k+1}, S_{k+2}, \widetilde{S}_k$ all correspond to portions of the sheets that meet at the swallowtail point. At $(+1,+1)$, sheet S_k is the top sheet of the swallow tail, and sheets S_{k+1} and S_{k+2} cross to the right of the swallow tail point; $\widetilde{S}_k$ lies above the closed subset of $[-1,1]\times[-1,1]$ that sits to the left of the cusp locus.

10.1. **Coordinate model near a swallowtail point.** We begin by giving an explicit coordinate description of the front projection of a Legendrian containing a single swallowtail point. Although only sheets involved with the swallowtail point are present in this model, we will still refer to them as sheets S_k, S_{k+1}, S_{k+2}, and $\widetilde{S}_k$ since we will later integrate this coordinate model with the remaining sheets of a Type (13) square.

The following description of the swallowtail is taken from[3][1, p.47]. Consider the function

$$F : \mathbb{R}^2 \times \mathbb{R} \to \mathbb{R}, \quad F(x_1, x_2; e) = e^4 - x_1 e^2 + x_2 e$$

which we view as a 2-parameter family of functions on $\mathbb{R}$ denoted $f_{x_1,x_2}(e) = F(x_1, x_2; e)$. The front projection of a Legendrian $L_{st} \subset J^1(\mathbb{R}^2)$ with a single swallowtail point at $(0,0)$ is given by

$$\pi_{xz}(L_{st}) = \{(x_1, x_2, f_{x_1,x_2}(e)) \mid f'_{x_1,x_2}(e) = 0\},$$

i.e. it is the collection of critical values of the map $\mathbb{R}^3 \to \mathbb{R}^3$ given by $(x_1, x_2, e) \mapsto (x_1, x_2, f_{x_1,x_2}(e))$.

Remark 10.1. The function F is called a generating family for the Legendrian L_{st}. The y_1 and y_2-coordinates of L_{st} are given by $y_i = \partial F/\partial x_i(x_1, x_2; e)$.

The number of sheets of L_{st} above a point (x_1, x_2) is determined by the number of real roots of

$$f'_{x_1,x_2}(e) = 4e^3 - 2x_1 e + x_2.$$

The projection of L_{st} to the base $\mathbb{R}^2$ is 3 sheeted where f'_{x_1,x_2} has 3 distinct real roots, and 1-to-1 where f'_{x_1,x_2} has a real root and 2 distinct complex conjugate roots. Cusp edge points (x_1, x_2) correspond to those points $(x_1, x_2, f_{x_1,x_2}(e))$ where e is a multiplicity 2 root of f'_{x_1,x_2}. The swallowtail point itself is the unique value of (x_1, x_2) where f'_{x_1,x_2} has a root of multiplicity 3.

Proposition 10.2. *Let S denote the closure of the portion of $\pi_{xz}(L_{st})$ that projects in a 3-to-1 manner to the x_1x_2-plane. The formulas*

$$\begin{aligned} x_1 &= 2[r^2 + s^2 + rs] \\ x_2 &= 4rs[r+s] \\ z &= -r^4 + 2r^3 s + 2r^2 s^2 \end{aligned} \tag{65}$$

[3]We have replaced x_1 in the reference with $-x_1$ here so that the swallow tail opens to the right rather than to the left.

parametrize S in a manner that is 2-to-1 except along ∂S where the mapping is 1-to-1, provided that we view S as the subset $\pi_{xz}^{-1}(S) \subset L_{st}$. The inverse image of the cusp edge is

$$\{s = r\} \cup \{s = -2r\};$$

the inverse image of ∂S is

$$\{s = -\frac{1}{2}r\}$$

with the swallow tail point itself at $(r, s) = (0, 0)$.

In a neighborhood of a point not belonging to the cusp edge, S is given by the graph of a locally defined function $z = z(x_1, x_2)$. The Euclidean gradients $\nabla z = (\partial_{x_1} z, \partial_{x_2} z)$ are given by

$$\nabla z(r, s) = \frac{J(r, s)}{J(r, s)}(-r^2, r) \tag{66}$$

where $J(r, s) = 8(r - s)(2r + s)(r + 2s)$.

Proof. As discussed in the previous paragraph, S is the subset of L_{st} for which f'_{x_1,x_2} has 3 real roots (with possible repetitions). For such values of (x_1, x_2), we can write

$$f'_{x_1,x_2}(e) = 4e^3 - 2x_1 e + x_2 e = 4(e - r_1)(e - r_2)(e - r_3). \tag{67}$$

Putting $r_1 = r$ and $r_2 = s$, the vanishing of the quadratic term in f'_{x_1,x_2} forces $r_3 = -r - s$. Making these substitutions and expanding the right hand side gives

$$4e^3 - 2x_1 e + x_2 e = 4e^3 - 4[r^2 + s^2 + rs]e + 4[rs(r + s)].$$

Equating coefficients, and setting $z = f_{x_1,x_2}(r)$ gives the parametrization (65).

Next we check that the parametrization is 2-to-1 except along ∂S. Note that replacing r and s with any 2 of the 3 roots, $r, s, -r - s$, of f'_{x_1,x_2} will lead to the same product in (67). Thus, substituting any of

$$(r, s), (r, -r - s), (s, r), (s, -r - s), (-r - s, r), (-r - s, s) \tag{68}$$

for (r, s) in the parametrization leads to a point on the swallowtail with the same x_1 and x_2 coordinates as $(x_1, x_2, z)(r, s)$. [Moreover, only these substitutions have this property, since a polynomial with leading coefficient 4 is uniquely determined by its roots.] By construction, we will have

$$z(r, s) = z(r, -r - s); \quad z(s, r) = z(s, -r - s); \quad z(-r - s, r) = z(-r - s, s), \tag{69}$$

and assuming the three roots of f'_{x_1,x_2} are distinct and take distinct values when f_{x_1,x_2} is applied, these 3-values will all be distinct. This shows that for values of x_1, x_2 in the complement of the cusp and crossing locus each of the 3 sheets above (x_1, x_2) has 2 preimages in the (r, s)-plane.

Next, note that f'_{x_1,x_2} has a multiplicity 2 root when $r = s$, $r = -r - s$, or $s = -r - s$. As claimed, the first two lines both parametrize the cusp edge (since r is the multiplicity 2 root). The third line parametrizes ∂S (since r is the other root), and the equality of s and $-r - s$ gives a 1-to-1 parametrization of ∂S.

To compute $\nabla z = (\partial_{x_1} z, \partial_{x_2} z)$, we use the inverse function theorem. The differential of $(r, s) \mapsto (x_1, x_2)$ is given in matrix form by

$$\begin{bmatrix} \frac{\partial x_1}{\partial r} & \frac{\partial x_1}{\partial s} \\ \frac{\partial x_2}{\partial r} & \frac{\partial x_2}{\partial s} \end{bmatrix} = \begin{bmatrix} 2s + 4r & 2r + 4s \\ 8rs + 4s^2 & 8rs + 4r^2 \end{bmatrix}.$$

When the determinant $J(r, s) = 8(r - s)(2r + s)(r + 2s)$ is non-zero, we can locally write $(r, s) = (r(x_1, x_2), s(x_1, x_2))$ and compute

$$\begin{bmatrix} \frac{\partial r}{\partial x_1} & \frac{\partial r}{\partial x_2} \\ \frac{\partial s}{\partial x_1} & \frac{\partial s}{\partial x_2} \end{bmatrix} = \frac{1}{J} \begin{bmatrix} 8rs + 4r^2 & -[2r + 4s] \\ -[8rs + 4s^2] & 2s + 4r \end{bmatrix}.$$

Finally, the chain rule gives

$$\partial_{x_1} z = \frac{\partial z}{\partial r}\frac{\partial r}{\partial x_1} + \frac{\partial z}{\partial s}\frac{\partial s}{\partial x_1} = \frac{J}{J} \cdot (-r^2),$$

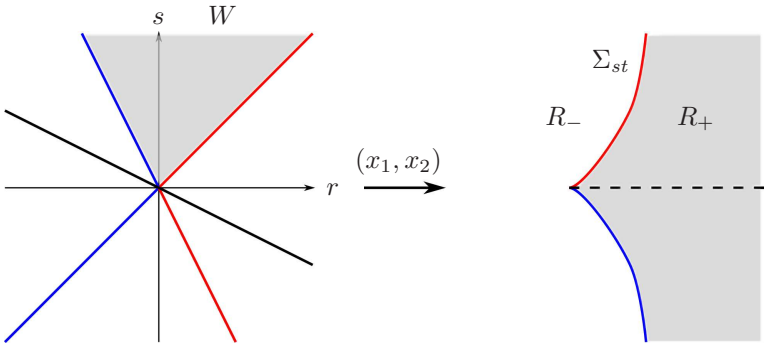

FIGURE 70. The parametrization (1) with the base projection of S pictured (schematically). The pictured lines, $\{r = s\}, \{2r + s = 0\}$, and $\{r + 2s = 0\}$ each project to the cusp locus Σ_{st} in the (x_1, x_2)-plane. The first two lines parametrize the cusp edge in S with the direction of parametrization indicated by coloring. The 3 lines divide the rs-plane into 6 wedges with the wedge W shaded. Any of these (closed) wedges homeomorphically parametrizes the base projection of S which is the shaded region R_+ in the x_1x_2-plane.

$$\partial_{x_2} z = \frac{\partial z}{\partial r}\frac{\partial r}{\partial x_2} + \frac{\partial z}{\partial s}\frac{\partial s}{\partial x_2} = \frac{J}{J} \cdot (r).$$

□

Note that it follows from Proposition 10.2 that the projection of the cusp edge to the (x_1, x_2) plane is the subset

$$\Sigma_{st} = \{(6r^2, 8r^3) \,|\, r \in \mathbb{R}\} = \{(x_1, x_2) \,|\, x_1 = \frac{3}{2}(x_2)^{\frac{2}{3}}\}. \tag{70}$$

Let

$$R_+ = \{(x_1, x_2) \,|\, x_1 \geq \frac{3}{2}(x_2)^{\frac{2}{3}}\} \quad \text{and} \quad R_- = \{(x_1, x_2) \,|\, x_1 \leq \frac{3}{2}(x_2)^{\frac{2}{3}}\}$$

denote the closed regions to the right and left of Σ_{st}. Figure 70 illustrates some features of the parametrization (65).

Lemma 10.3. *The crossing locus of L_{st} (in the base projection) is the ray consisting of the positive x_1-axis. The two arcs in L_{st} that cross one another in the front projection are the image of $\{s = 0\} \cup \{s + r = 0\}$ under the parametrization (65).*

Proof. The wedge $W = \{s \geq -2r\} \cap \{s \geq r\}$ homeomorphically parametrizes the base projection $\pi_x(S)$ (using $x_1 = x_1(r, s)$ and $x_2 = x_2(r, s)$ from (65)). Indeed, those points (u, v) such that $(x_1, x_2)(u, v) = (x_1, x_2)(r, s)$ were listed in (68), and for any (r, s) the list provides exactly one point in W. In fancier language, W is a fundamental domain for the action of the group of invariants of (x_1, x_2) on $\mathbb{R}^2$.

Following the discussion surrounding (69), the 3 sheets, S_k, S_{k+1}, and S_{k+2} above R_+ are homeomorphically parametrized by

$$W \xrightarrow{\cong} S_l, \quad (r, s) \mapsto (x_1(r, s), x_2(r, s), z_l(r, s)),$$

for $l = k, k + 1, k + 2$ where

$$z_k(r, s) = z(r, s), \quad z_{k+1}(r, s) = z(s, r), \quad z_{k+2}(r, s) = z(-r - s, s)$$

with $z(r, s)$ as in (65).

A computation shows

$$\begin{aligned} z_k - z_{k+1} &= (s + r)(s - r)^3; \\ z_k - z_{k+2} &= s(2r + s)^3; \\ z_{k+1} - z_{k+2} &= r(r + 2s)^3. \end{aligned}$$

It follows that for any $(r, s) \in W$, and hence any $(x_1, x_2) \in R_+$, $z_k(r, s) \geq z_{k+1}(r, s)$ (resp. $z_k(r, s) \geq z_{k+2}(r, s)$) with equality only when $s = r$ (resp. $s = -2r$) which is the upper (resp. lower) half of the cusp edge of L_{st}. In addition,

$$\operatorname{sgn}(z_{k+1} - z_{k+2}) = \operatorname{sgn}(r) = \operatorname{sgn}(x_2), \tag{71}$$

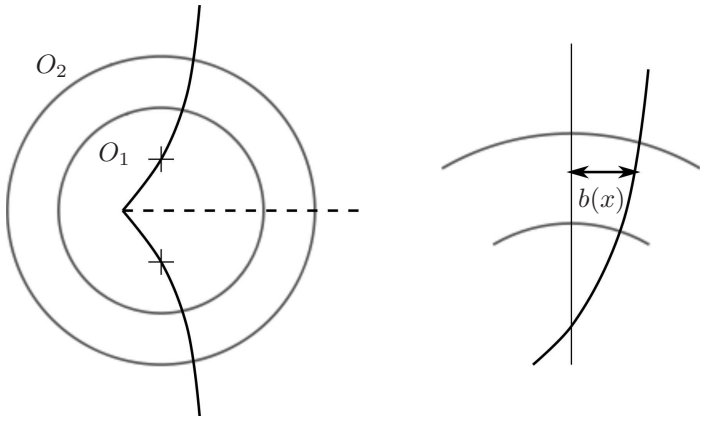

FIGURE 71. (left) The placement of the cusp and crossing locus within O_1 after applying S. The marked points are $(-3/8, \pm 1/32)$. (right) The function $b(x)$ when $x \in [1/16, +\infty)$.

so as claimed the crossing locus of L_{st} is $\{x_2 = 0\} \cap R_+$. For the statement about the preimage of the crossing sheets, note that $0 = x_2 = 4rs[r+s]$ only when $r = 0$, $s = 0$, or $r + s = 0$. The line $r = 0$ parametrizes a portion of S_k while the other two lines parametrize the crossing arc. □

10.1.1. *Local defining functions.* Let a_k, a_{k+1}, a_{k+2} denote defining functions with domain R_+ whose graphs are the 3 swallowtail sheets, S_k, S_{k+1}, and S_{k+2}, above R_+ so that $a_k(x_1, x_2) \geq a_{k+1}(x_1, x_2) \geq a_{k+2}(x_1, x_2)$ when $x_2 > 0$ and $a_k(x_1, x_2) \geq a_{k+2}(x_1, x_2) \geq a_{k+1}(x_1, x_2)$ when $x_2 < 0$. In addition, let b_k denote the defining function in R_- for $\widetilde{S}_k$. Note that along $\Sigma_{st} \cap \{x_2 \geq 0\}$ (resp. $\Sigma_{st} \cap \{x_2 \leq 0\}$) $a_k = a_{k+1}$ and $b_k = a_{k+2}$ (resp. $a_k = a_{k+2}$ and $b_k = a_{k+1}$).

As a corollary of Proposition 10.2, we can compute the gradients of local difference functions,

$$\nabla a_{i,j} = \nabla(a_i - a_j), \quad \text{for } i, j \in \{k, k+1, k+2\}.$$

Recall that, using the first two coordinates from (65), the wedge $W = \{s \geq -2r\} \cap \{s \geq r\}$ homeomorphically parametrizes R_+ in an orientation reversing manner.

Corollary 10.4. *For $(r, s) \in W$, we have*

$$\nabla a_{k,k+1}(x_1(r,s), x_2(r,s)) = (s - r)(s + r, -1) \tag{72}$$

$$\nabla a_{k,k+2}(x_1(r,s), x_2(r,s)) = (2r + s)(s, 1) \tag{73}$$

$$\nabla a_{k+1,k+2}(x_1(r,s), x_2(r,s)) = (r + 2s)(r, 1). \tag{74}$$

Proof. As in the proof of Lemma 10.3, we see that for $(r, s) \in W$, the S_k, S_{k+1}, and S_{k+2} sheets of L_{st} above $(x_1(r, s), x_2(r, s))$ are respectively the images of (r, s), (s, r), and $(-r - s, s)$. [That (s, r) and $(-r - s, s)$ corresponds to the S_{k+1} and S_{k+2} sheets respectively, as ordered when $x_2 > 0$, follows from (71).] The formulas then follow from (66). □

10.1.2. *Straightening the cusp edge.* In this subsection, we make two changes to the model L_{st}. Specifically, we place the swallowtail within O_1 and straighten the cusp locus in $O_2 \setminus O_1$ according to the following specifications.

Consider a diffeomorphism of the plane $S : \mathbb{R}^2 \to \mathbb{R}^2$ of the form $S(x_1, x_2) = (Mx_1 + X, Mx_2)$, i.e. the composition of a dialation and a horizontal translation. We can (and do) choose the constants X and M so that after applying the contactomorphism of $J^1(\mathbb{R}^2)$ induced by S to L_{st}

- (P1) The swallowtail point is on the x_1-axis within O_1 and left of the center of O_1, $(-3/8, 0)$.
- (P2) The cusp locus intersects the points $(-3/8, \pm 1/32)$, and is contained in the strip where $-3/8 - \epsilon_2 \leq x_1 \leq -3/8 + \epsilon_2$ when $|x_2| \leq 1/16$.
- (P3) When $|x_2| \geq 1/32$, the slope of the cusp locus is bounded below in magnitude by $9(2N + 1.1)$.
- (P4) We have $M > (2(2N + 1)480)^3$.

These conditions are obtainable by choosing M suitably large since the slopes of the two halves of the cusp locus, Σ_{st}, go to $+\infty$ and $-\infty$ as $x_1 \to +\infty$. See Figure 71.

Next, we apply a further diffeomorphism $T : \mathbb{R}^2 \to \mathbb{R}^2$ to L'_{st} to straighten the cusp locus within $O_2 \setminus O_1$. For the purpose of defining T, choose a function $b : [0, +\infty) \to \mathbb{R}$ satisfying

- $0 \leq b(x)$ with $b(x) = 0$ for $x \in [0, 1/32]$;
- $b(x) \leq c(x) - (-3/8)$ for $x \in [1/32, +\infty)$ with equality when $x \geq 1/16$ where $c(x)$ is the x_1 coordinate of the cusp locus of L'_{st} when $x = x_2$;
- b is non-decreasing; and
- $b'(x) < 1/(3 \times (2N + 1.1))$.

Lemma 10.5. *Such a function b exists.*

Proof. Let $\beta : [0, +\infty) \to \mathbb{R}$ be a smooth cutoff function with $\beta(x) = 0$ for $x \in [0, 1/32]$; $\beta(x) = 1$ for $x \in [1/16, +\infty)$; and $0 \leq \beta'(x) \leq 33$ for all x. Set $b(x) = \beta(x)(c(x) + 3/8)$. To verify the third and fourth items, compute

$$\begin{aligned} 0 \leq b'(x) = \quad & \beta'(x)(c(x) + 3/8) + \beta(x)c'(x) \leq \\ & 33(1/32)(1/(9[2N + 1.1])) + 1(1/(9[2N + 1.1])) < 1/(3 \times (2N + 1.1)). \end{aligned}$$

For the 1st inequality, note that for $x > 0$, $c(x)$ is increasing, and $(c(x) + 3/8) \geq 0$ when $x \geq 1/32$ by (P2). For the 2nd inequality, use (P2) and (P3) to estimate $(c(x) + 3/8)$ when $1/32 \leq x \leq 1/16$ and (P3) for $c'(x)$ when $1/32 \leq x$. □

Now, define $T(x_1, x_2) = (x_1 + b(|x_2|), x_2)$. Let $L''_{st} \subset J^1(\mathbb{R}^2)$ denote the Legendrian obtained from L'_{st} by applying the contactomorphism induced by T. We denote the local defining functions for the front projection of L''_{st} as A_k, A_{k+1}, A_{k+2}, and B. They are related to the local defining functions of L_{st} via

$$A_i = a_i \circ S \circ T, \text{ for } i = k, k+1, k+2, \quad \text{and} \quad B = b \circ S \circ T. \tag{75}$$

The respective domains of the A_i and B are $T^{-1}(S^{-1}(R_+))$ and $T^{-1}(S^{-1}(R_-))$. The cusp locus of L''_{st} is

$$\Sigma = T^{-1}(S^{-1}(\Sigma_{st})). \tag{76}$$

10.1.3. *Properties of model.* We record and establish several properties of L''_{st} for later use. For $i, j \in \{k, k+1, k+2\}$, denote difference functions by $A_{i,j} = A_i - A_j$.

Lemma 10.6. *The following properties of L''_{st} hold.*

A1 *Within O_2, the cusp locus is contained in $\{-3/8 - \epsilon_2 \leq x_1 \leq -3/8 + \epsilon_2\}$, and in $O_2 \setminus O_1$ it agrees with the vertical line segment $x_1 = -3/8$. Furthermore, when $1/32 \leq |x_2| \leq 1/16$ the absolute value of the slope of the cusp locus is bounded below by $2N + 1.1$.*

A2 *The crossing locus is the horizontal ray extending to the right from the swallowtail point.*

A3 *For all $(x_1, x_2) \in T^{-1}(S^{-1}(R_+))$,*

$$\partial_{x_1} A_{k,k+1}(x_1, x_2) \geq 0; \quad \partial_{x_1} A_{k,k+2}(x_1, x_2) \geq 0; \quad \text{and } sgn(\partial_{x_1} A_{k+1,k+2}(x_1, x_2)) = sgn(x_2).$$

Moreover, in the first (resp. second) inequality, we have equality only when (x_1, x_2) belongs to the upper (resp. lower) half of the cusp locus.

A4 *For points $(x_1, 0)$ belonging to the crossing locus*

$$\partial_{x_2} A_{k+1,k+2}(x_1, 0) \geq 0$$

with equality only at the swallow tail point itself.

Moreover, for $(x_1, x_2) \in O_1$ with $|x_2| \leq 1/32$,

$$\partial_{x_2} A_{k+1,k+2}(x_1, x_2) \geq 0, \quad \partial_{x_2} A_{k,k+2}(x_1, x_2) \geq 0, \quad \partial_{x_2} A_{k,k+1}(x_1, x_2) \leq 0.$$

A5 *In $(O_2 \setminus O_1) \cap \{x_2 \geq 1/32\}$, the gradient $\nabla A_{k,k+1}$ points into the wedge $\{x_1 \geq 0\} \cap \{x_1 \geq x_2\}$. In $(O_2 \setminus O_1) \cap \{x_2 \leq -1/32\}$, the gradient $\nabla A_{k,k+2}$ points into the wedge $\{x_1 \geq 0\} \cap \{x_1 \geq -x_2\}$.*

Proof. A1. Denote the cusp locus of L'_{st} by $\Sigma'_{st} = \{(c(x_2), x_2)\}$. The cusp locus of L''_{st} is $T^{-1}(\Sigma'_{st})$, and for $(c(x_2), x_2) \in \Sigma'_{st}$ with $|x_2| \geq 1/16$ we compute

$$T^{-1}(c(x_2), x_2) = (c(x_2) - b(|x_2|), x_2).$$

From the definition of b, and (P2) we have

$$\begin{aligned} &-3/8-\epsilon_2 \le c(0) \le c(x_2) = c(x_2) - b(|x_2|) \le -3/8, && \text{for } |x_2| \le 1/32; \\ &-3/8 = c(x_2) - (c(x_2)+3/8) \le c(x_2) - b(|x_2|) \le c(x_2) \le -3/8+\epsilon_2, && \text{for } 1/32 \le |x_2|, \end{aligned}$$

with $c(x_2) - b(|x_2|) = -3/8$ when $|x_2| \ge 1/16$.

To prove the slope bound, note that the differential of T^{-1} is

$$\begin{bmatrix} 1 & -b'(|x_2|)\cdot \operatorname{sgn}(x_2) \\ 0 & 1 \end{bmatrix}.$$

By property (P3), for a point $T^{-1}(a) \in T^{-1}(\Sigma'_{st})$ in the cusp locus of L''_{st} with $1/32 \le |x_2| \le 1/16$, we have that the tangent to Σ'_{st} at a is given by a vector of the form $\begin{bmatrix} 1 \\ y \end{bmatrix}$ with $|y| > 9(2N+1.1)$. Thus, a tangent vector to $T^{-1}(\Sigma'_{st})$ at $T^{-1}(a)$ is given by $\begin{bmatrix} 1 - b'(|x_2|)\cdot \operatorname{sgn}(x_2)\cdot y \\ y \end{bmatrix}$. The slope therefore satisfies

$$|\text{slope}| = \left| \frac{y}{1 - b'(|x_2|)\cdot \operatorname{sgn}(x_2)\cdot y} \right| \ge \frac{|y|}{1 + |b'(|x_2|)|\cdot |y|} = \frac{1}{1/|y| + |b'(|x_2|)|}.$$

Again using (P3) and a defining property of b, we have

$$1/|y| + |b'(|x_2|)| \le \frac{1}{9(2N+1.1)} + \frac{1}{3(2N+1.1)} = \frac{4}{9(2N+1.1)},$$

so it follows that $|\text{slope}| \ge \frac{9}{4}(2N+1.1) > 2N+1.1$.

A2. This statement is clearly true for L'_{st} (using Lemma 10.3), and $T(x_1,x_2) = (x_1,x_2)$ when $|x_2| < 1/32$.

A3. The differentials of S and T are given by

$$dS = \begin{bmatrix} M & 0 \\ 0 & M \end{bmatrix} \quad \text{and} \quad dT = \begin{bmatrix} 1 & b'(|x_2|)\cdot \operatorname{sgn}(x_2) \\ 0 & 1 \end{bmatrix}.$$

Using the chain rule we compute the differential of $A_{i,j} = a_{i,j} \circ S \circ T$ to be

$$[\partial_{x_1} A_{i,j}, \partial_{x_2} A_{i,j}] = dA_{i,j} = da_{i,j} \cdot dS \cdot dT,$$

and carrying out the matrix multiplication gives

$$\partial_{x_1} A_{i,j} = M \cdot \partial_{x_1} a_{i,j}(S \circ T(x_1,x_2)); \tag{77}$$

$$\partial_{x_2} A_{i,j} = M \cdot \left[\operatorname{sgn}(x_2)\cdot b'(|x_2|)\cdot \partial_{x_1} a_{i,j}(S\circ T(x_1,x_2)) + \partial_{x_2} a_{i,j}(S\circ T(x_1,x_2)) \right]. \tag{78}$$

Using Corollary 10.4 and its surrounding notation, we have that for any $(r,s) \in W = \{s \ge -2r\} \cap \{s \ge r\}$ (and hence any $(x_1,x_2) \in R_+$)

- $\partial_{x_1} a_{k,k+1} = (s-r)(s+r) \ge 0$, with equality only when $r = s$;
- $\partial_{x_1} a_{k,k+2} = (2r+s)\cdot s \ge 0$, with equality only when $s = -2r$; and
- $\partial_{x_1} a_{k+1,k+2} = (r+2s)\cdot r$ which shows that $\operatorname{sgn}(\partial_{x_1} a_{k+1,k+2}) = \operatorname{sgn}(r)$.

Since the images of $\{r=s\}\cap W$ and $\{s=-2r\}\cap W$ are respectively the upper and lower halves of the cusp locus the statements from *A3* concerning $A_{k,k+1}$ and $A_{k,k+2}$ both follow. To deduce the claim about $A_{k+1,k+2}$, note that $\operatorname{sgn}(r) = \operatorname{sgn}(x_2)$ and that the diffeomorphism $S\circ T$ preserves the sign of the x_2 coordinate.

A4. When $|x_2| \le 1/32$, (78) simplifies to

$$\partial_{x_2} A_{k+1,k+2}(x_1,x_2) = M \cdot \partial_{x_2} a_{k+1,k+2}(S\circ T(x_1,x_2)),$$

and, as $r+2s$ is positive everywhere in W except for $(0,0)$, Corollary 10.4 shows that $\partial_{x_2} a_{k+1,k+2}$ is positive everywhere except for the swallowtail point itself. Similar computations using Corollary 10.4 verify the signs of $\partial_{x_2} A_{k,k+1}$ and $\partial_{x_2} A_{k,k+2}$.

A5. With *A3* established we need only show that $\partial_{x_2} A_{k,k+1} \le \partial_{x_1} A_{k,k+1}$ when $x_2 \ge 1/32$ and $-\partial_{x_2} A_{k,k+2} \le \partial_{x_1} A_{k,k+2}$ when $x_2 \le -1/32$. For the first inequality, note that when $x_2 \ge 1/32$,

$$\operatorname{sgn}(x_2) b'(|x_2|) \partial_{x_1} a_{k,k+1}(S\circ T(x_1,x_2)) \le 1 \cdot \partial_{x_1} a_{k,k+1}(S\circ T(x_1,x_2))$$

and

$$\partial_{x_2} a_{k,k+1}(S \circ T(x_1, x_2)) \leq 0$$

where we have used the properties of b and Corollary 10.4 respectively. In view of (77) and (78), adding these inequalities and multiplying both sides by M gives $\partial_{x_2} A_{k,k+1} \leq \partial_{x_1} A_{k,k+1}$ as desired. When $x_2 \leq -1/32$, note that Corollary 10.4 gives $\partial_{x_2} a_{k,k+2}(S \circ T(x_1, x_2)) \geq 0$, and then estimate

$$-\partial_{x_2} A_{k,k+2} = M[-\mathrm{sgn}(x_2) b'(|x_2|) \partial_{x_1} a_{k,k+2}(S \circ T(x_1, x_2)) - \partial_{x_2} a_{k,k+2}(S \circ T(x_1, x_2))] \leq$$
$$M[\partial_{x_1} a_{k,k+2}(S \circ T(x_1, x_2)) + 0] = \partial_{x_1} A_{k,k+2}.$$

□

10.2. **Defining functions away from the swallowtail point.** The edges of the Type (13) square have the following types: The L edge is (PV) with $n-2$ sheets. Edges U and D are (Cu) with n sheets and a left cusp between sheets k and $k+1$. The R edge is (1Cr) with n sheets and a single crossing between the sheets $k+1$ and $k+2$. We let f_i^L, f_i^U, f_i^D, f_i^R denote the 1-skeleton functions associated to each of these types of edges as constructed in Section 9.

In constructing the swallowtail square we have occasion to introduce 5 new 1-variable functions which we denote by $f_k^{ST}, f_{k+1}^{ST}, f_{k+2}^{ST}, \widehat{f}_{k+1}$, and $\widehat{f}_{k+2}$. The three f^{ST} will serve as substitutes for the functions $f_{k-0.5}^L$ that were used in defining the Type (9)-(12) squares (see Section 9.3) while $\widehat{f}_{k+1}$ and $\widehat{f}_{k+2}$ will be used in combination with $f_{k+1}^U = f_{k+1}^D$ and $f_{k+2}^U = f_{k+2}^D$.

10.2.1. *Definition of $\widehat{f}_{k+1}$ and $\widehat{f}_{k+2}$.* We construct functions $\widehat{f}_{k+1} : [-1, 1] \to \mathbb{R}$ and $\widehat{f}_{k+2} : [-3/8, 1] \to \mathbb{R}$ to satisfy

$$\widehat{f}_{k+1}(x) = \begin{cases} f_{k+2}^U(x) & \text{for } x \in [-1, -7/8], \\ f_{k+1}^U(x) & \text{for } x \in [-3/8 + R_1/2, 1], \end{cases} \tag{79}$$

and

$$\widehat{f}_{k+2}(x) = \begin{cases} f_{k+1}^U(x) + C & \text{near } x = -3/8, \\ f_{k+2}^U(x) & \text{for } x \in [-3/8 + R_1/2, 1], \end{cases} \tag{80}$$

where C is some additive constant, along with several technical requirements. A schematic depiction of the constructions appears in Figure 72.

Lemma 10.7. *There exist functions $\widehat{f}_{k+1}$ and $\widehat{f}_{k+2}$ satisfying (79) and (80) as well as the following conditions:*

- *For $x \in [-3/8, -1/4]$,*

$$d_x \widehat{f}_{k+1} < d_x f_k^U \quad \text{and} \quad d_x \widehat{f}_{k+2} \leq d_x f_{k+1}^U. \tag{81}$$

- *For $x \in [-3/8, 1]$,*

$$f_{k+2}^U(x) \leq \widehat{f}_{k+2}(x) < f_{k+1}^U(x) \quad \text{and} \quad f_{k+2}^U(x) < \widehat{f}_{k+1}(x) \leq f_{k+1}^U(x). \tag{82}$$

  with all inequalities strict at $x = -3/8$.

- *For $x \in [-1, -3/8]$,*

$$f_{k+2}^U(x) \leq \widehat{f}_{k+1}(x) < f_{k-1}^U(x). \tag{83}$$

- *For $x \in [-3/8 - \epsilon_2, -3/8 + \epsilon_2]$,*

$$\widehat{f}_{k+1} \quad \text{is linear and} \quad d_x f_{k+2}^U(x) < d_x \widehat{f}_{k+1}(x) < d_x f_{k+1}^U(-3/8). \tag{84}$$

- *For $(x_1, x_2) \in (\{-3/8 \leq x_1 \leq -1/4\} \cap \{x_2 > 0\}) \setminus O_1$,*

$$\phi(x_2) d_x(f_{k+1}^U - f_{k+2}^U)(x_1) \geq [1 - \phi(x_2)] d_x(\widehat{f}_{k+1} - \widehat{f}_{k+2})(x_1). \tag{85}$$

Proof. Note that for $-3/8 + R_1/2 \leq x_1$ (79) and (80) will imply (85) since $\phi(x_2) \geq 1 - \phi(x_2)$ when $x_2 > 0$. For (x_1, x_2) where (85) is required to hold, when $-3/8 \leq x_1 \leq -3/8 + R_1/2$ we will have $x_2 \geq \sqrt{3} R_1/2 = \sqrt{3}/32$ by trigonometry. Thus, (85) will follow provided we have (79), (80) and the condition

$$\left[\frac{\phi(\sqrt{3} R_1/2)}{1 - \phi(\sqrt{3} R_1/2)} \right] \cdot d_x(f_{k+1}^U - f_{k+2}^U)(x_1) \geq d_x(\widehat{f}_{k+1} - \widehat{f}_{k+2})(x_1) \tag{86}$$

holds for $-3/8 \leq x_1 \leq -3/8 + R_1/2$.

Therefore, it suffices to obtain $\widehat{f}_{k+1}$ and $\widehat{f}_{k+2}$ satisfying (79)-(84) and (86). Begin by setting $\widehat{f}_{k+1} = f^U_{k+1}$ and $\widehat{f}_{k+2} = f^U_{k+2}$ for $x \geq -3/8 + R_1/2$. Then, proceeding from right to left, we modify the derivatives of $\widehat{f}_{k+1}$ and $\widehat{f}_{k+2}$ in a small interval to the left of $-3/8 + R_1/2$ but to the right of $-3/8 - \epsilon_2$ to momentarily make $d_x\widehat{f}_{k+1}$ slightly larger than $d_x f^U_{k+1}$ and $d_x\widehat{f}_{k+2}$ slightly smaller than $d_x f^U_{k+2}$ in such a way that (81) and (86) continue to hold. The latter is achievable because

$$\left[\frac{\phi(\sqrt{3}R_1/2)}{1-\phi(\sqrt{3}R_1/2)}\right] = \frac{8+\sqrt{3}}{8-\sqrt{3}} > 1.5, \tag{87}$$

where we used (63) to evaluate ϕ. Next, return the derivatives to equality, $d_x\widehat{f}_l = d_x f^U_l$, $l = k+1, k+2$. Continuing from right to left, we now have an interval where $\widehat{f}_{k+1} = f^U_{k+1} - \alpha_1$ and $\widehat{f}_{k+2} = f^U_{k+2} + \alpha_2$ for positive constants α_1 and α_2. Moreover, the previous construction can be arranged so that $\alpha_1 = \alpha_2 = \alpha$ with $0 < \alpha << 1$ as small as desired.

To complete the definition of $\widehat{f}_{k+2}$, just prior to $-3/8$, interpolate the derivative $d_x\widehat{f}_{k+2}$ from $d_x f^U_{k+2}$ to $d_x f^U_{k+1}$ to arrange that $\widehat{f}_{k+2} = f^U_{k+1}(x) + C$ in a interval to the right of and including $x = -3/8$. This can be done to maintain the estimates for $d_x\widehat{f}_{k+2}$ and $\widehat{f}_{k+2}$ from (81) and (82) provided the interpolation is carried out in a small enough neighborhood of $-3/8$ and α was taken to be suitably small.

To complete the definition of $\widehat{f}_{k+1}$, just to the right of $x_1 = -3/8 + \epsilon_2$ interpolate $d_x\widehat{f}_{k+1}$ from being equal to $d_x f^U_{k+1}$ to being constant with

$$d_x\widehat{f}_{k+1}(x) = d_x f^U_{k+1}(-3/8) - \delta$$

with $\delta > 0$ small, and then continue the definition of $\widehat{f}_{k+1}$ by interpolating between the linear function and f^U_{k+2} somewhere on the interval $[-7/8, -3/8 - \epsilon_2)$.

We now verify the required inequalities for $\widehat{f}_{k+1}$ from (81)-(84). Note that (81) continues to hold since

$$d_x\widehat{f}_{k+1}(x) \leq d_x f^U_{k+1}(-3/8) - \delta = d_x f^U_k(-3/8) - \delta < d_x f^U_k(x), \qquad \text{for } x \in [-3/8, -3/8 + \epsilon_2]$$

where the 2nd inequality follows from Proposition 9.5 (8'). In addition, $\widehat{f}_{k+1}(x) \leq f^U_{k+1}(x)$ continues to hold (part of (82)) provided δ is chosen small enough, since $f^U_{k+1} > \widehat{f}_{k+1}(x)$ holds to the right of $-3/8 + \epsilon_2$, and for $x \in [-3/8, -3/8 + \epsilon_2]$

$$d_x(f^U_{k+1} - \widehat{f}_{k+1})(x) < d_x f^U_{k+1}(-3/8) - (d_x f^U_{k+1}(-3/8) - \delta) = \delta.$$

[When working from right to left $f^U_{k+1} - \widehat{f}_{k+1}$ could conceivably decrease, but by taking δ sufficiently small, we guarantee that the total decrease from $x = -3/8 + \epsilon_2$ to $x = -3/8$ is less than the value of the difference at $-3/8 + \epsilon_2$.] To verify the bound from (84) for $x \in [-3/8 - \epsilon_2, -3/8 + \epsilon_2]$, we note that $d_x f^U_{k+2}$ is also constant (by Proposition 9.5 (8')) with

$$d_x f^U_{k+2} < d_x f^U_{k+1}(-3/8).$$

Next, note that to the right of $x = -3/8 + \epsilon_2$,

$$\begin{aligned}(f^U_{k+1} - f^U_{k+2})(x) &\geq (f^U_{k+1} - f^U_{k+2})(-3/8) = .08\epsilon_1, \quad \text{and}\\ (f^U_{k-1} - f^U_{k+1})(x) &\geq (f^U_{k-1} - f^U_{k+1})(-3/8) \geq .08\epsilon_1\end{aligned}$$

(evaluated using (48)), and $\widehat{f}_{k+1}$ is approximately equal to f^U_{k+1}. Since

$$\begin{aligned}d_x(\widehat{f}_{k+1} - f^U_{k+2}) &\leq d_x f_{k-1,k+2} = 3\\ d_x(f^U_{k-1} - \widehat{f}_{k+1}) &\leq d_x f_{k-1,k+2} = 3\end{aligned}$$

on $[-3/8 - \epsilon_2, -3/8 + \epsilon_2]$, the total change in magnitude to both $(\widehat{f}_{k+1} - f^U_{k+2})(x)$ and $(f^U_{k-1} - \widehat{f}_{k+1})(x)$ on this interval is less than $6\epsilon_2$ which is much smaller than $.08\epsilon_1$. It follows that

$$f^U_{k+2}(x) \leq \widehat{f}_{k+1}(x) < f^U_{k-1}(x)$$

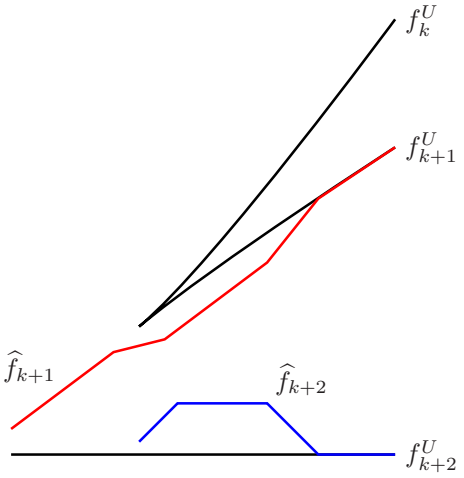

FIGURE 72. Schematic graphs of f_k^U, f_{k+1}^U, $\widehat{f}_{k+1}$ (red), $\widehat{f}_{k+2}$ (blue), and f_{k+2} with f_{k+2} pictured as 0.

holds on $[-3/8-\epsilon_2, -3/8+\epsilon_2]$ (and this gives the other part of (82)). As long as the interpolation from the linear function defining $\widehat{f}_{k+1}(x)$ near $-3/8-\epsilon_2$ to $f_{k+2}^U(x)$ is done close enough to $-3/8-\epsilon_2$, the previous inequality remains valid on all of $[-1,-3/8]$ as required by (83).

Finally, we check (85), for $x \in [-3/8, -3/8+\epsilon_2]$. We have

$$d_x(\widehat{f}_{k+1}-\widehat{f}_{k+2})(x) \le d_x f_{k+1}^U(-3/8) - \delta - d_x f_{k+2}^U(x) =$$

$$d_x(f_{k+1}^U)(-3/8+\epsilon_2) + (3/2)(\epsilon_2)^{1/2} - \delta - d_x f_{k+2}^U(x) \le d_x(f_{k+1}^U - f_{k+2}^U)(x) + (3/2)(\epsilon_2)^{1/2}.$$

[Use the definition of $d_x\widehat{f}_{k+1}$ and $d_x\widehat{f}_{k+2}$; then, the explicit formula for $d_x f_{k+1}^U$ in $[-3/8, -3/8+\epsilon_2]$ from Proposition 9.5 (8'); then, that $d_x f_{k+1}^U$ decreases on $[-3/8, -3/8+\epsilon_2]$.] Also, using (87) and $d_x(f_{k+1}^U)(x) - d_x f_{k+2}^U(x) \ge 1.5 - (3/2)(\epsilon_2)^{1/2}$ (by the explicit formula for $d_x f_{k+1,k+2}^U(-3/8) = 1.5$ found in equation (48)), we get

$$\left[\frac{\phi(\sqrt{3}R_1/2)}{1-\phi(\sqrt{3}R_1/2)}\right] \cdot d_x(f_{k+1}^U - f_{k+2}^U)(x) \ge (3/2) d_x(f_{k+1}^U - f_{k+2}^U)(x) \ge$$

$$d_x(f_{k+1}^U - f_{k+2}^U)(x) + .5\left(1.5 - (3/2)(\epsilon_2)^{1/2}\right) \ge d_x(f_{k+1}^U - f_{k+2}^U)(x) + (3/2)(\epsilon_2)^{1/2}.$$

Combining these inequalites shows that (86) holds.

□

We will make use of the estimates

$$|\widehat{f}_{k+1}(x)| < N\epsilon_1, \quad |\widehat{f}_{k+2}(x)| < N\epsilon_1, \quad \text{for } x \in [-1,-1/4] \tag{88}$$

that follow from (82), (83), and the corresponding estimate for the f^U from (3) of Corollary 9.6.

10.2.2. *Definition of the f^{ST}.* To begin, fix a bump function $\psi : [-1,1] \to [0,1]$ related to the cutoff function ϕ from Section 9.3 by

$$\psi(x) = \begin{cases} \phi(x), & x \le -R_1/2 \\ 1-\phi(x), & x \ge +R_1/2 \end{cases}$$

and with a single local maximum on $[-1/4, 1/4]$ at $x = 0$. In addition, we require that ψ is an even function satisfying the bounds

$$0 \le \psi(x) \le \text{Min}\{\phi(x), 1-\phi(x)\}, \quad |\psi'(x)| < 3, \quad \text{and} \quad |\psi''_{[-1/16,1/16]}| < 65. \tag{89}$$

See Figure 69. [To obtain $\psi(x)$, set $\psi(x) = \phi(x)$ for $x \le -R_1/2 = -1/32$. Then, interpolate the derivative of $\psi(x)$, which is 2 at $x = -1/32$, to agree with $-x$ in a neighborhood of $x = 0$. If the interpolation is done in a manner that is roughly linear, then the bound $|\psi''(x)| < 65$ will hold. Finally, extend $\psi(x)$ to be an even function and note that $\psi(x) = 1-\phi(x)$ for $x \ge R_1/2$ follows from (63).]

Lemma 10.8. *There exists a function $f_k^{ST} : [-1,1] \to \mathbb{R}$ satisfying*

$$f_k^{ST}(x) - f_{k+1}^L(x) = 1.5Q_\pm(x), \qquad \text{for } |x-(\pm 1)| \le 1/16, \tag{90}$$

$$f_k^{ST}(x) := f_k^L(x) + \psi(x)[\widehat{f}_{k+2}(-3/8) - f_{k+1}^U(-3/8)] \qquad \text{on } [-3/8, 3/4]; \tag{91}$$

with

$$\forall x \in [-1,-1/4] \cup [3/4,1], \quad f_k^L(x) \le f_k^{ST}(x) \le f_{k-1}^L(x); \tag{92}$$

$$\forall x \in (-1,-1/4], \quad (f_{k-1}^L - f_k^{ST})'(x) > 0, \quad \text{and } (f_k^{ST} - f_{k+1}^L)'(x) > 0; \tag{93}$$

$$\forall x \in [3/4,1), \quad (f_{k-1}^L - f_k^{ST})'(x) < 0, \quad \text{and } (f_k^{ST} - f_{k+1}^L)'(x) < 0; \tag{94}$$

$$||f_k^{ST} - f_k^L||_{C^0([-1,-1/4])} < 2N\epsilon_1, \quad \text{and} \quad ||f_k^{ST} - f_k^L||_{C^0([3/4,1])} < 2N\epsilon_1. \tag{95}$$

Proof. We need to show that the definition of f_k^{ST} resulting from (90) and (91) can be extended over $[-15/16, -3/8] \cup [3/4, 15/16]$ while retaining the properties (92)-(95).

Extending over $[3/4, 15/16]$**:** For small $\delta > 0$, fix $\beta : [7/8, 1] \to \mathbb{R}$ with

$$\beta \equiv -\delta \text{ near } 7/8, \quad \beta \equiv .5 \text{ on } [15/16, 1],$$

$$\beta' \ge 0, \quad ||\beta'||_{C^0} < 9.$$

In $[3/4, 1]$, we will define $f_k^{ST} - f_k^L$. Start by setting

$$(f_k^{ST} - f_k^L)(x) = \beta(x)\epsilon_2(x-1)^2 + .5\epsilon_2, \quad \forall x \in [7/8, 1]. \tag{96}$$

Notice that, since $Q_+(x) = \epsilon_2(x-1)^2 + \epsilon_2$, (90) holds. Moreover, for $x \in [7/8, 1]$ we can verify (94) by using Corollary 9.6 (4) to compute

$$(f_{k-1}^L - f_k^{ST})(x) = (1-\beta(x))\epsilon_2(x-1)^2 + .5\epsilon_2;$$
$$(f_k^{ST} - f_{k+1}^L)(x) = (1+\beta(x))\epsilon_2(x-1)^2 + 1.5\epsilon_2.$$

Then, estimate for $x \in [7/8, 1)$,

$$(f_{k-1}^L - f_k^{ST})'(x) = -\beta'(x)\epsilon_2(x-1)^2 + (1-\beta(x))2\epsilon_2(x-1) < 0 + 0;$$

$$(f_k^{ST} - f_{k+1}^L)'(x) = \beta'(x)\epsilon_2(x-1)^2 + (1+\beta(x))2\epsilon_2(x-1) \le ||\beta'||_{C^0}\epsilon_2(x-1)^2 + (1-\delta)2\epsilon_2(x-1) \le$$
$$(x-1)\epsilon_2\left(9(x-1) + (1-\delta)2\right) < 0$$

where the last inequality requires that $\delta < 7/16$.

With $f_k^{ST} - f_k^L$ now defined on $[7/8, 1]$, we extend it to $[1/2, 1]$ using Lemma 9.2 to agree with 0 on $[1/2, 3/4]$ and to meet the requirements

$$0 \le (f_k^{ST} - f_k^L)'(x) < (f_{k+1}^L - f_k^L)'(x). \tag{97}$$

To apply Lemma 9.2, first extend $f_k^{ST} - f_k^L$ slightly past 3/4 to make the first inequality strict, and then verify the two requirements:

(1) That (97) already holds for x near 3/4 and 7/8. This is straightforward since $d_x f_{k,k+1}^L < 0$ near 3/4 (by Proposition 9.4) and near 7/8 Corollary 9.6 (4) and (96) give explicitly

$$0 < (f_k^{ST} - f_k^L)'(x) = -2\delta\epsilon_2(x-1) < -2\epsilon_2(x-1) = (f_{k+1}^L - f_k^L)'(x).$$

(2) The other required inequality is

$$0 < (f_k^{ST} - f_k^L)(7/8) - (f_k^{ST} - f_k^L)(3/4) < (f_{k+1}^L - f_k^L)(7/8) - (f_{k+1}^L - f_k^L)(3/4).$$

We have

$$(f_k^{ST} - f_k^L)(7/8) - (f_k^{ST} - f_k^L)(3/4) = -\delta\epsilon_2(-1/8)^2 + .5\epsilon_2 \tag{98}$$

which is positive provided δ is sufficiently small and

$$(f_{k+1}^L - f_k^L)(7/8) - (f_{k+1}^L - f_k^L)(3/4) \ge -(65/64)\epsilon_2 + y_{k,k+1}^L - N\epsilon_1 > .5$$

where we bounded below the second term using Proposition 9.4 (2).

With the definition now complete, we note that (97) implies both inequalities from (94) for $x \in [3/4, 7/8]$. [Adding f_k^L everywhere gives

$$d_x f_k^L(x) \leq d_x f_k^{ST}(x) < d_x f_{k+1}^L(x).$$

Multiplying the first inequality by -1 and adding $d_x f_{k-1}^L$ gives

$$(f_{k-1}^L - f_k^{ST})'(x) \leq d_x f_{k-1,k}^L(x) < 0,$$

and subtracting $d_x f_{k+1}^L(x)$ from the second inequality gives $(f_k^{ST} - f_{k+1}^L)'(x) < 0$.] To check the second inequality of (95) note that, by (97), $(f_k^{ST} - f_k^L)|_{[3/4,7/8]}$ has its maximum absolute value at $7/8$ and the required bound holds in $[7/8, 1]$ by (96).

Finally, we check (92). For small enough $\delta > 0$, check (92) directly in $[7/8, 1]$ using (96) and the equation that immediately follows it. To verify that $f_k^L \leq f_k^{ST}$ holds on $[3/4, 7/8]$ use the first inequality from (97) together with $(f_k^{ST} - f_k^L)(3/4) = 0$. To verify that $f_k^{ST} \leq f_{k-1}^L$ holds on $[3/4, 7/8]$, use that $(f_{k-1}^L - f_k^{ST})' < 0$ and that the inequality holds at $x = 7/8$.

Extending over $[-15/16, -3/8]$**:** Using a similar procedure, set

$$(f_k^{ST} - f_k^L)(x) = \beta(-x)\epsilon_2(x+1)^2 + .5\epsilon_2, \quad \forall x \in [-1, -7/8].$$

Then, extend for $x \in [-7/8, -3/8]$ in a manner that satisfies

$$0 \leq (f_k^L - f_k^{ST})'(x) < d_x f_{k,k+1}^L(x).$$

The verification that this can be done and that the required properties of f_k^{ST} all hold is similar to the above. Here, we only mention that the definition of $f_{k,k+1}^L$ in (40) may be consulted to obtain the inequality

$$f_{k,k+1}^L(-3/8) - f_{k,k+1}^L(-7/8) > [f_k^L - f_k^{ST}](-3/8) - [f_k^L - f_k^{ST}](-7/8) > 0$$

that is required for the application of Lemma 9.2.

□

With f_k^{ST} defined as in Lemma 10.8, we complete the definition of the f^{ST} by setting

$$f_{k+2}^{ST} := f_k^{ST} \quad \text{on } [-1, -1/4]; \tag{99}$$

$$f_{k+2}^{ST} := f_k^L \quad \text{on } [-1/4, 1]; \tag{100}$$

$$f_{k+1}^{ST} := f_k^L \quad \text{on } [-1, 3/4]; \text{ and} \tag{101}$$

$$f_{k+1}^{ST} := f_k^{ST} \quad \text{on } [3/4, 1]. \tag{102}$$

Note that ψ vanishes near outside of $(-1/4, 1/4)$ so that the definitions of f_{k+1}^{ST} and f_{k+2}^{ST} piece together smoothly.

10.2.3. *Definition of* 2*-variable defining functions in* $I^2 \setminus O_1$. With these 1-variable functions in hand, we now give 2-variable functions

$$\begin{aligned} G_k, G_{k+1}, G_{k+2} : &\quad \{x_2 \geq -3/8\} \setminus \mathrm{Int}(O_1) \to \mathbb{R}, \\ H : &\quad \{x_2 \leq -3/8\} \setminus \mathrm{Int}(O_1) \to \mathbb{R}, \end{aligned}$$

whose graphs will together form the swallow tail sheets outside of O_2. The definitions are as follows:

$$G_k(x_1, x_2) = (1 - \phi(x_1))f_k^{ST}(x_2) + \phi(x_1)f_k^R(x_2) + f_k^U(x_1). \tag{103}$$

$$\begin{aligned} G_{k+1}(x_1, x_2) =& (1 - \phi(x_1))f_{k+1}^{ST}(x_2) + \phi(x_1)f_{k+1}^R(x_2) + \\ & (1 - \phi(x_2)) \begin{cases} \widehat{f}_{k+2}(x_1), & \text{if } x_2 \geq 0 \\ f_{k+2}^D(x_1), & \text{if } x_2 \leq 0, \end{cases} + \phi(x_2) \begin{cases} f_{k+1}^U(x_1), & \text{if } x_2 \geq 0 \\ \widehat{f}_{k+1}(x_1), & \text{if } x_2 \leq 0. \end{cases} \end{aligned} \tag{104}$$

$$\begin{aligned} G_{k+2}(x_1, x_2) =& (1 - \phi(x_1))f_{k+2}^{ST}(x_2) + \phi(x_1)f_{k+2}^R(x_2) + \\ & (1 - \phi(x_2)) \begin{cases} \widehat{f}_{k+1}(x_1), & \text{if } x_2 \geq 0 \\ f_{k+1}^D(x_1), & \text{if } x_2 \leq 0 \end{cases} + \phi(x_2) \begin{cases} f_{k+2}^U(x_1), & \text{if } x_2 \geq 0 \\ \widehat{f}_{k+2}(x_1), & \text{if } x_2 \leq 0. \end{cases} \end{aligned} \tag{105}$$

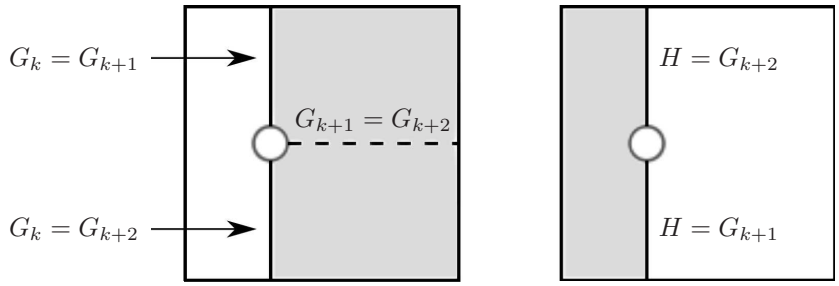

FIGURE 73. The shaded region in the left (resp. right) square indicates the portion of $[-1,1]^2$ where the graphs of G_k, G_{k+1}, and G_{k+2} (resp. H) are used. The agreement of various functions along parts of the lines $x_1 = -3/8$ and $x_2 = 0$ is indicated.

$$H(x_1,x_2) = (1-\psi(x_2))f^U_{k+2}(x_1) + \psi(x_2)\widehat{f}_{k+1}(x_1) + f^L_k(x_2). \tag{106}$$

(Note that G_{k+1} and G_{k+2} are well defined and smooth along $x_2 = 0$, since $\widehat{f}_{k+1}(x_1) = f^U_{k+1}(x_1) = f^D_{k+1}(x_1)$ and $\widehat{f}_{k+2}(x_1) = f^U_{k+2}(x_1) = f^D_{k+2}(x_1)$ for $x_1 \geq -3/8 + R_1$. Also, the definition of H makes sense for all $(x_1,x_2) \in [-1,1]^2$.) We follow our usual notation by setting $G_{i,j} = G_i - G_j$ for $i,j \in \{k, k+1, k+2\}$.

The graphs of the G_l and H fit together to form the front projection of a smooth Legendrian above $[-1,1] \setminus \mathrm{Int}(O_1)$ with features described in the following Proposition. See Figure 73.

Lemma 10.9. *With G_k, G_{k+1}, G_{k+2}, H defined as above,*

1. *The sheets defined by G_k and G_{k+1} (resp. G_k and G_{k+2}) line up at a cusp edge along $\{x_1 = -3/8\} \cap \{x_2 \geq R_1\}$ (resp. along $\{x_1 = -3/8\} \cap \{x_2 \leq -R_1\}$). Moreover, for $x_1 \leq -1/4$ and $|x_2| \leq 1/4$, these are the only points (in the domain of definition) where $G_{k,k+1} = 0$ (resp. $G_{k,k+2} = 0$).*
2. *The sheets defined by H and G_{k+1} (resp. H and G_{k+2}) fit together smoothly along $\{x_1 = -3/8\} \cap \{x_2 \leq -R_1\}$ (resp. along $\{x_1 = -3/8\} \cap \{x_2 \geq R_1\}$).*
3. *The sheets defined by G_{k+1} and G_{k+2} cross along $\{x_1 \geq R_1\} \cap \{x_2 = 0\}$. Moreover, for $x_1 \leq -1/4$, these are the only points (in the domain of definition) where $G_{k+1,k+2} = 0$.*

Proof. (1): Consider (x_1,x_2) where $G_{k,k+1}$ is defined and satisfying $x_1 \leq -1/4$. Letting $f^{ST}_{k,k+1} = f^{ST}_k - f^{ST}_{k+1}$, we have

$$\begin{aligned} G_{k,k+1}(x_1,x_2) =& f^{ST}_{k,k+1}(x_2) + \\ & (1-\phi(x_2)) \begin{cases} (f^U_k - \widehat{f}_{k+2})(x_1), & x_2 \geq 0 \\ f^U_{k,k+2}(x_1), & x_2 \leq 0, \end{cases} + \phi(x_2) \begin{cases} f^U_{k,k+1}(x_1), & x_2 \geq 0 \\ (f^U_k - \widehat{f}_{k+1})(x_1), & x_2 \leq 0. \end{cases} \end{aligned}$$

Letting $C = \widehat{f}_{k+2}(-3/8) - f^U_{k+1}(-3/8) < 0$, using (89) we have for $x_2 \geq -1/4$

$$f^{ST}_{k,k+1}(x_2) = \psi(x_2)C \geq (1-\phi(x_2))C \tag{107}$$

with equality for $x_2 \geq R_1/2$. From the evenness of ψ, and the symmetry in the formulas defining G_{k+1} and G_{k+2}, we observe that $G_{k,k+2}(x_1,-x_2) = G_{k,k+1}(x_1,x_2)$, so it suffices to establish (1) for $G_{k,k+1}$.

The inequality (107) leads to

$$G_{k,k+1} \geq (1-\phi(x_2)) \begin{cases} (f^U_k - \widehat{f}_{k+2})(x_1) + C, & x_2 \geq 0 \\ f^U_{k,k+2}(x_1) + C, & x_2 \leq 0, \end{cases} + \phi(x_2) \begin{cases} f^U_{k,k+1}(x_1), & x_2 \geq 0 \\ (f^U_k - \widehat{f}_{k+1})(x_1), & x_2 \leq 0. \end{cases}$$

Note that the terms that appear when $x_2 \leq 0$ are both strictly positive. [The left term becomes $\widehat{f}_{k+2}(-3/8) - f^U_{k+2}(-3/8) > 0$ when $x_1 = -3/8$ by (82), and remains positive as x_1 increases since $d_x f^U_{k,k+2}(x_1) > 0$. Positivity of the right term also follows from (82).] In addition, those terms that appear when $x_2 \geq 0$ are non-negative and vanish only when $x_1 = -3/8$. [The left term is 0 when $x_1 = -3/8$, and then increases by (81).] Thus, the only possible place where $G_{k,k+1} = 0$ is along $\{x_1 = -3/8\} \cap \{x_2 \geq R_1\}$. Moreover, equality holds when $x_2 \geq R_1/2$, and both terms agree with

$f^U_{k,k+1}(x_1)$ when x_1 is in a neighborhood of $-3/8$ by (80). Thus, we see that the sheets indeed meet at a cusp edge at the stated location.

(2): When $x_2 \geq R_1/2$ and $x_1 \leq -1/4$, recall that $f^{ST}_{k+2}(x_2) = f^L_k(x_2)$ and $\psi(x_2) = 1-\phi(x_2)$ to easily verify that the formulas for G_{k+2} and H agree. Similarly, check that $G_{k+1} = H$ when $x_2 \leq -R_1/2$ and $x_1 \leq -1/4$.

(3): For $x_1 \geq R_1$, $\widehat{f}_i(x_1) = f^U_i(x_1) = f^D_i(x_1)$ for $i = k+1$ or $k+2$. This allows us to evaluate

$$G_{k+1}(x_1,0) = (1-\phi(x_1))f^{ST}_{k+1}(0) + \phi(x_1)f^R_{k+1}(0) + \frac{1}{2}f^D_{k+2}(x_1) + \frac{1}{2}f^U_{k+1}(x_1)$$

and

$$G_{k+2}(x_1,0) = (1-\phi(x_1))f^{ST}_{k+2}(0) + \phi(x_1)f^R_{k+2}(0) + \frac{1}{2}f^D_{k+1}(x_1) + \frac{1}{2}f^U_{k+2}(x_1).$$

Since there is the R edge is (1Cr) with sheets S_{k+1} and S_{k+2} crossing, we have $f^R_{k+1}(0) = f^R_{k+2}(0)$ (as in Proposition 9.4 (1)), and by definition $f^{ST}_{k+1}(0) = f^{ST}_{k+2}(0) = f^L_k(0)$. In addition, U and D have the same edge type, so the result follows.

To see that $G_{k+1,k+2}(x_1,x_2) \neq 0$ when $x_2 \neq 0$ and $x_1 \leq -1/4$, we compute

$$\begin{aligned} G_{k+1,k+2} =& f^{ST}_{k+1,k+2}(x_2) + \\ & (1-\phi(x_2))\begin{cases} \widehat{f}_{k+2}(x_1) - \widehat{f}_{k+1}(x_1), & x_2 \geq 0 \\ f^U_{k+2}(x_1) - f^U_{k+1}(x_1), & x_2 \leq 0, \end{cases} + \phi(x_2)\begin{cases} f^U_{k+1}(x_1) - f^U_{k+2}(x_1), & x_2 \geq 0 \\ \widehat{f}_{k+1}(x_1) - \widehat{f}_{k+2}(x_1), & x_2 \leq 0, \end{cases} \end{aligned}$$

When $x_2 > 0$, we have $f^{ST}_{k+1,k+2}(x_2) \geq 0$ by (99)-(102) and (92); $\phi(x_2) > 1-\phi(x_2)$; and $f^U_{k+1}(x_1) - f^U_{k+2}(x_1) \geq \widehat{f}_{k+1}(x_1) - \widehat{f}_{k+2}(x_1)$ by (82). This shows that $G_{k+1,k+2}(x_1,x_2) > 0$. When $x_2 < 0$, similar reasoning gives $G_{k+1,k+2}(x_1,x_2) < 0$. □

10.2.4. *Properties of defining functions.* We record some properties of G_k, G_{k+1}, G_{k+2}, H and their differences for later use. In the following, we let K denote the closed subset

$$K = \{(x_1,x_2) \,|\, -3/8 \leq x_1 \leq -1/4,\ -1/4 \leq x_2 \leq 1/4\} \setminus \mathrm{Int}(O_1).$$

Lemma 10.10. *The following properties of G_k, G_{k+1}, G_{k+2}, H and their differences hold.*

B1 *For any $l \in \{k, k+1, k+2\}$, we have*

$$\|H - G_l\|_{C^0(K)} \leq 6N\epsilon_1$$

and

$$\|\partial_{x_2}(H - G_l)\|_{C^0(K)} \leq 18N\epsilon_1.$$

B2 *For all $(x_1,x_2) \in K$,*

$$\partial_{x_1}G_{k,k+1}(x_1,x_2) \geq 0; \quad \partial_{x_1}G_{k,k+2}(x_1,x_2) \geq 0; \quad \text{and } sgn(\partial_{x_1}G_{k+1,k+2}(x_1,x_2)) = sgn(x_2).$$

Moreover, in the first (resp. second) inequality, we have equality only when (x_1,x_2) belongs to the upper (resp. lower) half of the cusp locus.

B3 *Along the crossing locus, $\{(x_1,0) \,|\, -3/8 + R_1 \leq x_1 \leq -1/4\}$,*

$$\partial_{x_2}G_{k+1,k+2}(x_1,0) > 0.$$

B4 *For $(x_1,x_2) \in K$ with $x_2 \geq R_1/2$, $\partial_{x_2}G_{k,k+1}(x_1,x_2) \leq 0$; and for $(x_1,x_2) \in K$ with $x_2 \leq -R_1/2$, $\partial_{x_2}G_{k,k+2}(x_1,x_2) \geq 0$.*

Proof. (B1) For $l \in \{k, k+1, k+2\}$ and $(x_1,x_2) \in K$, we have

$$H(x_1,x_2) - G_l(x_1,x_2) =$$

$$f^L_k(x_2) - f^{ST}_l(x_2) + \psi(x_2)\widehat{f}_{k+1}(x_1) + [1-\psi(x_2)]f^U_{k+2}(x_1) - [1-\phi(x_2)]a_1(x_1) - \phi(x_2)a_2(x_1)$$

where a_1 and a_2 are each one of $f^U_k, f^U_{k+1}, f^U_{k+2}, \widehat{f}_{k+1}$, or $\widehat{f}_{k+2}$ depending on l and the location of (x_1,x_2). Corollary 9.6 (3) and the definitions of $\widehat{f}_{k+1}, \widehat{f}_{k+2}$ imply that all five of these functions are bounded in absolute value by $N\epsilon_1$ when $-1 \leq x_1 \leq -1/4$. Moreover, each of ψ, $1-\psi$, ϕ, and $1-\phi$ are bounded by 1. Thus, the sum of the last 4 terms is bounded by $4N\epsilon_1$. In addition, (91), (100), and (101) imply

that $f_k^L(x_2) - f_l^{ST}(x_2) = \psi(x_2)[\widehat{f}_{k+2}(-3/8) - f_{k+1}^U(-3/8)]$ if $l = k$ and is 0 when $l = k+1$ or $k+2$. Thus, $|f_k^L(x_2) - f_l^{ST}(x_2)| \leq 1 \cdot [N\epsilon_1 + N\epsilon_1]$, so the triangle inequality gives

$$|H(x_1, x_2) - G_l(x_1, x_2)| \leq 6N\epsilon_1.$$

To obtain the second inequality, compute the derivative and estimate

$$|\partial_{x_2}(H - G_l)(x_1, x_2)| \leq$$

$$|d_x(f_k^L - f_l^{ST})(x_2)| + |d_x\psi(x_2)| \cdot \left(|\widehat{f}_{k+1}(x_1)| + |f_{k+2}^U(x_1)|\right) + |d_x\phi(x_2)| \cdot (|a_1(x_1)| + |a_2(x_1)|) \leq$$

$$|d_x\psi(x_2)| \cdot \left(|\widehat{f}_{k+2}(-3/8)| + |f_{k+1}^U(-3/8)|\right) + 3(2N\epsilon_1) + 3(2N\epsilon_1) \leq 18N\epsilon_1,$$

where we used that $|d_x\psi(x_2)|, |d_x\phi(x_2)| \leq 3$, see (63), (89).

(B2) In K,

$$G_{k,k+1}(x_1, x_2) = f_k^{ST}(x_2) - f_{k+1}^{ST}(x_2) +$$

$$f_k^U(x_1) - (1 - \phi(x_2)) \begin{cases} \widehat{f}_{k+2}(x_1), & \text{if } x_2 \geq 0 \\ f_{k+2}^D(x_1), & \text{if } x_2 \leq 0 \end{cases} - \phi(x_2) \begin{cases} f_{k+1}^U(x_1), & \text{if } x_2 \geq 0 \\ \widehat{f}_{k+1}(x_1), & \text{if } x_2 \leq 0. \end{cases}$$

Thus,

$$\partial_{x_1} G_{k,k+1} = (1 - \phi(x_2)) \begin{cases} d_x(f_k^U - \widehat{f}_{k+2})(x_1), & \text{if } x_2 \geq 0 \\ d_x(f_k^U - f_{k+2}^D)(x_1), & \text{if } x_2 \leq 0 \end{cases} + \phi(x_2) \begin{cases} d_x(f_k^U - f_{k+1}^U)(x_1), & \text{if } x_2 \geq 0 \\ d_x(f_k^U - \widehat{f}_{k+1})(x_1), & \text{if } x_2 \leq 0. \end{cases}$$

By Proposition 9.5 applied to the $f_i^U = f_i^D$ and (81), all 4 of the derivatives that appear in the 2 piecewise defined terms of $\partial_{x_1} G_{k,k+1}$ are non-negative when $-3/8 \leq x_1 \leq -1/4$. Moreover, of these 4 terms only the 2 that are used when $x_2 \geq 0$ can vanish, and this happens precisely when $x_1 = -3/8$. The statement concerning $G_{k,k+1}$ follows.

The statement about $G_{k,k+2}$ is established in a similar manner. In fact, $\partial_{x_1} G_{k,k+2}$ is nearly identical to $G_{k,k+1}$ except that the upper and lower rows in the piecewise definitions are interchanged.

Next, observe that $G_{k+1,k+2}(x_1, -x_2) = -G_{k+1,k+2}(x_1, x_2)$. Thus to show $\operatorname{sgn}(\partial_{x_1} G_{k+1,k+2}) = \operatorname{sgn}(x_2)$, it suffices to show that $\partial_{x_1} G_{k+1,k+2}(x_1, x_2) > 0$ when $x_2 > 0$. To this end, for $x_2 > 0$ we compute

$$\partial_{x_1} G_{k+1,k+2} = (1 - \phi(x_2)) d_x(\widehat{f}_{k+2}(x_1) - \widehat{f}_{k+1}(x_1))(x_1) + \phi(x_2) d_x(f_{k+1}^U - f_{k+2}^U)(x_1)$$

which is positive on $K \cap \{x_2 > 0\}$ by (85).

(B3) When $-3/8 + R_1 \leq x_1 \leq -1/4$, $\widehat{f}_{k+1}(x_1) = f_{k+1}^U(x_1)$ and $\widehat{f}_{k+2}(x_1) = f_{k+2}^U(x_1)$. Near $x_2 = 0$, $f_{k+1}^{ST}(x_2) = f_{k+2}^{ST}(x_2)$. So we compute

$$\partial_{x_2} G_{k+1,k+2}(x_1, 0) = \phi'(0) \cdot 2(f_{k+1}^U(x_1) - f_{k+2}^U(x_1)) > 0.$$

(B4) We prove the first statement with the second statement proved by similar considerations. Note that when $x_2 \geq R_1/2$ we have $\psi(x_2) = 1 - \phi(x_2)$, and $f_k^{ST}(x_2) - f_{k+1}^{ST}(x_2) = \psi(x_2)[\widehat{f}_{k+2}(-3/8) - f_{k+1}^U(-3/8)]$. These observations allow us to compute

$$\partial_{x_2} G_{k,k+1} = \phi'(x_2) \left[\widehat{f}_{k+2}(x_1) - f_{k+1}^U(x_1) - (\widehat{f}_{k+2}(-3/8) - f_{k+1}^U(-3/8))\right] \leq 0.$$

The inequality is deduced as follows: The multiplier $\phi'(x_2)$ is non-negative; the term in brackets is 0 when $x_1 = -3/8$, so using (81) it follows that this term is non-positive for all $-3/8 \leq x_1 \leq -1/4$. □

10.3. **The formula over the square.** We now complete the construction of the Type (13) squares. The sheets S_k, S_{k+1}, S_{k+2}, and $\tilde{S}_k$ that meet at the swallowtail point are to be defined as the union of graphs of functions $F_k, F_{k+1}, F_{k+2}, \tilde{F}_k$ that will be obtained by interpolating between the defining functions of Section 10.2 and a suitable constant multiple of those from Section 10.1.

Using polar coordinates, (r, θ), centered at $(-3/8, 0)$, consider the subsets of the annulus $A = O_2 \backslash O_1$,

$$\begin{aligned} V_1 &= \{(r, \theta) \,|\, R_1 \leq r \leq R_2,\ \pi/3 \leq \theta \leq \pi/2\}, \\ V_2 &= \{(r, \theta) \,|\, R_1 \leq r \leq R_2,\ -\pi/2 \leq \theta \leq -\pi/3\}, \end{aligned} \tag{108}$$

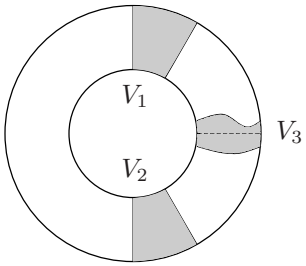

FIGURE 74. The closed subsets V_1, V_2, and V_3.

as in Figure 74. Note that the closure of $A \setminus V_1$ (resp. $A \setminus V_2$) in the domain of $G_{k,k+1}$ (resp. $G_{k,k+2}$) is a compact set where $G_{k,k+1}$ (resp. $G_{k,k+2}$) is positive by Lemma 10.9 (1) (because we are away from the cusp edge). Thus by compactness, there exist constants $C_1, C_2 > 0$ such that

$$\forall (x_1,x_2) \in A \setminus V_1, \quad G_{k,k+1}(x_1,x_2) > C_1, \quad \text{and} \quad \forall (x_1,x_2) \in A \setminus V_2, \quad G_{k,k+2}(x_1,x_2) > C_2. \tag{109}$$

Next, using Lemma 10.6.A4 and Lemma 10.10.B3 and continuity, we can find a neighborhood, V_3, of the crossing locus in $O_2 \setminus O_1$ such that the directional derivatives in the θ direction satisfy

$$\forall (x_1,x_2) \in V_3, \quad \partial_\theta A_{k+1,k+2}(x_1,x_2) > 0, \quad \text{and} \quad \partial_\theta G_{k+1,k+2}(x_1,x_2) > 0. \tag{110}$$

Within A, $G_{k+1,k+2}$ vanishes only at the crossing locus by Lemma 10.9 (3), so we can find $C_3 > 0$ such that

$$\forall (x_1,x_2) \in A \setminus V_3, \quad |G_{k+1,k+2}(x_1,x_2)| > C_3. \tag{111}$$

Using compactness of O_2, we can now fix $C > 0$ such that for $(i,j) = (k,k+1),(k,k+2)$, or $(k+1,k+2)$ and $l = k, k+1$, or $k+2$, we have

$$C\|A_{i,j}\|_{C^0(O_2)} \leq \text{Min}\{C_1, C_2, C_3\}; \tag{112}$$

$$C\|A_l\|_{C^0(O_2)}, C\|B\|_{C^0(O_2)} < \epsilon_1; \quad \text{and} \quad \text{Max}\{C\|\partial_{x_m} A_l\|_{C^0(O_2)}, C\|\partial_{x_m} B\|_{C^0(O_2)} \,|\, m = 1,2\} < \epsilon_1; \tag{113}$$

$$C < \frac{1}{2(2N+1)(M+M^{4/3})}, \qquad \text{where } M \text{ is from Section 10.1.2.} \tag{114}$$

(In the preceding formulas, by abuse of notation, $\|\cdot\|_{C^0(O_2)}$ indicates the sup norm of the functions on the intersection of their domain with O_2.)

In addition, we fix a non-decreasing cutoff function $\alpha : [0,+\infty) \to \mathbb{R}$ such that $\alpha(r) = 0$ for $r \leq R_1$ and $\alpha(r) = 1$ for $r \geq R_2$ such that

$$0 \leq \alpha'(r) \leq 33. \tag{115}$$

With these preparations complete, we make the definitions for $l \in \{k, k+1, k+2\}$,

$$\begin{aligned} F_l(x_1,x_2) &= (1-\alpha(r)) \cdot (H(x_1,x_2) + C\, A_l(x_1,x_2)) + \alpha(r) \cdot G_l(x_1,x_2), \\ \widetilde{F}_k(x_1,x_2) &= (1-\alpha(r)) \cdot (H(x_1,x_2) + C\, B(x_1,x_2)) + \alpha(r) \cdot H(x_1,x_2). \end{aligned} \tag{116}$$

Recall A_l, B, G_l, H are defined in (75), (103)-(106). For $i \notin \{k, k+1, k+2\}$ we define

$$F_i(x_1,x_2) = f_i^U(x_1) + (1-\phi(x_1)) f^L_{\sigma_L(i)}(x_2) + \phi(x_1) f_i^R(x_2). \tag{117}$$

We form the front projection of a Legendrian to be used for the Type (13) square, as follows: Take the union of the graphs of F_k, F_{k+1}, F_{k+2} in the region to the right of the cusp locus of L''_{st} with the graph of $\widetilde{F}_k$ to the left of the cusp locus of L''_{st}.

Lemma 10.11. *The graphs of the F_i and $\widetilde{F}_k$ fit together to form the front projection of a smooth Legendrian with a single swallowtail point. The base projection of the cusp locus agrees with that of the Legendrian L''_{st} from Section 10.1.*

Proof. The graphs of the A_l and B as well as the G_l and H fit together to form front projections of smooth Legendrians (by construction of the A_l and by Lemma 10.9). In addition, these two collections of defining functions have the same cusp locus (in the base projection) in their common domain. Thus, when we interpolate to form the F_l and $\widetilde{F}_k$, the result is again a smooth Legendrian with the same cusp locus. Moreover, up to scaling and the addition of a common function, the sheets defined by F_l, $l = k, k+1, k+2$ and $\widetilde{F}_k$ agree with L''_{st} within O_1 (where $\alpha(r) = 0$), and hence have a single swallowtail point. □

11. Proof of Theorem 5.1 Part 3: Verification of Properties

Let us recall where we are. We wish to construct $\tilde{L}_0$ satisfying all of the properties of Theorem 5.1 except possibly the 1-regular condition. Over each square of $\mathcal{E}_{\pitchfork}$, we take the front projection of $\tilde{L}_0$ to be the union of graphs of the functions defined using equation (64) for (1)-(12) square types, or using equation (116) for square (13) (and analogous for (14)).

In Section 11.1, we verify that $\tilde{L}_0$ pieces together over adjacent squares to form a smooth, globally defined Legendrian, and fix a metric from Construction 3.1 for computation of gradient vector fields. In Section 11.2, we confirm that the singular set of $\tilde{L}_0$ above each square is as prescribed by the square types (1)-(14), and verify properties of the Reeb chords. Properties 1, 4, 5, 6, 8, and 9 are proved in this section. In Section 11.3, we verify the remaining Properties 2, 3, 7, and 10-19, which concern gradient vector fields of local difference functions.

11.1. **Gluing the square models together.** For each square type, the defining functions correspond in an obvious way to the sheets of the Legendrian. Explicitly, for squares with types (1)-(12) the function F_i corresponds to sheets S_i that are labeled in descending order as they appear above $(+1, +1)$; for the Type (13) square functions F_i correspond to sheets S_i which, when $i = k, k+1, k+2$, are only defined to the right of the cusp locus, while the function $\widetilde{F}_k$ corresponds to the sheet $\tilde{S}_k$ defined to the left of the cusp locus.

Proposition 11.1. *Fix any square type.*

(1) *Assume there are n_c sheets defined above the corner $c = (c_1, c_2)$. (Here, $c_i \in \{\pm 1\}$). Suppose that for some $1 \le j \le n_c$, the defining function F corresponds to the sheet that appears in position j above c. Then, for $|x_i - c_i| \le 1/16$,*

$$F(x_1, x_2) = (n_c - j)\epsilon_2((x_1 - c_1)^2 + (x_2 - c_2)^2 + 2). \tag{118}$$

(2) *Assume that along the edge E where $x_2 = e$ equals $+1$ or -1, $n_\pm$ sheets exist above $(\pm 1, e)$. Suppose that for some $1 \le j \le n_+$, the defining function F corresponds to the sheet above E that appears in position j (resp. $\sigma_-(j)$) at $(+1, e)$ (resp. at $(-1, e)$). Then, for $|x_2 - e| \le 1/16$ we have*

$$F(x_1, x_2) = (1 - \phi(x_1))(n_- - \sigma_-(j))\epsilon_2((x_2 - e)^2 + 1) + \phi(x_1)(n_+ - j)\epsilon_2((x_2 - e)^2 + 1) + f_j(x_1) \tag{119}$$

with f_j the 1-dimensional function associated to the edge type of E. A similar formula holds along edges of the form $x_1 = e$ equals $+1$ or -1.

Note that in (2), if E is a (Cu) edge type with $j = k$ or $k+1$, then we take $\sigma_-(k) = \sigma_-(k+1) = k - 0.5$ as usual.

Proof. Both statements follow from the formulas (64) and (116), together with the standard form of the 1-dimensional functions near $x = \pm 1$ stated in Corollary 9.6 (4) (and variants for the functions $f_{k-0.5}$, f_l^{ST}, and $\widehat{f}_{k+1}$).

In more detail, consider the U edge of a (1)-(12) square type, and suppose $|x_2 - 1| \le 1/16$. Then, (64) simplifies to

$$F_j(x_1, x_2) = f_j^U(x_1) + (1 - \phi(x_1))f^L_{\sigma_L(j)}(x_2) + \phi(x_1)f_j^R(x_2).$$

Note that σ_L agrees with σ_- as associated to the edge type of U, so the formula follows from Corollary 9.6 (4) (and Lemma 9.7 (4) in the case that U is a (Cu) edge and $j = k$ or $k+1$). For the D edge, when $|x_2 - (-1)| \le 1/16$,

$$F_i(x_1, x_2) = f^D_{\sigma_D(i)}(x_1) + (1 - \phi(x_1))f^L_{\sigma_L(i)}(x_2) + \phi(x_1)f_i^R(x_2).$$

Since F_i corresponds to the sheet that appears in position $\sigma_D(i)$ above D the $f^D_{\sigma_D(i)}(x_1)$ term is consistent with (119). The remaining two terms are seen to have the desired form via Corollary 9.6 (4) (and Lemma 9.7 (4) if necessary).

If in addition, $|x_1-(\pm 1)|\leq 1/16$, then (119) reduces to (118) after another application of Corollary 9.6 (4).

To conclude the proof we consider the (13) square type where the functions F_l, $l=k,k+1,k+2$ and $\widetilde{F}_k$ are defined by (116). When $|x_i-(\pm 1)|\leq 1/16$ for $i=1$ or 2, $\alpha(r)=1$ in (116), so for $l=k,k+1,k+2$, we have $F_l=G_l$ and $\widetilde{F}_k=H$. Observe that Lemma 10.8 together with (99)-(102) shows that, letting n_L be the number of sheets to the left of the cusp locus, for $|x_2-1|\leq 1/16$,

$$f^{ST}_k(x_2)=f^{ST}_{k+1}(x_2)=(n_L-(k-0.5))Q_+(x_2), \text{ and } f^{ST}_{k+2}(x_2)=(n_L-k)Q_+(x_2);$$

and for $|x_2-(-1)|\leq 1/16$,

$$f^{ST}_k(x_2)=f^{ST}_{k+2}(x_2)=(n_L-(k-0.5))Q_-(x_2), \text{ and } f^{ST}_{k+1}(x_2)=(n_L-k)Q_-(x_2).$$

Moreover, in (103)-(105) and (106) when $|x_2-(\pm 1)|\leq 1/16$ all appearances of the functions $\widehat{f}_{k+1}$ and $\widehat{f}_{k+2}$ are with 0 coefficients. It follows that F_l and $\widetilde{F}_k$ have the required form near the edges U and D.

Near the R edge, when $|x_1-1|\leq 1/16$, in (103)-(105), we have $\phi(x_1)=1$; and $\widehat{f}_{k'}(x_1)=f^U_{k'}(x_1)=f^D_{k'}(x_1)$ for $k'=k+1,k+2$ so that $F_l(x_1,x_2)=f^R_l(x_2)+(1-\phi(x_2))f^D_{\sigma_D(l)}(x_2)+\phi(x_2)f^U_l(x_1)$ as with all the other square types. Finally, near the L edge when $|x_1-(-1)|\leq 1/16$, we have $\widehat{f}_{k+1}(x_1)=f^U_{k+2}(x_1)$ by (79), so that

$$\widetilde{F}_k(x_1,x_2)=H(x_1,x_2)=f^U_{k+2}(x_1)+f^L_k(x_2)=f^D_{k+2}(x_1)+f^L_k(x_2).$$

□

Recall from Section 5.2 that we have for any 0-cell a neighborhood, $N(e^0_\alpha)$. Using polar coordinates in a smooth chart centered at e^0_α, $N(e^0_\alpha)$ is the subset $\{(r,\theta)\,|\,0\leq r\leq 1/16\}$.

Proposition 11.2. *Suppose that n_c sheets exist above e^0_α. Then, in coordinates on $N(e^0_\alpha)$, the local defining functions of $\tilde{L}_0$ are given by*

$$F_i(r,\theta)=(n_c-i)\epsilon_2(r^2+2), \quad \text{for } i=1,\dots,n_c \tag{120}$$

Proof. The intersection of $N(e^0_\alpha)$ with a square containing e^0_α is a ball of radius 1/16 centered at the corner of $[-1,1]\times[-1,1]$ corresponding to e^0_α, and the distance from the corner agrees with the coordinate r on $N(e^0_\alpha)$. (See Section 3.1 (2).) Thus, (120) follows from Proposition 11.1 (1). □

Any 1-cell, e^1_α, appears as an edge of precisely two 2-cells of $\mathcal{E}_{\Cap}$. Recall that the regularity requirement (3) from Section 3.1 allows us to combine the coordinates of these bordering 2-cells to smoothly parametrize a neighborhood of e^1_α by $(-1,1)\times(-1/16,1/16)$. (This neighborhood consists of the portion of the interior of the bordering 2-cells that lies within 1/16 from e^1_α.)

Proposition 11.3. *Let f_i be the one dimensional defining functions associated to the edge type of e^1_α, and let $n_\pm$ and σ_- be as in Proposition 11.1. Above the subset $(-1,1)\times(-1/16,1/16)$ the defining functions for $\tilde{L}_0$ have the form*

$$F_i(x_1,x_2)=f_i(x_1)+\big[(1-\phi(x_1))(n_- -\sigma_-(i))+\phi(x_1)(n_+-i)\big]\epsilon_2(x_2^2+1) \tag{121}$$

for $1\leq i\leq n_+$.

Moreover, the critical points of $F_{i,j}$ located along $(-1,1)\times\{0\}$ are precisely the points $(x_1,0)$ with x_1 a critical point of $f_{i,j}$.

Proof. When parametrizing by $(-1,1)\times(-1/16,1/16)$, the $[-1,1]\times[-1,1]$ parametrizations of the two bordering squares are shifted (and possibly reflected) so that the edge corresponding to e^1_α is at $x_2=0$. Thus, x_2^2 in the current formula corresponds to $(x_2-e)^2$ in (119), and (121) follows from Proposition 11.1 (2).

For the statement concerning critical points of $F_{i,j}$, note that

$$\partial_{x_2}F_{i,j}(x_1,0)\equiv 0 \quad \text{and} \quad (\partial_{x_1}F_{i,j})|_{[-1,-1/4]\cup[1/4,1]}=d_xf_{i,j}(x_1),$$

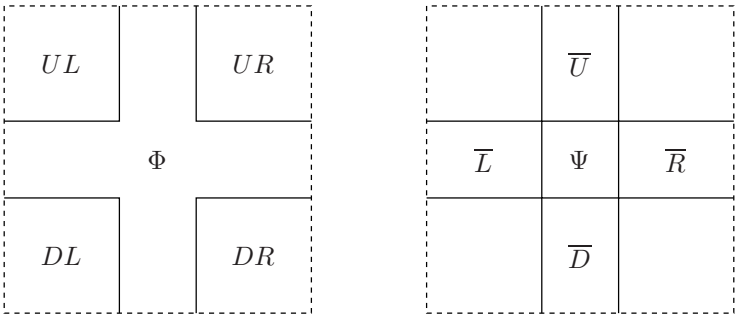

FIGURE 75. Notations used for different subsets of $[-1,1]\times[-1,1]$.

while for $x_1 \in [-1/4, 1/4]$ both $\partial_{x_1} F_{i,j}(x_1, 0)$ and $d_x f_{i,j}(x_1)$ are non-vanishing. [For $d_x f_{i,j}(x_1)$, this follows from item (2) of Propositions 9.4 and 9.5. For $\partial_{x_1} F_{i,j}(x_1, 0)$, using item (5) of the same propositions (with the values of the $y_{i,j}$ found above Proposition 9.4) we see that either:

(a.) $d_x f_{i,j}(x_1) > 1/8$ and therefore dominates the other term of

$$\partial_{x_1} F_{i,j}(x_1, 0) = d_x f_{i,j}(x_1) + d_x\phi(x_1)\left[(j-i) - (\sigma_-(j) - \sigma_-(i))\right]\epsilon_2 \tag{122}$$

in absolute value. (Using (63) the second term is bounded by $3 \cdot 2N\epsilon_2$.)

(b.) Or, e^1_α is a (1Cr) edge with S_i and S_j crossing above L. In this case, the second term becomes $d_x\phi(x_1)2\epsilon_2$, so that both terms in (122) have the same sign.

□

Corollary 11.4. *The Legendrian $\tilde{L}_0$ formed by piecing together the local defining functions assigned to the square types (1)-(14) above the transverse square decomposition $\mathcal{E}_{\Uparrow}$ is a smooth Legendrian submanifold of $J^1(S)$. Moreover, there exists a Riemannian metric on S such that the gradients of all local difference functions agree with the Euclidean gradients computed in $[-1,1]\times[-1,1]$ coordinates on each square.*

Proof. Smoothness follows from Propositions 11.2 and 11.3, since the interiors of the given neighborhoods of 0-cells and 1-cells, together with the 2-cells themselves form an open cover of S. In each of these regions, the coordinate formulas show that the front projection of $\tilde{L}_0$ is smooth except at cusp edges and swallowtail points which have been arranged to be standard so that the Legendrian $\tilde{L}_0$ is smooth in $J^1(S)$. (Smoothness in the interior of Type (13)-(14) squares was established in Lemma 10.11.)

Proposition 11.2 shows that Construction 3.1 may be applied to produce the required metric on S. □

11.2. **Properties involving Reeb chords, cusp loci and crossing loci.**

Proposition 11.5. *Consider the functions $F_i : [-1,1]\times[-1,1] \to \mathbb{R}$ defined in (64) (for (1)-(12) square types) or (116) (for (13)-(14) square types). In each case, the singular set of the Legendrian front defined by the F_i (and $\widetilde{F}_k$ in the (13)-(14) case) topologically agrees with the singular set prescribed by the square type. Moreover the crossing and/or cusp loci (if they exist) satisfy Property 1.*

Note that this proves the first itemized claim of Theorem 5.1.

Before we prove this proposition, we spend some time confirming that there are no unintentional Reeb chords. Locations of Reeb chords along the boundary of a square I^2 are determined by Propositions 11.2 and 11.3. In Lemmas 11.6 and 11.7, we identify all Reeb chords in the interior, $Int(I^2)$.

Let

$$\Phi := \{(x_1, x_2) \mid |x_i| < 1/4 \text{ for some } i\} \cap Int(I^2), \tag{123}$$

$$\Psi := \{(x_1, x_2) \mid |x_i| < 1/4 \text{ for both } i\}. \tag{124}$$

Label the four components of $Int(I^2)\setminus\Phi$ as XY where $X \in \{U, D\}$ and $Y \in \{R, L\}$ according to which two edges (up, right, down, left) of ∂I^2 intersect the closure of XY. Label each of the four components of $\Phi \setminus \Psi$ as $\overline{U}, \overline{R}, \overline{D}, \overline{L}$ based on which boundary sits in the component's closure. See Figure 75.

Lemma 11.6. *The difference function $F_{i,j}$ for two sheets has a critical point at (x_1, x_2) in the interior XY if and only if $F_{i,j}$ has a critical point on edge X at $(x_1, \pm 1)$ and a critical point on edge Y at $(\pm 1, x_2)$. (This includes the statement that if $F_{i,j}$ is not defined above X or Y due to a cusp edge, then $F_{i,j}$ has no critical points in XY.)*

Proof. For squares (1)-(12), since $|x_1| \geq 1/4$ and $|x_2| \geq 1/4$,

$$F_{i,j}(x_1, x_2) = (f^X_{i'} - f^X_{j'})(x_1) + (f^Y_{i''} - f^Y_{j''})(x_2) \tag{125}$$

for appropriate i', j' and i'', j''. If sheets S_i and S_j exist above X and Y, then the result follows from (125) and Proposition 11.3. If either S_i or S_j does not exist over X, then (i) Y must be a (Cu) edge and (ii) within XY we have $-1 < x_2 \leq -1/4$. From item (2) of Proposition 9.5 (and Lemma 9.7, in the case of the (11) square), it follows that

$$\partial_{x_2} F_{i,j}(x_1, x_2) = d_x(f^Y_{i''} - f^Y_{j''})(x_2)$$

is non-zero. A similar argument applies if S_i or S_j does not exist over Y.

For squares (13) and (14), recall $\alpha(r) = 1$ in (116). So (125) remains valid if we allow for the possibility that one or more of the f's above could be of type f^{ST}, see (103)-(106). Above UL and DL where some sheets are not defined and the f^{ST} functions may appear, the f^U and f^D functions are (Cu) functions, so that $\partial_{x_2} F_{i,j}(x_1, x_2) \neq 0$ as above.

□

Lemma 11.7. *For any pairs of sheets (i, j) in any of the 14 squares, $F_{i,j}$ has no critical points in Φ.*

Proof. Sections 11.2.1 and 11.2.2 constitute the proof of this lemma, in which we treat the non-swallowtail and swallowtail cases separately.

For squares (1)-(12), we show in Lemmas 11.9, 11.10 and 11.11 that $F_{i,j}$, for $i < j$, has no critical points in $\overline{U}$, $\overline{D}$, and Ψ. The arguments for $\overline{L}$ and $\overline{R}$ are similar, provided we consider all reflections in the $x_1 = x_2$ line of the square types (1)-(12) . To indicate this, let (n') label the reflected square type (n).

We then show in Lemmas 11.15 and 11.14 how slight modifications apply to square (13) for $\overline{U}, \overline{R}, \overline{D}, \Psi$. The argument for $\overline{L}$ given in Lemma 11.16 is more substantial. Square (14) is analogous to (13).

□

11.2.1. *Proof of Lemma 11.7 for squares (1)-(12).* First we prove a technical Lemma which will be used to prove Lemma 11.9.

Lemma 11.8. *Fix $i < j$ and a square (1)-(12). Then,*

$$\begin{aligned} \sigma_L(i) < \sigma_L(j) \quad &\longrightarrow \quad \partial_{x_1} F_{i,j}|_{[-1/4,1/4]\times[1/4,3/4]} > 1/5 \\ \sigma_D(i) < \sigma_D(j) \quad &\longrightarrow \quad \partial_{x_2} F_{i,j}|_{[1/4,3/4]\times[-1/4,1/4]} > 1/5, \end{aligned}$$

with the single exception of a Type (4) square with $(i, j) = (k, k+1)$ in which case the first inequality fails.

Proof. Say $\sigma_L(i) < \sigma_L(j)$ and $(x_1, x_2) \in [-1/4, 1/4] \times [1/4, 3/4]$. We prove

$$\partial_{x_1} F_{i,j}(x_1, x_2) = d_x f^U_{i,j}(x_1) + d_x\phi(x_1)(f^R_{i,j}(x_2) - f^L_{\sigma_L(i),\sigma_L(j)}(x_2)) > 1/5.$$

We prove the second implication at the same time by considering the reflected square types (n') as well.

For $X = U, D, R, L$, let $y^X_{i,j}$ denote the $y_{i,j}$ value which satisfies

$$|f^X_{i,j}(x) - y_{i,j}| < N\epsilon_1, \quad \text{for } x \in [1/4, 3/4]$$

as stated in (2) of Propositions 9.4 and 9.5. [The values of $y_{i,j}$ are listed above Proposition 9.4.] If U or R is a (Cu) edge we need to allow i and/or j to have the form $k - 0.5$ when $X = L$ or D. In these cases, we let $y^X_{i,j}$ denote the appropriate constant $C_{i,k-.5}$ or $C_{k-.5,j}$ from Lemma 9.7 (2), or 0 if

$i = j = k - 0.5$. Since $-1/4 \le x_1 \le 1/4$ and $1/4 \le x_2 \le 3/4$, the previous inequality and item (5) of Corollary 9.6 and Lemma 9.7 give

$$|d_x f^U_{i,j}(x_1) - 2y^U_{i,j}| < N\epsilon_1, \quad |f^R_{i,j}(x_2) - y^R_{i,j}| < N\epsilon_1,$$
$$|f^L_{\sigma_L(i),\sigma_L(j)}(x_2) - y^L_{\sigma_L(i),\sigma_L(j)}| < N\epsilon_1.$$

We have that $\sigma_L(i) < \sigma_L(j)$ implies $y^U_{i,j} \ge 1/8$. [The only case in which $y_{i,j} < 1/8$ is when sheets i and j cross along a 1-crossing edge.] So if $f^R_{i,j}(x_2) - f^L_{\sigma_L(i),\sigma_L(j)}(x_2) \ge 0$, then the lower bound of 1/5 holds. If $f^R_{i,j}(x_2) - f^L_{\sigma_L(i),\sigma_L(j)}(x_2) \le 0$, then (using also (63))

$$\begin{aligned} d_x f^U_{i,j}(x_1) + d_x\phi(x_1)(f^R_{i,j}(x_2) - f^L_{\sigma_L(i),\sigma_L(j)}(x_2)) &\ge 2y^U_{i,j} - N\epsilon_1 + (2+\epsilon_2)((y^R_{i,j} - N\epsilon_1) - (y^L_{\sigma_L(i),\sigma_L(j)} + N\epsilon_1)) \\ &\ge 2(y^U_{i,j} + y^R_{i,j} - y^L_{\sigma_L(i),\sigma_L(j)}) - 20N\epsilon_1. \end{aligned}$$

Thus, the lemma follows once we verify

$$y^U_{i,j} + y^R_{i,j} - y^L_{\sigma_L(i),\sigma_L(j)} \ge 1/8. \tag{126}$$

It suffices to show equation (126) for all consecutive pairs, $j = i+1$ since the other cases $j > i+1$ follow. [If $L_{i,j}$ denotes the left hand side of the inequality, then we have $L_{i,m} + L_{m,j} = L_{i,j}$.] Moreover, $y^U_{i,i+1} = y^R_{i,i+1} = y^L_{i,i+1} = 1$ if neither i or $i+1$ is a crossing or cusp sheet, so in this case the left hand side of (126) is 1.

For squares (2)-(6), (8)-(9) and (12), suppose the single crossing/cusp edges involve sheets (S_k, S_{k+1}) and/or (S_{k+1}, S_{k+2}), and the double crossing involves sheets (S_k, S_{k+1}, S_{k+2}). Then, in squares (2), (3), (4), (9) (and their reflections) we need only show equation (126) for pairs (S_{k-1}, S_k), (S_k, S_{k+1}), (S_{k+1}, S_{k+2}), and in squares (5), (6), (8), (12) (and their reflections) we need only consider pairs (S_{k-1}, S_k), (S_k, S_{k+1}), (S_{k+1}, S_{k+2}), (S_{k+2}, S_{k+3}).

For squares (7), (10), (11) (and their reflections), assume the crossing/cusp involves two pairs of sheets, S_k, S_{k+1} (vertical locus) and S_l, S_{l+1} (horizontal locus). By interchanging the role of (n) and (n') if necessary, we may assume without loss of generality that $k+1 < l$. However, this assumption requires us to consider two versions of square (10), denoted (10a) and (10b) where the vertical locus is respectively a cusp locus and a crossing locus. Moreover, we only consider the case $k+1 = l-1$, since for all other cases the crossing and cusp sheets are not adjacent so the calculation follows from squares (2) and (9). Thus for figures (7), (10), (11) (and their reflections) we need to consider pairs of sheets $(S_{k-1}, S_k), (S_k, S_{k+1}), (S_{k+1}, S_{k+2}), (S_{k+2}, S_{k+3}), (S_{k+3}, S_{k+4})$.

To avoid excessive sub/superscripts, we introduce notation (in the remainder of this proof only) to represent the different $y_{i,i+1}$ values as defined above Proposition 9.4.

$$a = 0,\ z = 1.5,\ y_0 = 1.125,\ y_1 = 0.625,\ y_2 = 0.125,\ y_3 = 2.125.$$

The below tables list the left-hand side of equation (126) for different sheet pairs and different squares. In all cases where $y^L_{\sigma_L(j),\sigma_L(j)}$ is of the form $C_{i,k-.5}$ or $C_{k-.5,j}$ we use the larger of the two possible values, and marked this term with *. (We have used a for the 0's that represent $y_{i,i+1}$ from a (1Cr) edge where i crosses $i+1$. Other 0's also appear in $y^L_{\sigma_L(k),\sigma_L(k+1)}$ when sheets k and $k+1$ meet at a cusp above U as in squares (9)-(12).)

Square \ Sheet Pair	(S_{k-1}, S_k)	(S_k, S_{k+1})	(S_{k+1}, S_{k+2})
(2)	$z+1-2$	$a+1--1$	$z+1-2$
(2′)	$1+z-z$	$1+a-a$	$1+z-z$
(3)	$1+1-z$	$1+1-a$	$1+1-z$
(4)	$1+z-1$	$1+a-1$	$1+z-1$
(4′)	$z+1-(z+a)$	$a+1-(-a)$	$z+1-(a+z)$
(9)	$1+1-1^*$	$1+1-0$	$1+1-1^*$
(9′)	$1+1-1$	$1+1-1$	$1+1-1$

	(S_{k-1}, S_k)	(S_k, S_{k+1})	(S_{k+1}, S_{k+2})	(S_{k+2}, S_{k+3})
(5)	$1 + y_0 - y_0$	$1 + y_1 - y_1$	$1 + y_2 - y_2$	$1 + y_3 - y_3$
(5′)	$y_0 + 1 - 2$	$y_1 + 1 - 1$	$y_2 + 1 - (-2)$	$y_3 + 1 - 3$
(6)	$1 + y_0 - 1$	$1 + y_1 - z$	$1 + y_2 - a$	$1 + y_3 - z$
(6′)	$y_0 + 1 - (z + a)$	$y_1 + 1 - z$	$y_2 + 1 - (-a - z)$	$y_3 + 1 - (a + z + 1)$
(8)	$z + y_0 - (y_0 + y_1)$	$a + y_1 - -y_1$	$z + y_2 - (y_1 + y_2)$	$1 + y_3 - y_3$
(8′)	$y_0 + z - (1 + z)$	$y_1 + a - a$	$y_2 + z - (-z - a)$	$y_3 + 1 - 3$
(12)	$1 + y_0 - 1^*$	$1 + y_1 - 0$	$1 + y_2 - 1^*$	$1 + y_3 - 1$
(12′)	$y_0 + 1 - (1 + 1)$	$y_1 + 1 - 1$	$y_2 + 1 - (-1 - 1)$	$y_3 + 1 - 3$

	(S_{k-1}, S_k)	(S_k, S_{k+1})	(S_{k+1}, S_{k+2})	(S_{k+2}, S_{k+3})	(S_{k+3}, S_{k+4})
(7)	$z + 1 - 2$	$a + 1 - (-1)$	$z + z - (z + 1)$	$1 + a - a$	$1 + z - z$
(7′)	$1 + z - z$	$1 + a - a$	$z + z - (z + 1)$	$a + 1 - (-1)$	$z + 1 - 2$
(10a)	$1 + 1 - z^*$	$1 + 1 - 0$	$1 + z - z^*$	$1 + a - a$	$1 + z - z$
(10a')	$1 + 1 - 1$	$1 + 1 - 1$	$z + 1 - 2$	$a + 1 - (-1)$	$z + 1 - 2$
(10b)	$z + 1 - 2$	$a + 1 - (-1)$	$z + 1 - 2$	$1 + 1 - 1$	$1 + 1 - 1$
(10b')	$1 + z - z$	$1 + a - a$	$1 + z - z^*$	$1 + 1 - 0$	$1 + 1 - z^*$
(11)	$1 + 1 - 1^*$	$1 + 1 - 0$	$1 + 1 - 1^*$	$1 + 1 - 1$	$1 + 1 - 1$
(11′)	$1 + 1 - 1$	$1 + 1 - 1$	$1 + 1 - 1^*$	$1 + 1 - 0$	$1 + 1 - 1^*$

Plug in the values of z, y_0, y_1, y_2, y_3 to get that, with the exception of the (S_k, S_{k+1}) entry for the Type (4) square, each table entry is greater than the right-hand side of equation (126).

	(S_{k-1}, S_k)	(S_k, S_{k+1})	(S_{k+1}, S_{k+2})	(S_{k+2}, S_{k+3})	(S_{k+3}, S_{k+4})
(2)	0.5	2	0.5	N/A	N/A
(2′)	1	1	1	N/A	N/A
(3)	0.5	2	0.5	N/A	N/A
(4)	1.5	0	1.5	N/A	N/A
(4′)	1	1	1	N/A	N/A
(5)	1	1	1	1	N/A
(5′)	0.125	0.625	3.125	0.125	N/A
(6)	1.125	0.125	1.125	1.625	N/A
(6′)	0.625	0.125	2.625	.625	N/A
(7)	0.5	2	0.5	1	1
(7′)	1	1	0.5	2	0.5
(8)	0.875	1.25	0.875	1	N/A
(8′)	0.125	0.625	3.125	0.125	N/A
(9)	1	2	1	N/A	N/A
(9′)	1	1	1	N/A	N/A
(10a)	0.5	2	1	1	1
(10a')	1	1	0.5	2	0.5
(10b)	0.5	2	0.5	1	1
(10b')	1	1	1	2	0.5
(11)	1	2	1	1	1
(11′)	1	1	1	2	1
(12)	1.125	1.625	0.125	2.125	N/A
(12′)	0.125	0.625	3.125	0.125	N/A

□

Lemma 11.9. *Fix $i < j$ and a square (1)-(12). $F_{i,j}$ has no critical points in $\overline{U}$ or $\overline{R}$.*

Proof. By considering the reflected squares (1')-(12') as well, we only need to show there are no critical points in $\overline{U}$.

If $\sigma_L(i) \geq \sigma_L(j)$ and $(x_1, x_2) \in \overline{U}$, then the first two terms in

$$\partial_{x_1} F_{i,j}(x_1, x_2) = d_x f^U_{i,j}(x_1) + d_x\phi(x_1)(f^R_{i,j}(x_2) - f^L_{\sigma_L(i),\sigma_L(j)}(x_2))$$

are strictly positive and the third term is non-negative.

If $\sigma_L(i) < \sigma_L(j)$ and $(x_1, x_2) \in [-1/4, 1/4] \times [1/2, 3/4]$, then the result follows from Lemma 11.8, except when $(i, j) = (k, k+1)$ and the square is Type (4). In this exceptional case, $f^U_{i,j} = f^L_{\sigma_L(i),\sigma_L(j)} = f^{PV}_{k,k+1}$ and $f^R_{i,j}(x_2) = f^{1Cr}_{k,k+1}$ where $f^{PV}_{k,k+1}$ and $f^{1Cr}_{k,k+1}$ are the 1-dimensional functions defined in (40) and (42) during the proof of Proposition 9.4. Using (40) and (42) we explicitly evaluate

$$\partial_{x_1} F_{i,j}(x_1, x_2) = 2 + d_x\phi(x_1)(-1 + (1/6)\epsilon_1),$$

and using (63)

$$\partial_{x_1} F_{i,j}(x_1, x_2) > 2 + (2 + \epsilon_2)(-1 + (1/6)\epsilon_1) = (1/3)\epsilon_1 - \epsilon_2 + (1/6)\epsilon_1\epsilon_2 \geq (1/4)\epsilon_1 > 0.$$

If $\sigma_L(i) < \sigma_L(j)$ and $(x_1, x_2) \in \overline{U} \setminus [-1/4, 1/4] \times [1/2, 3/4]$, then

$$\partial_{x_2} F_{i,j}(x_1, x_2) = \phi(x_1) d_x f^R_{i,j}(x_2) + (1 - \phi(x_1)) d_x f^L_{\sigma_L(i),\sigma_L(j)}(x_2)$$

is a convex linear combination of strictly positive terms on $[-1/4, 1/4] \times [1/4, 1/2]$ and a convex linear combination of strictly negative terms on $[-1/4, 1/4] \times [3/4, 1)$.

□

Lemma 11.10. *Fix $i < j$ and a square (1)-(12). $F_{i,j}$ has no critical points in $\overline{D}$ or $\overline{L}$.*

Proof. By considering the reflected squares (1')-(12') as well, we only show that there are no critical points in $\overline{D}$. Note that if $(x_1, x_2) \in \overline{D}$ then

$$\partial_{x_1} F_{i,j}(x_1, x_2) = d_x f^D_{\sigma_D(i),\sigma_D(j)}(x_1) + d_x\phi(x_1)(f^R_{i,j}(x_2) - f^L_{\sigma_L(i),\sigma_L(j)}(x_2)), \tag{127}$$

$$\partial_{x_2} F_{i,j}(x_1, x_2) = \phi(x_1) d_x f^R_{i,j}(x_2) + (1 - \phi(x_1)) d_x f^L_{\sigma_L(i),\sigma_L(j)}(x_2). \tag{128}$$

Case 1: R is a (Cu) edge.

In this case, for x_2 in the domain of $f^R_{i,j}$, we always have

$$f^R_{i,j}(x_2) \geq 0, \quad \text{and} \quad d_x f^R_{i,j}(x_2) \geq 0$$

with equality only when $(i, j) = (k, k+1)$ and $x_2 = -3/8$, by (1), (2), and (8') of Proposition 9.5, and

$$\begin{aligned} d_x f^D_{\sigma_D(i),\sigma_D(j)}(x_1) &> 0, \qquad \text{for } (i,j) \neq (k,k+1), \\ d_x f^D_{\sigma_D(i),\sigma_D(j)}(x_1) &= 0, \qquad \text{for } (i,j) = (k,k+1). \end{aligned}$$

[Here, in addition to Proposition 9.4 (2) and Proposition 9.5 (2) and (8'), we use Lemma 9.7 (2).]

SubCase 1: $d_x f^L_{\sigma_L(i),\sigma_L(j)}(x_2) > 0$. Note that this includes the case where $(i, j) = (k, k+1)$ for $x_2 \neq 3/8$, since sheets S_k and S_{k+1} must meet above a cusp edge along edge L as well.

In this case, $\partial_{x_2} F_{i,j}(x_1, x_2) > 0$ is a convex combination of two strictly positive values.

SubCase 2: $d_x f^L_{\sigma_L(i),\sigma_L(j)}(x_2) \leq 0$. Since L is a (Cu) edge, it must be the case that $f^L_{\sigma_L(i),\sigma_L(j)}(x_2) \leq 0$ holds as well. As long as, $(i, j) \neq (k, k+1)$, then $\partial_{x_1} F_{i,j}(x_1, x_2) > 0$ since the first term in (127) is strictly positive and the second is non-negative. Finally, if $(i, j) = (k, k+1)$, then $x_2 = -3/8$ and the sheets in question meet at a cusp edge above (x_1, x_2) so that there is nothing to prove.

Case 2: Sheets S_k and S_{k+1} cross along D. Then, $\operatorname{sgn}(f^R_{i,j}(x_2)) = -\operatorname{sgn}(f^L_{\sigma_L(i),\sigma_L(j)}(x_2))$, and since

$$f^R_{i,j}(x_2) < 0 \longleftrightarrow \sigma_D(i) > \sigma_D(j) \longleftrightarrow d_x f^D_{\sigma_D(i),\sigma_D(j)}(x_1) < 0$$

all terms in equation (127) are of the same sign.

Case 3: All remaining cases. Since $\sigma_D(i) \neq \sigma_D(j)$; neither of these values are half integers; and sheets S_i and S_j do not cross above D, we see from Corollary 9.6 (5) that

$$\left| d_x f^D_{\sigma_D(i),\sigma_D(j)}(x_1) \right| > 2y^D_{i,j} - N\epsilon_1 \geq 2/8 - N\epsilon_1.$$

In addition, (63) together with Corollary 9.6 (3) and (if necessary) Lemma 9.7 (3) give

$$|d_x\phi(x_1)|(|f^R_{i,j}(x_2)| + |f^L_{\sigma_L(i),\sigma_L(j)}(x_2)|) \leq (2 + \epsilon_2)(N\epsilon_1 + N\epsilon_1) \leq 6N\epsilon_1.$$

Combining these inequalities, we have

$$|\partial_{x_1} F_{i,j}(x_1, x+2)| > 2/8 - N\epsilon_1 - 6N\epsilon_1 > 0.$$

□

Lemma 11.11. *Fix $i < j$ and a square (1)-(12). $F_{i,j}$ has no critical points in Ψ.*

Proof. **Main case:** After possibly reflecting across $x_1 = x_2$, suppose that

(1) S_i and S_j do not meet one another at a crossing or cusp along U;
(2) $d_x f^L_{\sigma_L(i),\sigma_L(j)}(x) \geq 1/10$ for $-1/4 \leq x \leq 1/4$; and
(3) S_i and S_j are not the crossing sheets in a Type (4) square.

We will show that for $(x_1, x_2) \in \Psi$,

$$\begin{aligned} \partial_{x_2} F_{i,j} &= \phi(x_1) d_x f^R_{i,j}(x_2) + (1-\phi(x_1)) d_x f^L_{\sigma_L(i),\sigma_L(j)}(x_2) \\ &+ d_x\phi(x_2)(f^U_{i,j}(x_1) - f^D_{\sigma_D(i),\sigma_D(j)}(x_1)) \end{aligned} \tag{129}$$

is positive.

Our assumption implies

$$f^U_{i,j}(x_1) > 0, \quad d_x f^L_{\sigma_L(i),\sigma_L(j)}(x_2) \geq 1/10. \tag{130}$$

In addition, since the case of a Type (4) square with S_i and S_j crossing is prohibited, we see from the estimate (126) proved in Lemma 11.8 (with U, D replacing R, L and vice versa, which amounts to interchanging the estimates for the Type (n) and (n') squares) that

$$y^R_{i,j} + y^U_{i,j} - y^D_{\sigma_L(i),\sigma_L(j)} \geq 1/8. \tag{131}$$

If $-1/4 \leq x_1 \leq -1/4 + \frac{1}{1000N}$ (recall $\epsilon_1 < \frac{1}{1000N}$), then we estimate

$$\begin{aligned} \partial_{x_2} F_{i,j} &\geq (1-\phi(x_1)) d_x f^L_{\sigma_L(i),\sigma_L(j)}(x_2) - d_x\phi(x_2) f^D_{\sigma_D(i),\sigma_D(j)}(x_1) \\ &\geq \left(1 - 2((-1/4 + \frac{1}{1000N}) + 1/4)\right) d_x f^L_{\sigma_L(i),\sigma_L(j)}(x_2) - (2+\epsilon_2)\left|f^D_{\sigma_D(i),\sigma_D(j)}(x_1)\right| \\ &\geq \left(1 - \frac{2}{1000N}\right)(1/10) - (3)\left(\frac{1}{1000N}(2y^D_{\sigma_D(i),\sigma_D(j)} + N\epsilon_1) + N\epsilon_1\right) \\ &\geq 1/10 - (\frac{2}{10000N} + \frac{6}{1000} + 6N\epsilon_1) > 0. \end{aligned}$$

[At the 1st inequality we used (130); at the 2nd inequality we used (63); at the 3rd inequality we used that $f^D_{\sigma_D(i),\sigma_D(j)}(x_1) = (x_1 + 1/4) d_x f^D_{\sigma_D(i),\sigma_D(j)}(-1/4) + f^D_{\sigma_D(i),\sigma_D(j)}(-1/4)$ and applied estimates from items (3) and (5) of Corollary 9.6 and Lemma 9.7; at the 4th inequality, we used $y_{l,m} \leq N$.] So the lemma holds in this region.

Finally, consider the region $-1/4 + \frac{1}{1000N} < x_1 \leq 1/4$. Assume $f^U_{i,j}(x_1) - f^D_{\sigma_D(i),\sigma_D(j)}(x_1) < 0$ since otherwise the left hand side of equation (129) is positive because of equation (130). We have

$$\begin{aligned} \partial_{x_2} F_{i,j} &\geq \phi(x_1) d_x f^R_{i,j}(x_2) + d_x\phi(x_2)(f^U_{i,j}(x_1) - f^D_{\sigma_D(i),\sigma_D(j)}(x_1)) \\ &\geq 2(x_1 + 1/4)(2y^R_{i,j} - N\epsilon_1) + (2+\epsilon_2)(f^U_{i,j}(x_1) - f^D_{\sigma_D(i),\sigma_D(j)}(x_1)) \\ &\geq 2(x_1 + 1/4)(2y^R_{i,j} - N\epsilon_1) \\ &+ (2+\epsilon_2)(2y^U_{i,j} - 2y^D_{\sigma_D(i),\sigma_D(j)} - 2N\epsilon_1)(x_1 + 1/4) \\ &- (2+\epsilon_2)(|f^U_{i,j}(-1/4)| + |f_{\sigma_D(i),\sigma_D(j)}(-1/4)|) \\ &= 4(x_1 + 1/4)\left(y^R_{i,j} + y^U_{i,j} - y^D_{\sigma_D(i),\sigma_D(j)}\right) \\ &+ (x_1 + 1/4)\left(-2N\epsilon_1 + 2y^U_{i,j}\epsilon_2 - 2y^D_{\sigma_D(i),\sigma_D(j)}\epsilon_2 - (2+\epsilon_2)(2N\epsilon_1)\right) \\ &- (2+\epsilon_2)(|f^U_{i,j}(-1/4)| + |f_{\sigma_D(i),\sigma_D(j)}(-1/4)|) \\ &\geq 4\left(\frac{1}{1000N}\right)(1/8) - (1/2)(10N\epsilon_1) - (3)(2N\epsilon_1) > 0. \end{aligned}$$

[We used in the 1st inequality (130); in the 2nd inequality item (5) of Corollary 9.6 and properties of ϕ from (63) including the estimate $\phi(x_1) \geq 2(x_1 + 1/4)$ which holds since $x_1 \geq \frac{1}{1000N}$; and in the 3rd inequality item (5) from Corollary 9.6 and Lemma 9.7. In the 4th inequality, we used that $-1/4 + \frac{1}{1000N} < x_1 \leq 1/4$, that $|2y_{l,m}\epsilon_2| \leq N\epsilon_1$ and $2 + \epsilon_2 < 3$, and applied (131) as well as item (3) from Corollary 9.6 and Lemma 9.7.]

Remaining cases: First, we determine those cases where the requirements (1)-(3) imposed in the main case can fail.

Lemma 11.12. *After possibly reflecting across $x_1 = x_2$, we can arrange that either S_i and S_j satisfy requirements (1)-(3) or one of the following conditions is satisfied:*

(A) *S_i and S_j cross above L and R.*
(B) *S_i and S_j cross above L and D.*
(C) *S_i and S_j are the crossing sheets of a Type (4) square.*
(D) *S_i and S_j belong to a Type (11) square with a cusp edge between sheets S_k and S_{k+1} above R and a cusp edge between S_{k+2} and S_{k+3} above U, and we have $i \in \{k, k+1\}$ and $j \in \{k+2, k+3\}$.*
(E) *S_i and S_j belong to a Type (12) square with $j = k+2$ and $i \in \{k, k+1\}$.*

Proof. The only time when condition (3) fails is as in (C). Notice that for any of the square types, it is the case that no pair of sheets meets (at a crossing or cusp) above both R and U. Therefore, reflecting across $x_1 = x_2$ if necessary, we may assume that S_i and S_j do not meet above U, so that (1) holds. Before considering condition (2), if either of S_i or S_j ends at a cusp edge, if necessary we attempt to reflect so that neither S_i or S_j meets a cusp edge above U. Such a reflection is possible except when we have

(D') a Type (11) square with the pairs of sheets S_k, S_{k+1} and S_l, S_{l+1} meeting at cusp edges and $i \in \{k, k+1\}$ and $j \in \{l, l+1\}$.

Moreover, condition (1) will still hold after this reflection except when S_i and S_j are as in (E), since this is the only instance where cusp sheets have crossings with another sheet.

Now, item (5) from Corollary 9.6 and Lemma 9.7, gives

$$d_x f^L_{\sigma_L(i),\sigma_L(j)} > y^L_{\sigma_L(i),\sigma_L(j)} - N\epsilon_1.$$

Since we have arranged that S_i and S_j do not meet above U so that $\sigma_L(i) < \sigma_L(j)$, we have $y^L_{\sigma_L(i),\sigma_L(j)} - N\epsilon_1 > 1/10$ as required by (2) except possibly when

- L is a (1Cr) edge with S_i and S_j crossing above L; or
- $\sigma_L(i) - \sigma_L(j) = 0.5$.

In the first case, either (A) or (B) holds. The second case, can only happen when at least one of S_i or S_j ends at a cusp edge above U, and as arranged above, this can only be when (D') is satisfied. In order for $\sigma_L(i) - \sigma_L(j) = .5$ it must be the case that the two pairs of cusping sheets are adjacent so that $(l, l+1) = (k+2, k+3)$. □

We now prove Lemma 11.11 for each of the cases (A)-(E).

(A): In this case, $d_x f^L_{\sigma_L(i),\sigma_L(j)}(x_2), d_x f^R_{i,j}(x_2), f^U_{i,j}(x_1)$, and $-f^D_{\sigma_D(i),\sigma_D(j)}(x_1)$ are all positive, so that $\partial_{x_2} F_{i,j} > 0$ follows from (129).

(B): This only occurs in the Type (3) square with $i = k$, and $j = k+1$. Since edge D is (1Cr), $sgn\left(f^D_{\sigma_D(k),\sigma_D(k+1)}(x_1)\right) = sgn(x_1)$ by item (1) of Proposition 9.4. Thus, when $x_1 < 0$, the argument from (A) applies, while when $x_1 \geq 0$ (in fact when $x_1 \geq -1/4 + 1/(1000N)$) the final estimate used in the Main Case applies.

(C): For the (4) square, with $(i, j) = (k, k+1)$, the 1-dimensional functions satisfy

$$d_x f^L_{\sigma_L(k),\sigma_L(k+1)}(x_2) \geq 2 - N\epsilon_1; \quad d_x f^R_{k,k+1}(x_2) > 0; \quad f^U_{i,j}(x_1) > 0;$$

$$sgn\left(f^D_{\sigma_D(k),\sigma_D(k+1)}(x_1)\right) = sgn\left(f^D_{k+1,k}(x_1)\right) = -sgn(x_1); \quad \text{and} \quad |f^D_{\sigma_D(k),\sigma_D(k+1)}(x_1)| < N\epsilon_1.$$

(The estimates are from items (2), (3), and (5) of Proposition 9.4.) When $x_1 > 0$, all terms in (129) are positive. When $x_1 \leq 0$,

$$(1-\phi(x_1))d_x f^L_{\sigma_L(k),\sigma_L(k+1)}(x_2) \geq (1/2)(2-N\epsilon_1)$$

and this dominates the only negative term $-d_x\phi(x_2)f^D_{\sigma_D(k),\sigma_D(k+1)}(x_1)$ which is bounded as

$$|-d_x\phi(x_2)f^D_{\sigma_D(k),\sigma_D(k+1)}(x_1)| < 3N\epsilon_1$$

using (63).

(D): In this case, $\sigma_L(i) = i \in \{k, k+1\}$ and $\sigma_L(j) = k+1.5$. The statement of Lemma 9.7 only explicitly gives that $d_x f^L_{i,k+1.5} > 2C_{i,k+1.5} - N\epsilon_1$ with $C_{i,k+1.5} \in \{y^L_{i,k+1}, y^L_{i,k+2}\}$. However, in examining the proof, since it is the sheet in position $k+2$ above edge L that is appears adjacent to the S_{k+2} and S_{k+3} cusp sheets above both U and D, the construction produces $C_{i,k+1.5} = y^L_{i,k+2}$, so that for $i \in \{k, k+1\}$ the estimate $d_x f^L_{i,k+1.5} > 1/10$ holds and the Main Case applies.

(E): For the Type (12) square (as pictured, and not reflected) with $i \in \{k, k+1\}$ and $j = k+2$, the 1-dimensional functions satisfy

$$d_x f^L_{\sigma_L(i),\sigma_L(j)}(x_2) = d_x f^L_{k-.5,k}(x_2) > 0, \quad d_x f^R_{i,j}(x_2) > 0,$$
$$f^U_{i,k+2}(x_1) > 0, \quad \text{and} \quad -f^D_{\sigma_D(i),\sigma_D(j)}(x_1) > 0$$

since $\sigma_D(i) > \sigma_D(j) = k$. Thus, all terms in (129) are positive.

□

11.2.2. *Proof of Lemma 11.7 for squares (13) and (14).* We focus on square (13) as the other is similar. In Lemmas 11.13-11.15, we prove there are no Reeb chords in $\Psi, \overline{U}, \overline{D}, \overline{R}$ by showing that for (x_1, x_2) in each of the various regions considered one of the $\partial_{x_i} F_{i,j}$ does not vanish. That there are no Reeb chords in $\overline{L}$ is proved in Lemma 11.16.

Outside of $\overline{L}$, we have $F_l = G_l$ in (116), $\widehat{f}_{k+1} = f^U_{k+1}$ in (79), and $\widehat{f}_{k+2} = f^U_{k+2}$ in (80). Plugging these into (103)-(105), we get

$$\begin{aligned}
\partial_{x_1} F_{i,j} &= \phi(x_2)d_x f^U_{i,j}(x_1) + (1-\phi(x_2))d_x f^D_{\sigma_D(i),\sigma_D(j)}(x_1) \\
&+ d_x\phi(x_1)(f^R_{i,j}(x_2) - f^{ST}_{i,j}(x_2)) \\
\partial_{x_2} F_{i,j} &= \phi(x_1)d_x f^R_{i,j}(x_2) + (1-\phi(x_1))d_x f^{ST}_{i,j}(x_2) \\
&+ d_x\phi(x_2)(f^U_{i,j}(x_1) - f^D_{\sigma_D(i),\sigma_D(j)}(x_1)).
\end{aligned} \tag{132}$$

Here $f^{ST}_{i,j} := f^{ST}_i - f^{ST}_j$, and $f^{ST}_i(x)$ is defined as $f^L_{\sigma_L(i)}(x)$ if $i \neq k, k+1, k+2$, and by (90)-(102) otherwise. Set $y^{ST}_{k-1,k} = 1$, $y^{ST}_{k,k+1} = 0 = y^{ST}_{k+1,k+2}$, $y^{ST}_{k+2,k+3} = 1$ and all other $y^{ST}_{i,i+1} = 1$. For $i < j$, make $y^{ST}_{i,j}$ the summation as done above Proposition 9.4. Note for $\{i,j\} \cap \{k, k+1, k+2\} = \emptyset$, $y^{ST}_{i,j} = y^L_{\sigma_L(i),\sigma_L(j)}$.

Lemma 11.13. *The $y^{ST}_{i,j} \geq 0$ satisfy properties analogous to Proposition 9.4 (2) and (5), and equation (126) holds. Namely,*

1. $|f^{ST}_{i,j}(x)| \leq y^{ST}_{i,j} + N\epsilon_1$ *if* $\{i,j\} \not\subset \{k, k+1, k+2\}$,
2. $|d_x f^{ST}_{i,j}|_{[-1/4,1/4]} - 2y^{ST}_{i,j}| \leq 7N\epsilon_1$ *for all* $i < j$,
3. $y^R_{i,j} + y^U_{i,j} - y^D_{\sigma_D(i),\sigma_D(j)} \geq 1/2 \geq 1/8$ *for all* $i < j$,
4. $y^U_{i,j} + y^R_{i,j} - y^{ST}_{i,j} \geq 1 \geq 1/8$ *for all* $i < j$.

Proof. (2): If we set

$$\sigma'(i) = \begin{cases} i, & i \leq k-1, \\ k, & i = k, k+1, k+2, \\ i-2, & i \geq k+3, \end{cases} \tag{133}$$

then for all $1 \leq i \leq n$ on $[-1/4, 1/4]$ we have

$$f^{ST}_i(x) = f^L_{\sigma'(i)}(x) + \delta_{i,k} \cdot \psi(x)(\widehat{f}_{k+2}(-3/8) - f^U_{k+1}(3/8)), \quad \text{and} \quad y^{ST}_{i,j} = y^L_{\sigma'(i),\sigma'(j)}.$$

Thus, using Corollary 9.6 (5), (89), and (88), we have

$$\begin{aligned}|d_x f^{ST}_{i,j}(x) - 2y^{ST}_{i,j}| &\leq |d_x f^{L}_{\sigma'(i),\sigma'(j)}(x) - 2y^{L}_{\sigma'(i),\sigma'(j)}| + |d_x\psi(x)(\widehat{f}_{k+2}(-3/8) - f^{U}_{k+1}(3/8))|\\ &\leq N\epsilon_1 + 3\cdot(N\epsilon_1 + N\epsilon_1) = 7N\epsilon_1.\end{aligned}$$

(1): For $i < k$, $k+2 < j$, and $l \in \{k, k+1, k+2\}$, since locally f^{ST}_l agrees with f^L_k or f^{ST}_k, the combination of (93) and item (2) of Proposition 9.4 show that $f^{ST}_{i,l}$ and $f^{ST}_{l,j}$ have positive (resp. negative) derivative on $(-1, 1/2]$ (resp. on $[3/4, 1)$). Within $[1/2, 3/4]$ $f^{ST}_l = f^L_k$, so we see that $f^{ST}_{i,l}$, $f^{ST}_{l,j}$ and $f^{ST}_{i,j}$ all have a unique local maximum in $[1/2, 3/4]$. This maximum agrees with the maximum of $f^L_{\sigma'(i),\sigma'(j)}$ which is within $N\epsilon_1$ of $y^{ST}_{i,j} = y^L_{\sigma'(i),\sigma'(j)}$ by Proposition 9.4 (2). The result follows.

(3) and (4): We compute $y^R_{i,i+1} + y^U_{i,i+1} - y^D_{\sigma_D(i),\sigma_D(i+1)}$. The general case follows.

$(i \leq k-1, i+1)$	$(k, k+1)$	$(k+1, k+2)$	$(k+2, k+3)$	$(i \geq k+3, i+1)$
$1+1-1$	$1.5+1-2$	$0+1-(-1)$	$1.5+1-2$	$1+1-1$

Similarly, $y^U_{i,i+1} + y^R_{i,i+1} - y^{ST}_{i,i+1}$ equals

$(i \leq k-1, i+1)$	$(k, k+1)$	$(k+1, k+2)$	$(k+2, k+3)$	$(i \geq k+3, i+1)$
$1+1-1$	$1+1.5-0$	$1+0-0$	$1+1.5-1$	$1+1-1$

□

Lemma 11.14. *For any pairs of sheets (i, j) in either square (13) or (14), $F_{i,j}$ has no critical points in Ψ.*

Proof. **Case 1:** $(i, j) = (k+1, k+2)$. For $(x_1, x_2) \in \Psi$ we have

$$\begin{aligned}F_{k+1,k+2}(x_1, x_2) =& \phi(x_1) f^R_{k+1,k+2}(x_2) + (1-\phi(x_1)) f^{ST}_{k+1,k+2}(x_2)\\ &+ \phi(x_2) f^U_{k+1,k+2}(x_1) + (1-\phi(x_2)) f^D_{k+2,k+1}(x_1)\\ =& \phi(x_1) f^R_{k+1,k+2}(x_2) + (2\phi(x_2) - 1) f^U_{k+1,k+2}(x_1);\end{aligned}$$

$$\begin{aligned}\partial_{x_1} F_{k+1,k+2} =& d_x\phi(x_1) f^R_{k+1,k+2}(x_2) + (2\phi(x_2)-1) d_x f^U_{k+1,k+2}(x_1);\\ \partial_{x_2} F_{k+1,k+2} =& \phi(x_1) d_x f^R_{k+1,k+2}(x_2) + 2 d_x\phi(x_2) f^U_{k+1,k+2}(x_1).\end{aligned}$$

Since R is a (1Cr) edge with sheets $k+1$ and $k+2$ crossing, we get using item (1) of Proposition 9.4 that $\operatorname{sgn}(\partial_{x_1} F_{k+1,k+2}(x_1, x_2)) = \operatorname{sgn}(x_2)$. Thus, $\partial_{x_1} F_{k+1,k+2}$ vanishes only when $x_2 = 0$ in which case

$$\partial_{x_2} F_{k+1,k+2}(x_1, 0) \geq 2 d_x\phi(0) f^U_{k+1,k+2}(x_1) = 4 f^U_{k+1,k+2}(x_1) > 0.$$

Case 2: $i = k$ and $j \in \{k+1, k+2\}$. From equations (63), (99)-(102), as well as Corollary 9.6 (5) we have

$$\phi(x_2) d_x f^U_{i,j}(x_1) + (1-\phi(x_2)) d_x f_{\sigma_D(i),\sigma_D(j)}(x_1) \geq 2\min\{y^U_{i,j}, y^D_{\sigma_D(i),\sigma_D(j)}\} - N\epsilon_1 = 2 - N\epsilon_1; \tag{134}$$

$$d_x\phi(x_1)(f^R_{i,j}(x_2) - f^{ST}_{i,j}(x_2)) \geq -d_x\phi(x_1) f^{ST}_{i,j}(x_2) \geq -(2+\epsilon_2)(\psi(x) 2N\epsilon_1) \geq -6N\epsilon_1. \tag{135}$$

So $\partial_{x_1} F_{i,j} > 0$.

Case 3: $\{i, j\} \not\subset \{k, k+1, k+2\}$. We use an argument almost identical to the one from the Main Case of the proof of Lemma 11.11, where $f^{ST}_{i,j}$ replaces $f^L_{\sigma_L(i),\sigma_L(j)}$ throughout. Recall that we split the proof into two regions: $\{-1/4 \leq x_1 \leq -1/4 + \frac{1}{1000N}\}$ and $\{-1/4 + \frac{1}{1000N} \leq x_1 \leq 1/4\}$.

In the first region, we used that $d_x f^L_{\sigma_L(i),\sigma_L(j)} \geq 1/10$ which still holds by Lemma 11.13 (2) along with properties of ϕ and the f^D, f^U, and f^R that remain true in square (13). The argument applies as written.

In the second region, $f^L_{\sigma_L(i),\sigma_L(j)}$ is never used other than in the first step which assumes $d_x f^L_{\sigma_L(i),\sigma_L(j)}(x_2) \geq 0$. The proof still applies with the estimates from Lemma 11.13 (3) and (4) used in place of (126).

□

Lemma 11.15. *For any pairs of sheets (i, j) in either square (13) or (14), $F_{i,j}$ has no critical points in $\overline{U}, \overline{D}, \overline{R}$.*

Proof. Note that in $\overline{R}$, the f_l^{ST} functions are not used and, since $x_1 \geq 1/4$, the f^U and f^D functions share all of the properties of the (PV) 1-dimensional functions. Thus, in this region, the result follows from the case of the (2') square.

We are left to consider the regions $\overline{U}$ and $\overline{D}$.

Case 1: $(i,j) = (k+1, k+2)$. We have

$$\forall (x_1,x_2) \in \overline{U}, \quad \partial_{x_1} F_{k+1,k+2}(x_1,x_2) = d_x f^U_{k+1,k+2}(x_1) + d_x\phi(x_1)(f^R_{k+1,k+2}(x_2) - f^{ST}_{k+1,k+2}(x_2));$$

$$\forall (x_1,x_2) \in \overline{D}, \quad \partial_{x_1} F_{k+1,k+2}(x_1,x_2) = d_x f^D_{k+2,k+1}(x_1) + d_x\phi(x_1)(f^R_{k+1,k+2}(x_2) - f^{ST}_{k+1,k+2}(x_2)).$$

For $x_1 \in [-1/4, 1/4]$, Corollary 9.6 (5) gives

$$|d_x f^U_{k+1,k+2}(x_1)| = |d_x f^D_{k+2,k+1}(x_1)| \geq 2 - N\epsilon_1 > 1.$$

Since sheets $k+1$ and $k+2$ cross along R which is a (1Cr) edge, Proposition 9.4 gives

$$|f^R_{k+1,k+2}(x_2)| < N\epsilon_1, \quad \forall x_2 \in [-1,1].$$

From (99)-(102) we see that

$$|f^{ST}_{k+1,k+2}(x_2)| = \begin{cases} |f^{ST}_k(x_2) - f^L_k(x_2)|, & x_2 \in [-1,-1/4] \cup [3/4,1], \\ 0 & x_2 \in [-1/4, 3/4], \end{cases}$$

so that (95) gives

$$|f^{ST}_{k+1,k+2}(x_2)| < 2N\epsilon_1, \quad \forall x_2 \in [-1,1].$$

Thus, for $(x_1,x_2) \in \overline{U} \cup \overline{D}$ we have

$$|\partial_{x_1} F_{k+1,k+2}(x_1,x_2)| > 1 - 3(N\epsilon_1 + 2N\epsilon_1) > 0.$$

Case 2: $i = k$ and $j \in \{k+1, k+2\}$. For $(x_1,x_2) \in \overline{U} \cup \overline{D}$, the inequality (134) still holds, and since

$$|f^{ST}_{i,j}(x_2)| \leq |f^{ST}_k(x_2) - f^L_k(x_2)| \leq 2N\epsilon_1$$

holds by (95) the inequality (135) remains valid as well. Thus, $\partial_{x_1} F_{i,j} > 0$.

Case 3: $\{i,j\} \not\subset \{k, k+1, k+2\}$. We follow an argument almost identical to the proofs of Lemmas 11.8, 11.9 and 11.10, mindful of the possible modifications done in the proof of Lemma 11.14: (i) $f^{ST}_{i,j}$ and $y^{ST}_{i,j}$ replace $f^L_{\sigma_L(i),\sigma_L(j)}$ and $y^L_{\sigma_L(i),\sigma_L(j)}$; (ii) equation (126) is replaced by (3) and (4) from Lemma 11.13.

For $(x_1,x_2) \in [-1/4, 1/4] \times [1/2, 3/4] \subset \overline{U}$, we see by applying modifications (i) and (ii) to the proof of Lemma 11.8 that

$$\partial_{x_1} F_{i,j} \quad = \quad d_x f^U_{i,j}(x_1) + d_x\phi(x_1)(f^R_{i,j}(x_2) - f^{ST}_{i,j}(x_2)) > 1/5.$$

(Here, Lemma 11.13 (1) is used to bound $|f^{ST}_{i,j}(x_2)|$ by $y^{ST}_{i,j} + N\epsilon_1$.) For $(x_1,x_2) \in \overline{U} \setminus [-1/4,1/4] \times [1/2,3/4]$,

$$\partial_{x_2} F_{i,j} \quad = \quad \phi(x_1) d_x f^R_{i,j}(x_2) + (1 - \phi(x_1)) d_x f^{ST}_{i,j}(x_2)$$

is a convex linear combination of terms of the same sign on the two components of $\overline{U} \setminus [-1/4,1/4] \times [1/2,3/4]$, see Lemma 10.8 and (91)-(102), with (94) used to check that $d_x f^{ST}_{i,j}(x_2)$ is negative for $x_2 \geq 3/4$.

Next, we apply modification (i) to the proof of Lemma 11.10. For $(x_1,x_2) \in \overline{D}$,

$$\partial_{x_1} F_{i,j} \quad = \quad d_x f^D_{\sigma_D(i),\sigma_D(j)}(x_1) + d_x\phi(x_1)(f^R_{i,j}(x_2) - f^{ST}_{i,j}(x_2)).$$

The right-hand side is non-zero from Corollary 9.6 (3) and (5), plus an application of (95) to bound $|f^{ST}_{i,j}(x_2)|$,

$$\left| d_x f^D_{\sigma_D(i),\sigma_D(j)}(x_1) \right| > 2y^D_{i,j} - N\epsilon_1 \geq 2 - N\epsilon_1,$$

$$|d_x\phi(x_1)|(|f^R_{i,j}(x_2)| + |f^{ST}_{i,j}(x_2)|) \leq (2+\epsilon_2)(N\epsilon_1 + 3N\epsilon_1).$$

□

Lemma 11.16. *For any pairs of sheets (i,j) in either square (13) or (14), $F_{i,j}$ has no critical points in $\overline{L}$.*

Proof. This statement is established by the following Claims 1-5.

Claim 1. For $i<j$ with $\{i,j\}\cap\{k,k+1,k+2\}=\emptyset$, we have $\partial_{x_1}F_{i,j}(x_1,x_2)>0$ and $\partial_{x_2}F_{i,j}(x_1,x_2)>0$ for all $(x_1,x_2)\in\overline{L}$.

In $\overline{L}$, (117) leads to $F_{i,j}(x_1,x_2)=f^L_{\sigma_L(i),\sigma_L(j)}(x_2)+f^U_{i,j}(x_1)$ (since $f^D_{\sigma_D(i),\sigma_D(j)}=f^U_{i,j}$). As $\sigma_L(i)<\sigma_L(j)$, $\partial_{x_2}F_{i,j}>0$ holds by Corollary 9.6 (5).

Claim 2. For $i<k$ and $j>k+2$, we have $\partial_{x_2}(F_i-w)(x_1,x_2)>0$ and $\partial_{x_2}(w-F_j)(x_1,x_2)>0$ for all $(x_1,x_2)\in(\text{domain of } w)\cap\overline{L}$ where w is any of F_k,F_{k+1},F_{k+2} or $\widetilde{F}_k$.

We prove the statement about F_i as a similar argument establishes the statement about F_j.

To begin, we compute and estimate $\partial_{x_2}(F_i-H)$. In $\overline{L}$, (64) and (106) give

$$F_i-H=f^L_i(x_2)+f^U_i(x_1)-f^L_k(x_2)-(1-\psi(x_2))f^U_{k+2}(x_1)-\psi(x_2)\widehat{f}_{k+1}(x_1),$$

so we have

$$\partial_{x_2}(F_i(x_1,x_2)-H(x_1,x_2))=d_xf^L_{i,k}(x_2)+d_x\psi(x_2)\cdot\left(f^U_{k+2}(x_1)-\widehat{f}_{k+1}(x_1)\right)\geq \tag{136}$$
$$1-|\psi'(x_2)|\cdot(|f^U_{k+2}(x_1)|+|\widehat{f}_{k+1}(x_1)|)\geq 1-3(N\epsilon_1+N\epsilon_1).$$

The bounds of 3 for $|\psi'(x_2)|$ and $N\epsilon_1$ for $|f^U_{k+2}|$ and $|\widehat{f}_{k+1}|$ on $[-1,-1/4]$ follow from (89), (88) and item (3) of Corollary 9.6. Next, (116) implies

$$H(x_1,x_2)-w(x_1,x_2)=-(1-\alpha(r))u(x_1,x_2)+\alpha(r)\cdot(H(x_1,x_2)-v(x_1,x_2))$$

where u is one of $C\,A_l$ or $C\,B$, and v is one of G_l or H with $l\in\{k,k+1,k+2\}$. (Here, (r,θ) is a polar coordinate centered at $(-3/8,0)$.) Thus, using that

$$|\partial_{x_2}(\alpha(r))|=\left|\alpha'(r)\cdot\frac{x_2}{\sqrt{(x_1+3/8)^2+x_2^2}}\right|\leq|\alpha'(r)|,$$

we have

$$|\partial_{x_2}(H-w)(x_1,x_2)|\leq|\alpha'(r)|\cdot|u(x_1,x_2)|+(1-\alpha(r))|\partial_{x_2}u(x_1,x_2)|+ \tag{137}$$
$$|\alpha'(r)|\cdot|H(x_1,x_2)-v(x_1,x_2)|+\alpha(r)|\partial_{x_2}(H-v)(x_1,x_2)|\leq$$
$$33\|u\|_{C^0(O_2)}+\|\partial_{x_2}u\|_{C^0(O_2)}+33\|H-v\|_{C^0(K)}+\|\partial_{x_2}(H-v)\|_{C^0(K)}\leq$$
$$33\epsilon_1+\epsilon_1+33(6N\epsilon_1)+18N\epsilon_1=250N\epsilon_1.$$

In the second to last line, the notation K is from Section 10.2.4 and we used (115). In the last line, we used (113) and Lemma 10.10.B1.

Now, combining (136) and (137) gives the desired inequality:

$$\partial_{x_2}(F_i-w)(x_1,x_2)\geq\partial_{x_2}(F_i-H)(x_1,x_2)-|\partial_{x_2}(H-w)(x_1,x_2)|\geq 1-6N\epsilon_1-250N\epsilon_1>0. \tag{138}$$

Claim 3. The only critical points of $F_{k,k+1}$ in the intersection of $\bar{L}$ with the domain of definition of $F_{k,k+1}$ are along the upper half of the cusp locus (where sheets k and $k+1$ meet at the cusp edge).

First, consider $(x_1,x_2)\notin V_1$ where V_1 is defined in (108). We have

$$\begin{aligned}\partial_{x_1}F_{k,k+1}(x_1,x_2) &= (1-\alpha(r))C\partial_{x_1}A_{k,k+1}(x_1,x_2)+\alpha(r)\cdot\partial_{x_1}G_{k,k+1}(x_1,x_2)\\ &+ [\partial_{x_1}(\alpha(r))]\cdot(G_{k,k+1}(x_1,x_2)-CA_{k,k+1}(x_1,x_2)).\end{aligned} \tag{139}$$

The combination of Lemmas 10.6.A3 and 10.10.B2 show that the sum of the first two terms is non-negative and, in fact, strictly positive everywhere except for the upper half of the cusp locus. The values of (x_1,x_2) where $\alpha'(r)$ is non-zero and $F_{k,k+1}$ is defined consist of only the right half of the annulus $A=O_2\setminus O_1$, and in this half the chain rule gives $\partial_{x_1}(\alpha(r))\geq 0$. In addition, since $(x_1,x_2)\notin V_1$, (109) and (112) give $G_{k,k+1}(x_1,x_2)-A_{k,k+1}(x_1,x_2)>0$. Thus, for such (x_1,x_2) we have shown

$$\partial_{x_1}F_{k,k+1}(x_1,x_2)\geq 0$$

with equality only along the upper half of the cusp locus.

In the remaining case of $(x_1,x_2)\in V_1$ we show that $\partial_\theta F_{k,k+1}(x_1,x_2)<0$ unless (x_1,x_2) belongs to the cusp locus. Note that since $\partial_\theta(\alpha(r))=0$, we simply have

$$\partial_\theta F_{k,k+1}(x_1,x_2)=(1-\alpha(r))\cdot\partial_\theta A_{k,k+1}(x_1,x_2)+\alpha(r)\cdot\partial_\theta G_{k,k+1}(x_1,x_2). \tag{140}$$

The definition of V_1 and trigonometry show that $x_2 \geq \sqrt{3}R_1/2 > R_1/2$, so that both Lemmas 10.6.A5 and 10.10.B4 apply. Lemma 10.10.B2 and B4 place $\nabla G_{k,k+1}(x_1, x_2)$ in the 4-th quadrant where the angle from the positive x-axis is between $-\pi/2$ and 0, while Lemmas 10.6.A5 has the angle between $\nabla A_{k,k+1}(x_1, x_2)$ and the positive x-axis bounded between $-\pi/2$ and $+\pi/4$. On the other hand, in V_1 $\partial/\partial\theta$ has angle between $5\pi/6$ and π and equal to π only along the cusp edge. Thus, except at the cusp edge the angle between $\partial/\partial\theta$ and either gradient is strictly larger than $\pi/2$, so geometric properties of the dot product give that both

$$\partial_\theta A_{k,k+1}(x_1, x_2) = \frac{\partial}{\partial\theta} \bullet \nabla A_{k,k+1}(x_1, x_2) \leq 0 \quad \text{and} \quad \partial_\theta G_{k,k+1}(x_1, x_2) = \frac{\partial}{\partial\theta} \bullet \nabla G_{k,k+1}(x_1, x_2) \leq 0$$

where in both cases equality holds only along the upper half of the cusp locus. At other points the gradient vectors are non-zero by Lemmas 10.6.A3 and 10.10.B2.

Claim 4. The only critical points of $F_{k,k+2}$ in its domain of definition are along the lower half of the cusp locus (where sheets k and $k+2$ meet at the cusp edge).

Arguments parallel to those used in Claim 3 show that $\partial_{x_1} F_{k,k+2}(x_1, x_2) > 0$ everywhere except V_2 and the lower half of the cusp locus, while, in V_2, $\partial_\theta F_{k,k+2}(x_1, x_2) > 0$ except at the cusp locus.

Claim 5. The only critical point of $F_{k+1,k+2}$ in its domain of definition is at the swallowtail point (where sheets $k+1$ and $k+2$ merge together).

For $(x_1, x_2) \notin V_3$ (see (110)), we check that $\operatorname{sgn}(\partial_{x_1} F_{k+1,k+2}(x_1, x_2)) = \operatorname{sgn}(x_2)$ as follows. The computation of $\partial_{x_1} F_{k+1,k+2}(x_1, x_2)$ is as in (139) with subscripts $k, k+1$ replaced with $k+1, k+2$. Lemmas 10.6.A3 and 10.10.B2 give that

$$\operatorname{sgn}\left((1-\alpha(r)) \cdot \partial_{x_2} A_{k+1,k+2}(x_1, x_2) + \alpha(r) \cdot \partial_{x_2} G_{k+1,k+2}(x_1, x_2)\right) = \operatorname{sgn}(x_2),$$

while (111) and (112) together with the fact that $\operatorname{sgn}(A_{k+1,k+2}) = \operatorname{sgn}(G_{k+1,k+2}) = \operatorname{sgn}(x_2)$ (from the location of the crossing locus) show that $(\partial_{x_1}(\alpha(r)))\,(G_{k+1,k+2}(x_1, x_2) - A_{k+1,k+2}(x_1, x_2))$ is greater than (resp. less than) or equal to 0 when $x_2 > 0$ (resp. when $x_2 < 0$). Putting these observations together completes the check.

Finally, if $(x_1, x_2) \in V_3$, then the defining property (110) of V_3 shows that $\partial_\theta F_{k+1,k+2} > 0$ since the computation of $\partial_\theta F_{k+1,k+2}$ is as in (140). In addition, for points not in V_3 but belonging to the crossing locus (where $x_2 = 0$), Lemma 10.6.A4 and Lemma 10.10.B3 show that $\partial_\theta F_{k+1,k+2} > 0$.

□

We now prove Proposition 11.5.

Proof. For squares (1)-(12):

Step 1: The cusp loci are as described in Property 1, i.e. vertical (resp. horizontal) cusp loci agree with $\{x_1 = -3/8\}$ (resp. $\{x_2 = -3/8\}$).

Suppose a cusp locus occurs on edges U and D involving S_k, S_{k+1}, as in squares (9)-(12). (The case of a cusp locus connecting edges L and R, which only occurs in square (11), is similar.) Then, $f^L_{\sigma_L(k),\sigma_L(k+1)}(x_2) = 0$, and edges U and D are (Cu) edges with cusps between $k, k+1$ and $\sigma_D(k), \sigma_D(k+1)$ respectively. Therefore, using Proposition 9.5 (8'), for $x_1 \in [-3/8, -3/8 + \epsilon_2]$, the formula for $F_{k,k+1}(x_1, x_2)$ reduces to

$$F_{k+1,k+2}(x_1, x_2) = 2(x_1 + 3/8)^{3/2},$$

so that the sheets meet at a cusp edge along $x_1 = -3/8$.

Step 2: All crossing loci are as in Property 1, i.e. they must sit inside Φ.

For $X \in \{U, D\}, Y \in \{R, L\}$, we need to show sheets S_i and S_j do not cross in the region XY (from Figure 75). For squares (1)-(12), we have

$$F_{i,j}|_{XY}(x_1, x_2) = f^X_{i',j'}(x_1) + f^Y_{i'',j''}(x_2) \tag{141}$$

for some i', j', i'', j'' (some of which may be half integers). Here, $i' = j'$ (resp. $i'' = j''$) occurs only when $X = D$ (resp. $Y = L$) and sheets S_i and S_j meet at a cusp above R and L (resp. U and D). These conditions cannot simultaneously occur. In the case $i' = j'$ (the case $i'' = j''$ is similar), we get that $F_{i,j}|_{XY}(x_1, x_2) = f^Y_{i'',j''}(x_2)$ and $f^Y_{i'',j''}$ is a function for a (Cu) edge type with i'' and j'' the cusp

sheets. From Proposition 9.5 (8'), we see that $(f^Y_{i'',j''})^{-1}(0) = \{-3/8\}$, so the only place that sheets S_i and S_j meet within XY is at their cusp edge.

We are left to consider the case when $i' \neq j'$ and $i'' \neq j''$. Note that:

(i) By item (1) from Propositions 9.4 and 9.5 and item (1) from Lemma 9.7, we have (possibly empty)
$$(f^X_{i',j'})^{-1}(0), (f^Y_{i'',j''})^{-1}(0) \subset [-1/4, 1/4].$$

(ii) For $(x_1, x_2) \in XY$, $\mathrm{sgn}(f^X_{i',j'}(x_1)) = \mathrm{sgn}(f^Y_{i'',j''}(x_2))$. [This is because $\mathrm{sgn}(f^X_{i',j'}(x_1))$ (resp. $\mathrm{sgn}(f^Y_{i'',j''}(x_2))$) is determined by whether S_i appears above or below S_j along the portion of edge X (resp. edge Y) that borders XY. But, edges X and Y meet at the corner of XY, so these signs are the same.]

Combining (i) and (ii) shows that (141) is never 0 in XY.

Step 3: Along a cusp edge, the only time that a third sheet (not one of the cusp edge sheets) intersects the cusp edge is in the Type (12) square where S_{k+2} crosses the cusp edge of S_k and S_{k+1} at a single point $(-3/8, x_2)$ with $x_2 \in [-1/4, 1/4]$.

In verifying, we restrict to the case of a vertical cusp edge between sheets S_k and S_{k+1}, and make use of items (1) and (2) from Lemma 9.7. For $i \notin \{k, k+1\}$, and, in the case of square (12), $i \neq k+2$, the three terms $f^L_{\sigma_L(i),\sigma_L(k)}(x_2)$, $f^U_{i,k}(-3/8)$, and $f^D_{\sigma_D(i),\sigma_D(k)}(-3/8)$ all share the same (strict) sign which is positive if $i < k$ and negative if $k+1 < i$. Thus,
$$F_{i,k}(-3/8, x_2) = f^L_{\sigma_L(i),\sigma_L(k)}(x_2) + \phi(x_2) f^U_{i,k}(-3/8) + (1 - \phi(x_2)) f^D_{\sigma_D(i),\sigma_D(k)}(-3/8)$$
is non-zero everywhere.

For square (12) with $i = k+2$, we have
$$F_{k,k+2}(-3/8, x_2) = f^L_{k-.5,k}(x_2) + \phi(x_2) f^U_{k,k+2}(-3/8) + (1 - \phi(x_2)) f^D_{k+1,k}(-3/8). \tag{142}$$
Note that $f^U_{k,k+2}(-3/8) > 0$; $f^D_{k+1,k}(-3/8) < 0$; $f^L_{k-.5,k}(x_2)$ is positive (resp. negative) for $x_2 \geq 1/4$ (resp. $x_2 \leq -1/4$); and $d_x f^L_{k-.5,k}(x_2) > 0$ for $-1/4 \leq x_2 \leq 1/4$. It follows that $F_{k,k+2}(-3/8, x_2)$ is also positive for $x_2 \geq 1/4$, negative for $x_2 \leq -1/4$, and satisfies $\partial_{x_2} F_{k,k+2}(-3/8, x_2) > 0$ for $-1/4 \leq x_2 \leq 1/4$. Thus, $F_{k,k+2}(-3/8, x_2) = 0$ occurs for a unique x_2, and this value of x_2 has $x_2 \in [-1/4, 1/4]$.

Step 4: For any pair of sheets S_i and S_j with $i < j$, the (i,j)-crossing locus is topologically as pictured in Figure 4, i.e. it is either empty or is a single arc with endpoints on the specified edges of $[-1,1] \times [-1,1]$, or in the case of square (12) on the cusp locus.

Step 2 places $F^{-1}_{i,j}(0)$ in Φ, and Lemma 11.7 shows that $F_{i,j}$ has no critical points in Φ. Thus, 0 is a regular value for $F_{i,j}$, so that $F^{-1}_{i,j}(0)$ is a 1-manifold with boundary whose boundary points consist of the intersection of $F^{-1}_{i,j}(0)$ with the boundary of the domain of definition of $F_{i,j}$ in $[-1,1] \times [-1,1]$. A priori, $F^{-1}_{i,j}(0)$ may have end points on the cusp edge, but we have shown in Step 3 that the only case in which this occurs is the $(k, k+2)$- and $(k+1, k+2)$-crossing locus in square (12). Moreover, $F_{i,j}$ has a (unique) crossing on an edge $X \in \{U, R, L, D\}$ if and only if the 1-dimensional difference function $f^X_{\sigma_X(i),\sigma_X(j)}$ that corresponds to sheets S_i and S_j above X has a crossing.

[To verify the previous sentence, consider the case $X = L$ where, using item (4) of Corollary 9.6,
$$F_{i,j}(-1, x_2) = f^L_{\sigma_L(i),\sigma_L(j)}(x_2) + \phi(x_2)(\sigma_+(j) - \sigma_+(i))\epsilon_2 + (1 - \phi(x_2))(\sigma_-(j) - \sigma_-(i))\epsilon_2$$
where $\sigma_+(i)$ and $\sigma_-(i)$ denote the order that S_i appears above $(-1, +1)$ and $(-1, -1)$ respectively. Note that
$$\forall x_2 \in [1/4, 1], \quad \mathrm{sgn}(f^L_{\sigma_L(i),\sigma_L(j)}(x_2)) = \mathrm{sgn}(\sigma_+(j) - \sigma_+(i));$$
$$\forall x_2 \in [-1, -1/4], \quad \mathrm{sgn}(f^L_{\sigma_L(i),\sigma_L(j)}(x_2)) = \mathrm{sgn}(\sigma_-(j) - \sigma_-(i));$$
and $F_{i,j}(-1, x_2)$ is strictly monotonic for $x_2 \in [-1/4, 1/4]$ because either

(a.) by Corollary 9.6 item (5) $d_x f^L_{\sigma_L(i),\sigma_L(j)}(x_2) > 1/8$ and therefore dominates the other term of
$$\partial_{x_2} F_{i,j}(-1, x_2) = d_x f^L_{\sigma_L(i),\sigma_L(j)}(x_2) + d_x \phi(x_2)\epsilon_2((\sigma_+(j) - \sigma_+(i)) - (\sigma_-(j) - \sigma_-(i))) \tag{143}$$

in absolute value, or

(b.) edge L is (1Cr) with S_i and S_j crossing above L. In this case, both terms in (143) have the same sign.

Therefore, $F_{i,j}$ has a unique 0 on L if and only if $f^L_{\sigma_L(i),\sigma_L(j)}$ does by Intermediate and Mean Value Theorems.]

At this point, since the 1-dimensional functions have crossings as pictured in Figure 5 (by (1) of Propositions 9.4 and 9.5) we see that the non-closed components of the (i,j)-crossing locus, $F^{-1}_{i,j}(0)$, have their boundary points as specified in (1)-(12) of Figure 4. To complete Step 4, we need only rule out closed components of $F^{-1}_{i,j}(0)$. Within such a closed component, $|F_{i,j}|$ would attain a maximum value somewhere, but this is impossible since in Lemma 11.7 $F_{i,j}$ was shown to have no critical points in Φ.

Step 5: Up to ambient isotopy of $[-1,1]\times[-1,1]$, the base projections of crossing and cusp arcs appear as in Figure 4.

We need to check the following:

(A) For squares (5), (6), (12), the 2 crossing arcs do not intersect (in the base projection), except at their common endpoint in square (12).

(B) For squares (7), (10), (11), the intersection point of the two relevant arcs is transverse and unique.

(C) For square (8), there is a unique triple point and it is the only point in the projection of more than one crossing arc.

Observe that for any $i<j<m$, $F_{i,j}+F_{j,m}=F_{i,m}$. Therefore, if two of the three are zero at some (x_1,x_2), then the third must also be zero at (x_1,x_2). This implies (A), since the two pictured arcs are $(k+1,k+2)$- and $(k,k+2)$-crossing arcs, and they cannot intersect since there is no $(k,k+1)$-crossing arc.

Consider now a crossing locus between consecutive sheets $k,k+1$ which connects two opposite (1Cr) edges, say U and D (the R,L case is similar), as in squares (7), (10), and (8). In these cases, item (1) of Proposition 9.4 states that

$$f^U_{k,k+1}(0)=0=f^D_{\sigma_D(k),\sigma_D(k+1)}(0).$$

Moreover, our assumption implies that the edge types of R and L are the same (including the number of strands and location of crossing or cusp sheets); thus, $f^R_{k,k+1}(x_2)=-f^L_{\sigma_L(k),\sigma_L(k+1)}(x_2)$. By equation (63), $\phi(0)=1/2$. So we compute

$$\begin{aligned}F_{k,k+1}(0,x_2) &= \phi(x_2)f^U_{k,k+1}(0)+(1-\phi(x_2))f^D_{\sigma_D(k),\sigma_D(k+1)}(0)\\ &+ 1/2(f^R_{k,k+1}(x_2)+f^L_{\sigma_L(k),\sigma_L(k+1)}(x_2))\\ &= 1\times 0+1/2\times 0.\end{aligned}$$

Thus, the crossing loci in squares (7), (10), as well as the vertical crossing locus in square (8) are all straight lines. Therefore, (B) follows with the unique intersection actually orthogonal.

Finally, we need to exclude multiple triple points in square (8). All such points must lie in the $(k,k+1)$-crossing locus which is the line $\{x_1=0\}$. Computing

$$\begin{aligned}F_{k,k+2}(0,x_2) &= \phi(x_2)f^U_{k,k+2}(0)+(1-\phi(x_2))f^D_{k+1,k}(0)\\ &+ (1/2)\left(f^R_{k,k+2}(x_2)+f^L_{k+1,k+2}(x_2)\right)\end{aligned}$$

and keeping in mind that the D edge is (1Cr) with the crossing between the sheets in position $k+1$ and $k+2$ above D, we see that $F_{k,k+2}(0,x_2)>0$ for $x_2\geq 1/4$, and $F_{k,k+2}(0,x_2)<0$ for $x_2\leq 1/4$. In addition,

$$\begin{aligned}\partial_{x_2}F_{k,k+2}(0,x_2) &= d_x\phi(x_2)(f^U_{k,k+2}(0)-f^D_{k+1,k}(0))\\ &+ \phi(0)d_xf^R_{k,k+2}(x_2)+(1-\phi(0))d_xf^L_{k+1,k+2}(x_2),\end{aligned}$$

and for $x_2\in[-1/4,1/4]$ this is a sum of four positive terms. It follows that $F_{k,k+2}|_{\{x_1=0\}}$ must have exactly one zero.

For squares (13) and (14): We follow the same steps.

At Step 1, the cusp locus was already identified in Lemma 10.11, and is as in Property 1.

At Step 2, when considering (141), the $f^{ST}_{i,j}$ functions appear if $Y = L$ as

$$F_{i,j}|_{UL} = f^U_{i,j}(x_1) + f^{ST}_{i,j}(x_2); \qquad F_{i,j}|_{DL} = f^D_{\sigma_D(i),\sigma_D(j)}(x_1) + f^{ST}_{i,j}(x_2).$$

For $i < j$, away from the cusp edge $f^U_{i,j}(x_1)$ is strictly positive, as is $f^D_{\sigma_D(i),\sigma_D(j)}(x_1)$ except for $(i,j) = (k+1,k+2)$ in which case $f^D_{\sigma_D(i),\sigma_D(j)} = f^D_{k+2,k+1}$ is negative. Using (92), we see that $f^{ST}_{i,j}(x_2)$ has the same sign, but in a non-strict manner. For instance,

$$f^{ST}_{k+1,k+2}(x_2) = \begin{cases} f^{ST}_k(x_2) - f^L_k(x_2), & \text{for } x_2 \geq 1/4, \\ f^L_k(x_2) - f^{ST}_k(x_2), & \text{for } x_2 \leq -1/4, \end{cases}$$

and this is greater (resp. less) than or equal to 0 when $x_2 \geq 1/4$ (resp. $x_2 \leq -1/4$) by (92) together with (99)-(102).

We verify a slightly strengthened Step 3. in three parts:

(1) S_{k+2} does not intersect S_k or S_{k+1} along the $(k,k+1)$-cusp edge.
The formula for $F_{k,k+2}$ from (116) is

$$F_{k,k+2} = (1-\alpha(r))(CA_{k,k+2}) + \alpha(r)G_{k,k+2}. \tag{144}$$

That $A_{k,k+2}(x_1,x_2) \geq 0$ holds with equality only along the $(k,k+2)$-cusp edge follows from Lemma 10.6.A2. The corresponding statement for $G_{k,k+2}(x_1,x_2)$ follows from Lemma 10.9 (3). Thus, above the $(k,k+1)$-cusp locus, $F_{k,k+2}(x_1,x_2)$ is an interpolation of positive terms.

(2) S_{k+1} does not intersect S_k or S_{k+2} along the $(k,k+2)$-cusp edge.
This is similar to (1).

(3) For $i \notin \{k,k+1,k+2\}$, S_i does not intersect any of S_k, S_{k+1}, or S_{k+2} above the $(k,k+1)$- or $(k,k+2)$-cusp locus.
From (116), for $l \in \{k,k+1,k+2\}$,

$$F_{i,l} = (1-\alpha(r))(F_i - H - CA_l) + \alpha(r)(F_i - G_l). \tag{145}$$

Using the definition of H and G_l in (103)-(106), and the observation that $f^D_{\sigma_D(i)} = f^D_i = f^U_i$,

$$F_i - H = (1-\psi(x_2))f^U_{i,k+2}(x_1) + \psi(x_2)(f^U_i - \widehat{f}_{k+1})(x_1) + f^L_{\sigma_L(i),k}(x_2)$$

all of these terms have the same sign (for the middle term apply (83)), and $|f^L_{\sigma_L(i),k}(x_2)| \geq 1/4$ (by item (5) of Proposition 9.4) dominates $||CA_l||_{C^0(O_2)} < \epsilon_1$ (by (113)). Thus, where $(1-\alpha(r)) \neq 0$, $(F_i - H - CA_l) > 0$ holds if $i < k$, while $(F_i - H - CA_l) < 0$ holds if $k+2 < i$.
Moreover,

$$F_i - G_l = f^{ST}_{i,l}(x_2) + (1-\phi(x_2))(f^U_i - u)(x_1) + \phi(x_2)(f^U_i - v)(x_1)$$

for appropriate functions $u, v \in \{f^U_k, f^U_{k+1}, f^U_{k+2}, \widehat{f}_{k+1}, \widehat{f}_{k+2}\}$. For $i < k$ (resp. $k+2 < i$) all of these terms are positive (resp. negative). [This is verified for the $\widehat{f}$ functions using (82) and (83).

With Steps 1-3 in place the argument is completed as in the case of squares (1)-(12). Note that we use the strengthened statement of Step 3 to ensure that crossings between sheets S_{k+1} or S_{k+2} and another sheet S_i do not cross the border where these sheets merge with $\tilde{S}_k$. This allows us to see that closed components of the crossing locus must be in the zero set of a single difference function of the form $F_{i,j}$ or possibly $F_i - \tilde{F}_k$, and therefore would produce a critical point that is forbidden by Lemma 11.7.

□

Having eliminated any unwanted Reeb chords, we can now prove that Reeb chords exist in the desired places.

Proposition 11.17. *Properties 4, 5, 6, 8, 9, as well as their swallowtail counterparts (see Section 7.1) hold. We set the constants $\beta_{i,j}$, $\tilde{\beta}_{j,i}$, and ϵ that appear in Property 6 to be*

$$\beta_{i,j} = \eta_{i,j}, \quad \tilde{\beta}_{j,i} = \tilde{\eta}_{j,i}, \quad \epsilon = \epsilon_\eta$$

where ϵ_η was defined in equation (36).

Proof. Property 4 follows from Proposition 11.2 which shows that within $N(e^0_\alpha)$ each $F_{i,j}$ has a unique critical point at e^0_α itself.

With $(-1,1)\times(-1/16,1/16)$ coordinates obtained from gluing two adjacent squares used in a neighborhood of e^1_α, Proposition 11.3 identifies the critical points of $F_{i,j}$ that appear above the 1-cell itself as being located at points $(x_1,0)$ with x_1 a critical point of the 1-dimensional function $f_{i,j}$ associated to the edge type of e^1_α. That these critical points match the description from Properties 5 and 6 follows from item (2) of Propositions 9.4 and 9.5 with Proposition 9.3 (3) used to determine the relative location of the $\beta_{i,j}$. In the (2Cr) case, that $\tilde\beta_{k,k+2}<\tilde\beta_{k+1,k+2}$ follows since $d_x f_{k,k+2}=d_x f_{k,k+1}+d_x f_{k+1,k+2}$ will be positive at $\tilde\beta_{k+1,k+2}$. [That these are the only critical points in $\widehat N(e^1_\alpha)$ follows from Lemmas 11.6 and 11.7.]

Finally, Properties 8 and 9 follow from Lemmas 11.6 and 11.7 together with the location of critical points along ∂I^2.

□

Remark 11.18. As mentioned in Remark 6.1, there is some potentially confusing notation. The $\beta^X_{i,j}$ defined above Property 8 have $\beta^X_{i,j}=\beta_{\sigma_X(i),\sigma_X(j)}$, so that $\beta^X_{i,j}\neq\beta_{i,j}$ can occur when $X\in\{D,L\}$. To minimize this potential confusion, we denote critical points for $f^X_{i,j}$ by $\eta^X_{i,j}$. So in particular, $\beta^X_{i,j}=\eta^X_{\sigma_X(i),\sigma_X(j)}$ is the maximum for $f^X_{\sigma_X(i),\sigma_X(j)}$ when $X\in\{D,L\}$.

11.3. **Properties of GFTs.**

Proposition 11.19. *Property 2 holds.*

Proof. From Proposition 11.2, we have that, for $i<j$, above $N(e^0_\alpha)$, $F_{i,j}=(j-i)\epsilon_2(r^2+2)$. Thus, $\partial N(e^0_\alpha)=\{r=1/16\}$ is a level set of $F_{i,j}$ along which $-\nabla F_{i,j}$ points orthogonally into $N(e^0_\alpha)$.

□

Proposition 11.20. *Property 3 holds.*

Proof. We use $(-1,1)\times(-1/16,1/16)$ coordinates as above in a neighborhood of $e^1_\alpha\cong(-1,1)\times\{0\}$, and we denote by $e^0_\pm$ the 0-cells that bound e^1_α at $x_1=\pm1$. We will construct the piecewise linear path P_1 of Property 3 in $(-1,1)\times[-1/32,0)$, and then take P_2 to be the reflection of P_1 across the x_1-axis.

To define P_1 we start at the point on $\partial N(e^0_+)$ with $x_2=-1/32+.01$ and then specify the slope of the various segments of P_1. All slopes will belong to $(-.001,.001)$ so that $P_1\subset(-1,1)\times[-1/32,-1/32+.02]$ will hold, and it follows that the neighborhood $N(e^1_\alpha)$ (bounded below and above by P_1 and P_2 and on the left and right end by portions of $\partial N(e^0_-)$ and $\partial N(e^0_+)$ will meet the requirements (1) and (2) of Property 3.

Before specifying P_1, we record the signs of components of the $-\nabla F_{i,j}=(-\partial_{x_1}F_{i,j},-\partial_{x_2}F_{i,j})$ in $(-1,1)\times(-1/32,0)$. Recall that for a given edge type (PV), (Cu), (1Cr), (2Cr) with $n\le N$ sheets and 1-dimensional functions $f_1,\dots,f_n$, we label sheets as they appear above $x_1=1$, with S_k, S_{k+1} crossing or meeting at a cusp for a (1Cr) and (Cu) edge, and S_{k+2} crossing sheets S_{k+1} and S_k for a (2Cr) edge. Moreover, $\sigma_-(i)$ denotes the position of S_i above $x_1=-1$ with $\sigma_-(k)=\sigma_-(k+1)=k-.5$ in the (Cu) case. Proposition 11.3, gives for $(x_1,x_2)\in(-1,1)\times(-1/32,1/32)$

$$F_{i,j}(x_1,x_2)=f_{i,j}(x_1)+\left[(1-\phi(x_1))(\sigma_-(j)-\sigma_-(i))+\phi(x_1)(j-i)\right]\epsilon_2(x_2^2+1)$$

leading to

$$\partial_{x_1}F_{i,j}(x_1,x_2)=d_xf_{i,j}(x_1)+d_x\phi(x_1)\left[(j-i)-(\sigma_-(j)-\sigma_-(i))\right]\epsilon_2(x_2^2+1); \tag{146}$$

$$\partial_{x_2}F_{i,j}(x_1,x_2)=\left[(1-\phi(x_1))(\sigma_-(j)-\sigma_-(i))+\phi(x_1)(j-i)\right]\epsilon_2(2x_2). \tag{147}$$

Let $i < j$. For $(x_1, x_2) \in (-1, 1) \times (-1/32, 0)$ and belonging to the domain of $F_{i,j}$, we observe the following sign behavior with the interval restricting the value of x_1:

If S_i and S_j do not cross,		$(-1, \eta_{i,j})$ $-\partial_{x_1} F_{i,j} < 0$	$(\eta_{i,j}, 1)$ $-\partial_{x_1} F_{i,j} > 0$
If S_i and S_j do cross,	$(-1, \tilde{\eta}_{j,i})$ $-\partial_{x_1} F_{i,j} > 0$	$(\tilde{\eta}_{j,i}, \eta_{i,j})$ $-\partial_{x_1} F_{i,j} < 0$	$(\eta_{i,j}, 1)$ $-\partial_{x_1} F_{i,j} > 0$
If $\sigma_-(i) < \sigma_-(j)$,			$(-1, 1)$ $-\partial_{x_2} F_{i,j} > 0$
(Cu) with $(i, j) = (k, k+1)$,		$(-3/8, 1/4)$ $-\partial_{x_2} F_{k,k+1} \geq 0$	$[1/4, 1)$ $-\partial_{x_2} F_{k,k+1} > 0$
(1Cr) with $(i, j) = (k, k+1)$,		$(-1, 0)$ $-\partial_{x_2} F_{k,k+1} < 0$	$(0, 1)$ $-\partial_{x_2} F_{k,k+1} > 0$
(2Cr) with $(i, j) = (k+1, k+2)$,		$(-1, 1/12)$ $-\partial_{x_2} F_{k+1,k+2} < 0$	$(1/12, 1)$ $-\partial_{x_2} F_{k+1,k+2} > 0$
(2Cr) with $(i, j) = (k, k+2)$,		$(-1, -1/12)$ $-\partial_{x_2} F_{k,k+2} < 0$	$(-1/12, 1)$ $-\partial_{x_2} F_{k,k+2} > 0$

[In verifying the inequalities for $\partial_{x_1} F_{i,j}$, note that $\partial_{x_1} F_{i,j}$ is non-vanishing for $x_1 \in [-1/4, 1/4]$ since $d_x f_{i,j}(x_1)$ dominates the second term of (146) in all cases besides (1Cr) with $(i, j) = (k, k+1)$, while in this latter case both terms have the same sign. To verify the inequalites for $\partial_{x_2} F_{i,j}$, in the special cases where $\sigma_-(i) > \sigma_-(j)$, substitute the values of $\sigma_-(i)$ and $\sigma_-(j)$ into (147) and use that $\phi(x_1) = 2(x_1 + 1/4)$ in $(-1/4 + \epsilon_1, 1/4 - \epsilon_1)$ to explicitly locate where $\partial_{x_2} F_{i,j} = 0$.]

We now construct P_1 and verify that (3) and (4) of Property 3 hold. We use the notation $\varphi(x_1, x_2)$ for the slope of P_1 at $(x_1, x_2) \in P_1$, noting that φ is multivalued at non-smooth points. In all cases, we set $\varphi(x_1, x_2) = 0$ for $1/4 \leq x_1$. Note that $-\nabla F_{i,j}$ points transversally into the region above P_1 when $1/4 \leq x_1$ since $-\partial_{x_2} F_{i,j}(x_1, x_2) > 0$, so (3) holds. For $x_1 \leq 1/4$, the definition of $\varphi(x_1, x_2)$ depends on the edge type.

(PV): Take $\phi(x_1, x_2) = 0$ for $x_1 \leq 1/4$; (3) follows since $-\partial_{x_2} F_{i,j} > 0$ everywhere.

(Cu): Take $\phi(x_1, x_2) = .001$ for $x_1 \leq 1/4$; (3) holds since all $-\nabla F_{i,j}$ belong belong to the closed upper left quadrant of the plane.

(1Cr): For small $0 < \delta \ll .001$, take

$$\phi(x_1, x_2) = \begin{cases} 0 & \text{for } |x_1| \geq .1, \\ -\delta & \text{for } -.1 \leq x \leq 0, \\ \delta & \text{for } 0 \leq x \leq .1. \end{cases}$$

See Figure 76. Note that by compactness and the computation of the sign of $\partial_{x_l} F_{i,j}$ above, we can choose δ so that for all $i < j$ with $(i, j) \neq (k, k+1)$,

$$0 < \delta < \left| \frac{\partial_{x_2} F_{i,j}}{\partial_{x_2} F_{i,j}} \right|, \quad \forall (x_1, x_2) \in [-1/4, 1/4] \times [-1/32, -1/32 + .02].$$

We verify that (3) holds as follows. For $(i, j) \neq (k, k+1)$, along segments with non-negative slope, this is because $-\nabla F_{i,j}$ points into the open upper left quadrant; along the segment with negative slope the choice of δ has $-\nabla F_{i,j}$ pointing transversally above P_1. For $(i, j) = (k, k+1)$, $-\nabla F_{k,k+1}$ points into the open upper left quadrant for $x_1 > 0$ (verifying (3)) and along the negative x_1-axis for $x_1 = 0$ (verifying (4)), while $-\nabla F_{k+1,k}$ points into the open upper right quadrant for $x_1 < 0$ and along the positive x_1-axis for $x_1 = 0$.

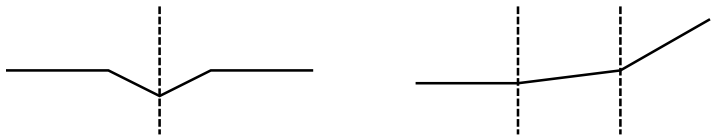

FIGURE 76. The path P_1 pictured schematically (slopes are exaggerated) near the crossing locus along a (1Cr) edge (left) and a (2Cr) edge (right).

(2Cr): Define P_1 for $x_1 \leq 1/4$, so that their are two non-smooth points which are located at the intersection of P_1 with the $(k,k+2)$ and $(k+1,k+2)$ crossing locus, and so that working from left to right $\varphi(x_1,x_2)$ takes the values 0, γ, and .001 where the value $0<\gamma<.001$ will be specified momentarily. Note that for $(i,j)\notin\{(k,k+1),(k,k+2)\}$, $-\nabla F_{i,j}$ points into the open upper left quadrant, so (3) holds in this case.

Note that both crossing loci (the $(k,k+2)$ locus is to the left of the $(k+1,k+2)$ locus) will intersect P_1 in the region where $-1/4<x_1<-1/4+10N\epsilon_1$. [This is because for $(x_1,x_2)\in[-1/4,1/4]\times[-1/32,-1/32+.02]$, since $d_x f_{i,j}(x_1)\geq y_{i,j}-N\epsilon_1\geq 1/5$ and $f_{i,j}(-1/4)\geq -N\epsilon_1$ (using item (3) and (5) of Corollary 9.6)

$$F_{i,j}(x_1,x_2)\geq f_{i,j}(x_1)-2N\epsilon_2((1/32)^2+1)\geq(-N\epsilon_1+1/5(x_1+1/4))-N\epsilon_1$$

which is positive for $x_1>-1/4+10N\epsilon_1$.]

For $(i,j)\in\{(k,k+1),(k,k+2)\}$, although $-\partial_{x_2}F_{i,j}$ becomes negative (well to the right of the crossing loci) so that $-\partial_{x_2}F_{i,j}$ points into the lower left quadrant, from (146) and (147) we have the slope bound

$$\left|\frac{\partial_{x_2}F_{i,j}}{\partial_{x_1}F_{i,j}}\right|<\frac{(N)(\epsilon_2)(2/32)}{(1/5)-(3)(2N)(\epsilon_2)(2)}<.001$$

so in the region where $\varphi=.001$ (3) and (4) hold. Also, to the left of both crossing loci where $F_{k+2,k},F_{k+2,k+1}>0$, we have $-\partial_{x_2}F_{k+2,k},-\partial_{x_2}F_{k+2,k+1}>0$, so that (3) and (4) hold when $\varphi=0$.

Finally, between the two crossing loci where $\varphi=\gamma$, $F_{k+2,k+1}>0$ and $F_{k,k+2}>0$. In this region, $-\nabla F_{k+2,k+1}$ (resp. $-\nabla F_{k,k+2}$) points into the upper right (resp. lower left) quadrant so that for (3) and (4) to hold we choose $0<\gamma<.001$ such that for all such (x_1,x_2),

$$\left|\frac{\partial_{x_2}F_{k,k+2}}{\partial_{x_1}F_{k,k+2}}\right|<\gamma<\left|\frac{\partial_{x_2}F_{k+2,k+1}}{\partial_{x_1}F_{k+2,k+1}}\right|.$$

To see that this is possible, use (146) and (147) to compute the following bounds when $(x_1,x_2)\in[-1/4,-1/4+10N\epsilon_1]\times[-1/32,-1/32+.02]$,

$$\begin{aligned}
|\partial_{x_1}F_{k,k+2}| &\geq (2y_{k,k+2}-N\epsilon_1)-(3)(2N)(\epsilon_2)(2)\geq 2(.625+.125)-.001\\
|\partial_{x_2}F_{k,k+2}| &= 2\epsilon_2|x_2|\cdot|-1+3\phi(x_1)|\leq\frac{2\epsilon_2}{32}\cdot 1\\
|\partial_{x_1}F_{k+2,k+1}| &= |\partial_{x_1}F_{k+1,k+2}|\leq(2y_{k+1,k+2}+N\epsilon_1)+(3)(2N)(\epsilon_2)(2)(.125)+.001\\
|\partial_{x_2}F_{k+2,k+1}| &= 2\epsilon_2|x_2|\cdot|-2+3\phi(x_1)|\geq 2\epsilon_2(1/32-.02)1.999
\end{aligned}$$

□

Proposition 11.21. *Property 7 holds.*

Proof. From Proposition 11.3, we have that for $(x_1,x_2)\in\widehat{N}(e^1_\alpha)\subset(-1,1)\times[-1/32,1/32]$ with $x_1\in(-1,-1/4]\cup[1/4,1)$,

$$\partial_{x_1}F_{i,j}(x_1,x_2)=d_x f_{i,j}(x_1)$$

where $f_{i,j}$ is the 1-dimensional difference function associated to the edge type of e^1_α. Therefore, (keeping in mind that $\beta_{i,j}=\eta_{i,j}$ here) Property 7 follows immediately from Propositions 9.4 and 9.5 which specify the sign of $d_x f_{i,j}$ everywhere on $[-1,1]$.

□

Proposition 11.22. *Properties 10 holds, including its extensions to the swallowtail case.*

Proof. Recall from Remark 11.18 the notation comparison: $\eta^L_{\sigma_L(i),\sigma_L(j)}, \eta^D_{\sigma_D(i),\sigma_D(j)}$ in this section are $\beta^L_{i,j}, \beta^D_{i,j}$ in the property statements.

For $X \in \{U, D\}, Y \in \{R, L\}$, the regions $C_{X,Y}$ appearing in Property 10 satisfy $C_{X,Y} \subset XY$ (with XY as in Figure 75). For any Type (1)-(12) square and $i < j$, within XY,

$$F_{i,j}(x_1, x_2) = f^X_{i',j'}(x_1) + f^Y_{i'',j''}(x_2),$$

for some i', j', i'', j'' which, because of the the assumption that neither S_i or S_j meet a cusp edge above XY, are both integers (i.e., the functions $f^L_{k-.5}$ and $f^D_{k-.5}$ of Lemma 9.7 do not appear here). In the case of the (13) square, the same considerations apply to the functions $F_{i,j}$ as well as $F_i - \widetilde{F}_k$ and $\widetilde{F}_k - F_j$. The key observation is that for the sheets that do not meet a cusp edge in $C_{L,U}$ and $C_{D,U}$ (so, for F_{k+2} and $\widetilde{F}_k$ in $C_{L,U}$ and F_{k+1} and $\widetilde{F}_k$ in $C_{L,D}$), the definition of the f^{ST}_l is such that the $f^Y(x_2)$ term arising from any of these functions will be $f^L_k(x_2)$. [See (116) where $\alpha(r) = 1$, then (104)-(106), then (100)-(101).]

Thus, the signs of the ∂_{x_1} and ∂_{x_2} partial derivatives respectively agree with the signs of the 1-dimensional functions $d_x f^X_{i',j'}(x_1)$ and $d_x f^Y_{i'',j''}(x_2)$. In particular, by Propositions 9.4 and 9.5, the sign of $\partial_{x_1} F_{i,j}$ (and also $\partial_{x_2} F_{i,j}$) is as specified in Property 10 with changes in sign of $\partial_{x_1} F_{i,j}$ occurring only when $x_1 = \eta^X_{i',j'} = \beta^X_{i,j}$ or $x_1 = \tilde{\beta}^X_{i,j}$.

□

Proposition 11.23. *Properties 11 and 14 hold.*

Proof. For Property 11 we establish the statement about $\partial_{x_2} F_{i,j}$ as the statement about $\partial_{x_1} F_{i,j}$ is similar. For $i < j$ and $(x_1, x_2) \in \widehat{N}(e^2_\alpha) \subset [-1, 1] \times [-1, 1]$, when $x_2 = 1/2$ we have

$$\partial_{x_2} F_{i,j} = \phi(x_1) d_x f^R_{i,j}(x_2) + (1 - \phi(x_1)) d_x f^L_{\sigma_L(i),\sigma_L(j)}(x_2). \tag{148}$$

The assumption that S_i and S_j do not cross or meet at a cusp edge above U implies that $\sigma_L(i) < \sigma_L(j)$, so that both terms are positive and $-\partial_{x_2} F_{i,j}(x_1, 1/2) < 0$ follows.

For the first statement of Property 14, note that for any of the difference functions $F_{i,j}, F_i - \widetilde{F}_k, \widetilde{F}_k - F_j$ considered there, since all f^{ST}_l functions agree with f^L_k in a neighborhood of $x_2 = 1/2$ (see (91) and (100)-(101)), (148) holds with σ_L redefined as

$$\sigma_L(i) = \begin{cases} i, & i < k \\ k, & i = k, k+1, k+2, \\ i-2, & i > k+2. \end{cases}$$

From the restrictions placed on i, j in the statement of Property 14, (148) is still a convex combination of positive terms.

To prove the second statement of Property 14, note that for $1/4 \le x_1 \le 3/4$,

$$\partial_{x_1} F_{i,j}(x_1, x_2) = \phi(x_2) d_x f^U_{i,j}(x_1) + (1 - \phi(x_2)) d_x f^D_{\sigma_D(i),\sigma_D(j)}(x_1).$$

For $(i, j) \neq (k+1, k+2)$, we have $\sigma_D(i) < \sigma_D(j)$, so

$$\begin{array}{llll} d_x f^U_{i,j}(x_1) > 0 \text{ (resp. } d_x f^D_{\sigma_D(i),\sigma_D(j)}(x_1) > 0) & \text{for } x_1 < \eta^U_{i,j} \text{ (resp. } x_1 < \eta^D_{\sigma_D(i),\sigma_D(j)}) & \text{and} \\ d_x f^U_{i,j}(x_1) < 0 \text{ (resp. } d_x f^D_{\sigma_D(i),\sigma_D(j)}(x_1) < 0) & \text{for } x_1 > \eta^U_{i,j} \text{ (resp. } x_1 > \eta^D_{\sigma_D(i),\sigma_D(j)}). & \end{array}$$

□

Proposition 11.24. *Property 12 holds.*

Proof. Recall that the constants $\beta^R_{i,j}$, $\beta^U_{i,j}$, and ϵ that appear in the statement of Property 12 have been defined as $\beta^R_{i,j} = \eta^R_{i,j}$, $\beta^U_{i,j} = \eta^U_{i,j}$, and $\epsilon = \epsilon_\eta$.

For $x_1, x_2 \ge 1/4$, $F_{i,j}(x_1, x_2) = f^U_{i,j}(x_1) + f^R_{i,j}(x_2)$. (For squares (13) and (14), $\alpha(r) = 1$ in (116), so the equation follows from (103)-(105).)

Let B_2 be the line segment with endpoints $(1/3 - \epsilon_1/2, 1/2)$ and $(1/3 + \epsilon_1/2, 3/4)$. Item (6) from Propositions 9.4 and 9.5, as well as the definition of M in equation (37) imply for $\{(x_1, x_2) \in B_2 \mid x_2 \le$

$\eta^R_{i,j} - \epsilon\}$,

$$\begin{aligned} \partial_{x_1} F_{i,j}(x_1, x_2) &= \begin{cases} (j-i)\epsilon_2, & \text{if } U \text{ is (PV), (1Cr), or (2Cr),} \\ (j-i)\epsilon_3, & \text{if } U \text{ is (Cu),} \end{cases} \\ \partial_{x_2} F_{i,j}(x_1, x_2) &\geq M. \end{aligned}$$

The definitions of ϵ_2 and ϵ_3 from equations (38) and (46) then give

$$\partial_{x_2} F_{i,j} / \partial_{x_1} F_{i,j} \geq \frac{M}{N\epsilon_2} > \frac{1}{4\epsilon_1} = \frac{3/4 - 1/2}{\epsilon_1}$$

which is the slope of B_2. As both components of $-\nabla F_{i,j}$ are negative along B_2, the inequality shows that $-\nabla F_{i,j}$ points transversally into the region to the right of B_2.

Let B_1 be the reflection of B_2 through $\{x_1 = x_2\}$. The calculation is similar. □

Proposition 11.25. *Property 13 holds.*

Proof. Suppose S_k, S_{k+1} cusp along $x_1 = -3/8$ for squares (1)-(12). The $x_2 = -3/8$ cusp locus case is similar. Fix distinct sheets S_i, S_j with $i \leq k$, $k+1 \leq j$, and $(i,j) \neq (k, k+1)$. Along the cusp locus,

$$\partial_{x_1} F_{i,j} = \phi(x_2) d_x f^U_{i,j}(-3/8) + (1 - \phi(x_2)) d_x f^D_{\sigma_D(i),\sigma_D(j)}(-3/8).$$

For all cases except when $(i,j) = (k, k+2)$ in square (12), we have $\sigma_D(i) < \sigma_D(j)$. Thus $\partial_{x_1} F_{i,j}$ (where defined) is a convex combination of two positive terms; see Proposition 9.5.

In the exceptional case, at the cusp point

$$d_x f^U_{k,k+2}(-3/8) = 1.5 = -d_x f^D_{k+1,k}(-3/8) = -d_x f^D_{\sigma_D(k),\sigma_D(k+2)}(-3/8).$$

[The first (resp. second) equality holds since U (resp. D) is a (Cu) edge with the cusp occurring between the sheets that appear above U (resp. D) in positions k and $k+1$ (resp. $k+1$ and $k+2$). The exact evaluation of these derivatives at $-3/8$ is in item (8) of Proposition 9.5.] Since $\phi^{-1}(0) = \{1/2\}$, see (63), this implies there is a unique $(k+1, k+2)$-switch point $P = \partial_{x_1} F^{-1}_{k,k+2}(0) \cap \{x_1 = -3/8\} = (-3/8, 0)$ with $-\nabla F_{k+1,k+2}$ pointing left (resp. right) of the cusp locus above (resp. below) P. (Recall that $F_{k,k+2}$ and $F_{k+1,k+2}$ agree to first order along the cusp edge.) Similarly, using (49) we evaluate $f^U_{k,k+2}(-3/8) = .12\epsilon_1 = -f^D_{k+1,k}(-3/8) = -f^D_{\sigma_D(k),\sigma_D(k+2)}(-3/8)$; so

$$\begin{aligned} F_{k,k+2}(-3/8, 0) &= f^L_{\sigma_L(k),\sigma_L(k+2)}(0) + \phi(0) f^U_{k,k+2}(-3/8) + (1 - \phi(0)) f^D_{\sigma_D(k),\sigma_D(k+2)}(-3/8) \\ &= f^L_{k-0.5,k}(0) > 0 \end{aligned}$$

where the inequality is from item (1) of Lemma 9.7. Thus, the unique intersection of the crossing locus and the cusp locus, $Q = F^{-1}_{k,k+2}(0) \cap \{x_1 = -3/8\}$, occurs below P on the cusp locus.

□

Proposition 11.26. *Property 15 holds.*

Proof. The claimed properties of the cusp locus $\Sigma \subset N(e^2_\alpha)$ are easily verified from the construction of Sections 10.1 and 10.1.2. [In Section 10.1, we started with an explicit model for the swallow tail with cusp locus

$$\Sigma_{st} = \{(6r^2, 8r^3) \,|\, r \in \mathbb{R}\}. \tag{149}$$

Then, Σ is obtained in Section 10.1.2 by straightening Σ_{st} outside of O_1 via the application of two diffeomorphisms, S then T. Here, S is a composition of a dialation and translation in the x_1-direction that relocates the swallowtail point to $Q = (q_1, 0)$ with $-3/8 - \epsilon_2 < q_1 < -3/8$. Then, leaving Σ fixed for $|x_2| \leq 1/32$, T translates points on the cusp locus in $N(e^2_\alpha) \cap \{|x_2| \geq 1/32\}$ horizontally so that outside of O_1 they agree with $x_1 = -1/32$. That the x_2-coordinate is monotonic along all of Σ is easily verified in (149), and is preserved by S and T. That the x_1-coordinate is monotonic along either branch of Σ when $|x_2| \leq 1/32$ is checked for (149) and is preserved by S, with T leaving this portion of Σ fixed. That the minimum of the x_1-coordinate is at Q follows when $|x_2| \leq 1/32$, and for $|x_2| \geq 1/32$ the cusp locus is at or to the right of $x_1 = -3/8$.]

We establish the claims about switch points in the following Steps 1-3.

Step 1. *There are no switch points outside of O_1.*

Along the $(k,k+1)$- and $(k,k+2)$-cusp edges, $\nabla F_k = \nabla F_{k+1}$ and $\nabla F_k = \nabla F_{k+2}$ respectively. Outside of O_1, Σ agrees with the vertical line $x_1 = -3/8$. Therefore, it suffices to check the following.

(i) For any $i<k$ or $j>k+2$, $\partial_{x_1}F_{i,k}$ and $\partial_{x_1}F_{k,j}$ are positive when $x_1=-3/8$ and $|x_2|\geq R_1$.
(ii) When $x_1=-3/8$ and $|x_2|\geq R_1$, $\partial_{x_1}F_{k+1,k+2}$ is non-vanishing.

Outside of $\overline{L}$, the result is clear since there $F_{i,k}$, $F_{k,j}$, and $F_{k+1,k+2}$ can each be written as the sum of a function of x_2 and a function of x_1 that does not have a critical point at $x_1=-3/8$. Within $\overline{L}$, (ii) was established in the proof of Lemma 11.16, Claim 5 where it was shown that $\operatorname{sgn}(\partial_{x_1}F_{k+1,k+2}) = \operatorname{sgn}(x_2)$ in a region of $\overline{L}$ that includes $x_1=-3/8$.

For (i), suppose $i<k$ and $k+2<j$. Assuming $(x_1,x_2)\in\overline{L}\cap\{x_1=-3/8\}$, we write

$$F_{i,k} = (F_i - H) + (H - F_k), \quad \text{and} \quad F_{k,j} = (F_k - H) + (H - F_j). \tag{150}$$

Computing from (64) and (106) (keeping in mind that $f_i^U = f_i^D$) gives

$$\begin{aligned}\partial_{x_1}(F_i-H)(-3/8,x_1) &= (1-\psi(x_2))d_x f^U_{i,k+2}(-3/8) + \psi(x_2)\cdot d_x(f_i^U - \widehat{f}_{k+1})(-3/8)\\ &\geq (1-\psi(x_2))d_x f^U_{i,k+2}(-3/8) + \psi(x_2)\cdot d_x f^U_{i,k}(-3/8)\end{aligned}$$

where we used that $d_x\widehat{f}_{k+1}(-3/8)\leq d_x f_k^U(-3/8)$ as in (81). Item (8') of Proposition 9.5 implies $d_x f^U_{i,k+2}(-3/8) = k+2-i$ and $d_x f^U_{i,k} = (-3/8) = k+1/2-i$. Thus,

$$\begin{aligned}\partial_{x_1}(F_i-H)(-3/8,x_2) &\geq (1-\psi(x_2))(k+2-i) + \psi(x_2)\cdot(k+1/2-i)\\ &\geq (1-\psi(x_2))(3) + \psi(x_2)\cdot(3/2) \geq 9/4.\end{aligned} \tag{151}$$

where in the last inequality we used that $(1-\psi(x_2))\geq 1/2$; see (89).

In a similar manner, with the estimate $d_x\widehat{f}_{k+1}(-3/8)\geq d_x f^U_{k+2}(-3/8)$ from (84) we find

$$\begin{aligned}\partial_{x_1}(H-F_j)(-3/8,x_2) &\geq [1-\psi(x_2)]d_x f^U_{k+2,j}(-3/8) + \psi(x_2)\cdot d_x f^U_{k+2,j}(-3/8)\\ &= (j-(k+2)) \geq 1.\end{aligned} \tag{152}$$

For the other terms in (150), we can compute from (116)

$$H - F_k = -[1-\alpha(r)]\cdot CA_k + \alpha(r)\cdot(H-G_k).$$

Since r is a polar coordinate centered at $(-3/8,0)$, when $x_1=-3/8$, $\partial r/\partial x_1 = 0$, and we have

$$\begin{aligned}\partial_{x_1}(H-F_k)(-3/8,x_2) &= -[1-\alpha(r)]\cdot C\partial_{x_1}A_k(-3/8,x_2) + \alpha(r)\cdot\partial_{x_1}(H-G_k)(-3/8,x_2)\\ &= O(\epsilon_1) + \alpha(r)\partial_{x_1}(H-G_k)(-3/8,x_2)\end{aligned} \tag{153}$$

where $O(\epsilon_1)$ indicates a term with absolute value bounded by ϵ_1; see (113). Equations (103)-(106) imply

$$\partial_{x_1}(H-G_k)(-3/8,x_2) = (1-\psi(x_2))\cdot d_x f^U_{k+2,k}(-3/8) + \psi(x_2)\cdot d_x(\widehat{f}_{k+1} - f_k^U)(-3/8) \tag{154}$$

Note that for all x_2, $1/2\leq(1-\psi(x_2))\leq 1$, so since $d_x f^U_{k+2,k}(-3/8) = -1.5$ (by (8') of Proposition 9.5) and $d_x(\widehat{f}_{k+1}-f_k^U)(-3/8)\leq 0$ (by (81)) we deduce from (153) and (154) that $\partial_{x_1}(H-F_k)(-3/8,x_2)<\epsilon_1$. Combining this observation with (152) and (150) then establishes

$$\partial_{x_1}F_{k,j} = \partial_{x_1}(F_k-H) + \partial_{x_1}(H-F_j) \geq -\epsilon_1 + 1 > 0.$$

The inequality $\partial_{x_1}F_{i,k}>0$ remains to be proven. For this we use (154), (81), and (84) to bound

$$|\partial_{x_1}(H-G_k)(-3/8,x_2)| \leq |d_x f^U_{k+2,k}(x_2)| = 1.5.$$

In view of (151) and (153), we then achieve the desired inequality by

$$\partial_{x_1}F_{i,k}(-3/8,x_2) = \partial_{x_1}(F_i-H)(-3/8,x_2) + (H-F_k)(-3/8,x_2) \geq 9/4 - (1.5+\epsilon_1) > 0.$$

Step 2. *Existence and uniqueness of (i,k) and $(k+1,j)$ switch points within $O_1\cap\{x_2\geq 0\}$ for $i<k$ and $k+2<j$.*

Our outline for proving Step 2 is as follows. We consider functions θ_1 and θ_2 defined on the upper branch of the cusp locus, $\Sigma_+ := \Sigma\cap O_1\cap\{x_2\geq 0\}$, that are respectively the slope of the tangent to Σ_+ and the slope of $\nabla F_{i,k}$ or $\nabla F_{k+1,j} = \nabla F_{k,j}$ along Σ_+. Our goal is to show that there is a unique point in Σ_+ where θ_1 and θ_2 agree.

We begin by establishing some slightly more detailed bounds for partial derivatives of $F_{i,k}$ in the strip $O_1 \cap ([-3/8-\epsilon_2, -3/8+\epsilon_2] \times [-1,1])$ that contains Σ (by Lemma 10.6.A1). The $F_{k,j}$ case is similar. Note that, within O_1, the formula (116) for F_k simplifies to $F_k = H + C\,A_k$. Thus, for any $(x_1, x_2) \in O_1$, we have

$$F_{i,k} = f^L_{i,k}(x_2) + [1-\psi(x_2)] \cdot f^U_{i,k+2}(x_1) + \psi(x_2) \cdot [f^U_i(x_1) - \widehat{f}_{k+1}(x_1)] - C\,A_k.$$

Now, for $-1/4 \le x_2 \le 1/4$, Corollary 9.6 item (5) gives $|d_x f^L_{i,k}(x_2) - 2(k-i)| \le N\epsilon_1$. In addition, using item (3) of Corollary 9.6 and (88), for $x_1 \le -1/4$ we have $|f^U_{i,k+2}(x_1)| < N\epsilon_1$ and $|f^U_i(x_1) - \widehat{f}_{k+1}(x_1)| < N\epsilon_1 + N\epsilon_1$. Combining these observations with $|\psi'(x_2)| < 3$ from (89) as well as (113) gives that

$$\begin{aligned} \partial_{x_2} F_{i,k}(x_1,x_2) &= d_x f^L_{i,k}(x_2) + \psi'(x_2) \cdot [-f^U_{i,k+2}(x_1) + f^U_i(x_1) - \widehat{f}_{k+1}(x_1)] - C\,\partial_{x_2} A_k \\ &\le 2(k-i) + N\epsilon_1 + 3 \cdot [3N\epsilon_1] + \epsilon_1 \le 2N+1. \end{aligned}$$

On the other hand, the previously established estimate (136) together with (113) gives the lower bound $1/2 \le \partial_{x_2} F_{i,k}(x_1,x_2)$. In summary, we have

$$1/2 \le \partial_{x_2} F_{i,k}(x_1,x_2) \le 2N+1, \quad \forall (x_1,x_2) \in O_1. \tag{155}$$

For the purpose of bounding

$$\partial_{x_1} F_{i,k} = \partial_{x_1}(F_i - H) - C\,\partial_{x_1} A_k = (1-\psi(x_2)) d_x f^U_{i,k+2}(x_1) + \psi(x_2) \cdot d_x(f^U_i - \widehat{f}_{k+1})(x_1) - C\,\partial_{x_1} A_k,$$

we restrict attention to $(x_1,x_2) \in O_1$ with $x_1 \in [-3/8-\epsilon_2, -3/8+\epsilon_2]$. Proposition 9.5, item (8') implies $d_x f^U_{i,k+2}(x_1) = k+2-i$, and in conjunction with (84) implies that $d_x(f^U_i - \widehat{f}_{k+1})(x_1) = K$ where K is constant with $k+1/2-i \le K \le k+2-i$. Thus, again using (113) to bound the $C\,\partial_{x_1} A_k$ term, we have

$$1 \le k+1/2-i-\epsilon_1 \le \partial_{x_1} F_{i,k} \le k+2-i+\epsilon_1 \le N, \tag{156}$$

for all $(x_1,x_2) \in O_1$ with $x_1 \in [-3/8-\epsilon_2, -3/8+\epsilon_2]$.

In proving uniqueness, we will also use some bounds on second order partial derivatives. Note that defining functions of sheets that meet a cusp edge are C^1 but not C^2 along the cusp edge; see the standard form in Proposition 9.5. However, we can write

$$F_{i,k} = E - CA_k \quad \text{where} \quad E = F_i - H \tag{157}$$

and E is C^∞. Consider $(x_1,x_2) \in O_1 \cap \{-3/8-\epsilon_2 \le x_1 \le -3/8+\epsilon_2\}$. The linearity of $f^U_i(x_1)$ (when $i \ne k, k+1$) and $\widehat{f}_{k+1}(x_1)$ from Proposition 9.5 item (8') and (84), the bounds on the derivative of ψ in (89), and the above computations imply the following upper bounds:

$$\left|\frac{\partial^2 E}{\partial x_1^2}(x_1,x_2)\right| = 0;$$

$$\left|\frac{\partial^2 E}{\partial x_2^2}(x_1,x_2)\right| = \left|\psi''(x_2) \cdot [-f^U_{i,k+2}(x_1) + f^U_i(x_1) - \widehat{f}_{k+1}(x_1)]\right| \le 65 \cdot [3N\epsilon_1] < 1/2;$$

$$\left|\frac{\partial^2 E}{\partial x_1 \partial x_2}(x_1,x_2)\right| = \left|\psi'(x_2) \cdot [K-k+2-i]\right| \le 3 \cdot 3/2 < 5.$$

With these preliminaries out of the way, we now examine the functions θ_1 and θ_2. For $(x_1,x_2) \in \Sigma_+$, by definition, we have

$$\theta_2(x_1,x_2) = \frac{\partial_{x_2} F_{i,k}}{\partial_{x_1} F_{i,k}}.$$

Using the inequalities (155) and (156) shows that for any $(x_1,x_2) \in \Sigma_+$,

$$\frac{1}{2\,N} \le \theta_2(x_1,x_2) \le 2N+1.$$

On the other hand, $\theta_1(x_1,x_2)$ is the slope of the tangent vector to Σ_+. For $0 \le x_2 \le R_1/2 = 1/32$, θ_1 takes non-negative real number values. Moreover, at the swallow tail point, θ_1 is 0 while by Lemma 10.6.A1 we have $\theta_1(-3/8, 1/32) > 2N+1.1$. Therefore, the Intermediate Value Theorem implies that there is at least 1 point in $\Sigma_+ \cap \{x_2 \le 1/32\}$ where $\theta_1 = \theta_2$, i.e. there is at least one (i,k)-switch point.

Observe that Lemma 10.6.A1 gives

$$\theta_1(x_1, x_2) \in [2N + 1.1, +\infty) \cup \{\infty\} \cup (-\infty, 0), \text{ when } x_2 \geq 1/32,$$

so to verify the uniqueness claim of Step 2 we need only check that there is only one point in $\Sigma_+ \cap \{0 \leq x_2 \leq 1/32\}$ where θ_1 and θ_2 agree. For this purpose, we use the parametrization

$$\left[0\,,\, \frac{M^{1/3}}{4^{4/3}}\right] \stackrel{\cong}{\to} \Sigma_+ \cap \{x_2 \leq 1/32\}, \quad t \mapsto (x_1(t), x_2(t)) = \left(\frac{1}{M}(6t^2 - X), \frac{1}{M}(8t^3)\right). \tag{158}$$

Here, the constants X and $M > 0$ are those used in the definition of the diffeomorphism, $S(x_1, x_2) = (M\, x_1 + X, M\, x_2)$, from Section 10.1.2. Now, the second diffeomorphism T used in that section is the identity when $|x_2| \leq 1/32$, so from (70) and (76) we have

$$\Sigma_+ = S^{-1}(\{(6t^2, 8t^3) \,|\, t \geq 0\ \}) \cap \{x_2 \leq 1/32\}$$

so that allowing $0 \leq t \leq \frac{M^{1/3}}{4^{4/3}}$ as in (158) does in fact parametrize Σ_+.

Now, as

$$x_1'(t) = \frac{12\, t}{M}, \quad \text{and} \quad x_2'(t) = \frac{24\, t^2}{M},$$

we compute

$$\theta_1(t) = \frac{x_2'(t)}{x_1'(t)} = 2t, \quad \text{and} \quad \theta_1'(t) = 2. \tag{159}$$

Therefore, the uniqueness statement will follow from the Mean Value Theorem provided we can show that $|\theta_2'(t)| < 2$ for all $0 \leq t \leq \frac{M^{1/3}}{4^{4/3}}$.

In verifying that $|\theta_2'(t)| < 2$, we will shorten notation to $F = F_{i,k}$. We have

$$\theta_2(t) = \frac{\partial_{x_2} F(x(t))}{\partial_{x_1} F(x(t))}.$$

Moreover, using notation as in (157),

$$\partial_{x_m} F(x(t)) = \partial_{x_m} E(x(t)) - C \partial_{x_m} A_k(x(t)). \tag{160}$$

The second term can be computed quite explicitly using Proposition 10.2. There, a parametrization of the preliminary version of the swallowtail L_{st} by variables (r, s) is given, and the upper half of the cusp edge is given by setting $r = s$ with the gradient of the local defining function along the cusp edge given by

$$\nabla a_k(x_1(s, s), x_2(s, s)) = (-s^2, s).$$

(as in equation (66)). After the modification of Section 10.1.2, for $0 \leq x_2 \leq 1/32$, the local defining function becomes

$$A_k(x_1, x_2) = a_k \circ S(x_1, x_2).$$

Moreover, the parametrization of the cusp edge used in (158) is related to the parametrization from Proposition 10.2 by

$$(x_1(t), x_2(t)) = S^{-1}(x_1(t, t), x_2(t, t)).$$

Therefore, since the chain rule gives

$$\nabla A_k(x_1, x_2) = M \cdot \nabla a_k(S(x_1, x_2)),$$

we have

$$\nabla A_k(x(t)) = (\partial_{x_1} A_k(x(t)), \partial_{x_2} A_k(x(t))) = M \cdot (-t^2, t). \tag{161}$$

Now, combining (160) and (161) gives

$$\theta_2(t) = \frac{\partial_{x_2} F(x(t))}{\partial_{x_1} F(x(t))} = \frac{\partial_{x_2} E(x(t)) - M \cdot C\, t}{\partial_{x_1} E(x(t)) + M \cdot C\, t^2}$$

We can then compute $\theta_2'(t)$ using the quotient and chain rules

$$\theta_2'(t) = \frac{\left[\frac{\partial^2 E}{\partial x_1 \partial x_2}\cdot x_1'(t) + \frac{\partial^2 E}{\partial x_2^2}\cdot x_2'(t) - M\cdot C\right]\cdot \partial_{x_1}F - \partial_{x_2}F\cdot\left[\frac{\partial^2 E}{\partial x_1^2}\cdot x_1'(t) + \frac{\partial^2 E}{\partial x_1 \partial x_2}\cdot x_2'(t) + 2M\cdot C\, t\right]}{\partial_{x_1}F(x(t))^2}.$$

Using that the absolute values of the second partial derivatives of E are bounded by 5, together with (155) and (156), we have

$$|\theta_2'(t)| \le \left[5|x_1'(t)| + 5|x_2'(t)| + M\cdot C\right]\cdot N + (2N+1)\cdot\left[5|x_1'(t)| + 5|x_2'(t)| + |2M\cdot C\, t|\right].$$

$$\mathrm{Max}\{|x_1'(t)|, |x_2'(t)|\} \le \mathrm{Max}\left\{\left|x_1'\left(\frac{M^{1/3}}{4^{4/3}}\right)\right|, \left|x_2'\left(\frac{M^{1/3}}{4^{4/3}}\right)\right|\right\} = \frac{24}{4^{8/3}M^{1/3}} < \frac{24}{M^{1/3}},$$

so we can estimate

$$\begin{aligned}|\theta_2'(t)| &\le \left[\frac{240}{M^{1/3}} + M\cdot C\right]N + (2N+1)\left[\frac{240}{M^{1/3}} + 2MC\left(\frac{M^{1/3}}{4^{4/3}}\right)\right]\\ &\le (2N+1)\left(\frac{480}{M^{1/3}} + (M + M^{4/3})C\right) < 1/2 + 1/2.\end{aligned}$$

where at the last inequality we used the lower bound on M from (P4) in Section 10.1.2 and the upper bound (114) on C. This gives the desired inequality $|\theta_2'(t)| < 2$.

Step 3. *Non-existence of (i,k) and $(k+2,j)$ switch points within $O_1 \cap \{x_2 \le 0\}$ for $i < k$ and $k+2 < j$.*

We establish the non-existence of (i,k) switch points. The $(k+2,j)$ switch points are similar. When $x_2 \le 0$, the slope of the cusp locus is negative or, when $x_2 \le -1/32$, contained in $(-\infty, -(2N+1.1)] \cup \{\infty\} \cup [2N+1.1, +\infty)$ by Lemma 10.6.A1. In contrast, (155) and (156) show that the slope of $\nabla F_{i,k}$ is positive and bounded above by $2N+1 < 2N+1.1$.

Step 4. *Existence and uniqueness of $(k+1,k+2)$ and $(k+2,k+1)$ switch points.*

Again, we let $\theta_1(t)$ and $\theta_2(t)$ denote the slope of the cusp locus and $\nabla F_{k+1,k+2}$ respectively at the point

$$(x_1(t), x_2(t)) = T^{-1}\circ S^{-1}(6t^2, 8t^3).$$

To obtain the entire portion of the cusp locus within O_1 where $-1/16 \le x_2 \le 1/16$ we need to consider $-M^{1/3}/2^{7/3} \le t \le M^{1/3}/2^{7/3}$. Within O_1, we have

$$F_{k+1,k+2} = CA_{k+1,k+2} = C\cdot a_{k+1,k+2}\circ S\circ T.$$

Thus, for a point $(w_1, w_2) = T^{-1}\circ S^{-1}(x_1, x_2)$ in O_1, we can compute the differential of $\left(\frac{1}{C}\right)F_{k+1,k+2}$ to be

$$d(a_{k+1,k+2}\circ S\circ T)(T^{-1}\circ S^{-1}(x_1,x_2)) = da_{k+1,k+2}(x_1,x_2)\cdot dS(S^{-1}(x_1,x_2))\cdot dT(w_1,w_2).$$

Now, from definitions of S and T in Section 10.1.2, we have

$$dS = \begin{bmatrix} M & 0\\ 0 & M\end{bmatrix} \quad\text{and}\quad dT(w_1,w_2) = \begin{bmatrix} 1 & b'(|w_2|)\cdot \mathrm{sgn}(w_2)\\ 0 & 1\end{bmatrix}. \tag{162}$$

To evaluate $da_{k+1,k+2}(x_1,x_2)$ using Corollary 10.4 we need to make use of the parametrization from (65) with parameter values belonging to the wedge W (see Figure 70). To parametrize the upper half of the cusp locus we take $(r,s) = (t,t)$ with $0 \le t \le M^{1/3}/2^{7/3}$, and for the bottom half we take $(r,s) = (t,-2t)$ with $-M^{1/3}/2^{7/3} \le t \le 0$. Notice that these substitutions into (65) produce $(x_1(t), x_2(t)) = (6t^2, 8t^3)$, so that plugging $(r,s) = (t,t)$ or $(r,s) = (t,-2t)$ into Corollary 10.4 to evaluate the $da_{k+1,k+2}(x_1,x_2)$ term from (162) and then transposing the result will give the vector whose slope is $\theta_2(t)$. In this manner, Corollary 10.4 produces

$$da_{k+1,k+2}(x_1(t), x_2(t)) = \begin{cases} (t+2t)(t,1) & \text{if } t \ge 0,\\ (t+2(-2t))(t,1) & \text{if } t \le 0.\end{cases}$$

Thus, regardless of the sign of t, using (162) we have

$$\theta_2(t) = \frac{t \cdot b'(|w_2|) \cdot \mathrm{sgn}(w_2) + 1}{t}.$$

When $|w_2| \leq 1/32$, this simplifies to $\theta_2(t) = 1/t$, and in this range we have already computed in (159) that $\theta_1(t) = 2t$. Therefore, there is a $(k+1, k+2)$-switch point at $t = 1/\sqrt{2}$, and a $(k+2, k+1)$-switch point $t = -1/\sqrt{2}$. These points are both in the range $|t| \leq M^{1/3}/2^{8/3}$ where $|w_2| \leq 1/32$ by the requirement (P4) from Section 10.1.2.

On the other hand, when $1/32 \leq |w_2| \leq 1/16$, Lemma 10.6.A1 gives that

$$|\theta_1(t)| \geq 2N + 1.1,$$

while we can use the defining properties of b in Section 10.1.2 to estimate

$$|\theta_2(t)| \leq |b'(|w_2|)| + \frac{1}{|t|} \leq \frac{1}{3(2N+1.1)} + \frac{1}{|t|} \leq 1$$

where we have used $M^{1/3}/2^{8/3} \leq |t| \leq M^{1/3}/2^{7/3}$ and the lower bound on M from (P4) of 10.1.2 to obtain the last inequality.

□

Proposition 11.27. *Property 16 holds.*

Proof. Let P_1 be the line segment from $(1/3 - \epsilon_1, -3/8)$ to $(1/3 + \epsilon_1, 3/4)$. To verify item (2) of the property, fix a pair of sheets S_i, S_j with $i < j$. For any $(x_1, x_2) \in P_1$, since $x_1 \geq 1/4$, equations (116) and (64) simplify to

$$F_{i,j}(x_1, x_2) = f^R_{i,j}(x_2) + \phi(x_2) f^U_{i,j}(x_1) + (1 - \phi(x_2)) f^D_{\sigma_D(i),\sigma_D(j)}(x_1).$$

Using item (6) of Corollary 9.6 gives

$$|\partial_{x_1} F_{i,j}(x_1, x_2)| \leq \phi(x_2)|d_x f^U_{i,j}(x_1)| + (1 - \phi(x_2))|d_x f^D_{\sigma_D(i),\sigma_D(j)}(x_1)| \leq N\epsilon_3.$$

On the other hand, for $(i,j) \neq (k+1, k+2)$, Lemma 11.8 (which, as observed in the proof of Lemma 11.15, remains true in the region $\overline{R}$ for the (13) square), combined with the fact that, when $|x_2| \geq 1/4$, $\partial_{x_2} F_{i,j} = d_x f^R_{i,j}(x_2)$ gives

$$\partial_{x_2} F_{i,j}(x_1, x_2) \geq \mathrm{Min}\{d_x f^R_{i,j}(x_2), 1/5\}.$$

Thus, when $x_2 < \beta^R_{i,j} - \epsilon = \eta^R_{i,j} - \epsilon_\eta$, the x_2-component of $-\nabla F_{i,j}$ is negative, and to see that $-\nabla F_{i,j}$ points to the right of P_1 it suffices to verify that

$$\frac{|\partial_{x_2} F_{i,j}(x_1, x_2)|}{|\partial_{x_1} F_{i,j}|} \geq \frac{\mathrm{Min}\{d_x f^R_{i,j}(x_2), 1/5\}}{N\epsilon_3} > \frac{9}{16\epsilon_1} = \mathrm{Slope}(P_1).$$

[At the second inequality we used the definition of ϵ_3 from (46).]

Next, define P_2 to go from the lower endpoint of P_1 to $x_1 = -7/8$ with slope $-\epsilon_1$, and then continue with slope 0 to the left boundary of $N(e^2_\alpha)$. For any (x_1, x_2), since $-3/8 \leq x_2 \leq -1/4$ and all f^{ST}_l functions agree with f^L_k in this region, we have

$$F_{i,j}(x_1, x_2) = f^D_{\sigma_D(i),\sigma_D(j)}(x_1) + (1 - \phi(x_1)) f^L_{\sigma'(i),\sigma'(j)}(x_2) + \phi(x_1) f^R_{i,j}(x_2).$$

where σ' is as in (133). In verifying item (4), we need only consider the case where $i < j$ and $(i,j) \neq (k+1, k+2)$, and this implies that for $-7/8 \leq x_1 \leq 1/2$,

$$\partial_{x_1} F_{i,j}(x_1, x_2) > 0$$

since when $-1/4 \leq x_1 \leq 1/4$, $d_x f^D_{\sigma_D(i),\sigma_D(j)}$ dominates the other terms which are each bounded by $4N\epsilon_1$ in absolute value via items (3) and (5) of Corollary 9.6 and (95). In addition, $\partial_{x_2} F_{i,j}(x_1, x_2)$ is an interpolation of non-negative terms. We conclude that for $-7/8 \leq x_1 \leq 1/2$, $-\nabla F_{i,j}(x_1, x_2)$ points into the closed lower left quadrant, and therefore into the region below P_2.

Now, when $x_1 \leq -7/8$ there is only one sheet (defined by $\tilde{F}_k$) that can produce an f^L_k term in $f^L_{\sigma'(i),\sigma'(j)}$. Therefore, when $0 \leq x_1 \leq -7/8$, we have strict inequality $-\partial_{x_2} F_{i,j}(x_1, x_2) < 0$ as required. Finally, by Property 7, $-\nabla F_{i,j}$ continues to point downward when P_2 passes into the part of $N(e^1_L)$ that lies in a neighboring square.

□

Proposition 11.28. *Property 17 holds.*

Proof. Let $j \in \{k, k+1, k+2\}$. The segment $x_1 = -17/64$ is to the left of $x_1 = -1/4$ (so $\phi(-17/64) = 0$), to the right of $x_1 = -3/8 + R_1/2$ (see (79)-(80)), and is disjoint from O_2. So (79)-(80), (103)-(105) and (116) imply that in a neighborhood of the segment

$$F_{i,j}(x_1, x_2) = F_i - G_j = f_i^L(x_2) - f_j^{ST}(x_2) + \phi(x_2) f_{i,j}^U(x_1) + (1 - \phi(x_2)) f_{i,\sigma_D(j)}^D(x_1)$$

where σ_D transposes $k+1$ and $k+2$. We compute

$$\partial_{x_1} F_{i,j}(x_1, x_2) = \phi(x_2) d_x f_{i,j}^U(x_1) + (1 - \phi(x_2)) d_x f_{i,\sigma_D(j)}^D(x_1) > 0.$$

The sum is a convex combination of positive terms since $i < j$ and $i < \sigma_D(j)$.

□

Proposition 11.29. *Property 18 holds.*

Proof. For any (x_1, x_2) considered in the Property 18 statement, we showed in (138) that $\partial_{x_2}(F_i - w) \geq 1 - 6\epsilon_1 - 250\epsilon_1$. The case for $\partial_{x_2}(w - F_j)$ is similar. This proves the first statement. Since $F_{k+1,k+2}^{-1}(0) \cap \{x_1 \leq -1/4\} \subset \{x_2 = 0\}$, this also proves the crossing locus statement.

□

Proposition 11.30. *Property 19 holds.*

Proof. Take $L_{k+1,k+2}$ to be a segment connecting the $(k+1, k+2)$-switch point to the $(k, k+2)$-cusp edge with sufficiently negative slope (but non-vertical) so that $L_{k+1,k+2}$ is contained in the portion of O_1 with $|x_2| \leq 1/32$. [Such an $L_{k+1,k+2}$ exists by Property 15.] Then, Lemma 10.6 items (A3) and (A4) implies that at points of $L_{k+1,k+2}$ above or on the cusp locus $-\nabla F_{k+1,k+2}$ points into the closed lower left quadrant, and hence to the left side of $L_{k+1,k+2}$. Also, at all points of $L_{k+1,k+2}$, except for the endpoint on the $(k, k+2)$-cusp locus where $\nabla F_{k,k+2} = 0$, $-\nabla F_{k,k+2}$ points into the closed lower left quadrant.

For $L_{k+2,k+1}$, take a segment from the $(k+2, k+1)$-switch point to the $(k, k+1)$-cusp edge that has positive slope and is contained in $|x_2| \leq 1/32$, and use Lemma 10.6 item (A3) and (A4) in a similar manner to verify the directionality of $-\nabla F_{k+2,k+1}$ and $-\nabla F_{k,k+1}$.

□

12. Proof of Theorem 5.1 Part 4: Transversality

The Legendrian metric pair $(\tilde{L}_0, g_0)$ constructed in Sections 9 and 10 has now been verified to satisfy all requirements of Theorem 5.1 except for the 1-regular condition. In combination, the following Propositions 12.2 and 12.3 show that the 1-regular condition may be obtained by a perturbation that preserves the other properties required in Theorem 5.1.

Convention 12.1. In this final section, the singular set of L refers to cusp edges and swallow tail points only. *Note that this differs from earlier sections, where we included crossings arcs in the singular set.*

Proposition 12.2. *Consider the Legendrian $L \subset J^1(S)$ with metric g on S as constructed in Sections 9 and 10. There exists an open neighborhood $U \subset L$ of the singular set of L (pre-image of cusp edges and swallowtail points) such that within any neighborhood of (L, g) in the C^∞-topology, there exist (L', g') such that L agrees with L' on U and L' is 1-regular with respect to g'.*

Proof. This is a modification of [4, Theorem 1.1a] which states that any Legendrian metric pair (L, g) can be made 1-regular by a C^∞-small perturbation. We will show that in our setting the perturbation procedure used in the proof of [4, Theorem 1.1a] can be carried out leaving a neighborhood $U \subset L$ of the cusp locus fixed.

We review the outline of the proof of [4, Theorem 1.1a]:

(1) After making a small perturbation if necessary, it is assumed that (L, g) satisfies certain Preliminary Transversality Conditions (PTC).

(2) When (L, g) satisfies PTC, any GFT, Γ, is assigned a *geometric dimension*, $gdim(\Gamma)$, and [4, Lemma 3.7] establishes the inequality

$$gdim(\Gamma) \leq fdim(\Gamma),$$

where $fdim(\Gamma)$ is the formal dimension of Γ. (See Section 2.)

(3) [4, Proposition 3.14] states that for any $D > 0$, there exists a C^∞-small perturbation of (L, g) after which any GFT with $fdim(\Gamma) \leq D$ is transversally cut out, and a space of nearby GFTs with the same geometric properties as Γ (e.g. homeomorphic domain trees) forms a manifold of dimension $gdim(\Gamma)$.

Taking $D = 1$, the Legendrian resulting after (3) is 1-regular. [A GFT of negative formal dimension would have to belong to a manifold of negative dimension and therefore cannot exist.]

To establish our strengthened result, we show that

(i) our (L, g) already satisfies PTC, and hence does not need to be perturbed at part (1) of the argument, and

(ii) there is a neighborhood U of the cusp locus that can be left fixed during the perturbation at part (3).

(i): We list the Preliminary Transversality Conditions following [4, p.1101–1103] simplified to our two-dimensional set-up. First L should have generic base and front projections. Then, the singular set $\Sigma \subset S$, that is, the set of points over which at least one sheet fails to be immersed has a stratification $\Sigma = \Sigma_1 \supset \Sigma_2$. Here, Σ_2 is an isolated set of points representing projections of standard swallowtail points and transverse intersections of the projection of two cusp edges. The Preliminary Transversality Conditions are:

(1) All switch points belong to $\Sigma_1 \setminus \Sigma_2$ and are non-degenerate.

(2) Let Σ and Σ' be the cusp loci of the two locally defined sheet pairs S_k, S_{k+1} and S_l, S_{l+1}. For $x \in \Sigma \cap \Sigma'$, $\nabla F_{k,l}(x)$ is non-vanishing.

(3) At a swallowtail point, all $\nabla F_{i,j}$ (involving at least one sheet that does not meet the swallowtail point) are transverse to the two cusp loci.

That (L, g) satisfies Condition 1 follows from Property 13 and 15. Condition 2 follows from Property 13. Condition 3 follows from Claim 1 and 2 in proof of Lemma 11.16 since the tangent to the cusp locus is horizontal at the swallowtail point.

(ii): The outline of the proof of [4, Proposition 3.14] is as follows. Spaces of PFTs and GFTs are made to be transversally cut out through an inductive procedure. At the inductive step, we are given a collection of spaces of PFTs and GFTs that have already been made transversally cut out. By a perturbation, transversality is then arranged for new spaces of GFTs arising from joining existing PFTs together at a vertex as allowed by the definition. (The perturbation is taken to be small enough to preserve transversality of existing spaces as well.) An a priori bound on the number of edges and vertices for GFTs satisfying a given bound on formal dimension and number of positive punctures is established in [4, Lemma 3.12], and this guarantees that the inductive procedure is completed after a finite number of steps.

It remains to verify that holding L fixed near its cusps does not disrupt the above transversality argument. From this Proposition's statement, let U be a small neighborhood of the cusp loci so that if $x \in U$ is close to the cusping sheets S_k, S_{k+1} then $F_{k,k+1}(x) < \delta$, where $\delta > 0$ is much smaller than the positive critical value for the smallest Reeb chord of L and the value of the smallest switch point. By this second condition, we mean if $\nabla F_{i,j}$ is tangent to the cusp locus of S_j, S_l at Q then $\delta < |F_{i,j}(Q)|$. Moreover, we can assume that the base projection of U sits in (one side of) a small neighborhood of Σ, and $\pi_x|_U$ is at most 2-to-1 except

(a.) in neighborhoods of swallow tail points that we take to be small enough so the difference between any of the 3 swallowtail sheets is less than δ, and

(b.) in Type (11) squares in a small region W near the intersection point of the two cusp loci at $(-3/8, -3/8)$. We now place some restrictions on W. At $(-3/8, -3/8)$, for all $F_i > F_j$ that do not meet one another at a cusp edge, $-\nabla F_{i,j}$ has both components strictly negative. [This is easily checked using (64).] Therefore, by compactness, there exist $0 < m < M$ such that in a

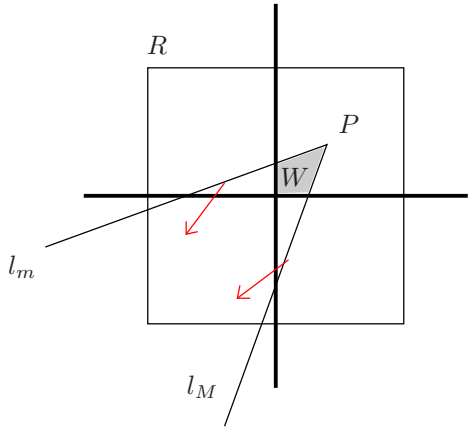

FIGURE 77. The projection of U to S is 2-to-1 or less outside of the shaded region W. The thickened lines represent Σ while the red arrows indicate the directionality of $-\nabla F_{i,j}$ (with F_i and F_j not meeting at a cusp) along the bordering segments l_m and l_M within the square R.

square R centered at $(-3/8, -3/8)$ all such $F_i > F_j$ satisfy

$$m < \frac{\partial_{x_2} F_{i,j}}{\partial_{x_1} F_{i,j}} < M;$$

i.e., in R, $-\nabla F_{i,j}$ points into the wedge in the down left quadrant bounded by lines through the origin of slope m and M. Consider a point $P = (-3/8 + \alpha, -3/8 + \alpha)$ with α chosen so that lines l_m and l_M of slope m and M through P intersect both cusp loci, $\{x_1 = -3/8\}$ and $\{x_2 = -3/8\}$, within R. Then, we require that the region W is contained in the closed subset with bounding segments $\{x_1 = -3/8\}$ (on left), $\{x_1 = -3/8\}$ (below), l_M (on right), and l_m (above). See Figure 77.

During the upcoming inductive perturbation, we can take all perturbations small enough to preserve the condition from (b.) that $-\nabla F_{i,j}$ points strictly into the wedge bounded by l_m and l_M within R.

As we consider only the case of GFTs with 1 positive puncture, we can carry out the inductive procedure starting with the output vertices and working up. To provide a slightly more detailed discussion of the induction from this point of view, we first introduce some terminology.

Recall that the projection of the singular set is stratified as $\Sigma = \Sigma_1 \supset \Sigma_2$, and via the Preliminary Transversality Conditions we can further refine Σ by adding the image of switch points into Σ_2. Given a subset $X \subset S$ with an upper and lower sheet of S assigned to each point of X, the **upward** (resp. **downward**) **flow out** manifold of X is the union of all flow lines for $-\nabla F_{i,j}$ starting at $x \in X$ when $t = 0$ and continued in negative (resp. positive) time for their maximal interval of definition, where F_i and F_j define the upper and lower sheet assigned to x.

We make some observations and technical remarks:

(1) Flow out manifolds are not embedded since for instance, a flow line for two sheets may follow the Legendrian around and return to the same point above S but with different upper and/or lower sheet. To address this issue, one can consider flow out manifolds as belonging to the subset of the fiber product $L * L = \{(a, b) \in L \times L \,|\, \pi_x(a) = \pi_x(b)\}$ with $z(a) \geq z(b)$. However, two or more of the initial points in X may belong to the same flow line of $-\nabla F_{i,j}$, so that even in $L * L$ flow outs are non-embedded. In the following, we (implicitly) view flow outs as maps to $L * L$.
(2) Flow lines may reach the end of their domain of definition in finite time. As such, flow out manifolds are stratified by their intersections with the various strata of Σ.
(3) When $X \subset \Sigma$ has points on a cusp edge for the upper or lower sheet, there are multiple upward/downward flow out manifolds determined by a choice of upper or lower sheet bordering the cusp edge.

(4) The sheet difference $F_{i,j}(x)$ decreases as t increases. In particular, at any point of an upward flow out manifold of X the sheet difference is larger than at the corresponding initial point on X.

Returning now to the inductive procedure, at the base case we begin with the ascending manifolds of critical points, $X_1, \dots, X_m$, and the upward flow out of all cusp edges (with respect to $-\nabla F_{k,k+1}$ where F_k and F_{k+1} are local defining functions for the upper and lower sheet at a cusp). Denote the latter flow out manifold by X_Σ. We arrange that $X_1, \dots, X_m, X_\Sigma$ intersect the descending manifolds of critical points and descending manifolds of the stratified parts of the cusp locus transversally. (The latter condition assures that the stratified components of this initial collection of manifolds, as in (2) are again manifolds.) In addition, we arrange that $X_1, \dots, X_m, X_\Sigma$ all intersect one another transversally, and that their stratified components intersect transversally in the various strata of Σ.

As discussed in [4, pg. 1113-1114], this is all accomplished by perturbing (L, g) in a neighborhood of the critical points. At any critical point of some $F_{i,j}$, at least one of the sheets is disjoint from U; perturbing this sheet accomplishes an arbitrary perturbation of $F_{i,j}$, so we can leave U fixed at this step. Note that no perturbation of X_Σ is required since it is top-dimensional and hence has intersections that are automatically transverse.

The intersection of the X_i (resp. X_Σ) with descending manifolds of critical points are identified with GFTs with a single edge ending at a Reeb chord (resp. e-vertex). The (iterated) intersections of (components of) the X_i and X_Σ with one another, restricted to points where the upper sheet of the first manifold agrees with the lower sheet of the second manifold, specify possible locations of a lower most vertex in a PFT or GFT. We write this collection of intersections as $Z_1, \dots, Z_n$, where if $Z_i = X_{i_1} \cap X_{i_2}$ with the lower sheet of X_{i_1} agreeing with the upper sheet of X_{i_2}, then the upper (resp. lower) sheet assigned to Z_i is the corresponding upper sheet of X_{i_1} (resp. lower sheet of X_{i_2}).

Now, we inductively arrange that the upward flow out of each Z_i is transverse to (i) descending manifolds of critical points, (ii) downward flow outs of the stratified components of Σ, (iii) all components of each of the X_i, X_Σ, and upward flow outs of Z_l with $l < i$ at points where lower (resp. upper) sheet of Z_i agrees with the upper (resp. lower) sheet of the other manifold. As discussed in [4, pages 1113–1114] this may be achieved by an arbitrarily small perturbation of (L, g) along the upward flow out of Z_i. We then append each non-empty intersection as in (iii), to the list of Y_j with the upper and lower sheet assigned as above, and proceed inductively with [4, Lemma 3.12] showing that the process is completed after finitely many steps.

Notice that since the sheet difference increases along ascending manifolds of critical points and upward flow out manifolds, we see that either:

(1) The Z_i arises (inductively) from some intersections of X_Σ with itself. In this case, since such intersections are top dimensional, there is no need to perturb Z_i.
(2) Or, the sheet difference of the upper sheet and lower sheet of Z_i must be larger than the value δ used to define U.

In case (2), the only way that both the upper and lower sheet of a point on Z_i or its upward flow out belong to U is if the endpoints are associated to two distinct cusp edges in a square of type (11) as in (b.) from the definition of U. We now rule out the possibility of such a Z_i existing, so that at this perturbation step we can always perturb a sheet disjoint from U.

A point on the upward flow out of Z_i is the initial point of a PFT. Thus, it suffices to show there is no PFT, Γ, that starts in the region W from (b.) with upper endpoint belonging to one of S_k, S_{k+1} and lower endpoint belonging to one of S_l, S_{l+1} where S_k, S_{k+1} and S_l, S_{l+1} are the two pairs of cusp sheets.

Supposing Γ exists, we build a path γ from a sequence of consecutive edges of Γ as follows. Begin at the inital point in W, and follow the domain of Γ according to its orientation. Note that as long as the image remains in the square R, whenever a vertex is reached, at least one outgoing edge can be found that is a flowline involving one of the sheets $S_k, S_{k+1}, S_l, S_{l+1}$, but is not a $(k, k+1)$-flow line or a $(l, l+1)$-flow line. We continue γ by following this edge. Note that while γ remains in R, it cannot cross the lines l_m or l_M (by the directionality of the $-\nabla F_{i,j}$). Moreover, γ cannot terminate at an e-vertex in R since none of its edges are $(k, k+1)$ or $(l, l+1)$ flow lines. Therefore, γ must eventually leave R, but doing so without crossing l_m or l_M forces the image to pass into the region where none

of the sheets $S_k, S_{k+1}, S_l, S_{l+1}$ exist. (See Figure 77.) This is impossible since along any edge of γ the upper or lower sheet belongs to $S_k, S_{k+1}, S_l, S_{l+1}$.

□

Proposition 12.3. *Let (L, g) denote the Legendrian and metric constructed in Sections 9 and 10 that satisfies Properties 1-19. Then, for any given open neighborhood, $U \subset L$, of the singular set, there exists some neighborhood $\mathcal{V}$ of (L, g) in the C^∞-topology such that if,*

(1) *$(L', g') \in \mathcal{V}$; and*
(2) *L' agrees with L on U,*

then (L', g') also satisfies Properties 1-19.

Given a neighborhood, $\mathcal{V}$, of (L, g) in the C^∞-topology, and an open set $U \subset L$, we write $\mathcal{V}_U$ to denote those $(L', g') \in \mathcal{V}$ such that L' agrees with L on U.

Proof. For a suitably chosen small neighborhood $\mathcal{V}$ of (L, g), it is the case that for $(L', g') \in \mathcal{V}_U$, L' has the same singular set as L (cusp edges and swallow tail points). We can further arrange that:

(I) The local defining functions of L' belong to chosen C^2-neighborhoods of the defining functions of L.
(II) Gradient vector fields of defining functions for L' with respect to g' belong to chosen C^2-neighborhoods of the gradient vector fields of defining functions of L with respect to g.
(III) For gradients of difference functions $-\nabla F_{k,k+1}$ that correspond to two sheets within U, we can arrange a uniform bound between the direction of $-\nabla_{g'} F_{k,k+1}$ (where non-zero), and the direction of $-\nabla_g F_{k,k+1}$. (We will need to use this property for two sheets that meet at a cusp edge. Since $\nabla_g F_{k,k+1}$ vanishes along the cusp edge, in a neighborhood of the cusp edge the uniform perturbation of direction does not follow from just the statement that $-\nabla_{g'} F_{k,k+1}$ C^2-approximates $-\nabla_g F_{k,k+1}$.)

[To verify (III), note that for (L, g) and $(L', g') \in \mathcal{V}_U$, the differentials $dF_{k,k+1}$ and $dF'_{k,k+1}$ are identical in U. Thus, the change between $-\nabla_g F_{k,k+1}$ and $-\nabla_{g'} F'_{k,k+1}$ is as a result of the isomorphism

$$TS \xrightarrow{g^\#} T^*S \xrightarrow{(g'^\#)^{-1}} TS.$$

This isomorphism induces a map between the unit sphere bundles $S(TS) \to S(TS)$, that by taking g' close enough to g can be made C^0 close to the identity on the base projection of U (which is a relatively compact subset of S).]

More concretely, for arbitrarily fixed $\epsilon > 0$, we can take $\mathcal{V}$ so that on any finite number of compact subsets $K_1, \ldots, K_r \subset S$, contained in the domains of local defining functions $F_1, \ldots, F_r$, we have that for any (L', g') in $\mathcal{V}_U$ the local defining functions for the same sheets $F'_1, F'_2, \ldots, F'_r$, satisfy, $||F'_i - F_i||_{C^2(K_i)} < \epsilon$ and $||\nabla F'_i - \nabla F_i||_{C^2(K_i)} < \epsilon$, for all $1 \leq i \leq r$. (We can use any choice of local coordinate on S to set up the $C^2(K_i)$-norms.) Moreover, $F_i = F'_i$ holds identically on U, and when $F_{k,k+1}$ is a difference function for two sheets that meet at a cusp edge, in the base projection of U, $\nabla F'_{k,k+1} \neq 0$ exactly where $\nabla F_{k,k+1} \neq 0$, and the angle between $\nabla F'_{k,k+1}$ and $\nabla F_{k,k+1}$ is less than ϵ.

We need to show that we can make all $(L', g') \in \mathcal{V}_U$ satisfy Properties 1-19 by an appropriate choice of K_i and ϵ.

Property 1. The cusp locus of L and L' agree exactly. In any particular square, the crossing locus between sheets defined by F_i and F_j is the zero set of $F_i - F_j$, and it is transversally cut out, i.e. 0 is a regular value, since L is embedded. Thus, a suitably C^2-small perturbation of $F_i - F_j$, results in the crossing locus of L' remaining within any chosen C^1-neighborhood of the crossing locus of L.

[By taking the F'_i and F'_j suitably close to F_i and F_j on $L \setminus U$, we can arrange that the crossing locus of F'_i and F'_j is contained in any given set of the form $\{|F_i - F_j| < \delta\}$, and hence keep the crossing locus of L' within an arbitrary neighborhood of the crossing locus of L. Moreover, the tangent to the crossing locus of L' is the orthogonal complement of $\nabla_{g'}(F'_i - F'_j)$. By keeping $\nabla_{g'}(F'_i - F'_j)$ close enough to $\nabla_g(F_i - F_j)$ and g' close enough to g, we can keep $\nabla_{g'}(F'_i - F'_j)$ non-zero along the crossing locus of L' and keep the respective g-orthogonal complements as close as desired.]

Properties 2, 3, 7, 10, 11, 12, 14, 16, 17, 18, 19. All of these properties involve the existence of certain compact subsets (sometimes explicitly defined) along which the gradients of particular difference

functions have their directions constrained. For instance, in Properties 2 and 3, gradients of positive local difference functions need to point strictly inward along the paths that form the boundary of $N(e^0_\alpha)$ and $N(e^1_\alpha)$, while Property 10 specifies that the x_1- and x_2-components of $\nabla(F_i - F_j)$ should have a particular (strict) sign along certain 2-dimensional compact subsets of $N(e^2_\alpha)$. In all cases, the constraints imposed on $-\nabla(F_i - F_j)$ can be rephrased as a finite number of properties of the form

$$\forall\, x \in K, \quad g_0(-\nabla(F_i - F_j), X) > 0 \tag{163}$$

with $K \subset N(e^d_\alpha)$ some compact set; X is an appropriately defined (continuous) vector field (with image in TS) defined along K, and g_0 is the euclidean metric in coordinates on some $N(e^2_\alpha)$ or $N(e^1_\alpha)$.

With properties 2, 7, 10, 11, 12, 14, 16, 17, there is no issue with using the same K for both (L, g) and (L', g), and since the inequality is strict on a compact set, it is preserved by suitably small perturbation of (L, g). Properties 3, 18, and 19 are handled similarly except that some extra subtleties need to be addressed.

Property 3 asserts the existence of polygonal paths P_1 and P_2 that in coordinates lie within 1/32 of boundary edges of the squares $[-1, 1] \times [-1, 1]$ that parametrize 2-cells. Along, P_1 and P_2, all $-\nabla F_{i,j}$ must point into $N(e^1_\alpha)$ at points where $F_i > F_j$.

In the case of a (PV) edge, this Property is maintained exactly as above. For a (Cu) edge, the only subtlety is that for the sheets F_k and F_{k+1}, the inequality (163) becomes non-strict at the point of P_1 that intersects the cusp edge. However, the angle between $-\nabla F_{k,k+1}$ and P_1 remains bounded away from 0 up to the cusp edge itself. [In equation (121) from Proposition 11.3, we will have $\sigma_-(k) = \sigma_-(k+1) = k - .5$. Thus, for $x_1 \leq -1/4$, $F_{k,k+1}(x_1, x_2) = f_{k,k+1}(x_1)$, so that the gradient $-\nabla F_{k,k+1}$ points in the negative x_1 direction everywhere along the cusp edge. From the proof of Proposition 11.20, P_1 has slope .001.] Therefore, we can instead use (III) to see that this condition can be maintained.

In the case of a (1Cr) or (2Cr) edge, any point $(x_1, x_2) \in P_l$ where distinct sheets F_i and F_j meet at a crossing, must be a vertex of P_l where edges Q_1 and Q_2 meet. Supposing $F_i \geq F_j$ above Q_1 and $F_j \geq F_i$ above Q_2, it is required that $-\nabla F_{i,j}$ (resp. $-\nabla F_{j,i}$) continues to point transversally to Q_1 (resp. Q_2) at (x_1, x_2).

To maintain this condition, for $(L', g') \in \mathcal{V}_U$ (for appropriate $\mathcal{V}$), we must modify P_l to P'_l because the crossing loci of L and L' are distinct (but C^1-close). This is done by, at each such crossing point (x_1, x_2), replacing Q_1 and Q_2 with new segments Q'_1 and Q'_2 as follows. Since $-\nabla F_{i,j}$ is transverse to Q_1 at the crossing point (x_1, x_2) it (as well as all other $-\nabla F_{k,l}$ with $F_k > F_l$) remains transverse to a small extension of the line segment Q_1 passed the crossing locus, call it $\widehat{Q}_1$, and to all close enough parallel translates of $\widehat{Q}_1$; a similar statement applies to $\nabla F_{j,i}$ and a small extension $\widehat{Q}_2$ of Q_2. Take $\mathcal{V}$ small enough so that (along with satisfying the other requirements) all $L' \in \mathcal{V}_U$ have (i) $F'_{i,j}$ and $F'_{j,i}$ are still transverse to translations of $\widehat{Q}_1$ and $\widehat{Q}_2$ and (ii) replace Q_1 and Q_2 with portions of parallel translates of the $\widehat{Q}_i$ chosen to intersect the crossing locus of L' at a common point. With this modification P'_l, (L', g) also satisfies Property 3.

In Property 18, the only extra subtlety is in the statement about the directionality of $-\nabla(F_i - w)$ along the crossing locus. This can be preserved by choosing $\mathcal{V}$ so that the crossing loci of $L' \in \mathcal{V}_U$ remain suitably C^1-close to that of L.

In Property 19, there are two extra issues to address: (i) The segments are required to start at switch points, and these locations may be distinct for (L, g) and (L', g'). (ii) Again, we require an inequality to hold along the segments $L_{k+1,k+2}$ and $L_{k+2,k+1}$ up to the crossing locus.

We discuss how to modify $L_{k+1,k+2}$ to $L'_{k+1,k+2}$ so that $L'_{k+1,k+2}$ starts at the switch point of (L', g') and retains the desired properties. (A similar argument applies to modify the segment $L_{k+2,k+1}$.) Using a suitable combination of (II) and (III) ((III) is used since $-\nabla F_{k,k+2}$ becomes 0 at the cusp edge), we can find a compact neighborhood of $L_{k+1,k+2}$, denoted by N, that is a union of line segments parallel to $L_{k+1,k+2}$ and such that the required transversality of $-\nabla F_{k+1,k+2}$ and $-\nabla F_{k,k+2}$ holds along each such segment. Taking $\mathcal{V}$ to be small enough, the $(k+1, k+2)$-switch point of any $L' \in \mathcal{V}_U$ will continue to lie in N, and the required transversality will still hold on all segments in N. Then, we can take $L'_{k+1,k+2}$ to be the line segment that is parallel to $L_{k+1,k+2}$ and starts at the $(k+1, k+2)$-switch point of (L', g').

Properties 13, 15. Statements about the location of the cusp locus of L hold as well for L' since the cusp loci of all $(L', g') \in \mathcal{V}_U$ agree. All remaining statements concern the direction of transversality of $-\nabla(F_i - F_k)$ and $-\nabla(F_{k+1} - F_j)$ to some $(k, k+1)$-cusp locus and the existence and location of non-degenerate switch points (which are precisely the tangencies of $-\nabla(F_i - F_k)$ and $-\nabla(F_{k+1} - F_j)$ to the cusp locus). Here, F_i and F_j are defining functions for sheets located above or below the cusp edge respectively. For notational convenience, we restrict attention to the case of $-\nabla(F_i - F_k)$.

As a preliminary, note that from the standard form for defining functions near a cusp edge, ∇F_k and ∇F_{k+1} are not differentiable along the cusp locus when considered as functions of two variables. However, their restrictions to the cusp edge are C^∞. Since for $(L', g') \in \mathcal{V}_U$, $F'_k = F_k$ and $F'_{k+1} = F_{k+1}$ in $\pi_x(U)$, a suitable choice of $\mathcal{V}$ results in $-\nabla(F_i - F_k)$ and $-\nabla(F'_i - F'_k)$ remaining C^2-close along the cusp locus. In particular, for any chosen neighborhood, N, of the (i,k)-switch point, we can preserve the property of having a unique (i,k)-switch point in N, and maintain the direction of transversality of $-\nabla(F_i - F_k)$ to the cusp locus outside of N. [Within N the (i,k)-switch point is the unique zero of a lift to $\mathbb{R}$ of the circle-valued difference $\theta_1 - \theta_2$ where θ_1 is the slope of the cusp locus and θ_2 is the slope of $-\nabla(F_i - F_k)$. The statement that switch points are non-degenerate is equivalent to 0 being a regular value, so the existence of a unique, non-degenerate 0 of $\theta_1 - \theta_2$ in N is preserved as long as the perturbation of $-\nabla(F_i - F_k)$ is suitably C^1-small.]

Properties 4, 5, 6, 8, 9. These properties concern the location and index of critical points of the difference functions $F_i - F_j$. Since all critical points are non-degenerate, it is standard that a suitably C^2-small perturbation of defining functions will result in a perturbation of the critical points of the $F_i - F_j$ that will preserve Morse indices. □

Conclusion of the proof of Theorem 5.1. With $(\tilde{L}_0, g_0)$ as constructed in Sections 9 and 10, let $U \subset \tilde{L}_0$ be a neighborhood of the singular set of L satisfying the conclusion of Proposition 12.2. Then, let $\mathcal{V}$ be a neighborhood of $(\tilde{L}_0, g_0)$, as in Proposition 12.3, with respect to U. The two Propositions show that within $\mathcal{V}$ there is a Legendrian metric pair, $(\tilde{L}, g)$, that satisfies the Properties 1-19 and such that $\tilde{L}$ is 1-regular with respect to g. That $\tilde{L}$ was smooth with crossing arcs and cusp arcs as prescribed by the square types (1)-(14) was verified in Section 11, and these conditions also continue to hold provided we take $\mathcal{V}$ small enough. □

References

[1] V.I. Arnold, S. M. Gusein-Zade and A.N. Varchenko. Singularities of differentiable maps. Volume 1. *Modern Birkhauser Classics*, Monogr. Math., 82, Birkhuser Boston, Boston, MA, 1985

[2] Yuri Chekanov. Differential algebra of Legendrian links. *Invent. Math.*, 150 (2002), no. 3, 441–483.

[3] Georgios Dimitroglou Rizell. Knotted Legendrian surfaces with few Reeb chords, *Algebr. Geom. Topol.* 11 (2011), no. 5, 2903–2936.

[4] Tobias Ekholm. Morse flow trees and Legendrian contact homology in 1-jet spaces. *Geom. Topol.*, 11:1083–1224, 2007.

[5] Tobias Ekholm, John Etnyre, Lenny Ng, and Michael Sullivan. Knot contact homology. *Geom. Topol.* 17 (2013), no. 2, 975–1112.

[6] Tobias Ekholm, John Etnyre, and Michael Sullivan. The contact homology of Legendrian submanifolds in $\mathbb{R}^{2n+1}$. *J. Differential Geom.*, 71(2):177–305, 2005.

[7] Tobias Ekholm, John Etnyre, and Michael Sullivan. Non-isotopic Legendrian submanifolds in $\mathbb{R}^{2n+1}$. *J. Differential Geom.*, 71(1):85–128, 2005.

[8] Tobias Ekholm, John Etnyre, and Michael Sullivan. Legendrian contact homology in $P \times \mathbb{R}$. *Trans. Amer. Math. Soc.*, 359(7):3301–3335 (electronic), 2007.

[9] Yakov Eliashberg. Invariants in contact topology, *Proceedings of the International Congress of Mathematicians*, Vol. II (Berlin, 1998). Doc. Math. 1998, Extra Vol. II, 327–338.

[10] Yakov Eliashberg, Alexander Givental, and Helmut Hofer. Introduction to symplectic field theory *Geom. Funct. Anal.*, 2000, Special Volume, Part II, 560–673.

[11] Michael Entov. Surgery on Lagrangian and Legendrian singularities *Geom. Funct. Anal.*, 1999, Vol. 9, 298–352.

[12] Andreas Floer. Wittens complex and infinite-dimensional Morse theory, *J. Differential Geom.*, 30 (1989) 207–221.

[13] Kenji Fukaya and Yong-Geun Oh. Zero-loop open strings in the cotangent bundle and Morse homotopy. *Asian J. Math.*, 1 (1997), no. 1, 96–180.

[14] John Harper and Michael Sullivan. A bordered Legendrian contact algebra, *J. Symp. Geom.*, Volume 12 (2014), no. 2, 237–255.

[15] Dan Rutherford and Michael Sullivan. Cellular computation of Legendrian contact homology for surfaces, Part I. *Preprint* (2016).

[16] Dan Rutherford and Michael Sullivan. In preparation.
[17] Steven Sivek. A bordered Chekanov-Eliashberg algebra, *J. Topology* 4 (2011), no. 1, 73–104.

Ball State University
E-mail address: rutherford@bsu.edu

University of Massachusetts, Amherst
E-mail address: sullivan@math.umass.edu